Sugar beet cell walls in relation to crop improvement

By

Rachel Elizabeth O'Neill

Submitted in accordance with the requirements for the degree of

Doctor of Philosophy

The University of Leeds

Faculty of biological sciences

September 2017

The candidate confirms that the work submitted is her own and that appropriate credit has been given where reference has been made to the work of others.

Acknowledgements

I would like to thank and acknowledge the support and mentoring I have received from my supervisors over the last four years. Prof. Paul Knox for always being available for guidance and advice as well as his positive attitude towards my project and all things cell wall. Dr Belinda Townsend for introducing me to the world of sugar beet and always giving me guidance exactly when I needed it.

A big thank you to Sue Marcus who has always guided me in the lab and been able to answer even the silliest of questions. Also a big thank you to the other members of the lab who have given advise and provided laughter even in stressful times; Valérie Cornuault, Sara Pose-Albacete, Mercedes Hernández Gómez and Andrew Galloway.

Also a thank you to staff and students at Rothamsted Research for making me feel welcome on research visits and during student symposiums. A big thank you to the staff at Brooms Barn for helping with the massive harvesting effort back in 2013. In addition, thank you to Julia Schückel for hosting and advising me at the University of Copenhagen during my research visit.

Special thanks to Patrick Jarvis and Matthew White for their supervision during my industrial placement at ABSugar. Thank you to Dr Mark Stevens, Colin MacEwan and everyone at the BBRO, all the members of the University of Nottingham Beet Team and the UK grower's community, for always taking a special interest in my project.

A huge thank you to my family; Mum, Dad, Deborah and Lucy for their continuing love and support in everything I do, I would never have come this far without you. Finally, thank you to Laura for always being there for me over the last three years and putting up with me through it all.

This work was supported by the Biotechnology and Biological Sciences Research Council (Grant No. BB/K011456/1) and the British Beet Research Organisation Future Generation Training Programme (Project No. 13/200).

Abstract

Sugar beet (*Beta vulgaris* L. subsp. *vulgaris*) is an economically important crop for the production of dietary sucrose. Breeding efforts towards crop improvement traditionally aim to increase sugar yield as well as in field performance. However, more recently the sugar beet pulp, a by-product of sucrose extraction, has been identified as a potential resource for additional industrial applications. Therefore breeding efforts could be directed towards the improved composition of sugar beet pulp for efficient use in these industries. Plant cell wall composition is integral to both crop performance as cell walls play a role in root growth, development and sucrose accumulation. In addition, plant cell walls make up the majority of sugar beet pulp and therefore cell wall composition influences post extraction applications. A developmental study of three *Beta vulgaris* varieties, utilising a monoclonal antibody directed to xylan, has allowed the visualisation of the xylem vessels within the successive cambial arrangement seen in beet roots. Importantly, a novel monoclonal antibody (LM26) directed towards phloem sieve elements has been characterised as part of this project (Torode et al., 2018). This mAb has allowed the visualisation of the relative location and abundance of phloem sieve elements *in situ* and how this could translate to sucrose accumulation. Monoclonal antibodies directed to several different cell wall polysaccharides were used to screen field grown commercial sugar beet (Sophia) using immunoassay techniques (Enzyme-linked immunosorbent assay (ELISA) and for the first time compared against the cell wall polysaccharide screening technique Comprehensive microarray polymer profiling (CoMPP)) on the same samples to compare the best use of these techniques. These screens indicated that sugar beet cell wall composition is modified throughout development and is influenced by environmental factors. The CoMPP technique was manipulated as a high throughput method to compare the cell wall composition of a unique population of recombinant inbred lines (RILs). Cell wall characteristics were identified which can influence the physiological properties such as sugar yield to aid the phenotyping of the varied population. From this analysis candidate lines have been selected from the RILs that have the potential to be used to direct breeding efforts towards crop improvement.

Table of Contents

Acknowledgements ..... **iii**

Abstract ..... **iv**

List of figures ..... **ix**

List of tables ..... **xii**

List of abbreviations ..... **xiii**

Chapter 1 ..... **1**

Introduction **1**

1.1 Sugar beet **2**

1.1.1 Sugar beet history 2

1.1.2 Sugar beet biology and physiology 3

1.2 Sugar beet industries **5**

1.2.1 Sugar beet breeding and commercial seed production 6

1.2.1.1 Genetic modification of sugar beets 8

1.2.2 Sugar beet processing for sugar production 9

1.2.3 Sugar beets for the production of biofuels 12

1.2.3.1 Bioenergy production 12

1.2.4 Additional uses for sugar beet by-products 15

1.3 Plant cell walls **16**

1.3.1 Cellulose 18

1.3.2 Pectic polysaccharides 20

1.3.2.1 Homogalacturonan 22

1.3.2.2 Rhamnogalacturonan I 23

1.3.2.3 Rhamnogalacturonan II 25

1.3.3 Non-cellulosic/non-pectic polysaccharides 26

1.3.3.1 Heteroxylan 26

1.3.3.2 Xyloglucan 27

1.3.3.3 Heteromannan 29

1.3.4 Cell wall proteins 31

1.3.4.1 Arabinogalactan-proteins 31

1.3.4.2 Extensins 31

1.4 Sugar beet root cell walls 32

1.5 Studying plant cell walls 35

1.6 Project aims and objectives 36

Chapter 2 38

Materials and Methods 38

2.1 Plant materials 39

2.1.1 Preparation of cell wall materials 40

2.1.1.1 Preparation of alcohol insoluble residue 41

2.1.1.2 Cell wall extractions 41

2.1.2 Preparation of plant materials for sectioning for light microscopy. 42

2.1.2.1 Resin embedding 42

2.1.2.2 Wax embedding 42

2.1.3 Calculation of sucrose concentrations for RIL study 43

2.2 Monoclonal antibodies 44

2.3 Immunolabeling of plant material for microscopy 46

2.3.1 Indirect immunofluorescence labelling for light microscopy 46

2.3.2 Immunogold labelling for TEM 46

2.4 Monoclonal antibody characterisation 48

2.4.1 Carbohydrate microarrays of polysaccharides for epitope characterisation 48

2.5 *In vitro* analysis of monoclonal antibody binding 49

2.5.1 Enzyme linked immunosorbent assay (ELISA) 49

2.5.2 Comprehensive microarray polymer profiling (CoMPP) for high throughout analysis of cell wall polysaccharides. 49

2.5.3 Epitope detection chromatography (EDC) 50

2.6 Data handling 51

Chapter 3 52

Sugar beet storage root anatomy and cell wall composition through development 52

3.1 Introduction 53

3.1.1 Sugar beet development 54
3.1.2 Supernumerary successive cambia 57

3.2 Results 58

3.2.1 Sugar beet storage roots have successive supernumerary cambia 58
3.2.2 Development of the successive supernumerary cambia in sugar beet roots 60
3.2.3 Comparison of different *Beta vulgaris* lines 61
3.3.4 Link between sugar beet storage root size, cambial ring number and sucrose content 67
3.3.5 Change in sugar beet cell wall composition throughout development 72
3.3.5.1 Enzyme linked immunosorbent assay (ELISA) for the detection of sugar beet root cell wall glycans through development 74
3.3.5.2 Comprehensive microarray polymer profiling (CoMPP) for the detection of sugar beet root cell wall glycans through development 80
3.4 Discussion 89
3.4.1 Sugar beet storage root anatomy is connected to relative sucrose content 90
3.4.2 Detection of cell wall polysaccharides throughout development 90
3.4.2.1 A comparison of using ELISA and CoMPP for the analysis of cell wall polysaccharides 92

Chapter 4 94

Characterisation of a phloem sieve element specific antibody (LM26) 94

4.1 Introduction 95

4.2 Results 97

4.2.1 Monoclonal antibody LM26 binds specifically to phloem sieve elements in a range of plant organs including sugar beet roots 97
4.2.2 LM26 binds to a β-1,6-galactosyl substitution of pectic β-1,4-galactan 102
4.2.3 LM26 binding occurs in most cell walls of garlic bulbs: an abundant source of the epitope for the characterisation of LM26 104

4.2.1 Use of LM26 to identify phloem development in sugar beet storage root. 107

4.5.1.1 Study of phloem developmental anatomy in sugar beet storage roots 107

4.3 Discussion 111

Chapter 5 113

Assessment of recombinant inbred lines of *Beta vulgaris* to identify candidate lines for future breeding targets 113

5.1 Introduction 114

5.2 Results 116

5.2.1 Verification of the method by correlations between monoclonal antibodies of the same class..... 117

5.2.2 Correlations of different monoclonal antibodies indicate *in muro* interactions between polysaccharide groups. 117

5.2.3 Correlation between physiological traits and cell wall epitope detection in RIL population 118

5.2.4 Identifying candidate lines..... 137

5.3 Discussion 141

5.3.1 Physiological trait analysis 141

5.3.*2 In muro* interactions 144

5.4 Conclusion..... 146

Chapter 6 147

General discussion..... 147

6.1 Conclusion..... 152

Chapter 7 154

References..... 154

List of figures

Figure 1.1 Sugar beet anatomy..... 4

Figure 1.2 Sugar beet seed 7

Figure 1.3 Sugar beet processing in the factory.....10

Figure 1.4 Structure and biosynthesis of cellulose.....18

Figure 1.5 Generalised structure of the pectin supramolecule.....20

Figure 1.6 Structure of homogalacturonan.....23

Figure 1.7 Structure of rhamnogalacturonan I 23

Figure 1.8 Structure of rhamnogalacturonan II 24

Figure 1.9 Structure of heteroxylan... 27

Figure 1.10 Structure of xyloglucan 27

Figure 1.11 Structure of heteromannan 29

Figure 1.12 Sugar beet pectin..... 33

Figure 3.1 Summary of BBCH-scale for sugar beet.....55

Figure 3.2 Structure of a sugar beet root in transverse sections.....57

Figure 3.3 Seedling development of the *Beta vulgaris* line Sophia 61

Figure 3.4 Seedling development of the *Beta vulgaris* line W357B.....62

Figure 3.5 Seedling development of the *Beta vulgaris* line C869.....63

Figure 3.6 Comparison of storage root morphology of three *Beta vulgaris* lines at 6 weeks after emergence 65

Figure 3.7 Storage root diameters of three *Beta vulgaris* lines 67

Figure 3.8 Number of cambial rings within three *Beta vulgaris* lines.....68

Figure 3.9 Inter-ring distance of cambial rings within three *Beta vulgaris* line... 69

Figure 3.10 Summary of weather conditions during developmental growth seasons 71

Figure 3.11 Initial detection of cell wall polysaccharides.....74

Figure 3.12 Plate layout to maximise analysis efficiency 75

Figure 3.13 Heat map of ELISA analysis of cell wall polysaccharides throughout a field development study 79

Figure 3.14 Heat map of the standard deviations associated with the analysis of cell wall polysaccharides throughout a field development study in Figure 3.13. 80

Figure 3.15 heat map of CoMPP analysis of cell wall polysaccharides throughout a field development study 83

Figure 3.16 Heat map of the standard deviations associated with the analysis of cell wall polysaccharides throughout a field development study in Figure 3.15. 84

Figure 3.17 Heat map of additional CoMPP analysis of cell wall polysaccharides throughout a developmental field study 88

Figure 3.18 Heat map of the standard deviations associated with the analysis of cell wall polysaccharides throughout a field development study in Figure 3.17. 89

Figure 4.1 *in situ* analysis of LM26 binding to *Beta vulgaris* L. (sugar beet) 91

Figure 4.2 *in situ* analysis of LM26 binding patterns 92

Figure 4.3 Overall vascular anatomy in sugar beet storage root.....93

Figure 4.4 Transmission electron microscopy of sugar beet phloem sieve elements 94

Figure 4.5 Summary of glycan microarray analysis of LM26 96

Figure 4.6 LM26 binding in garlic bulbs 97

Figure 4.7 Epitope detection chromatography (EDC) of garlic bulb cell wall material 99

Figure 4.8 Overall plant morphology and developmental study of phloem vasculature in the sugar beet line Sophia 102

Figure 4.9 Overall plant morphology and developmental study of phloem vasculature in the sugar beet line C869.....103

Figure 4.10 Overall plant morphology and developmental study of phloem vasculature in the red garden beet variety W357B 104

Figure 5.1 Correlation matrix of RIL population 113

Figure 5.2. Recombinant inbred lines ranked by sugar yield. 117

Figure 5.3. Recombinant inbred lines ranked by mean root diameter.....118

Figure 5.4. Recombinant inbred lines ranked by percentage dry matter.....119

Figure 5.5. Recombinant inbred lines ranked by percentage sucrose of dry matter 120

Figure 5.6. Recombinant inbred lines ranked by LM5 epitope detection.....121

Figure 5.7. Recombinant inbred lines ranked by LM13 epitope detection.....122

Figure 5.8. Recombinant inbred lines ranked by LM28 epitope detection.....123

Figure 5.9. Recombinant inbred lines ranked by LM10 epitope detection. 124

Figure 5.10. Recombinant inbred lines ranked by LM11 epitope detection. ...125

Figure 5.11 Recombinant inbred lines ranked by JIM13 epitope detection.....126

Figure 5.12 Recombinant inbred lines ranked by LM25 epitope detection.....127

Figure 5.13 Recombinant inbred lines ranked by LM18 epitope detection.....128

Figure 5.14 Recombinant inbred lines ranked by LM19 epitope detection.....129

Figure 5.15 Recombinant inbred lines ranked by LM12 epitope detection.....130

Figure 5.16 Comparison of highest sugar yielding recombinant inbred lines..133

Figure 5.17 Comparison of lowest sugar yielding recombinant inbred lines ...134

List of tables

Table 2.1 List of monoclonal antibodies to cell wall polysaccharides..... 43

Table 3.1 Conversion of developmental stage from WAE to BBCH-scale for three *Beta vulgaris* lines..... 58

Table 3.2 Developmental stages of sugar beet plants used for the detection of cell wall polysaccharides..... 69

Table 5.1 Selected candidate recombinant inbred lines for further study for crop improvement..... 140

Table 5.2 Selected candidate recombinant inbred lines for further study into decreased sugar yield..... 140

List of abbreviations

AG:	arabinogalactan
AGP:	arabinogalactan protein
AIR:	alcohol insoluble residue
AX:	arabinoxylan
BBRO:	British beet research organisation
CDTA:	cyclohexane diamine tetraacetic acid
CESA:	cellulose synthase A
CoMPP:	comprehensive microarray polymer profiling
CSC:	cellulose synthase complex
CW:	cell wall
EDC:	epitope detection chromatography
ELISA:	enzyme-linked immunosorbent assay
FITC:	fluorescein isothiocyanate
GalA:	galacturonic acid
GAX:	glucuronoarabinoxylan
GX:	glucuronoxylan
HG:	homogalacturonan
JIM:	John Innes monoclonal
LM:	Leeds monoclonal
mAb:	monoclonal antibody
NMR:	nuclear magnetic resonance
O/N:	over night
PBS:	phosphate buffered saline
RGI:	rhamnogalacturonan I
RGII:	rhamnogalacturonan II
RIL:	recombinant inbred line
RT:	room temperature
TBO:	toluidine blue O
TEM:	transmission electron microscopy
TS:	transverse sections
UV:	ultraviolet
WAE:	weeks after emergence
XG:	xyloglucan

Chapter 1

Introduction

1.1 Sugar beet

Sugar beet is a member of the *Beta vulgaris* L. species which is a highly variable species with many agriculturally significant groups including: garden beets (beetroot), fodder beet, leafy beets (chard) and sugar beet (*Beta vulgaris* subsp. *vulgaris).* The *Beta vulgaris* species is a member of the Amaranthaceae (formerly Chenopodiaceae) family. Other members of this diverse family include species such as spinach (*Spincia oleracea*) (Elliott and Weston, 1993, Lange et al., 1999).

1.1.1 Sugar beet history

Sugar beet as it is known today has been selectively bred for high sucrose content along with improved agricultural practice, sucrose concentration can be up to 20% fresh weight and 75% of dry weight. Sugar beets were grown initially as a garden vegetable and as animal fodder before they were used for sugar production. Sucrose was extracted experimentally from beets in the mid-eighteenth century by chemist Andreas Magraff; however at the time cane sugar was freely available and therefore the process did not take off (Draycott, 2006a). However, interest in sugar beet sugar grew during the Napoleonic wars when the British blocked cane sugar imports. Napoleon encouraged sugar beet research and sugar beet processing factories were built across France. By 1880 the industry had become well established across Europe. The industry expanded from there, with Britain introducing the crop as a bid to become more self-sufficient during the shortages experienced during World War I (Harveson, 2016).

Sugar beet is one of only two crops that provides sucrose (sugar) to the world food industry (Van der Poel, 1998). Sugar beet is grown in temperate regions including; the UK, many countries across Europe, USA and China providing about a 20% of the world sugar production and sugar cane in tropical regions providing the remaining 80%. Both crops produce chemically identical sugar. In the UK, all sugar beet is processed by British Sugar plc in one of four processing plants in the South East of England producing around 1.4 million tonnes of sugar per year (British Sugar, 2010).

1.1.2 Sugar beet biology and physiology

Sugar beet is a biennial plant, where sucrose produced by photosynthesis is accumulated in the storage root in the first year (Artschwager, 1926). Commercial sugar beet is usually harvested at the end of this first year when sucrose is at its highest concentration. A mature sugar beet consists of the vegetative storage organ the tap root (Fig 1.1A), usually white in colour and a rosette of leaves. While the storage organ is usually called the root about 10% of the "root" forms the crown and is derived from the hypocotyl (Hanson and Wyse, 1982). If allowed to continue into the second year of growth the plants will vernalise through the winter with stem elongation (bolting), flower production and seed set occurring through the second year (Fig 1.1B) (Elliott and Weston, 1993). Bolting in sugar beet for commercial sugar production is selected against as stem elongation utilises the stored sucrose in the root within the first year of growth and therefore reduces sucrose yield (El-Mezawy et al., 2002, Mutasa-Göttgens et al., 2010).

Sugar beet root anatomy

Current understanding of the vascular anatomy of the sugar beet storage root is that it is derived from a series of active concentric cambia which develop in the very early stages of growth at the peripheral of the primary root (Artschwager, 1926, Zamski and Azenkot, 1981). Each cambium is responsible for the production of secondary xylem inwards and secondary phloem outwards, resulting in a succession of rings visible with the naked eye (Fig 3.2). This cambial arrangement is referred to as a supernumerary successive cambium and is typical for members of the Amaranthaceae family and a few other species (Carlquist, 2007, Fahn and Zimmermann, 1982, Tamaio et al., 2009, Carlquist, 2003). There is little understanding of the development of these cambial rings and the evolutionary advantage of this vascular arrangement.

There have been previous studies looking at the relationship of cell size and structure to concentration of sugar in mature sugar beet roots discussed by Milford (1973), as well as sucrose concentration in cells relative to distance from the phloem (Milford, 1973, Geiger et al., 1973), however very little is known about the development of the root in detail and how this effects sucrose yield. The yield of sugar from sugar beet storage roots is determined by the root weight and the

concentration of sugar within it (Milford, 1973). Despite sugar yield being the most important factor for a sugar beet grower, very little is known about sugar assimilation and the factors that affect this. Sucrose is transported to the root via the phloem; however, the impact of development of the vascular anatomy of the root has been uncertain.

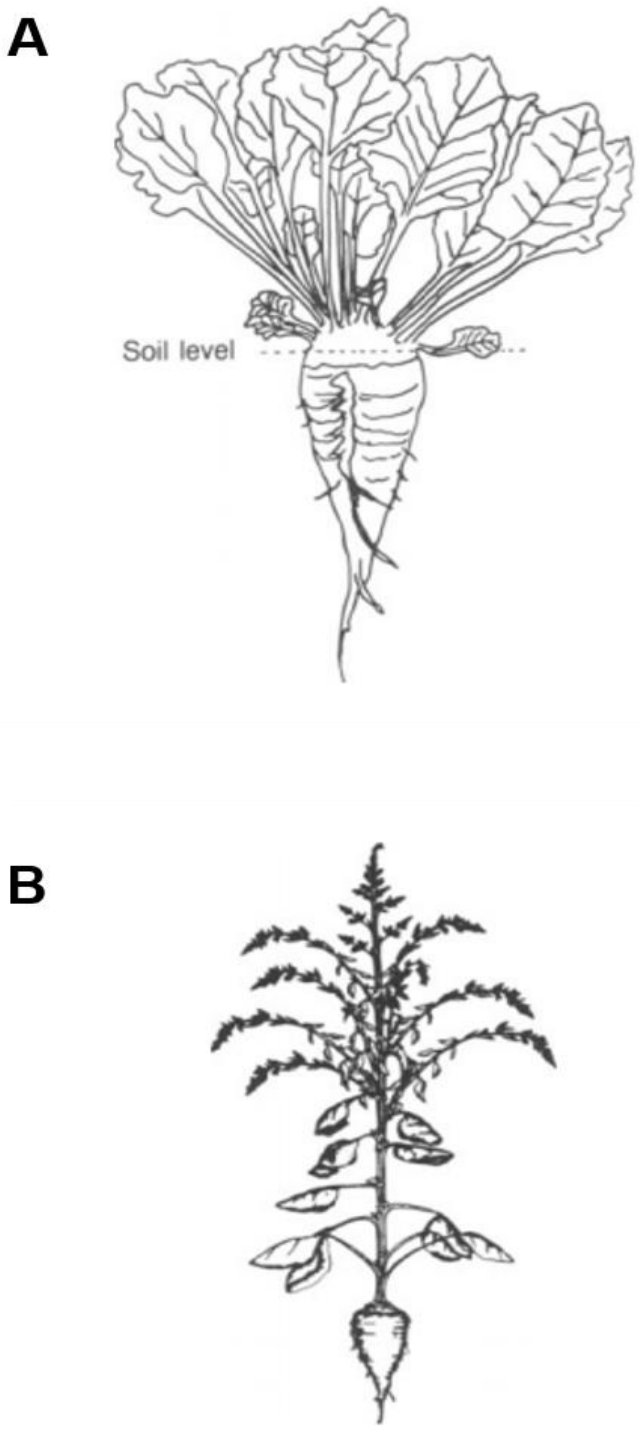

Figure 1.1 Sugar beet anatomy A; A mature sugar beet at the end of the first year of growth, as the plant would be at harvest for sugar production B; A flowering sugar beet with stem elongation (bolting). (Taken from Elliott and Weston (1993))

Physiology of sucrose transportation

An important factor in the success of the sugar beet to store relatively high levels of sucrose within its storage root is sucrose transportation from leaf to root. Higher plants accumulate sugars such as glucose, fructose and sucrose as a source of energy to drive metabolism as well as an energy store for future growth and develop or in times of stress.

Sucrose synthesised in the leaves is the most commercially valuable and the accumulation of this disaccharide in the vacuoles of sugar beet taproots makes sugar beet an important cash crop. Sucrose transport out of the leaves is facilitated by “SWEET-type transporters” which are involved in sucrose loading into phloem sieve elements and corresponding companion cells (Chen et al., 2010). The majority of sucrose that enters the root is destined for the vacuole however the molecular mechanisms for this in roots is poorly characterised. Many vacuolar transporters reported for movement of sucrose across the tonoplast have been described in leaves (Schulz et al., 2011, Eom et l., 2011, Klemens et al., 2013). In 2015 Jung et al described a sugar beet specific vacuolar sucrose transporter (BvTST 2.1) with a key role in sucrose accumulation in the sugar beet taproot.

It is clear that phloem have an important role in sucrose accumulation and it has been suggested that transportation of photosynthate and amino acids through the phloem can be a limiting factor in both sucrose accumulation and biomass yield (Zhang et al., 2014). In addition, it has been suggested to increase sugar yield in sugar cane that improvements to translocation from leaves to phloem and from phloem to sink to prevent negative feedback would be one of the most successful endeavours into yield increase (Shrivastava et al., 2015)

1.2 Sugar beet industries

Sugar beet is a summer crop usually grown as part of a rotation with maize or wheat to lessen the effects of crop specific diseases. Sugar beets have a growing period between 170 and 200 days and require a mild growing season with a well

distributed precipitation, as they suffer readily from water deficiency effecting sucrose assimilation (Camposeo and Rubino, 2003, Draycott and Farley, 1971).

Modern day farming practice for sugar beets have been adopted with deep plough after the preceding crop to produce a seed bed with good tilth (Baver and Farnsworth, 1941) and precision drilling of the pre-treated seeds. Fertilisers and herbicides applied to the crop at sowing and germination occurs about 10 days after (Tzilivakis et al., 2005). Fertilisers are applied throughout the growing period to increase root yield. Mature sugar beets can grow to be around 1-2 kg with 8-22% sucrose of fresh weight (Scott et al., 1973, Cooke and Scott, 2012).

Sugar beets are subject to a number of insect pest and diseases many of which effect sucrose concentrations in various ways. Foliage diseases such as leaf spot (*Cercospora* sp.), powdery mildew (*Erysiphe betae)* and sugar beet rust (*Uromyces betae*), where leaves become infected and this interferes with photosynthesis therefore reducing sucrose production (Draycott, 2006b, Cooke and Scott, 2012). Whereas, root borne pest and diseases such as root rots, rhizomania and nematodes reduce sucrose concentrations through root damages and stress (Buhre et al., 2009).

1.2.1 Sugar beet breeding and commercial seed production

Higher sucrose content and disease resistance are constantly sought after by sugar beet growers and in response sugar beet breeders produce new commercial varieties every year. Four main seed houses (KWS UK, Strube, Syngenta and SES vanderHave), provide sugar beet seed to the UK market with the BBRO (British Beet Research Organisation) providing a recommended list each year based on growth trials. The list recommends varieties based on sucrose concentration for various soil types and resistance to disease threats (BBRO, 2017).

Current sugar beet varieties are the result of over 100 years selective breeding for high sucrose content and improved performance in the field. As well as high sucrose yield the main objectives for sugar beet breeders are: to reduce yield losses from abiotic and biotic pressures, early bolting resistance, and particularly resistance to root diseases such as rhizomania (Biancardi et al., 2002, Lewellen

et al., 1987). The sugar beet seed that is planted is actually derived from the whole flower which has become woody, so for commercial use the seed is polished, primed and coated with fertilisers and fungicides (McQuilken et al., 1990, Duan and Burris, 1997) (Fig 1.2).

Sugar beet breeding has relied on mass selection of favourable traits. This strategy works well for traits that are easily scored, such as sucrose concentrations. Recurrent selection has also been used to some extent. With this method, selections are made and crossed with a common parent. The progeny is evaluated, and the best-performing families or lines are identified. Those seed parents whose progeny showed high performance are then inter-crossed and advanced to another round of selection. Frequently, progeny testing occurs with a promising pollinator crossed with a series of cytoplasmic male sterility (CMS) tester lines (Reif et al., 2010). Commercial varieties grown in the UK are monogerm, a recessive trait of the current breeding programmes along with CMS which has been developed over the last 60 years and is now slowing down future population improvement. The CMS lines (pollen sterile) are used to harvest seed and are planted in a population of pollen donors and the seed exclusively harvested from the CMS plants to maintain the monogerm traits (Richardson, 2010).

Figure 1.2. Sugar beet seed. From left to right: Sugar beet seed as harvested, polished sugar beet seed, coated sugar beet seed (blue). (Image from Strube (2017))

1.2.1.1 Genetic modification of sugar beets

Commercialised genetically modified (GM) sugar beets are cultivated outside of the EU, with 95% of all sugar beets in the USA being GM. GM sugar beets have been produced by Monsanto and KWS SAAT for glyphosate-resistance (Mannerlof et al., 1997). These “RoundUp ready” sugar beets have been grown in the USA and Canada since 2007 (KWS, 2005).

Sugar beet is considered one of the best candidates as a wide spread GM crop as the likelihood of becoming a pest plant is significantly reduced due to the cultivation practices within the industry (Khan, 2010). With selection against sugar beet entering reproductive growth to maximise sucrose yield, cross-pollination with other species’ is unlikely to occur (Bennett et al., 2004). In addition, sugar for GM sugar beets cannot be classed as GM as there is no genetic material in the products. Sugar and pulp from GM sugar beets is approved for human and animal consumption in many countries, including the UK (ISAAA, 2016). However, it may be some time until approval is granted to grow herbicide tolerant sugar beet in the UK (May, 2003)

1.2.2 Sugar beet processing for sugar production

Sugar beet processing occurs from field to factory and requires specialised factories; in the UK there are four sugar beet processing plants owned by British Sugar which process sugar beet and produce white sugar among other co-products (Fig 1.3).

Harvest

In the UK, the sugar beet harvest or 'campaign' takes place between September and March when the sugar content of the beet is at its highest. During this time, the leaves are cut off in the field (topped) where they are either ploughed back into the land as a fertiliser or used as animal feed. The beets are harvested and delivered immediately to the factory or stored in clamps for later delivery. Due to its bulk, transport distances are kept to a minimum with the average distance being 28 miles in Britain from field to factory British Sugar (2010).

Extraction

Upon arrival at the factory the beet is cleaned in large tanks to remove debris and then chopped into slices known as cossettes. The cossettes increase the surface area to ease the extraction process. The cossettes are mixed with hot water for about an hour at 70^{o}C causing the sucrose and other components of the sugar beet to diffuse from the plant cells into the surrounding water, this produces a brown liquid "Juice" (Koelsch, 1969).

Pressing

As the cossettes come to the end of the extraction step they still contain water with some sucrose therefore they are pressed with a screw press to ensure the maximum sucrose is extracted from the sugar beet. The pressed beet is now referred to as pulp and is usually dried and used as the main component of many animal feeds.

Carbonation

This process is used to clean the juice before sugar is produced. For this calcium hydroxide is added and carbon dioxide is bubbled through the mixture, while the pH and temperature of the reaction are carefully monitored. The carbon dioxide and the calcium hydroxide react to form solid calcium carbonate crystals which occlude the solids from the juice. This mixture is now passed through a filter or allowed to settle to remove the solids for the next phase.

Boiling

The liquid mixture is then boiled under vacuum to produce a thick syrup in which crystals appear. 'Seed' crystals are added to promote crystallisation. Sucrose naturally forms pure sucrose crystals expelling non-sugars, therefore throughout the process the remaining liquid becomes less pure. The crystallisation is repeated several times with the yield reducing each time until no more sucrose crystals can be produced. Using centrifugation, the crystals are separated from the syrup and dried to produce commercial white crystal sugar (Van der Poel, 1998).

Products

The sugar is now read to be packaged and used. In addition, the remaining juice which has been exhausted for crystal sugar production and is now used as molasses, used for animal feed (Huhtanen, 1988) or distilled for alcohol production (Ergun and Mutlu, 2000). As mentioned the pulp is a by-product of sugar production from sugar beet that is mostly composed of the plant cell walls. Downstream uses of this resource include - for example nutrition for animal feed (Brouns et al., 1997, Longland and Low, 1989)or alternative uses in the bio economy such as bioethanol (Dodić et al., 2009).

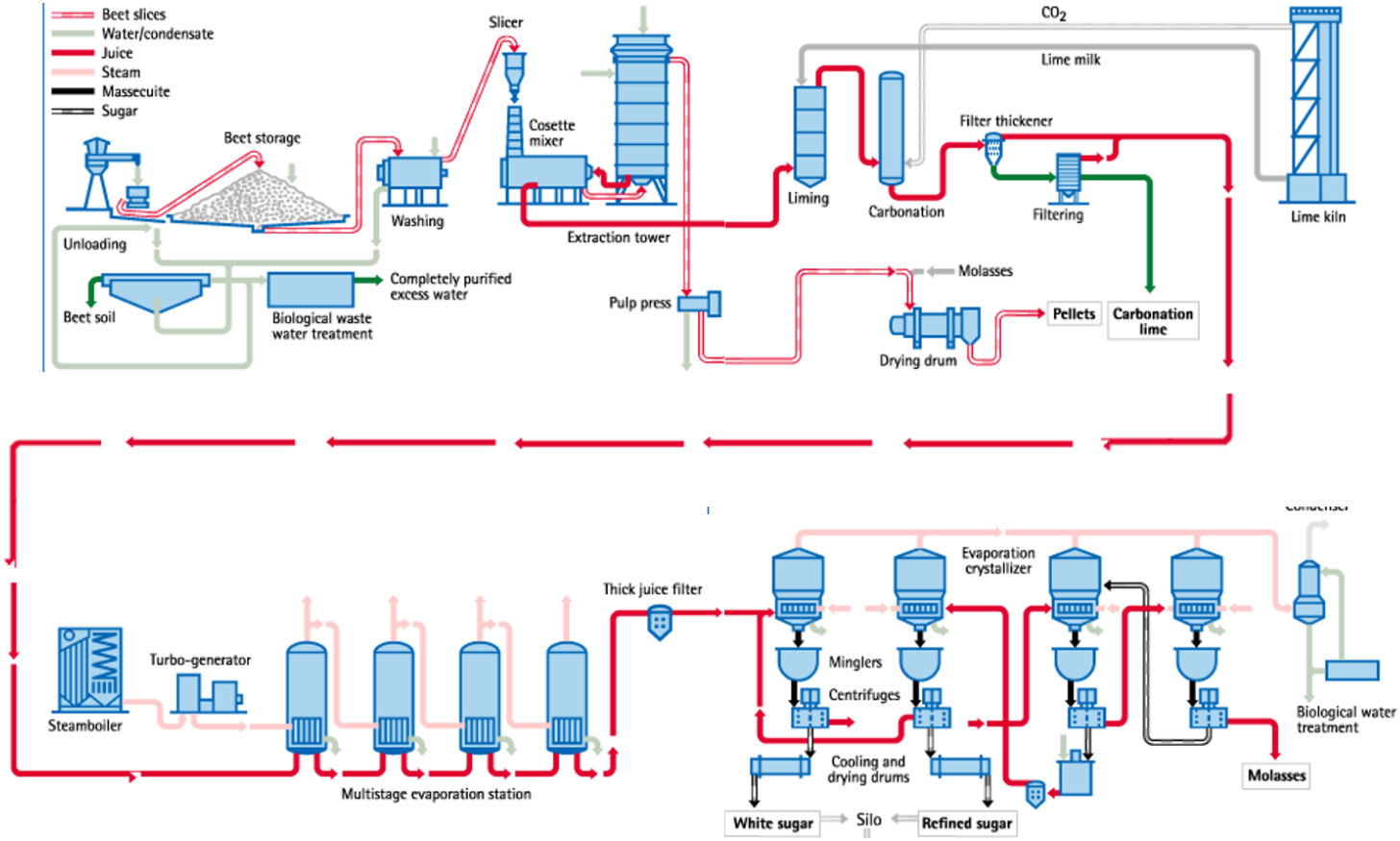

Figure 1.3. Sugar beet processing in the factory. Summarisation of the processes of a sugar beet processing factory to extract sugar (sucrose) from sugar beet including the co-products produced as part of the processing. Image modified from Kissner (2015)

1.2.3 Sugar beets for the production of biofuels

A renewed interest in renewable energy has occurred since the mid-1990s due to the pursuit to reduce greenhouse gas emissions and reduce climate change (Berndes et al., 2003) Currently about 10% of the world's energy demand is delivered using biomass.

Biofuels and bioenergy are seen as one of the options as a substitute for fossil fuels. The use of biomass as an energy source on a large scale can contribute to sustainable energy production as well as have positive social and economic advantages (Turkenburg and et al., 2000). However biomass energy potential is limited by resource, land use competition for other crops and other uses for the biomass , additionally other energy sources are available for less cost to the consumer (Berndes et al., 2003). Limitations also exist in that the techniques required to efficiently utilise crop residue biomass for energy are underdeveloped (Kim and Dale, 2004).

1.2.3.1 Bioenergy production

Combustion

Combustion is the most traditional use for biomass as an energy source is use of firewood for heating and cooking - a technique that has been used for centuries in open fires. The advancement of technologies has allowed for improve efficiency for domestic scale heating using combustion of diverse biomass with the development of heating systems catalytic gas cleaners and the use of the fuel in a standardised form (i.e. pellets). Biomass has also been utilised via combustion on an industrial scale to efficiently produce heat and electricity. Co-combustion of biomass in coal-fired power plants has been introduced in some European countries therefore increasing biomass based power with minimal investment as existing power plants are utilised for this purpose, with advantages over purely coal based power plants due to high efficiency combined with lower sulphur dioxide (SO_2) and nitrogen oxide (NO_x) emissions (Turkenburg and et al., 2000).

Fermentation

Fermentation is a well-known route for the conversion of sugar cane and maize on a large scale into ethanol. Conversion of sucrose to ethanol is simple and involves fermentation by yeast, however ethanol from cereal grains is slightly more complex is this first requires enzymes for the conversion of starch to sugars. Despite this, cereal grains were the feedstock for more than 50% of the ethanol produced in Europe in 2009. Sugar beet, was the next most common feedstock but is harder to store than cereal grains (Panella, 2010). The biological process for the conversion of lignocellulose biomass in to ethanol occurs as follows: A pre-treatment to remove lignin or hemicellulose and release cellulose, use of cellulases to produce free sugars from the polysaccharide polymers, fermentation of hexoses and pentoses to produce ethanol followed by distillation of ethanol. Bioethanol is an attractive alternative to non-renewable fuels as it can be readily utilised successfully in any combustion engine that require gasoline and therefore reduces air pollution and therefore eases climate change by reducing greenhouse gas emissions (Canilha et al., 2012)

Anaerobic digestion

Biogas produced by anaerobic microbial digestion of waste products can also be used to produce renewable energy. The gas, mostly methane and carbon dioxide can be produced from a wide range of substrates including plant material, crops and green waste. The gases produced can be combusted with oxygen and therefore can be used as a fuel, for example heating or cooking. Biogas can also be utilised in a similar way to natural gas, compressed and used in vehicles and has the potential to replace present motor fuels; however, these cannot be used in traditional combustion engines and require specialist vehicles to be able to utilise the fuel (Andrews, 2008).

Despite sugar beet being predominately grown for sugar, with breeding focused on high sucrose content and low impurities, there has been research into the use of fermentable sugars in the production of bioethanol to offer an alternative to fossil fuels in which case traditional breeding could be diverted to select solely for fermentable sugars (Draycott, 2006a).

At present ethanol can be easily produced as a first generation biofuel from sugar beet. This simply uses yeast fermentation to convert sucrose from the storage root in to ethanol. This is efficient compared to conversion of starch to sugars in cereal grains as no enzymes are required as a pre-treatment (Antoni et al., 2007). Per hectare sugar beet is one of the most efficient sources of bioalcohols, producing over 5000l/ha (fresh weight) of ethanol through fermentation. (Elbehri et al., 2013) For the aforementioned reasons sugar beet is the second most common ethanol feedstock after cereal grains.

It has been suggested that sugar beet is a good candidate for use as a substrate for anaerobic digestion to produce bio-methane by co-digestion with the waste water from sugar beet processing (Alkaya and Demirer, 2011). This process could also use the entire beets including the crown, which is currently unused when refining for sucrose extraction. (Weiland, 2003). As well as whole roots it is possible that sugar beet pulp, a co-product of sugar processing, could be used as a substrate for recombinant bacteria to produce ethanol as a second generation biofuel (Sutton and Doran Peterson, 2001).

Currently second generation biofuels from waste and lignocellulose feedstocks are limited (Kumar et al., 2009). The cell walls of the sugar beet make up the majority of the pulp that remains after sucrose extraction, this pulp is generally used to make animal feed but has potential to be processed as a second generation biofuel increasing the value of the pulp (Rezic et al., 2013). With the introduction of an anaerobic digestion (AD) plant at the British sugar factory in Bury St Edmunds in 2016, producing renewable electricity by processing pressed pulp from the factory, it is clear that the industry is moving towards increasing added-value to the products of sugar production. An improved understanding of the biochemical interactions and fundamental biology controlling sugar beet cell wall composition would allow for the opportunity to increase yield and efficiency of the processes involved in the production of economically valuable products.

1.2.4 Additional uses for sugar beet by-products

In addition to utilising the by-products produced from sucrose extraction from sugar beets for animal feed and biofuel production there have been many other studies into alternative uses for these resources. One example is the use of sugar beet pulp as a source of human dietary fibre. Nordic sugar has produced Fibrex® as a dietary fibre product from sugar beet. This product is marketed as a dietary additive for the promotion of improved bowel health and maintenance of healthy cholesterol levels. Cell wall composition of sugar beet pulp is described as beneficial, with lower levels of lignification as other sources (cereal bran), therefore providing a "unique fibre composition" with interesting physical properties, making this product superior to other fibre products on the market (Nordic Sugar, 2012). There have also been many studies into utilising sugar beet pulp in the dietary industry; as a source of phenolic compounds as a natural antioxidant (Mohdaly et al., 2010) and a source of betaine as a supplement (Ueland, 2011). A recent study by Modelska et al. (2017) developed a concept for utilising sugar beet pulp and leaves for the chemical and biotechnical industries. They describe acidic hydrolysis to produce furfurayl alcohols to be converted into propylene glycol.

1.3 Plant cell walls

Plant cell walls are important structures for a plant, giving rigidity and shape to individual cells is a key feature in the success of the whole organism by allowing structural strength and large size (Cosgrove, 1993). Plant cell walls are important in terms of biological research, as the functions of the plant cell walls extend much further than just strength and shape to include; cell expansion, protection, cell signalling and intercellular transport, among others (Vorwerk et al., 2004, McMahon and Gallop, 2005). This breadth of functions explains why the plant cell wall is such a complex structure whose biosynthesis is so well controlled (Cosgrove, 2005).

The plant cell wall is formed in a series of stages starting during cell division with the deposition of callose followed by cellulose at the cell plate (Chen and Kim, 2009, Amor et al., 1995). The cellulose forms a network of associations with non-cellulosic polysaccharides including, xylan, xyloglucan and mannans (Hosoya et al., 2007). This is embedded in a pectic network to provide flexibility (Moore et al., 2008, Caffall and Mohnen, 2009). The cell wall is usually described in three layers, with the middle lamella laid down initially between the cell plate and the plasma membrane, composed mostly of pectin this layer is thought to play a large part in cell adhesion (Carpita and Gibeaut, 1993, O'Neill et al., 1990, York et al., 1986). The middle lamella is often very thin between adjacent cells as the cell plate is stretched during cell growth. The primary cell wall is deposited during cell growth and the thickness is maintained at 0.1-1.0 µm and develops between the middle lamella and the plasma membrane. While relatively thin the primary cell wall structure confers strength against turgor pressure while being elastic enough to allow growth and expansion of the cell (Carpita and Gibeaut, 1993).

In flowering plants the primary cell wall is categorised based on composition, type I and type II. Type I primary cell walls are characterized by a framework of cellulose-xyloglucan at approximately equal amounts embedded in a pectic network and are found in dicotyledonous plants. While type II primary cell walls contain less xyloglucan and predominately have glucuronoarabinoxylan linking to the cellulose microfibrils contain less pectin and develop in non-commelinid monocotyledonous plants (Harris, 2006). In some cells the cell wall does not

develop any further than the primary cell wall however some specialised cells, e.g. xylem, deposit a secondary cell wall during differentiation (Brown et al., 2005, Wightman and Turner, 2008). Thicker than the primary cell wall, the secondary wall develops between the primary wall and the plasma membrane. The secondary cell wall is strong and restricts cell expansion thus maintaining the cell shape and size (Turner and Somerville, 1997). The secondary cell wall varies both biochemically and in its morphology, depending on cell function.

The major components of plant cell walls are cellulose, pectin, heteroxylans, xyloglucan, mannans, mixed-linkage glucans and proteins (Fry, 1988). The amount of each cell wall component varies between species, tissue, cell type and even areas within an individual cell (McCann et al., 1992). The plant cell wall is involved in the transportation of many molecules and ions and forms the apoplastic pathway (Schreiber et al., 1999, Steudle and Peterson, 1998). Cells will adapt their cell wall composition to meet their associated function whether it is to be porous to allow movement of nutrients or like xylem vessels being impermeable water for transport throughout the plant (De Boer and Volkov, 2003). The composition of plant cell walls is not fixed and can change in response to environmental and developmental stimuli to ensure that they have the appropriate physical and chemical composition for their required purpose (Brummell, 2006, Peaucelle et al., 2011).

1.3.1 Cellulose

Cellulose is the most abundant polysaccharide of plant cell walls making it the most abundant biological polymer on earth (Jarvis, 2003), and is produced by a taxonomically diverse group of organisms including vascular and lower plants, some algae, fungi and several bacterial species (Richmond, 2000). Cellulose is a homopolymer with a repeating unit of two β1, 4 linked D-glucose residues (cellobiose), each glucose molecule is rotated 180˚ allowing the chain to remain flat (Fig 1.4). Neighbouring chains will form intermolecular hydrogen bonds and Van der Waals interactions. These bonds between cellulose chains forms cellulose microfibrils, as they are found functionally in the plant cell walls at about 3 nm in thickness (Taylor, 2008). Cellulose biosynthesis is a coordinated process by the action of cellulose synthases. Cellulose synthases have been visualised in plasma membranes as cellulose synthases complexes (CSC) (Kimura et al., 1999, Richmond and Somerville, 2000). The CSCs consist of six synthase isoform (CesA) subunits which are arranged in a rosette formation, with each of these complexes then arranged again in a larger rosette formation. It is hypothesised that each of the CesA subunits can produce a single glucan chain and therefore each CSC produces six glucan chains. The coordinated production of glucan chains by the six CSC working together synthesises the 36-glucan chain microfibril (Fig 1.4) (Taylor, 2008, Beeckman et al., 2002)

Cellulose microfibrils play an essential structural role in plant structure, being strong and inflexible (Brett, 2000). These properties protect the plant cells from bursting due to osmotic pressure creating turgor pressure allowing plants to stand upright. The cellulose frame work consisting of microfibrils, with differing orientations that vary between cell type and species (Kerstens and Verbelen, 2002), is embedded in a gel matrix. The matrix consists of various polysaccharides which interact with the cellulose microfibrils, *in muro*. Interactions of pectin (Zykwinska et al., 2005), xylan (Busse-Wicher et al., 2014) and xyloglucan (Lima et al., 2004) with cellulose microfibrils by hydrogen bonds. Side chains and acetylation patterning play a role in the extent of cellulose polysaccharide interaction which contributes to the differing strength and rigidity of the cell wall and overall properties of different plant tissues (Kabel et al., 2007, Lima et al., 2004).

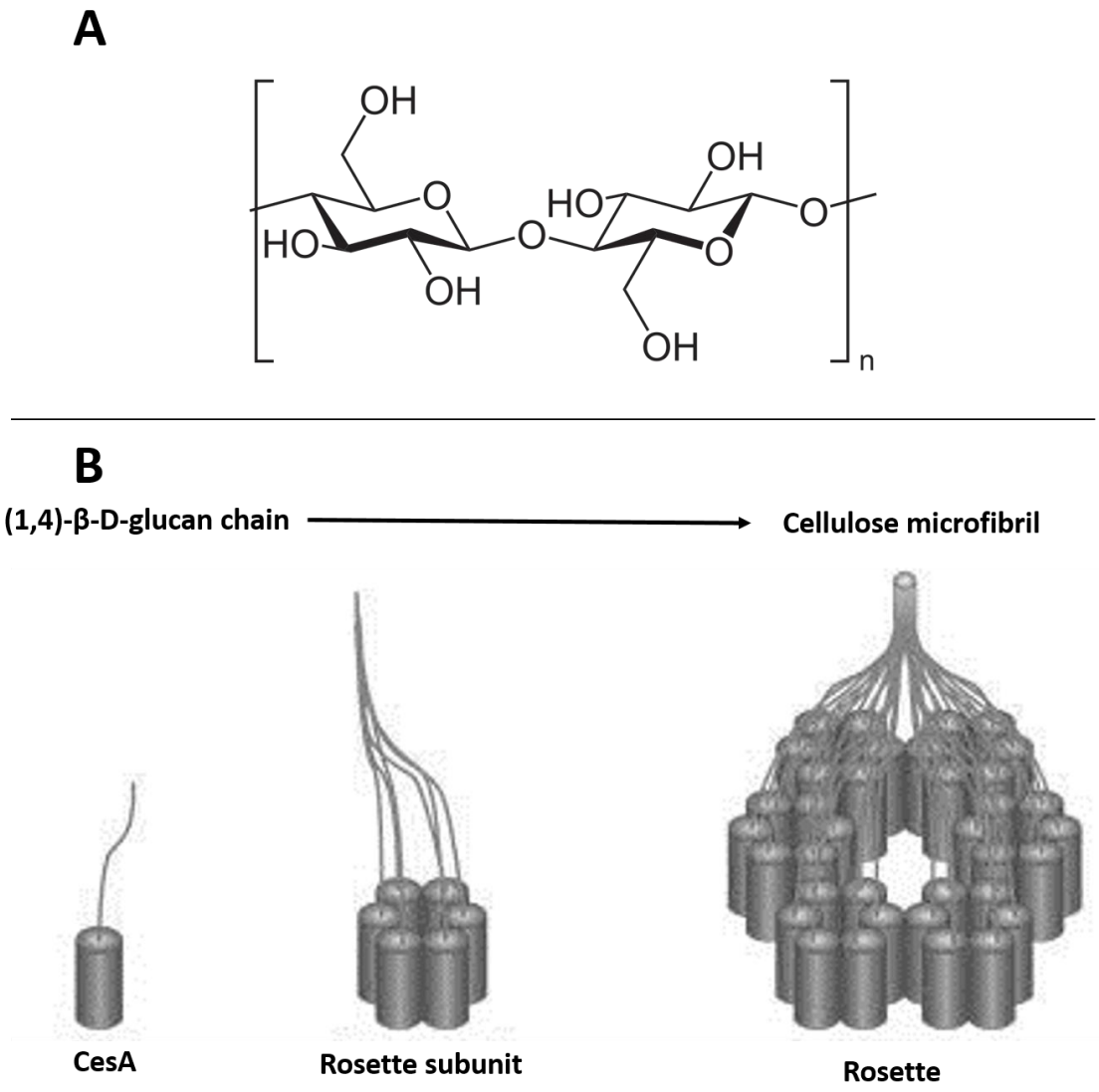

Figure 1.4. Structure and biosynthesis of cellulose. A. Chemical schematic of the repeating unit (Cellobiose) of a cellulose chain. B. Diagrammatic representation of the biosynthesis of cellulose microfibrils by cellulose synthases complexes (CSC), showing the assembly of the rosette formation from individual subunits. (Taken from Cosgrove (2005))

1.3.2 Pectic polysaccharides

Pectins are a group of polysaccharides that can be distinguished into four groups of molecules containing galacturonic acid residues; homogalacturonan (HG), xylogalacturonan (XGA), rhamnogalacturonan I (RGI) and rhamnogalacturonan II (RGII) (Willats et al., 2001). Current understanding states that the different groups of polysaccharides are not separate molecules but exist as covalently bonded domains of the pectic supramolecule as shown in Figure 1.5 (Yapo, 2011, Voragen et al., 2009, Caffall and Mohnen, 2009, Burton et al., 2010). Typically, HG is the most abundant of these polysaccharides accounting for about 65% of pectin, with RGI making up 20 to 35% (Mohnen, 2008) and the remaining 10% made up of RGII and XGA (Harholt et al., 2010, Zandleven et al., 2007), but the ratios of the polysaccharides varies between species. Pectin is essential to plant cell wall function and play a key role in cell adhesion and cell expansion (Caffall and Mohnen, 2009).

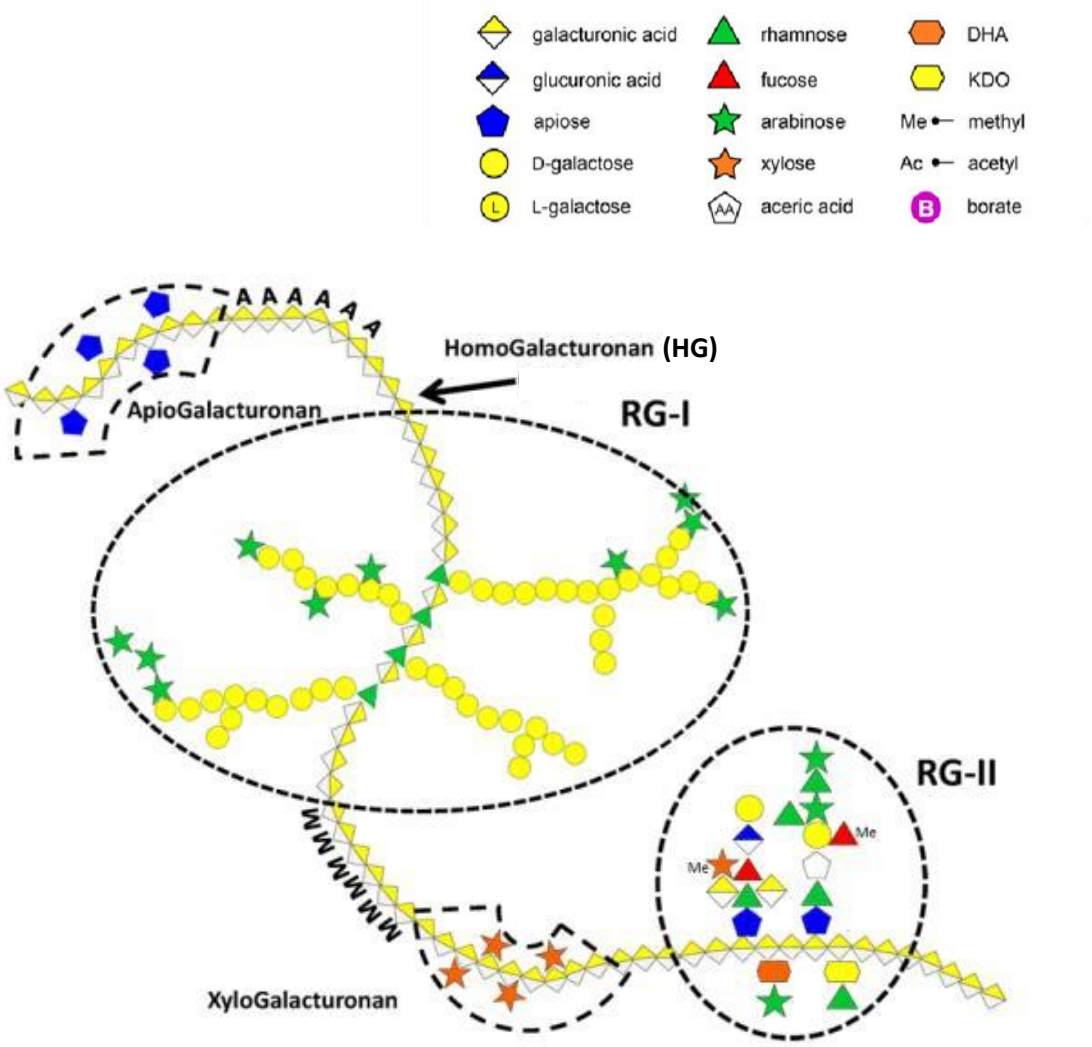

Figure 1.5 Generalised structure of the pectin supramolecule. A schematic representation of the different groups of polysaccharides within the pectin supramolecule structure. Key pectic domains are indicated by dashed circles, homogalacturonan (HG), rhamnogalacturonan I (RGI) and rhamnogalacturonan II (RGII). Substitutions of homogalacturonan with xylose and apiose are indicated by the dashed ellipses. **A**, indicates acetylation and **M**, indicates methylation (Perez et al., 2000)

1.3.2.1 Homogalacturonan

Homogalacturonan (HG) is made up of a backbone of α (1,4) linked galacturonic acid (GalA) of which some GalA may be methyl esterified at the *C*-6 and/or have acetyl groups attached at the *O*-2 and *O*-3. The methyl esterification distribution throughout the molecule affects the qualities of the pectin gel matrix with longer regions of unesterified HG more susceptible to interaction via Ca^{2+} ion bridges (Daas et al., 2001). GalA in HG can be substituted with xylose at *O*-3 to form xylogalacturonan (XGA), xylosylation can vary greatly between species from 20% to 75% (Schols et al., 1995) and, like HG XGA can also be methyl esterified (Fig 1.6)

While the mechanisms behind pectin biosynthesis are poorly understood the production of these long chain polysaccharides for the cell wall is hypothesised. Studies suggest synthesis in the Golgi apparatus and transportation via vesicles to the cell surface and assembled at the plasma membrane forming new cell wall material or incorporation into the existing cell wall. The degree of methylation can be selectively altered by wall-bound pectin methylesterases, the de-esterification *in muro* allows Ca^{2+}cross-linkage with existing HG. Due the complexity of pectin synthesis the identification of the enzymes involved in the mechanism did not occur until much after HG synthesis was observed for the first time by (Lin et al., 1966). The process involves a large number of enzymes including galacturonosyltransferases, galactosyltransferases, methyltransferases and acetyltransferases. The complexity of the pectin structure confers the necessity of a large number of different enzymes to give the structure its differing properties.

1.3.2.2 Rhamnogalacturonan I

Rhamnogalacturonan I (RGI) is a major component of the primary cell wall of dicotyledonous plants. The back bone of this molecule is made up of a repeating unit of α1,4-linked galacturonic acid (GalA) alternating with α1,2-linked rhamnose (Rha), this molecule can be made up of more than 100 of these repeating units (McNeil et al., 1980). RGI can have a number of neutral sugars substituted at the *O*-4 position of the Rha and acetyl groups can be present on the *O*-2 and *O*-3 of GalA. The branching of Rha residues can vary significantly depending on the source, from 20% to 80%. Side chains can be single unit (1,4) Gal or polymeric for example arabinan or arabinogalactan I (AGI) (Ridley et al., 2001). Arabinans can be highly branched molecules which have α(1,5)-linked arabinose backbone. Side chains can either be the addition of a single arabinose as linked via α(1,2) or α(1,3) bonds to the backbone or α(1,5)-linked arabinose oligosaccharides. Arabinogalactans are made up of β(1-4)-linked galactan chains commonly attached to the Rha residues in the RGI back bone, the galactosyl residues have arabinan attached to the O-3 position (Liwanag et al., 2012). The complex formed between RGI, AGI and arabinan lead to these being referred to as pectic hairy regions with the AGI and arabinan representing the 'hairs' (Fig 1.7). These side chains can form connections with other chains forming hydrogen bonds.

The composition of RGI can vary not only between species and cell type but spatially within a single cell. The variations are associated with function and these can include, cell expansion, cell adhesion, cell signalling and cell development (Verhertbruggen and Knox, 2006, Lee et al., 2011)

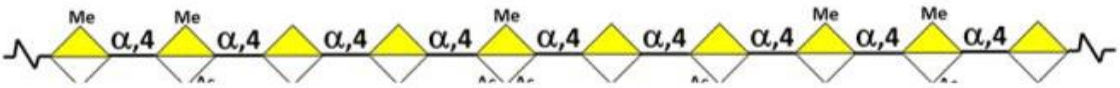

Figure 1.6. Structure of homogalacturonan. A schematic representation of the homogalacturonan. The galacturonic acid (GalA) are linked via an α (1,4) bond. Shown by **Me** is the potential methyl esterification of the GalA subunits. Adapted from (Joseleau and Perez, 2017)

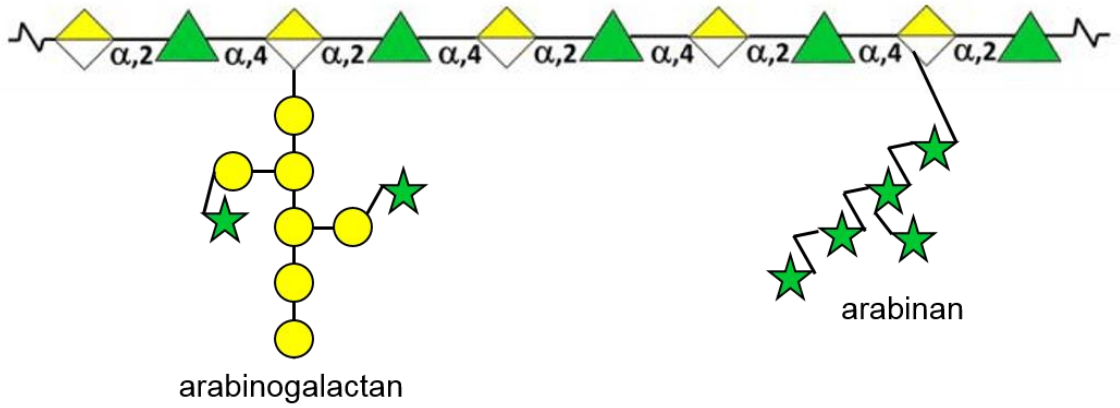

Figure 1.7 Structure of rhamnogalacturonan I. Schematic structure of rhamnogalacturonan I (RGI) showing associated chain substitutions. Substitutions of the RGI shown are; arabinan, chains of arabinose which can be linear or branched and arabinogalactan, chains of galactose with arabinose substitutions. Adapted from (Joseleau and Perez, 2017)

1.3.2.3 Rhamnogalacturonan II

Rhamnogalacturonan II (RG II) has a linear back bone of β(1-4) GalA, similar to HG but in contrast to RGI (Fig 1.8). RG II makes up about 1-4% of the primary walls of most dicots (O'Neill et al., 2004) and has been found to be a complex molecule containing 12 different glycosyl residues and several rare sugars (Melton et al., 1986). RG II molecules form cross links between each other via borate-diol ester links. It has been suggested that borate deficiency causes abnormal plant cell wall morphology due to lack of these links (O'Neill et al., 2001, Ishii et al., 1999), therefore making borate-diol links and RG II fundamental for plant development.

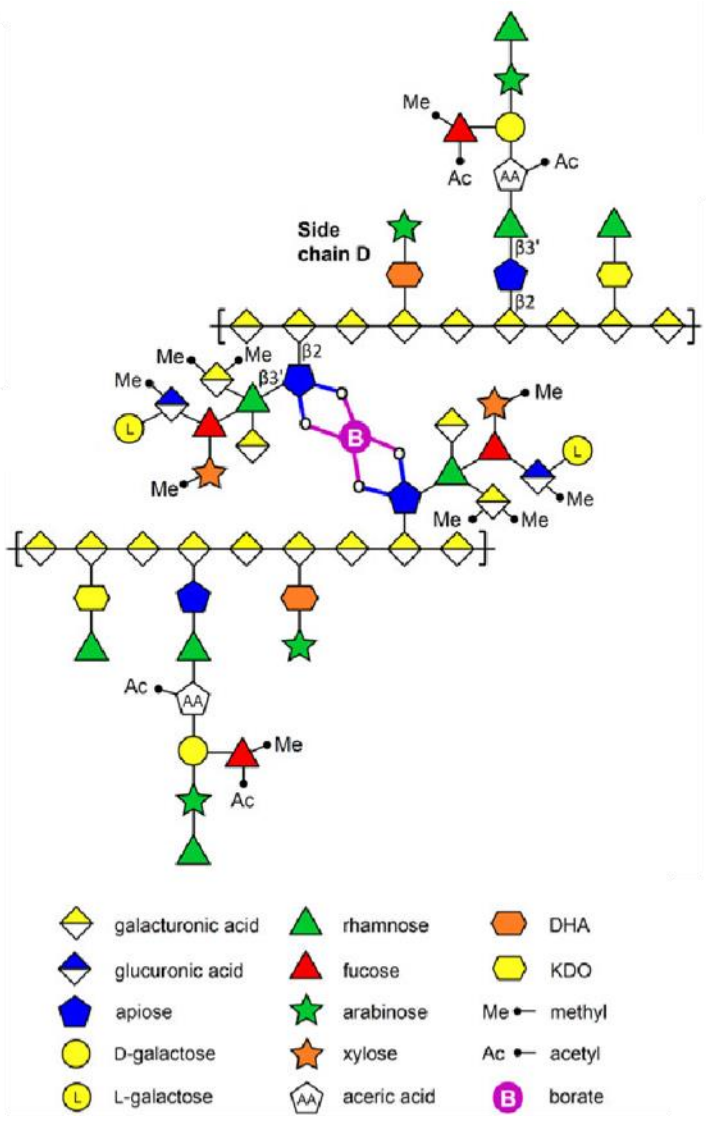

Figure 1.8 Structure of rhamnogalacturonan II. Schematic structure of two molecules of RGII connected via a borate- diol ester link. Adapted from O'Neill et al. (2004)

1.3.3 Non-cellulosic/non-pectic polysaccharides

Non-cellulosic polysaccharides (also known as hemicellulose) represent the remaining polysaccharides present in plant cell walls. These polysaccharides are responsible for cross-linking with cellulose to form a strong network. This group of polysaccharides includes; xylans, xyloglucans and mannans and are present in varying abundance in the cell walls of all terrestrial plants (Scheller and Ulvskov, 2010)

1.3.3.1 Heteroxylan

Heteroxylan (Xylan) is the main type of matrix polysaccharide in primary cell walls of monocotyledons and the secondary walls of dicotyledons and is a polymer of D-xylose (D-Xyl) connected via β(1-4) linkages (Fig 1.9). However *in muro* the xylan backbone is usually substituted in different ways depending on the species. Substitutions at *O*-2 and/or *O*-3 positions of the xylosyl backbone with α-arabinofuranosyl chain result in arabinoxylans (AX). An alternative substitution of α-glucosyluronic acid (sometimes methylated) results in glucuronoxylan (GX) and in some cases both substitutions can occur resulting in the nomenclature glucuronoarabinoxylans (GAX) (Fig 1.8) (Mazumder et al., 2012).

Xylan is a major component of both primary and secondary plant cell walls in monocot plants as AX and GAX. In dicots however, xylan is less abundant in the primary cell wall but still a major component in the secondary cell wall mostly in the form of GAX. It has been established that dicot xylans have unique sequences of glycosyl residues at their reducing ends required for xylan synthesis (Peña et al., 2007). In the secondary cell wall xylan is essential to the structure of xylem and is required to maintain shape and cope with water transportation via transpiration and the associated pressures. Xylan biosynthesis occurs mostly in the Golgi along with the addition of side chains (Rennie and Scheller, 2014). The enzymes associated with the synthesis of the xylan backbone are nominated as IRX9, IRX10 and IRX14. The addition of side chains to xylan have been shown to include; GUX1 and GUX2 which transfer glucuronic acid to the C-2 position of the xylosyl (Bromley et al., 2013), and glycosyl transferases which mediate the addition of arabinofuranose to the xylan backbone (Anders et al., 2012).

1.3.3.2 Xyloglucan

Xyloglucan is formed of a backbone of β(1-4) linked glucose like cellulose, however there is the addition of xylosyl residues attached at the *O*-6 position, hence the name xyloglucan (Fry, 1989) (Fig 1.10). The xylose residues can be further substituted with a galactose and occasionally by a fructose residue. The glucan backbone of xyloglucan forms hydrogen bonds with the cellulose microfibrils as well as forming covalent bonds to pectic polysaccharides and thus linking the pectin matrix with the cellulose microfibrils (Park and Cosgrove, 2015).

This polysaccharide is present in the cell walls for all land plants and plays a role in many cell functions including cell elongation regulation (Pauly et al., 2001), structural functions (Anderson et al., 2010) and energy storage in tamarind seeds (Meier and Reid, 1982, Edwards et al., 1988). The synthesis of xyloglucan is restricted to the Golgi and is deposited early on in cell wall formation (Moore and Staehelin, 1988)

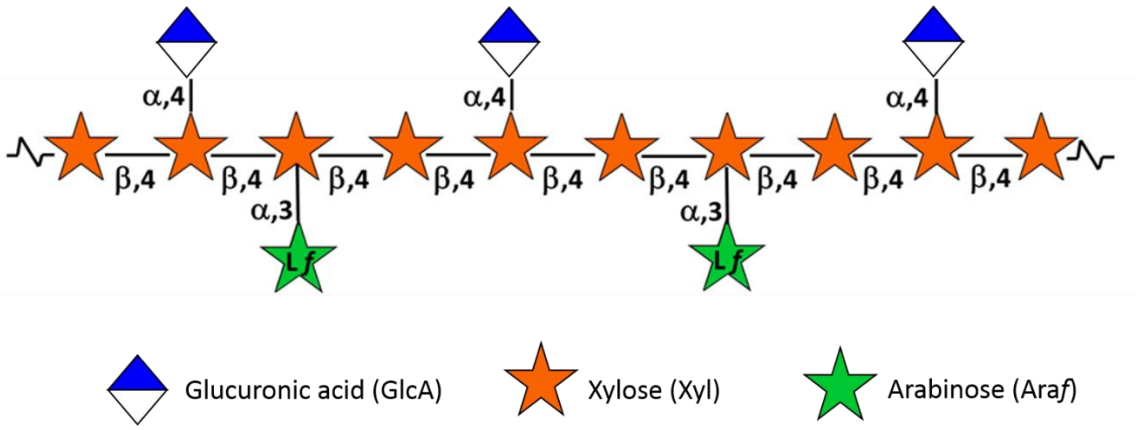

Figure 1.9 Structure of heteroxylan. Schematic of xylan structure and the associated substitutions which result in glucuronoxylan (GX), arabinoxylan (AX) and glucuronoarabinoxylan (GAX). Adapted from (Joseleau and Perez, 2017)

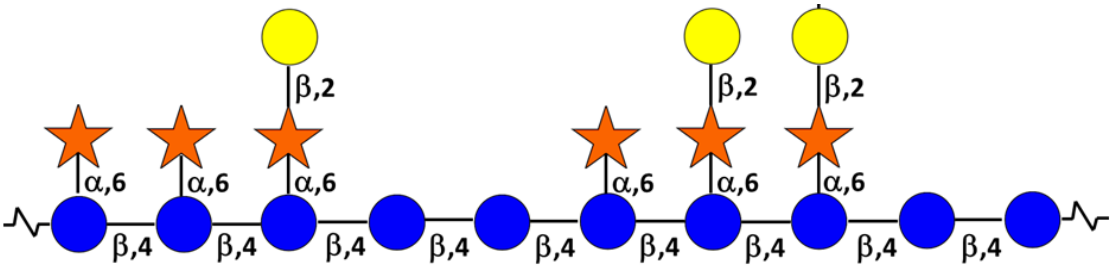

Figure 1.10 Structure of xyloglucan. Xyloglucan has a backbone of glucose (blue circles) substituted with xylose residues (orange stars). The xylose can be further substituted with galactose residues (yellow circles) and a fructose residue (red triangle). Adapted from (Joseleau and Perez, 2017)

1.3.3.3 Heteromannan

The mannan backbone is usually formed of β(1,4) linked mannosyl residues with α(1,6) galactosyl side chains (galactomannan) (Fig 1.11). However, mannans with a back bone containing glucosyl as well as mannosyl residues are referred to as glucomannans or galactoglucomannans if these also have galactosyl substitutions (Fig 1.11)

Mannans are commonly found in high abundance in the cell walls of early land plants including mosses and Charophytes (Pauly and Keegstra, 2008). Mannans are less abundant in the angiosperms where they have been replaced by other non-cellulosic polysaccharides through evolution. However, they have been in some dicot species (Scheller and Ulvskov, 2010, Rodríguez-Gacio et al., 2012). Mannans have been reported to be involved in oligosaccharide signalling and cell elongation (Hernandez-Gomez et al., 2015)

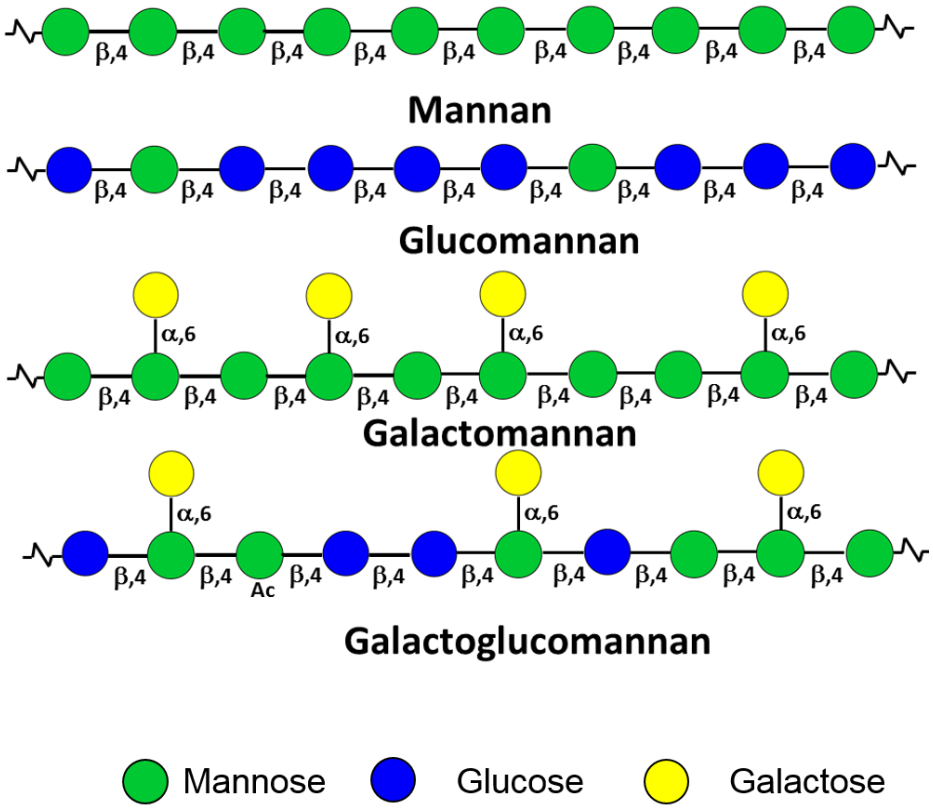

Figure 1.11 Structure of heteromannan. The structure of heteromannan varies, mannan has a back bone composed solely of mannose whereas glucomannan has some mannose replaced with glucose. When these backbones are substituted with a galactose residue on the mannose subunits they are known as galactomannan and galactoglucomannan respectively. Adapted from (Joseleau and Perez, 2017)

1.3.4 Cell wall proteins

In addition to polysaccharides plant cell walls contain proteins. These can have structural functions or be enzymes (Lamport, 1966). These proteins have various functions in cell wall architecture, signalling and defence (Showalter, 1993). Most of these proteins are only expressed in response to specific stimuli such as wounding and have been found to have specific spatial variations. The cell wall proteins are classified into groups according to their amino acid sequences; glycine-rich proteins (GRPs), proline-rich proteins (PRPs) and hydroxyproline-rich proteins (HRGPs). Some cell wall proteins are referred to arabinogalactan-protein to reflect their glycosylation and this group contains both PRPs and HRGPs.

1.3.4.1 Arabinogalactan-proteins

Arabinogalactan-proteins (AGPs) have a relatively low protein content compared to the glycan portion of the molecule with the ratio being about 10% protein (rich in hydroproline) to 90% glycan. The key characteristics of AGPs have been collected in a list by Lamport et al. (2014). According to this list AGPs are usually about 120 kDa in size, with 87 to 739 amino acids. The majority of AGPs (80%) are localised in the cell wall with the remaining 20% at the plasma membrane. The glycan portion of the AGPs are highly variable indicating that the composition of the glycan reflects it function. They have roles in various functions including, cell differentiation and tissue development, they are expressed in large amounts in response to wounding as well as having a role in plant-pathogen interactions (Fincher et al., 1983, Showalter, 2001).

1.3.4.2 Extensins

Extensins are specific type of HRGP which are highly conserved throughout the plant kingdom (Lamport, 1966). As their name would suggest extensins are thought to be one of the key components involved cell extension as they are known to have a role in wall rigidity (Cosgrove, 2000). It has also been demonstrated that extensins respond to stress such as wounding, pathogen attack and water deficiency by becoming insoluble (Showalter, 1993).

1.4 Sugar beet root cell walls

The cell wall components of the Amaranthaceae family, and sugar beet specifically, exhibit differences in abundance, ratios and substitutions thereof to other plant species, with sugar beet pectin exhibiting several differing structural characteristics (Fig 1.8) (Ralet et al., 2003).

Sugar beet cell walls contain feruloylated arabinose and galactose pectic side chains (Ralet et al., 1994). Feruloylation occurs on the O-2 of arabinose residues attached to the backbone of α(1-5) linked arabinan chains and the O-6 of galactose residues attached to the backbone of β(1-4) linked galactan chains (Colquhoun et al., 1994, Oosterveld et al., 2000). *In muro* ferulate monomers couple to form dehydrodimers or cyclodimers (Oosterveld et al., 1997) enabling covalent cross linkages between polysaccharide chains within the plant cell walls to form via diferulate bridges (Levigne et al., 2004a, Saulnier and Thibault, 1999). These cross-linkages dramatically alter the mechanical properties of the cell wall and have been known to decrease digestibility by bacterial and fungal enzymes. However reduction of this key cross-linkage could have impacts on cell wall strength and therefore in field and harvest performance.

It has been shown that the release of these ferulic acids greatly increases the degradation of arabinoxylans by xylanases in grasses (Kroon et al., 1999a, Molinari et al., 2013), however, the effect of ferulic acid removal from pectin has on the digestibility of sugar beet cell walls is undemonstrated. Therefore, the ferulic acids are of interest to the biofuel industry as a potential target to improve the application of sugar beet pulp as a feedstock (Levigne et al 2004).

Acetylation of pectin in the sugar beet occurs abundantly on HG, whereas in the cell walls of most other plant species acetylation is mostly concentrated on the RGI backbone (Bonnin et al., 2002a, Ralet et al., 2005, Fares et al., 2001). Acetylation occurs on galacturonic acid (GalA) groups, 90% of which in sugar beet are HG derived with only the remaining 10% associated with RGI (Rombouts and Thibault, 1986). Reduced acetylation of beet pectin would significantly improve applications for the food industry, such as for gelling and emulsification properties. In comparison to other species used for cell wall research sugar beet have a relatively large percentage of pectin (Huang et al., 2017, Ma et al., 2013)

and therefore can be used as an abundant source of pectin for research; however structural differences between species should be noted.

There is some debate over the abundance levels of xyloglucan in sugar beet pulp, Oosterveld et al. (2000) extracted xyloglucans from sugar beet pulp and characterised the xyloglucan similar to that of apple xyloglucans in terms of substitution with Fructose (Fuc) and Galactose (Gal). However this study disagreed with Renard and Jarvis (1999) who concluded that the amounts of xyloglucan are insufficient for them to have a significant role in the architecture of the sugar beet cell walls.

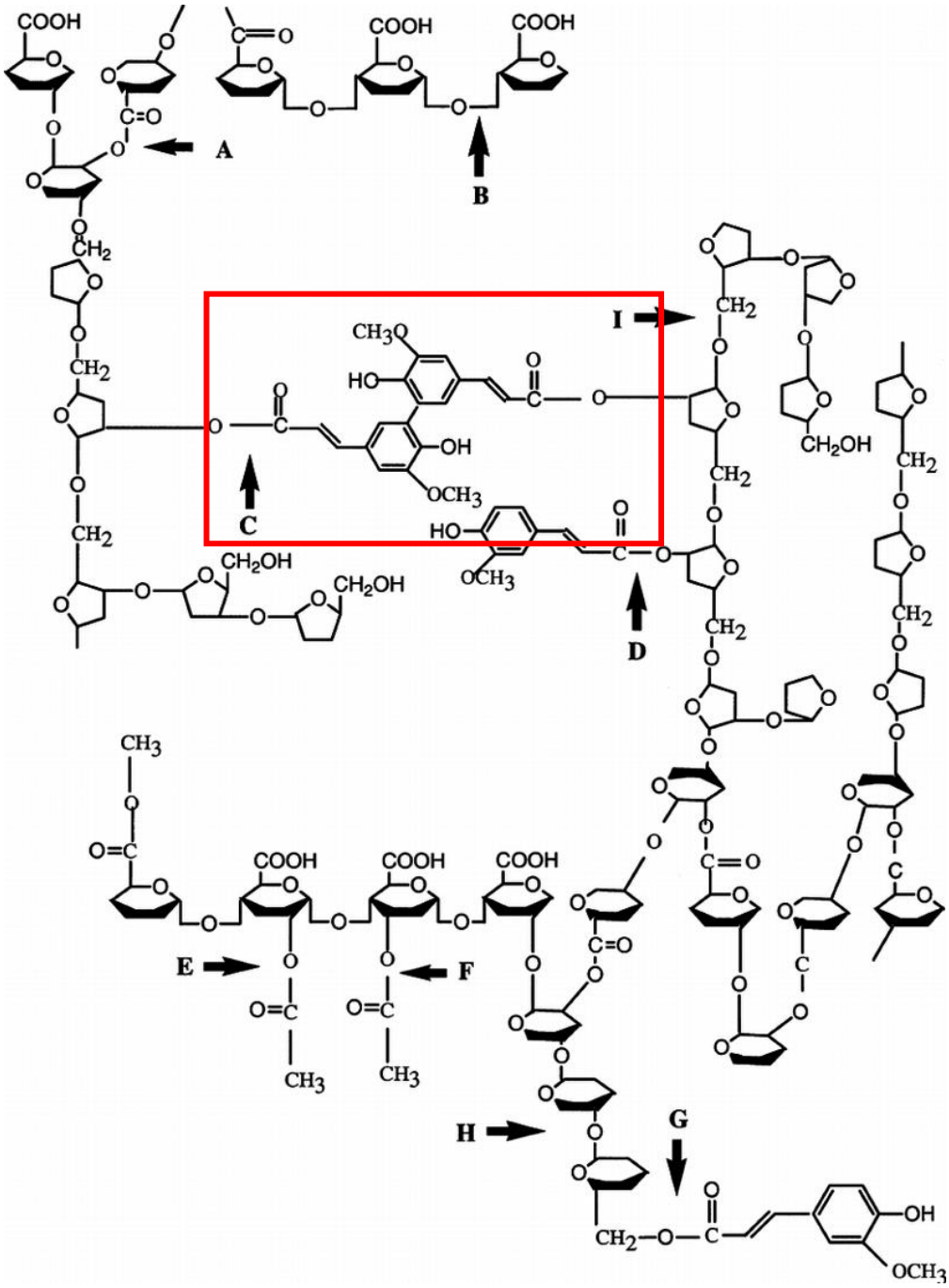

Figure 1.12. Sugar beet pectin. Generalised structure of sugar beet pectin. A, Backbone of alternating residues of Galacturonic acid and Rhamnose (RGI), B, α -(1-4) linked galacturonic acid residues (HG), C, Diferuloyl group attached to C-2 of arabinose, indicated by the red box an example of a diferulate bridge linking polysaccharides, D: Feruloyl group attached to C-2 of arabinose, E: 2-O-acetyl group, F: 3-O-acetyl group, G: Feruloyl group attached to C-6 of galactose, H: β -(1-4) linked galactose, I: α -(1,5) linked arabinan chains. (Mathew and Emilia Abraham, 2004)

1.5 Studying plant cell walls

Studying the architecture and composition of the plant cell wall polysaccharides requires several differing techniques based on the specific information required. A combination of methodologies is usually required to construct a meaningful interpretation of the composition of discrete cell wall components and their impact relative to the cell wall as a whole.

To identify the monosaccharide composition and linkage within a component of the cell wall a combination of techniques can be used. For example, by coupling gas chromatography and mass spectrometry (GC/MS) it is possible to quantify and identify the monomers which make up the polymer (Pettolino et al., 2012). Additionally, chemical structures can be deduced using Fourier Transformed Infra-Red Spectroscopy (FTIR) and Nuclear Magnetic resonance (NMR) (Him et al., 2001, Thomas et al., 2013).

To understand the molecular linkages between components of the cell wall it is possible to use specific enzymatic action to degrade plant materials at selected sites. Using analytic techniques such as polysaccharide gel electrophoresis (PACE) or High Pressure Liquid Chromatography (HPLC) on the degraded plant material can identify the oligosaccharides which make up the plant cell walls (Goubet et al., 2002).

Knowledge on the composition and interactions of the cell wall sometimes requires the analysis of the plant material without the complete destruction of the polysaccharides. Monoclonal antibodies (mAbs) are a powerful tool to analyse the composition of the plant cell wall (Knox et al., 1990b, Pattathil et al., 2010) . Highly specific sets of mAbs have been produced directed to a large array of cell wall polysaccharides (Andersen et al., 2016, Verhertbruggen et al., 2009b, McCartney et al., 2005b, Verhertbruggen et al., 2009a). These mAbs can be used on fixed and sectioned plant material to image the cell wall glycans *in situ* using fluorescence and electron microscopy to identify tissue locate cell wall polysaccharides (Jones et al., 2003, Marcus et al., 2008). In addition, these can be used in combination with other techniques to quantify cell wall polysaccharides using ELISA techniques, or to identify the interactions between different polysaccharides *in muro*. A recently developed technique termed, Epitope

Detection Chromatography (EDC) utilises the sensitivity of mAbs and the separating power of anion exchange chromatography to identify epitopes of cell wall polysaccharides and indicate interactions occurring within the cell wall structure (Cornuault et al., 2014).

1.6 Project aims and objectives

Knowledge of the sugar beet root cell wall composition is a driving power for the improvement of this important commercial crop. The plant cell wall dictates the overall structure and characteristics of the sugar beet root down to a cellular level, meaning that the cell wall influences how well the crop performs during both growth in the field and processing at the factory. The cell wall structure in specific tissues and cells within the root contributes to the sucrose accumulation within the cells of the root, with the anatomy and relative positioning of cell types playing a part in the potential sucrose yield.

Understanding the properties and structure of sugar beet cell walls is also key in identifying the alternative uses for the abundant sugar beet pulp available. Sugar beet pulp is comprised of up to 30% pectin (Levigne et al., 2002) and is therefore a good resource of pectin for many industries. Pulp is also a source of agricultural cellulose, which is currently not being used to its full potential (Kumar et al., 2009). Sugar beet cell walls have been identified as a potential source of biofuels (Draycott, 2006a) for second generation production. To utilise this resource for secondary biofuel production an improved understanding of the biochemical interactions and fundamental biology controlling sugar beet cell wall composition will need to be obtained through careful and detailed analysis.

This project utilises monoclonal antibodies which have emerged as a powerful tool to detect the relative abundance of cell wall components including pectic elements and non-cellulosic polysaccharides (McCartney et al., 2005a). Increasing the initial sugar yield potential and the diversity of valuable co-products of sugar production has the potential improve the economic value of the sugar beet crop.

The main project objectives followed and described in this thesis were:

- The comparative analysis of three strategic *Beta vulgaris* lines through development, including cell wall composition and anatomical variances.
- Characterisation and use of a phloem specific monoclonal antibody to study the development and relative position of phloem vessels within the root anatomy of three *Beta vulgaris* lines.
- Identify variation in cell wall composition from a Recombinant Inbred Line of *Beta vulgaris*, to demonstrate a correlation with performance parameters and to identify candidate genetic regions for use in crop improvement.

Chapter 2

Materials and Methods

2.1 Plant materials

The plant materials used in this project were:

1. A commercial sugar beet variety, Sophia (KWS) (*Beta vulgaris* L. subsp. *vulgaris* var. *altissima*)
2. A seed parent sugar beet variety, C869 (*Beta vulgaris* L. subsp. *vulgaris* var. *altissima*)
3. A red garden beet variety, W357B (Beta vulgaris L. subsp. *vulgaris* var. *vulgaris*)
4. Garlic bulbs (*Allium sativum*)

For light and electron microscopy (Chapter 3 and Chapter 4) *Beta vulgaris* seeds (Sophia, W357B and C869) were steeped overnight in Thiram solution (22°C in darkness with gentle shaking) prior to sowing in compost (Levington's F2+sand) in greenhouses at Rothamsted Research. Greenhouse temperature was maintained at approximately 22°C with natural lighting. Sugar beet plants were harvested in triplicate at the appropriate developmental stage for the study. Plants were recorded and sample material was excised and fixed immediately as described below

In Chapter 4, sugar beet (Sophia) were grown in the greenhouses at the University of Leeds under the same growth conditions as above for light microscopy. Garlic bulbs, *Allium sativum,* were sourced locally for the EDC analysis.

A field plot of the commercial sugar beet variety, Sophia, was grown for cell wall analysis through development (Chapter 3). Sugar beet plants were grown from establishment through to vegetative maturity then overwintered for flowering and seed production at Rothamsted Research – Broom's Barn (Higham, Suffolk). This growth season was replicated with sowing occurring in April 2009, 2010 and 2011 with field management as a commercial crop with appropriate applications of fertilisers, pesticides, fungicides and irrigation. Six individual roots were harvested and processed at throughout the growing seasons beginning at seedling development (4WAE) followed by two harvests at 3 week intervals which incorporated rapid root expansion (harvest 2 and 3). The next 10 harvests were taken at 4 week intervals until the final 3 harvest which were timed to correspond

with developmental points, early bolting, late bolting and flowering. At each harvest three biological replicates were taken.

A population of recombinant inbred lines (RIL) were developed by J. Mitchell McGrath of the USDA Sugar beet and bean research unit. The population was derived from a cross between a USDA sugar beet breeding line (C869) and a garden beet (W357B) via single seed descent (McGrath et al., 2005) .Seed of the F_7 generation were kindly provided for this study by J. Mitchell McGrath. Field grown plants were grown for the recombinant inbred lines (RIL) study (Chapter 5) at Rothamsted Research – Brooms Barn and subject to appropriate agricultural practises. 172 sugar beet RILs, the parent C869 (C), the parent W (a red garden beet, W357B) and the commercial variety Sophie (S) as an independent control were grown in a randomised block design with 400 plots in total. Six plants were grown per plot, and the two central plants were taken for measurement as technical replicates. Biological replication of the RILs was afforded by an independent plot of each RIL per block.

2.1.1 Preparation of cell wall materials

For the study of cell wall components by enzyme linked immunosorbent assay (ELISA) and epitope chromatography (EDC) plant material was collected frozen in liquid nitrogen, freeze dried and lysed using a TissueLyser LT (Qiagen).

Alternatively plant material for RIL analysis was collected coarsely cut using a food processor, frozen in liquid nitrogen and freeze dried. These were powdered using a Genogrinder (SpexPrep) for 90 seconds at 1500 rpm with three 9.5 mm steel balls, freeze dried again, and further powdered with a coffee grinder and sieved to a uniform 150-250 microns.

Garlic bulb material (25 g) was prepared by chopping a garlic bulb into small pieces which were frozen and freeze dried. This material was then ground to a powder using a TissueLyser (Qiagen, http://qiagen.com) for 10 min at 50 oscillations s^{-1}.

2.1.1.1 Preparation of alcohol insoluble residue

Plant samples prepared into powder as above were washed with 70% (v/v) ethanol for 1 h at room temperature (RT) with rocking, the pellet was collected by centrifugation (10 min at 1300 x g) and supernatant removed and discarded. The pellet was then subjected to successive washes with 80%, 90% and 100% (v/v) ethanol. Then the resulting pellet was washed with 100% acetone followed by methanol: chloroform (2:3 v/v) to produce an alcohol insoluble residue (AIR) pellet which was air dried overnight under a fume hood.

2.1.1.2 Cell wall extractions

For ELISA analysis AIR powder (10 mg) was placed into Eppendorf tubes with two 5 mm diameter stainless steel balls and ground using the TissueLyser for 2 min at 50 oscillations s^{-1}, 2 ml of dH_2O was added to the tube and ground again in the TissueLyser for 20 min at the same speed. After centrifugation at 1300 x g for 10 min the supernatant was removed and the pellet re-suspended in 50 mM CDTA (cyclohexanediamine tetraacetic acid) for pectin extraction. Following lysing and centrifugation the final extraction with 4M KOH + 1% (w/v) $NaBH_4$ was collected in the same way. The resulting supernatant was neutralized with 80% acetic acid (v/v). All cell wall extracts were stored at -20°C.

To prepare a water extract for EDC freeze-dried garlic bulb material was ground to a powder using a TissueLyser (Qiagen, http://www.qiagen.com) for 10 min at 50 oscillations s-1 and the powder stored at -20˚C until use. The powder (15 mg) was used to produce AIR which was air-dried overnight. AIR (8 mg) was placed into Eppendorf tubes with two ball bearings and ground using the TissueLyser for 2 min at 50 oscillations s-1 followed by 2 ml of water in the TissueLyser for 20 min at the same speed. After centrifugation at 1300 x g for 10 min the supernatant was collected and used for analysis.

2.1.2 Preparation of plant materials for sectioning for light microscopy.

2.1.2.1 Resin embedding

For light microscopy excisions were made from 2 cm below the widest diameter of the root into 0.5 cm^3 blocks. Immediately after collection the blocks were submerged in 4% (v/v) paraformaldehyde in PEM buffer (0.1 M PIPES (piperazine - ethanesulfonic acid), 2 mM EGTA (ethylene glycol- tetraacetic acid), 2 mM $MgSO_4$) for 1 h at RT with vacuum infiltration.

For electron microscopy 16 week old sugar beet plants (Sophia variety) were harvested and the crown removed. Samples were taken from the widest part of the root, between the second and third cambial ring and trimmed to a maximum diameter of 6 mm and thickness of 200 µm ensuring that each sample contained both vascular and parenchyma regions. Samples were high pressure frozen using a Leica Microsystems EM HPM100 and stored in liquid nitrogen before freeze substitution using dry ethanol in a Leica Microsystems EM AFS. Following freeze substitution, samples were stored at -20°C for 24 h, then 4°C until resin infiltration. Samples were infiltrated with a dry ethanol: LR White resin series and polymerised under nitrogen at 60°C. 70 nm ultrathin sections were cut using a Leica Microsystems UC7 ultra microtome and collected on nickel grids coated with formvar and carbon.

2.1.2.2 Wax embedding

Excisions were made from 2 cm below the widest diameter; these 1 cm^3 blocks of root material were sliced transversely to roughly 2 mm thick blocks and fixed in PEM buffer (0.1M PIPES, 5mM EGTA, 2mM $MgSO_4$) containing 4% paraformaldehyde for 1 h at RT with an initial vacuum infiltration. Following this the sections were washed with phosphate-buffered saline (PBS) twice. After fixation the sections were dehydrated in an ethanol series of 30%, 50%, 70%, 90% and 97% ethanol, each at 4˚C for 30 min. Samples were then moved to 37˚C and allowed to warm. At 37˚C the sections were transferred into Steedmans wax and ethanol 1:1 and left at 37˚C O/N. The sections were transferred into 100% wax for 1 h (2x at 37˚C). The sections were then placed into sample moulds filled with molten wax (ensuring the sections are at the correct orientation) and left to

solidify at RT (12 h minimum). The sections were then cut to a thickness of 10 µm using a microtome and placed on poly-L-lysine coated microscope slides. The sections were then dewaxed and rehydrated through an ethanol series consisting of; 97% ethanol (3x 10 min), 90% ethanol (10 min), 50% ethanol (10 min), water (10 min), water (90 min) and immunolabelled as described below.

2.1.3 Calculation of sucrose concentrations for RIL study

The quantification of sucrose in RILs was conducted by Dr Belinda Townsend at Rothamsted research using an enzymatic method as described here (Spackman and Cobb, 2002).

2.2 Monoclonal antibodies

A range of monoclonal antibodies were used throughout this project (Table 2.1)

Table 2.1. List of monoclonal antibodies to cell wall polysaccharides

mAb	Specificity	Reference
Anti-Homogalacturonan		
LM18	Partially Me-homogalacturonan	(Verhertbruggen et al., 2009a)
LM19	Non-Me-homogalacturonan	(Verhertbruggen et al., 2009a)
JIM7	Partially Me-homogalacturonan	(Knox et al., 1990a)
JIM5	Partially Me-homogalacturonan	(Knox et al., 1990a)
Anti-Rhamnogalacturonan I		
LM5	β(1,4) galactan	(Jones et al., 1997)
LM6	α(1,5) arabinan	(Willats et al., 1998)
LM13	Linearised α(1,5) arabinan	(Moller et al., 2008)
LM16	Processed arabinan	(Verhertbruggen et al., 2009b)
LM9	Feruloylated β(1,4) galactan	(Clausen et al., 2004)
LM12	Feruloylated pectin	(Pedersen et al., 2012)
LM26	Phloem sieve elements	*****
LM6-M	α(1,5) arabinan	(Cornuault et al., 2017)
Anti-Xyloglucan		
LM15	XXXG motif of xyloglucan	(Marcus et al., 2008)
LM25	Galactosylated xyloglucan	(Pedersen et al., 2012)
Anti- Xylan		
LM10	(1,4)-β-D-xylan	(McCartney et al., 2005b)
LM11	(1,4)-β-D-xylan/arabinoxylan	(McCartney et al., 2005b)
LM28	Glucoronoxylan	(Cornuault et al., 2015)
Anti-mannan		
LM21	Heteromannan	(Marcus et al., 2010)
Anti-AGP		
LM2	β-linked-GlcA in AGP glycan	(Yates et al., 1996)
JIM4	AGP glycan	(Knox et al., 1989)
JIM13	AGP glycan	(Knox et al., 1991)
JIM16	AGP glycan	(Knox et al., 1991)
Anti-Extensin		
LM1	Extensin	(Smallwood et al., 1995)
JIM20	Extensin	(Smallwood et al., 1994)

*LM26 is an unpublished monoclonal antibody which has been characterised during this project. The LM26 rat hybridoma cell line was isolated from a screen

of cell lines derived subsequent to immunizations that led to the isolation of the pectic homogalacturonan MAb LM7 (Willats et al. 2001). It was cloned by standard limiting dilution procedures as described (Willats et al. 2001). The isotype of LM26 is rat IgG1 and in all analyses it was used in the form of un-purified hybridoma cell culture supernatant. This work was conducted by Sue Marcus (University of Leeds)

2.3 Immunolabeling of plant material for microscopy

2.3.1 Indirect immunofluorescence labelling for light microscopy

Wax-embedded sections were used for developmental studies. Wax sections were prepared on to glass slides using a microtome followed by a dewaxing procedure were the slides were immersed in 100% (v/v) ethanol, then rehydrated in dilutions of ethanol, 90% (v/v), 70% (v/v), 50% (v/v), 30% (v/v), 100% dH2O. Resin embedded sections were sectioned using an ultramicrotome onto Vectabond coated glass slides and did not require rehydration before use.

Resin and wax embedded samples were prepared the same way for light microscopy detection of cell wall epitopes. Slides were blocked with PBS with 5% (w/v) milk protein was added at RT for 30 min. Primary antibodies were added at a 1:5 dilution in 5% milk/PBS for 90 min. Following a wash with PBS, anti-rat FITC (anti-rat IgG linked to fluorescein isothiocyanate) was added as a secondary antibody at a 1:100 dilution in 5% milk/PBS for 60 min. Calcofluor White (Sigma-Alderich) was added at 0.02 mg/ml in PBS for 5 min to stain cellulose in all cell walls. Toluidine Blue O (TBO) 1% (w/v) was added for 2 min to remove auto-fluorescence and excess was thoroughly washed with PBS. Anti-fade reagent Citifluor glycerol/PBS (Agar scientific) was added before a coverslip was placed. Slides were stored at 4°C in the dark prior to analysis.

Microscopy imaging was performed using an Olympus BX61 microscope with epifluorescence irradiation. Images were captured using a Hamamatsu ORCA285 camera and Velocity software (PerkinElmer). Micrographs for comparative analysis were captured using calibrated settings and processed in an equivalent manner.

2.3.2 Immunogold labelling for TEM

Nickel grids containing ultra-thin sections were blocked with 1% BSA in 0.01M PBS-tween, 30 min. After blocking, sections were incubated with the LM26 monoclonal antibody (undiluted), 60 min at 37°C and blocked again for 30 min. The grids were then labelled with a secondary goat polyclonal antibody to rat IgG conjugated to 10 nm gold particles (1:10 dilution in PBS, Sigma), for 60 min at

37°C. The grids were then washed thoroughly with PBS-Tween and then dH_2O before staining. The sections were post stained with uranyl acetate, 15 min and lead citrate, 2 min to increase contrast. Images were obtained using a JEOL 2011 transmission electron microscope at 200kV and a Gatan Ultrascan CCD camera. This work was conducted by Rebecca Lauder (Rothamsted Research).

2.4 Monoclonal antibody characterisation

2.4.1 Carbohydrate microarrays of polysaccharides for epitope characterisation

Glycan synthesis has been previously described (Andersen et al., 2016b, Pedersen et al., 2012). Carbohydrate screening was performed as described (Andersen et al., 2016a, Andersen et al., 2016b). In brief, functionalised oligosaccharides were printed onto NHS-activated Slide-H microarrays (Schott, Mainz, Germany) using the ArrayJet Sprint microarray printer (ArrayJet, Roslin, UK). The microarrays were blocked with 50 mM ethanolamine in 50 mM sodium phosphate buffer pH 9.2. After blocking the slides were covered with the antibodies LM5 or LM26 at a 1:100 dilution of hybridoma supernatant in PBS for 2 h. Mab binding was detected using the AlexaFluor 488 goat anti-rat IgG antibody (ThermoFisher Scientific, Waltham, USA) at a 1:500 dilution in PBS for 2 h. Microarrays were scanned with a GenePix 4400A microarray scanner and quantified using Array-Pro Analyser 6.3 (Media Cybernetics, Rockville, USA). This work was conducted at the Technical University of Denmark by Mads Clausen.

2.5 *In vitro* analysis of monoclonal antibody binding

2.5.1 Enzyme linked immunosorbent assay (ELISA)

ELISAs were performed using 96-well microtitre plates Nunc, Fisher Scientific, Denmark). Firstly, these were coated O/N (4˚C) with up to 50 µg/ml of antigen in PBS, 100 µl per well. Plates were washed with tap water 3x. A blocking solution of 5% Milk/PBS (200 µl per well) was added for 2 h at RT. After vigorous washing (9X with tap water) the primary antibody was added at a dilution of 1 in 10 in 5% Milk/PBS (100 µl per well). After an hour incubation the plates were washed vigorously with tap water (9X) and the secondary antibody, anti-rat IgG HRP, (100 µl per well of 1 in 1000 dilution with 5% Milk/PBS) was added for an hour. The plates were washed thoroughly and antibody binding was detected with the addition of the HRP substrate (18 ml water, 2 ml 1 M sodium acetate buffer pH 6.0, 200 µl tetramethyl benzidine, 20 µl 6% hydrogen peroxide). After 5 minutes the reaction was stopped by the addition of 2.5 M sulphuric acid. The absorbance at 450 nm was read on the Thermo scientific Multiscan FC ELISA reader.

2.5.2 Comprehensive microarray polymer profiling (CoMPP) for high throughout analysis of cell wall polysaccharides.

CoMPP was used to identify cell wall polysaccharides at the University of Copenhagen. Samples were prepared as AIR and initially extracted with 50 mM CDTA (diamino-cyclohexane-tetraacetic acid) at 300 µl/10 mg of sample. A glass bead was added to each tube and shaken for 2 min at 30 oscillations/s followed by 120 min at 6 oscillations/s using a Qiagen TissueLyser II. Samples were then centrifuged for 10 min at 2700 g and supernatant removed and kept for analysis. The pellet was then re-suspended in 300 µl/10 mg of 4 M NaOH (+ 0.1% $NaBH_4$) and shaken then centrifuged as before. The supernatant was collected from this extraction and kept for analysis.

Both the CDTA and NaOH extractions were pipetted onto 128 well plates, diluted 50% (v/v) with ArrayJet buffer (46% glycerol (v/v), 1.4% 69.5 mM Triton X (v/v)) then with three further serial dilutions of 1:5. The plates were and placed into an ArrayJet Sprint microarray printer (ArrayJet, Roslin, UK) O/N for printing onto

nitrocellulose sheets. Nitrocellulose sheets were blocked with 5% milk/PBS and then incubated with primary monoclonal antibodies at 1:10 dilution in 5% milk/PBS with shaking for 2 h. These were thoroughly washed with PBS and incubated with the secondary antibody, alkaline phosphatases anti-rat, at 1:5000 dilution in 5% milk/PBS with shaking for 2 h. The nitrocellulose was rinsed thoroughly with PBS then rinsed in dH_2O. The nitrocellulose was developed using the development solution (10 mL AP buffer (100 mM NaCl, 5 mM $MgCl_2$ and 100 mM Tris-HCl), 82.5 µl BCIP and 66 µl NBT) for 2-10 min until dot are visible, these were then washed in dH_2O to stop over development. After drying O/N the nitrocellulose were scanned using a flatbed scanner and the spots analysed using ArcSoft PhotoStudio and Array-Pro Analyser software where spot density is calculated.

CoMPP analysis for developmental study in Chapter 3 was conducted by Julia Schückel (University of Copenhagen).

2.5.3 Epitope detection chromatography (EDC)

12 µl aliquots of the garlic bulb water extract (diluted in 2.5 ml of 20 mM sodium acetate buffer, pH 4.5) was injected into an anion-exchange column (1 ml Hi-Trap ANX FF, GE Healthcare) using a Bio-Rad BioLogic LP system. A step elution gradient was used as follows: 20 mM sodium acetate buffer, pH 4.5 at a flow rate of 1 ml/min from 0-20 min with a step change to 20% 0.6 M NaCl at 20 min. Followed by step increases of 0.6 M NaCl at 30 min to 20%, 40 min to 30%, 50 min to 40% and 60 min to 100%. Ninety-six 1 ml fractions were collected. The collected fractions were adjusted to pH 7 by adding 50 µl of 1 M Na_2CO_3 before 100 µl of each fraction were incubated overnight at 4˚C in microtitre plates for detection with mAbs using ELISA. For pre-treatment with sodium carbonate the aliquots of water extract were mixed with an equal volume of 0.1 M sodium carbonate and left at room temperature for 3 h prior to EDC analysis.

2.6 Data handling

Analysis of CoMPP data for the field development in Chapter 3 was conducted using a programme developed at the University of Copenhagen where data was normalised and ranked based on density with the highest density assigned 100. Densities below 5 were removed and shown as 0. This analysis was completed by Julia Schückel (University of Copenhagen) according to methods described in Sørensen and Willats (2011) and (Moller et al., 2007)

For the analysis of RIL samples, the CoMPP data was used as raw density values. Principal coordinates analysis (PCO) were applied to the data for each of the monoclonal antibodies and extracts plus the physiological trait data was included: fresh root weight (g), average root diameter (cm), % dry matter, root dry weight (g), % sucrose of dry matter, % sucrose of fresh weight and sugar yield (kg/ha). This work was conducted by Stephen Powers (Rothamsted Research) using The GenStat statistical package (2014, 17th edition, © VSN International Ltd., Hemel Hempstead, UK).

Chapter 3

Sugar beet storage root anatomy and cell wall composition through development

3.1 Introduction

The internal anatomy of sugar beet storage roots have not been studied in detail for many decades with Artschwager (1926) detailing the internal anatomy of mature sugar beet storage roots with a few observations from young seedlings . These anatomical studies outlined the relative positioning of the cambial rings describing these as being “more or less equidistant” with the rings often not comprising of a complete ring. This study utilised staining practises in combination with light microscopy and many observations were recorded with hand drawings. Shortly after these the studies the scientific papers that followed focused on physiological development field studies in relation to root growth (Milford, 1973), sucrose accumulation (Watson and Baptiste, 1938, Watson and Selman, 1938, Giaquinta, 1979), fertilisation (Brentrup et al., 2001, Hergert, 2010), crop protection (Esau and Hoefert, 1972, Williams and Asher, 1996) and weather variables (Ulrich, 1952, Kenter et al., 2006) as the crop became more economically important

For the purpose of this project it was important to produce a detailed anatomical study of the internal anatomy of young sugar beet seedlings. Focusing on the development of young seedlings allows identification of when the successive cambia development begins and how this can impact sucrose accumulation and downstream processing of mature sugar beet roots. In this study three *Beta vulgaris* lines were selected with differing sucrose concentrations; Sophia KWS, a commercial sugar beet variety (KWS, 2011), C869, a sugar beet seed parent line and W357B, a garden beet (McGrath et al., 2005). The work described in this chapter provides information on the sugar beet storage root anatomy and the formation of important tissues through development.

In this project there has been several approaches to widen understanding of sugar beet root development including; microscopy, immunochemistry and high throughput approaches. The information collected in this chapter has underpinned the work collated in the chapters following. Visualisation of the internal structures using histochemistry techniques combined with immunolabelling with monoclonal antibodies has provided a novel view of the

structures and anatomy of the roots, including the successive supernumerary cambia, a cambial formation limited to a few genera but is characteristic of *Beta vulgaris*. It has been previously identified that the sucrose content and sugar beet root yield are controlled by cambial formation and the distance between rings of vascular tissue is a key parameter involved in this control (Wyse, 1979). In addition to microscopy analysis a study of sugar beet cell wall composition throughout development has allowed the understanding of how storage root cell walls adapt and change in response to changing developmental, environmental and mechanical signals.

3.1.1 Sugar beet development

Sugar beet is a biennial with a two year development from germination to seed production. The vegetative phase (year 1) includes establishment and the main biomass production of the plant with this being the stage where most commercial crops are harvested. Year 2 is the reproductive phase which occurs following a period of vernalisation in the field during the winter months, this would only usually occur in sugar beet seed production.

Sugar beets emerge with two cotyledons which usually turn yellow and die upon the growth of the first two true leaves. During this period of canopy development photosynthate is utilised for new leaf production and rapid canopy growth starts after the production of the first six true leaves. Once the canopy closes light interception is at its maximum and from this stage energy from photosynthesis is stored in the root as sucrose for the next growing season. At the end of the vegetative stage the roots would be harvested before the sucrose is relocated to support the period of stem elongation and flower production during the second year of growth. Flowers reach anthesis five to six weeks after initiation of reproductive development and continues for several weeks. Pollen is transmitted from mature anthers mostly by wind.

Over the years there have been many improvements of how to assess the development stage of a sugar beet root. Due to the harvestable material being concealed underground it has been necessary to conclude the development of the root by the stage of the visible part of the crop, i.e. the leaves. Therefore most

scales for the identification infer root developmental stage from the development of the leaves. One example of such a scale is the BBCH-scale (Biologische Bundesanstalt, Bundessortenamt und CHemische Industrie) (Meier et al., 1993), this allows the identification of developmental stage of an individual plant by studying the leaf development and assigning a growth stage code to the plant. The scale begins at the different stages of germination: growth stage 0, with additional codes 0-9 depending on the stage of germination the seeds is currently at, for example when the radicle has emerged from the seed this is assigned the code 05. The growth stages included on this scale are; 0: Germination, 1: Leaf development (youth stage), 2: Rosette growth (crop cover), 3: Principal growth stage, 4: Development of harvestable vegetative plant parts, 5: Inflorescence emergence (2nd year of growth), 6: Flowering, 7: Development of fruit, 8: Ripening, 9: Senescence. A summary of this scale is shown in Fig. 3.1. This scale is especially useful when harvesting plants for experimental purposes that require roots of similar size/developmental stage, in this project work has mostly concentrated on the vegetative development of sugar beets with one exception in this chapter.

Sugar Beet Growth Stages

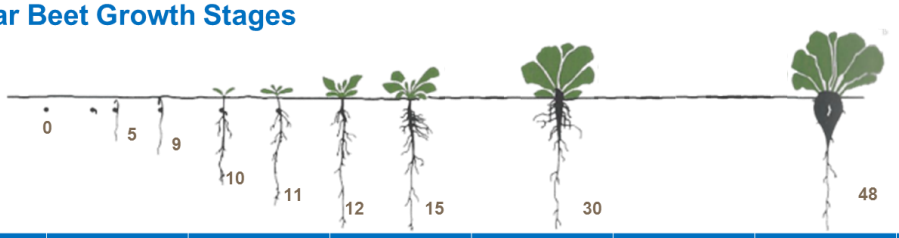

Growth Stage	Description of stage	Growth Stage	Description of stage	Growth Stage	Description of stage	Growth Stage	Description of stage
Germination		**Leaf Development (Youth stage)**		**Principal Growth Stage 3**		**Development of harvestable vegetative plant parts**	
00	Dry Seed	10	First leaf visible (pinhead-size): cotyledons horizontally unfolded	31	Beginning of crop cover: leaves cover 10% of ground	49	Beet root has reached harvestable size
01	Beginning of imbibition: seeds begins to take up water	11	First pair of leaves visible, not yet unfolded (pea-size)	33	Leaves cover 30% of ground		
03	Seed imbition complete (pellet cracked)	12	2 leaves (first pair of leaves) unfolded	39	Beet root has reached harvestable size		
05	Radicle emerged from seed (pellet)	14	4 leaves (2nd pair of leaves) unfolded				
07	Shoot emerged from seed (pellet)	15	5 leaves unfolded				
09	Emergence: shoot emerges through soil surface	19	9 and more leaves unfolded				

Figure 3.1 Summary of the BBCH-scale for sugar beet. The BBCH-scale showing the vegetative stages of sugar beet development and the associated development stages. Adapted from (Jensen and Spliid, 2003)

3.1.2 Supernumerary successive cambia

Successive cambia are responsible for the familiar concentric rings seen in beet species. The production of secondary phloem associated with secondary xylem in bands surrounded by conjunctive tissue are agreed to be the product of a successive cambium (Stevenson and Popham, 1973). This vascular plan where secondary growth occurs at more than one vascular cambium. The tell-tale ringed patterning can be seen in the stems and roots of several other well-known plant species, many being members of the Amaranthaceae family along with sugar beets. Well known genera which also have this successive cambial arrangement include *Amaranthus* (Bhambie and Sharma, 1985), *Chenopodium* (Fahn and Zimmermann, 1982), *Avicennia* (Robert et al., 2011) and surprisingly the gymnosperm, *Welwitshia* (Carlquist and Gowans, 1995). Terminology of this multiple cambia has in the past been an issue as the ontogeny and adaptive values of the successive cambia are unknown, however some studies have suggested that the distribution of phloem in this was play a role in survival in harsh environments (Robert et al., 2011). In this study Robert et al. (2011) observed that the majority of species with a successive cambial arrangement originate from dry or saline environments. This includes sugar beet having been selected from sea beets, *Beta vulgaris* subsp. *maritima* (Draycott, 2006b), which grow in coastal areas.

A series of stages of cell production are required for secondary vascular cambium to become differentiated from the master cambium (Carlquist, 2007). Differing from ‘interxylary phloem’ where a single cambium is present and secondary phloem are distributed within the secondary xylem, successive cambia results in secondary phloem external to secondary xylem separated by what is known as conjunctive tissue (Stevenson and Popham, 1973). This vascular growth is then repeated by individual cambia each separated by storage parenchyma producing rings of xylem and phloem associated with each cambia. This feature is of interest for crop improvement in sugar beet as this cambial arrangement could contribute to the root storing higher concentrations of sucrose in the roots. Having phloem dispersed throughout the root shortens diffusion pathways from phloem sieve

elements and storage tissue allowing more effective assimilation of sucrose (Giaquinta, 1979, Saftner et al., 1983, Wyse, 1979).

3.2 Materials and methods

Plants for the early development series for three *Beta vulgaris* were grown in 9 x 9 cm pots until cotyledons emerged and transferred to 9 L pots to allow root expansion. These plants were grown in green houses at Rothamsted Research (Harpenden, UK) and planted by Belinda Townsend on behalf of the author. Harvesting was conducted by the author and the samples were fixed at the time of harvest and transported to the University of Leeds where the samples were set in wax as described in chapter 2. Microscopy and further analysis of these samples was completed by the author.

Field development plants were grown and harvested by staff at Broom's barn. These samples were dried and ground to a powder and stored at Rothamsted research before being made available for the author for ELISA analysis as described in chapter 2. Weather data was collected at Brooms barn and graphical presentation produced by Aiming Qi.

CoMPP analysis in this chapter was completed by Julia Schückel at the University of Copenhagen and the raw data was provided to the author for tabulation and interpretation.

3.3 Results

3.3.1 Sugar beet storage roots have successive supernumerary cambia

To understand the details of the supernumerary cambia in mature sugar beet storage roots microscopy was used to form a compound image of the overall internal anatomy (Fig 3.2).

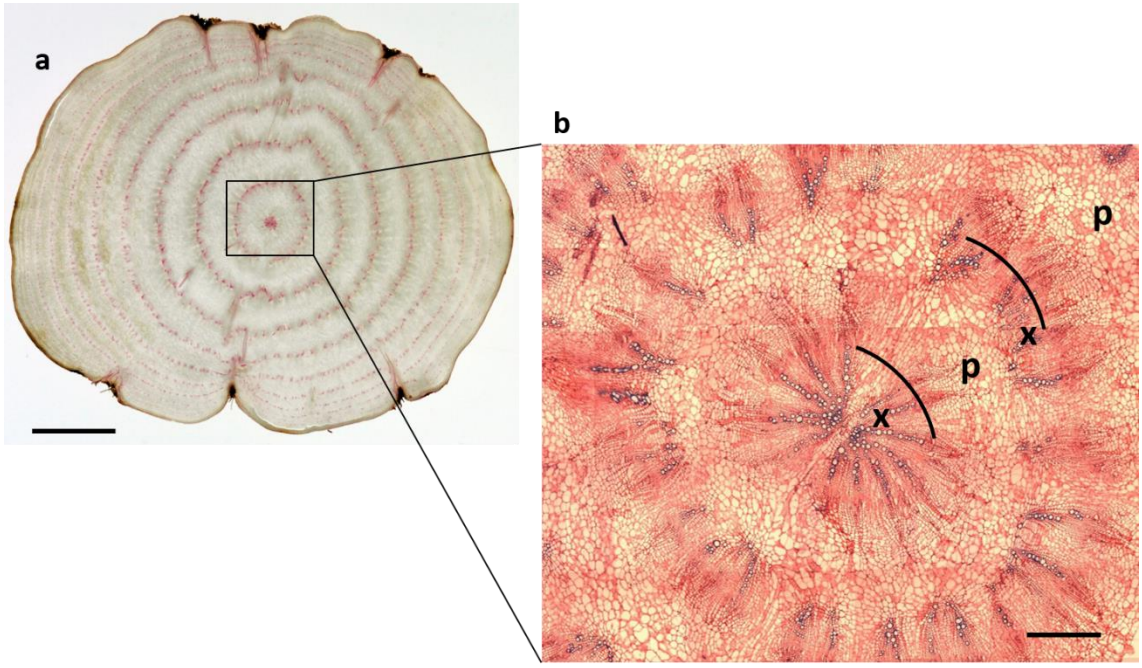

Figure 3.2 Structure of a sugar beet root in transverse sections. a; Transverse image of a topped mature sugar beet stained with phloroglucinol-HCl, xylem vessels (pink) indicate position of cambial rings. Black box indicates the relative position of section detailed in figure 3.1b. Scale bar = 5 cm b; Transverse image of mature sugar beet central stele, a composite of multiple bright field micrographs stained with Toluidine blue O to give an overview of cambial formation. x; xylem, easily identified by the secondary cell wall formation, p, parenchyma cells, identifiable by their comparatively large size. Black arcs detail hypothesised position of cambia. Scale bar = 100 µm

Initial studies of sugar beet storage roots clearly show that they have a specialised vascular system which give beets the familiar ringed pattern when they are topped (rosette and crown removed). This ringed pattern (Fig 3.1a) which can be seen with the naked eye in mature beets is the result of xylem vessels developing in concentric rings throughout the root. The development of the cambium throughout the root is not uniform through all regions of the root with areas where the cambium is more pronounced. When studied using bright field microscopy (Fig 3.1b) there is clear distinction between the rings of vascular tissue with bands of parenchyma between each consecutive ring. While it is clear by the secondary cell wall where xylem cells are located due to secondary cell wall thickening, the phloem cells are less easily identified. This is an issue for studying this species as it is commercially used to accumulate and store sucrose. It is clear that a tool is required to locate phloem cells in order to study the sugar beet vascular anatomy in more detail.

3.3.2 Development of the successive supernumerary cambia in sugar beet roots.

The three *Beta vulgaris* lines were harvested at 7 points throughout the early development; 1 week after emergence (WAE), 2 WAE, 3 WAE, 4 WAE, 6 WAE, 8 WAE and 10 WAE. Their developmental stages were recorded according to the BBCH-scale described in Figure 3.1. Table 3.1 outlines the conversion between WAE and BBCH-scale for each of the three lines.

Table 3.1 Conversion of developmental stage from WAE to BBCH-scale for three *Beta vulgaris* lines.

Weeks after emergence (WAE)	BBCH-scale		
	Sophia	C869	W357B
1	11	11	11
2	12	12	12
3	13	13	13
4	15	14	14
6	20	18	18
8	26	24	25
10	30	28	28

Initially the Sophia variety was used to study the cambial formation in sugar beet root as this has the most direct link to industrial applications. The focused study of the Sophia variety (Fig 3.3) shows the early stage development using the combination of fluorescence microscopy and a monoclonal antibody, LM11, which is specific to xylan which allows the *in situ* identification of the xylem vessels (McCartney et al., 2005). By tracking the very early stages of development, from one week after emergence (1WAE) through to ten weeks after emergence (10WAE), it has been possible to identify the development of new vasculature as well as development in terms of root diameter and inter ring-distance. At 1WAE primary xylem has developed and the cortical cells are still intact which is similar to 2WAE where there is increased primary growth and an increase in parenchyma between the vascular tissue and the endodermis. By 3WAE the secondary cambium develops in a similar way to the primary, at the pericycle, this development produces the second ring of vasculature outside the relative position of the initial primary cambium as there is now a band of parenchyma separating this new development and the initial vasculature. This process is repeated throughout the seedling development resulting in the concentric rings which make up the successive supernumerary cambia. As more rings are added the diameter of the root increases leading to the vasculature no longer creating complete rings but rather separating and forming in zones of vasculature radiating round the root at the same distance from the centre creating an interrupted ring. These interrupted rings can be seen at 6 WAE where the root has become so large that a singular zone of vasculature has been imaged as a representative for its given ring. These vascular rays continue to form at both the 8WAE and 10WAE stage where the ring number is at its maximum for this line. While the rings are being formed the parenchyma band between the rings also increases contributing to the overall increase in root diameter through development.

3.3.3 Comparison of different *Beta vulgaris* lines

There is an understanding that ring number and distance between the rings can be connected with root sucrose content (Wyse, 1979, Milford, 1973). In order to look into this hypothesis the same developmental investigation was undertaken

on two other *Beta* lines, W357B – a red garden beet and C869 – a sugar beet representative used for breeding studies (McGrath et al., 2005). The red garden beet is known to have a lower sucrose concentration than that of a sugar beet therefore it was necessary to study the internal anatomy of the storage roots of the W357B as a comparison to the Sophia line to investigate if the number of cambial rings is an indicator of sucrose content. In addition, Sophia is a commercial sugar beet, it is hypothesised that an increased cambial ring number contributes to increased sucrose content, therefore conducting the same analysis on a sugar beet line which is used as a parent line in breeding programmes rather than for sucrose production could indicate if this hypothesis is correct.

While the development of the additional cambial rings in the W375B (Fig 3.4) and C869 (Fig 3.5) storage roots is similar to that of the Sophia storage root (Fig 3.3), there are some differences. Due to the diameter of Sophia being much larger than the other two lines the xylem vessels are much more separated where only one cluster of xylem vessels can be viewed within the micrograph. In addition, the shape of the xylem clusters also differs between lines. Where the Sophia and C869 lines show extended rays of xylem vessels the W357B has much shorter clusters of relatively smaller xylem vessels. The binding patterning of LM11 in the C869 line differs from the other two lines with the cells between the large circular shaped xylem vessels also being bound by the LM11 antibody.

These comparative studies show in detail how cambial rings develop to give rise to the successive ring anatomy that is familiar in this genus. Cambial rings develop very early in development starting within three weeks after emergence of the cotyledons from the soil. The commercial variety Sophia develops more cambial rings than the lines with lower sucrose concentration and the xylem vessels become more spread out as the root develops.

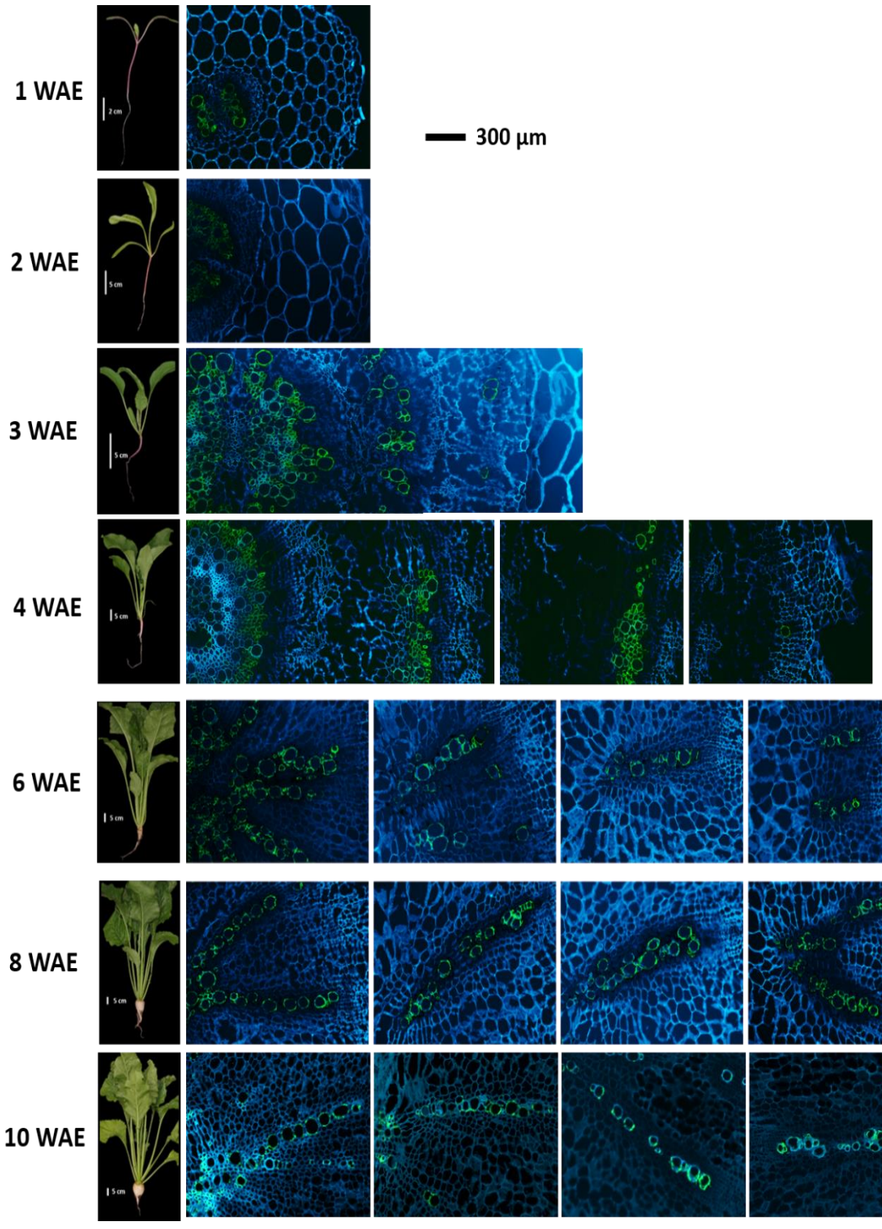

Figure 3.3 Seedling development of the *Beta vulgaris* line Sophia. Overall plant morphology and transverse sections (TS) showing development of the commercial variety Sophia from 1 week after emergence (WAE) through to 10 WAE. Gaps between micrographs indicate a section of parenchyma with no vasculature present. Xylem vessels are indicated in green by fluorescence microscopy using the monoclonal antibody LM11 which detects xylan. Calcofluor White (Blue) staining has been used to highlight all cell types.

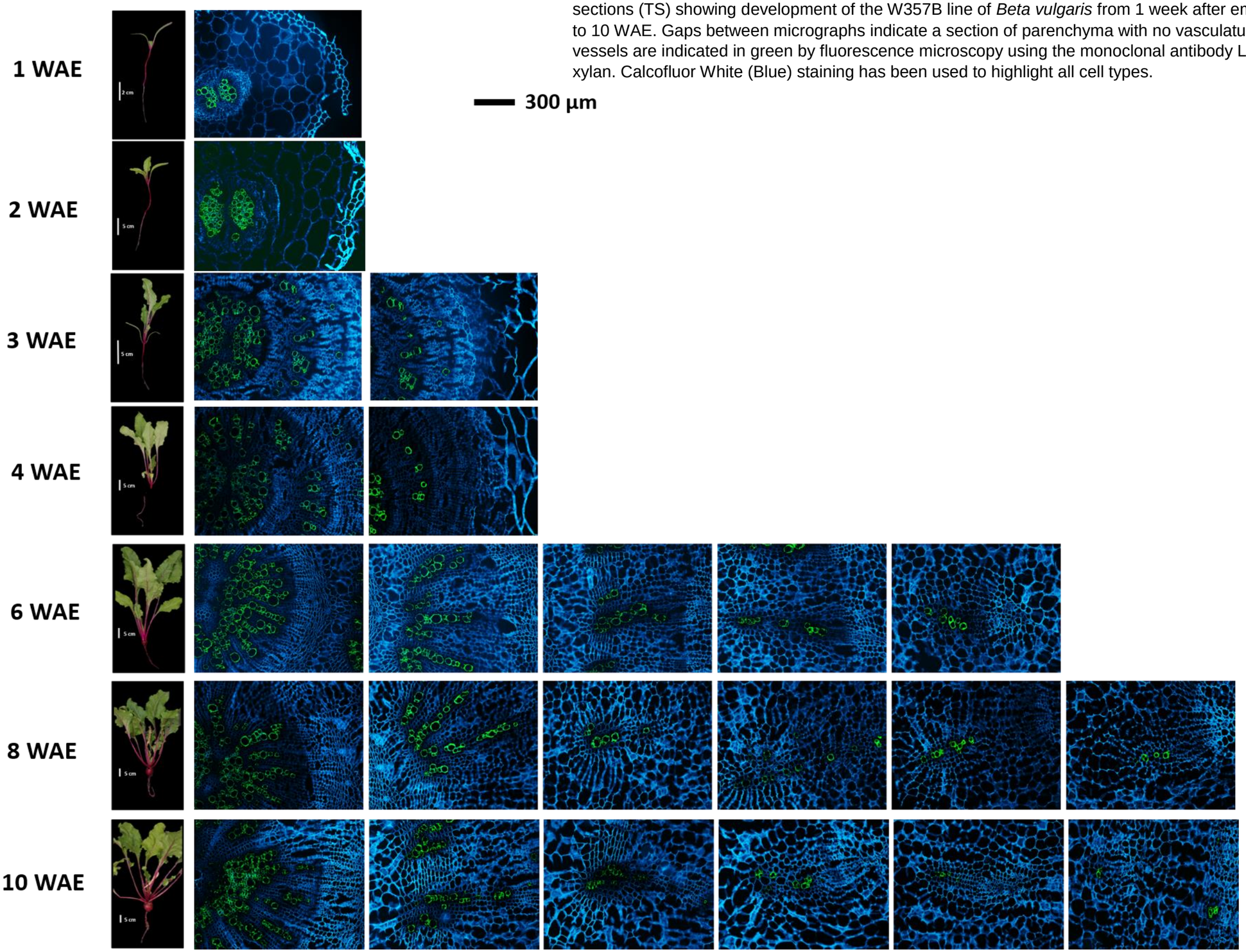

Figure 3.4 Seedling development of the *Beta vulgaris* line W357B. Overall plant morphology and transverse sections (TS) showing development of the W357B line of *Beta vulgaris* from 1 week after emergence (WAE) through to 10 WAE. Gaps between micrographs indicate a section of parenchyma with no vasculature present. Xylem vessels are indicated in green by fluorescence microscopy using the monoclonal antibody LM11 which identifies xylan. Calcofluor White (Blue) staining has been used to highlight all cell types.

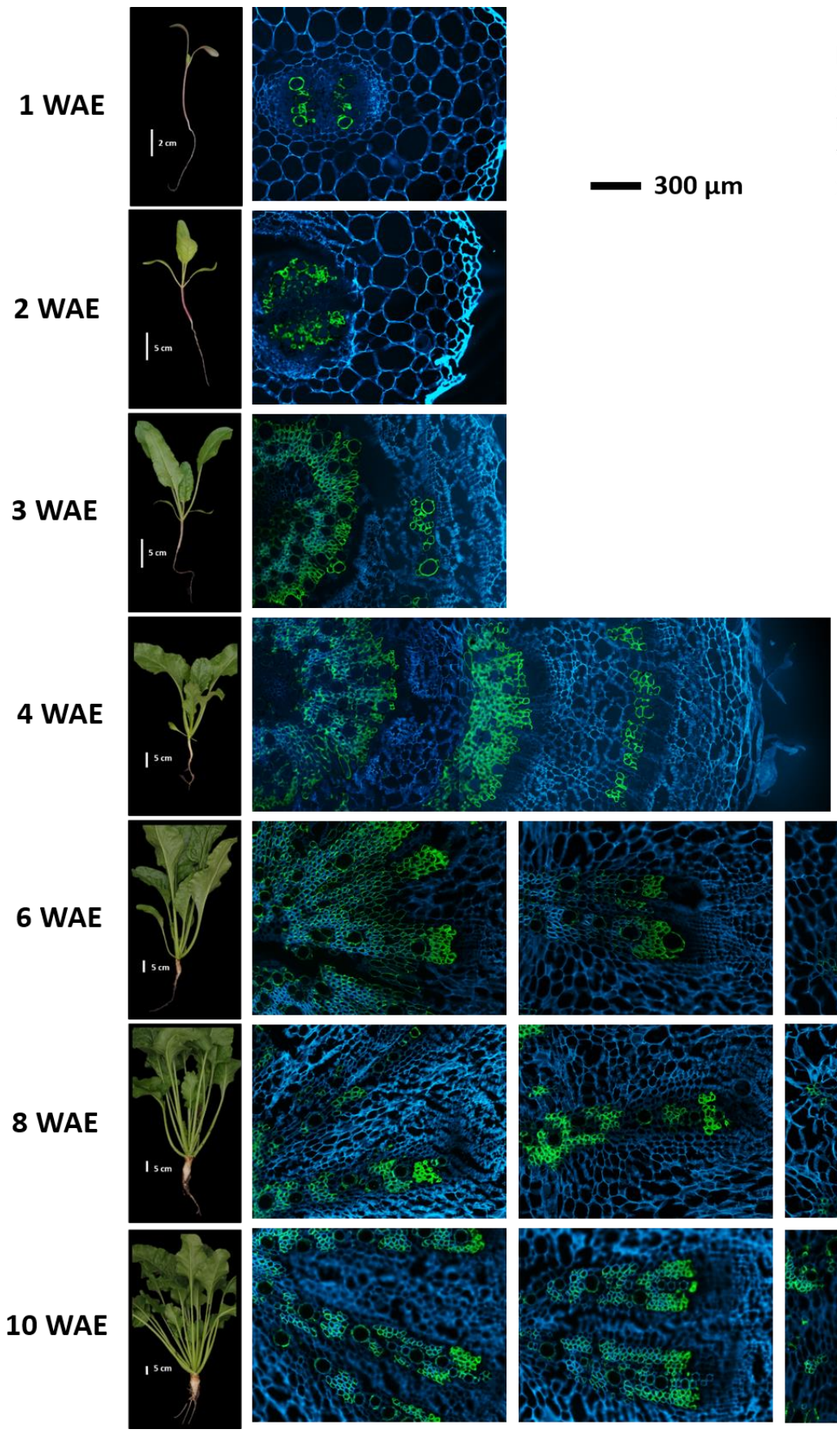

Figure 3.5 Seedling development of the *Beta vulgaris* line C869. Overall plant morphology and transverse sections (TS) showing development of the C869 line of *Beta vulgaris* from 1 week after emergence (WAE) through to 10 WAE. Gaps between micrographs indicate a section of parenchyma with no vasculature present. Xylem vessels are indicated in green by fluorescence microscopy using the monoclonal antibody LM11 which identifies xylan. Calcofluor White (Blue) staining has been used to highlight all cell types.

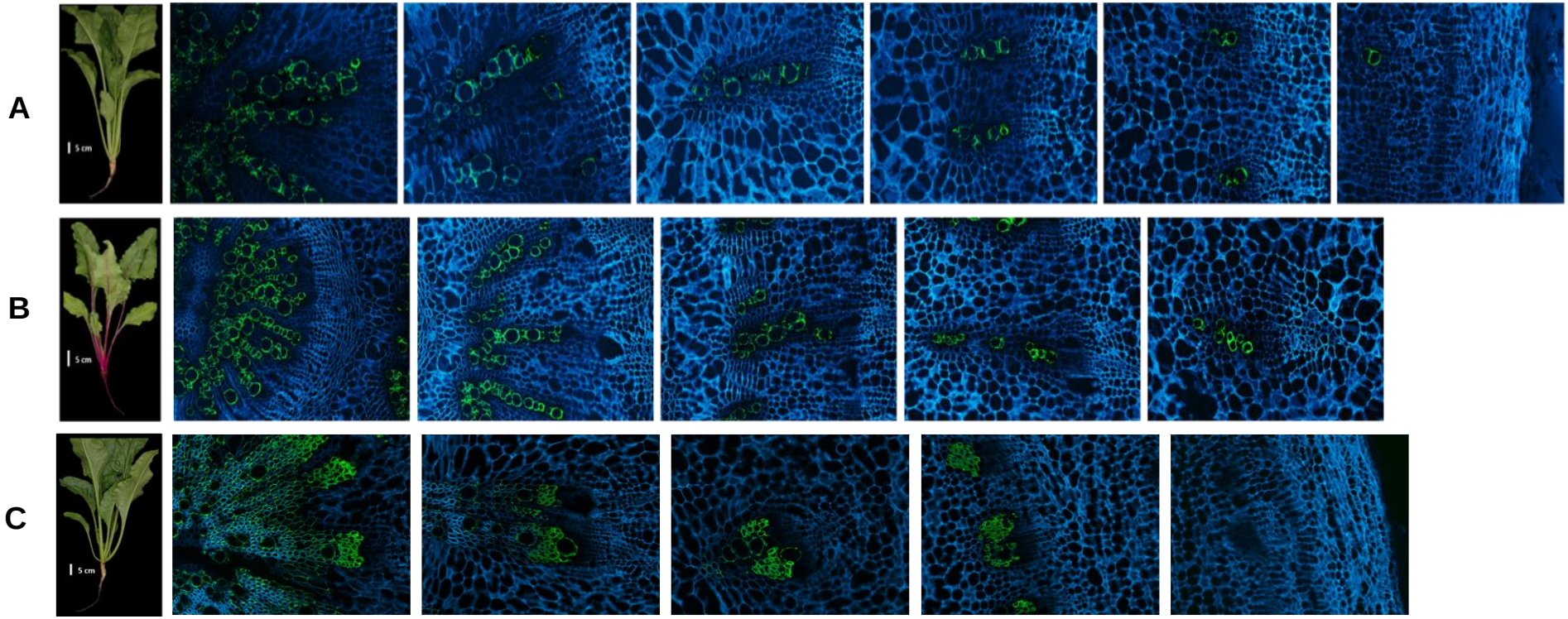

Figure 3.6 Comparison of storage root morphology of three *Beta vulgaris* lines at 6 weeks after emergence. Comparative transverse sections (TS) of **A**. Sophia line of *Beta vulgaris*. **B**. W357B line of *Beta vulgaris*. **C**. C689 line of *Beta vulgaris*. Images taken from Figure 3.3, Figure 3.4 and Figure 3.5 respectively to give a clear view of differences in development at this representative stage. Xylem vessels are indicated in green by fluorescence microscopy using the monoclonal antibody LM11 which identifies xylan. Calcofluor White (Blue) staining has been used to highlight all cell types.

3.3.4 Link between sugar beet storage root size, cambial ring number and sucrose content

The link between root size, ring number and sucrose content has long been a topic of discussion for sugar beet breeders. There is seemingly an inverse relationship between sucrose content and root yield (biomass), in that agronomic practises that increase root yield decrease relative sucrose yield and vice versa. With the increase of sucrose yield of novel commercial cultivars slowing there is a need for new selection criteria. One of these selection criteria to be considered is an increase in cambial ring number.

In order to study this hypothesis, the mean diameter and interring distances have been calculated for three *Beta* lines; a commercial sugar beet line (SOPHIA), the seed parent line (C869), and a red garden beet (W357B). The mean diameter has been measured throughout the first 10 weeks after emergence (WAE) as an indicator of overall root size (Fig 3.7). For all three *Beta* lines the average root diameter increases through development with the SOPHIA line having the greatest diameter of 56 cm at 10 WAE. Initially the C869 line has a larger mean diameter than the W357B line however at 6 WAE the W375B line mean diameter increases beyond C869. By 8 WAE and 10 WAE the W357B and C869 line's mean diameter were not significantly different with 31 (± 2.4 SEM) and 29 (± 1.6 SEM) mean diameters at 10 WAE respectively. To assess the relationship between sucrose content, root yield and cambial ring number the mean cambial rings for each of the three *Beta* lines have been recorded (Fig 3.8) along with the inter ring distances (Fig 3.9)

The Sophia line develops an additional cambial rings to the central stele at 2 WAE whereas the C869 and W357B lines do not start to develop one additional cambial rings until 3 WAE where the ring number of the Sophia line has increased to two. All three lines have the same ring number at 4 WAE with two additional cambial rings. All three lines increase at 6 WAE where both C869 and W357B have four cambial rings and Sophia has increased its additional ring number to five. Both the Sophia and C869 lines have an increase in cambial ring number to six and W357B remains unchanged with four cambial rings. The Sophia line

cambial ring number increases to eight at 10 WAE as does the W375B line to five cambial rings. The C869 line cambia ring number remains the same as 8 WAE at six rings.

Measurement has been taken for the relationship between individual cambium rings throughout development (Fig 3.9). Throughout the weeks studied cambial rings are established at varying times in each *Beta vulgaris* line, as the root develops the distance between successive rings increases. The Sophia line develops cambial rings earlier than the other two lines at 2WAE. At 3WAE all three lines have at least one additional cambial ring with C869 and Sophia having their ring at similar distance from the central stele, in addition at this stage the Sophia line has a second ring. The distance from the central stele to the first cambial ring increases for all three of the lines at 4WAE. For both Sophia and C869 the distance nearly doubles between this stage and the previous. Development has continued through to 6WAE with W357B showing five additional cambial rings where C869 has only added one more ring to the previous developmental stage. At 6WAE the distance between rings is still increasing with distances between the first, second and third additional rings equalising in the Sophia line. Additional rings are continuing to be developed at 8WAE with W357B and C869 with five rings and Sophia having six rings. The distances between rings are continuing to increase at 8WAE from the previous stage. In the final developmental stage studied 10WAE, C869 and W357B both have the same number of rings with six, whereas the Sophia line has added another four additional rings to increase the total number to 10 cambial rings. The additional cambial rings contribute to an increase in diameter (Fig 3.7). The Sophia line shows that the rings move away from each other as cell division occurs in the regions between the rings, the distance between the rings that developed earlier shows equalising distances between them at just under 5mm. Cambial rings which have developed later are relatively closer together towards the epidermis.

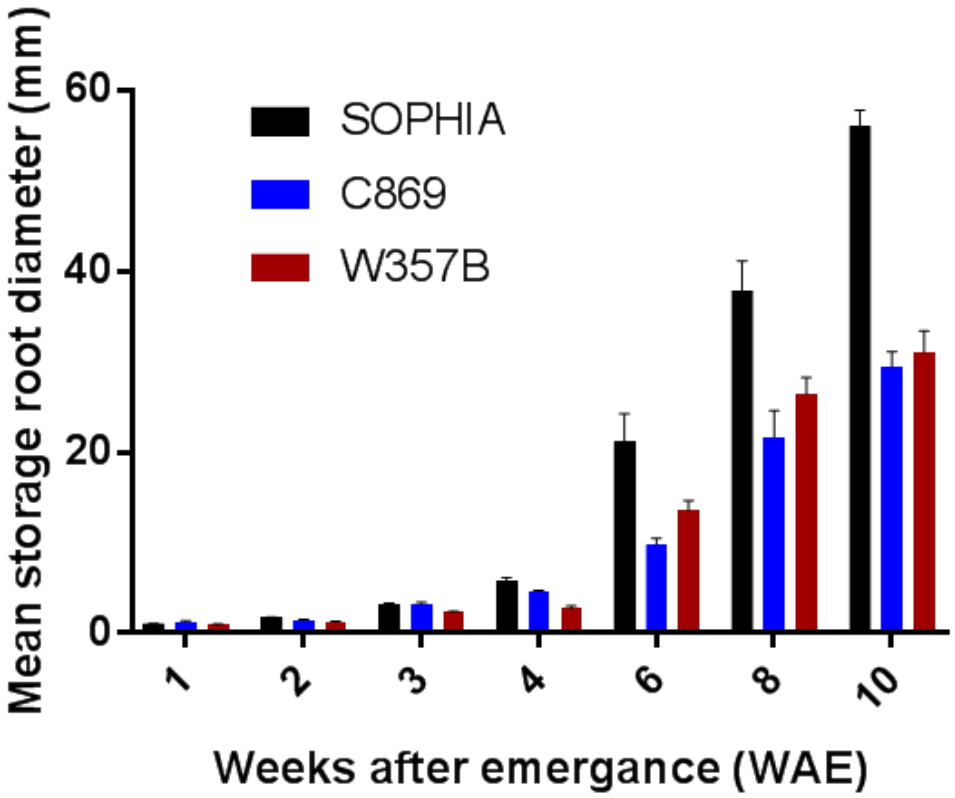

Figure 3.7 Storage root diameters of three *Beta vulgaris* lines. Mean storage root diameters of Sophia, C869 and W357B *Beta vulgaris* lines through the first 10 weeks after emergence (WAE). Bars: SEM, n=3.

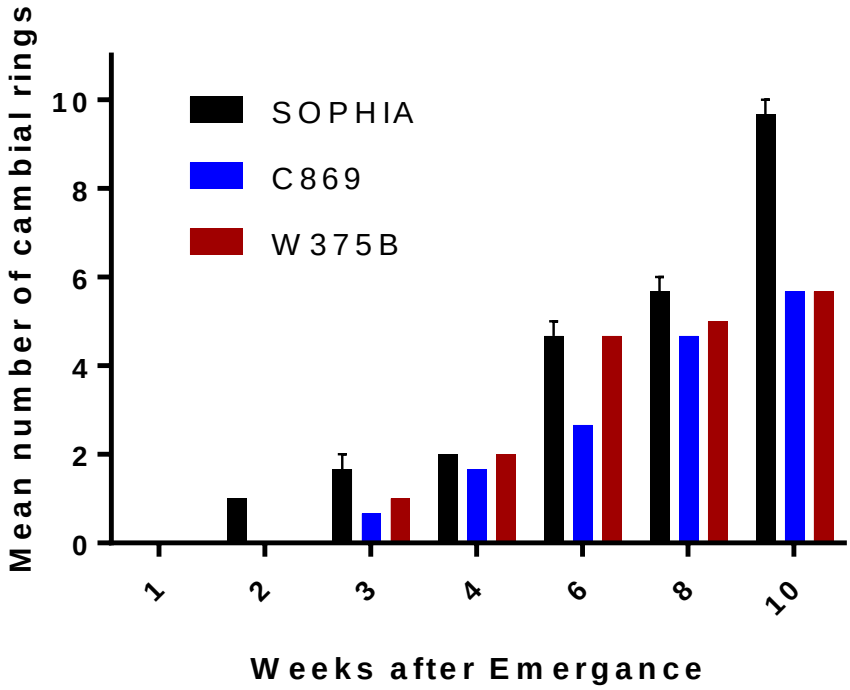

Figure 3.8 Number of cambial rings within three *Beta vulgaris* lines. The mean number of successive cambial rings of Sophia, C869 and W357B lines of *Beta vulgaris* through the first 10 weeks after emergence (WAE). Bars: SEM, n=3.

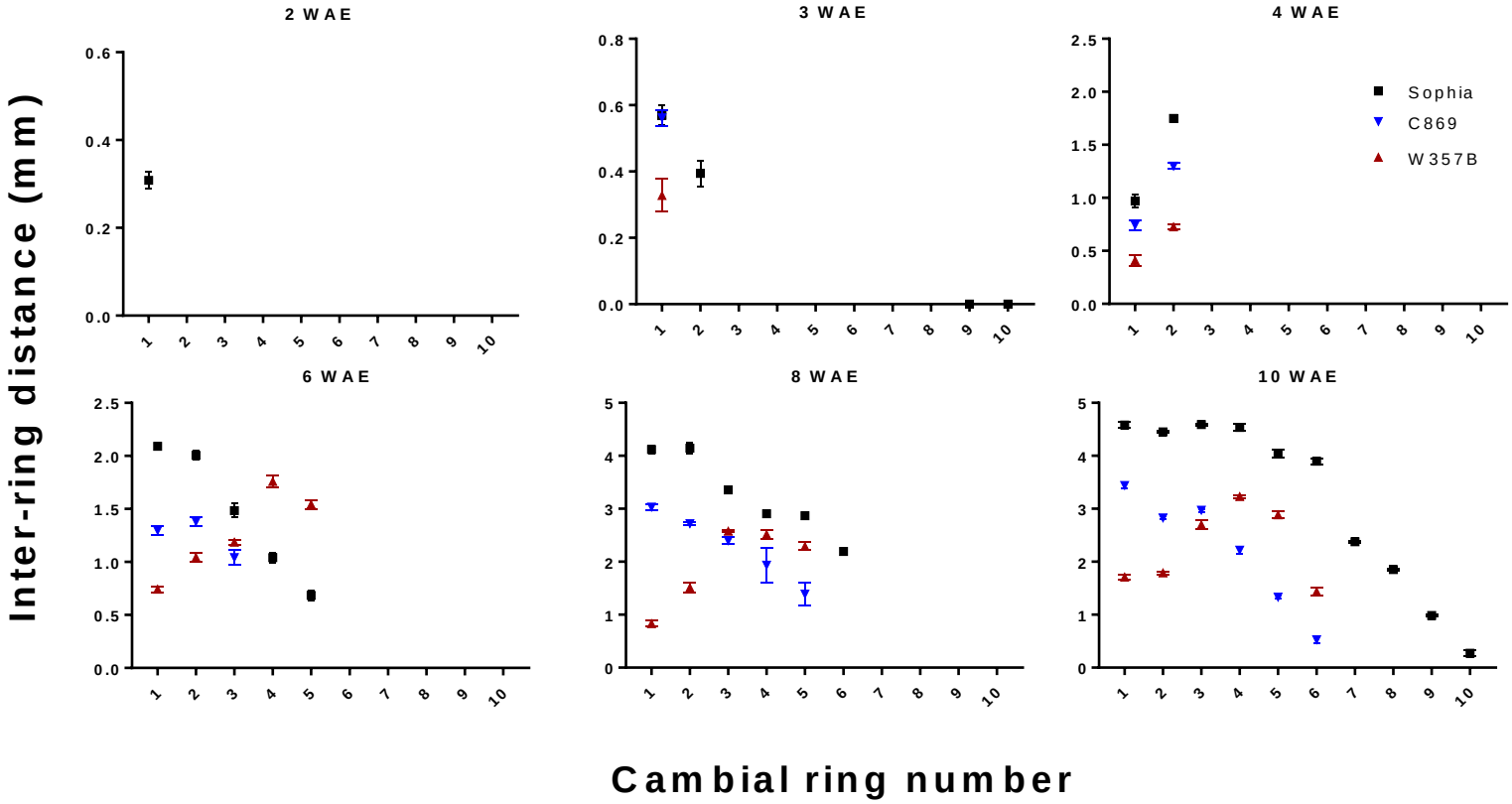

Figure 3.9 Inter-ring distances of cambial rings within three *Beta vulgaris* lines. The distances between each cambial ring throughout the first 10 weeks after emergence (WAE) of three *Beta* lines, SOPHIA, C869 and W357B. Bars: SEM, n=3

3.3.5 Change in sugar beet cell wall composition throughout development

Assessment of cell wall components is important in understanding how the sugar beet storage root partitions assimilated carbon between dry matter as sucrose and non-sucrose dry matter

Identifying changes in cell wall composition throughout plant development can be a challenge as the genes responsible for modification and biosynthesis if cell wall components are expressed at differing levels throughout cells and tissues. As an alternative approach monoclonal antibodies (mAbs) directed to distinct cell wall polysaccharides, were used for the study of plant cell wall structures throughout the growing season. Due to the sensitivity of the mAbs structural heterogeneity of plant cell wall polysaccharides can be detected with mAbs directed to specific epitopes of structures within polysaccharides relatively quickly. The plant cell wall specific mAbs have also been utilised for the quantitative detection of the relative abundance of major cell wall polysaccharides at differing time points throughout development. The field grown material was grown as described in Chapter 2 at Brooms Barn (Rothamsted Research). There were a total of 16 harvests and specific harvests were selected for the polysaccharide analysis (Table 3.2)

Table 3.2 Developmental stages of sugar beet plants used for the detection of cell wall polysaccharides. Developmental stages of sugar beet plants harvested for the quantitative detection of cell wall glycans. Observations for triplicate field experiments have been averaged. (Data provided by Belinda Townsend, Rothamsted Research)

Harvest number	Approximate date	Weeks after emergence (WAE)	Developmental stage at harvest	BBCH-scale
2	Mid June	7	12 leaf	22
3	Early July	10	20 leaf	30
5	Late August	18	Closed canopy (<30 leaf)	39
7	Late October	26	Maturity	49
12	Early March	46	New growth	51
13	Early April	50	New growth	52
15	Late May	57	Late bolting	52
16	Late June	62	Flowering and seed set	55-59

The analysis of the plant material collected form the three growing seasons was initially assessed by enzyme linked immunosorbent assay (ELISA) using nine mAbs directed at different cell wall glycans. The same samples were then sent to the University of Copenhagen to be assessed using the comprehensive microarray polymer profiling (CoMPP) method. The same nine antibodies were used in this assay as well as an additional 16 mAbs due to the CoMPP technique being a semi-automated high-through put process.

Due to being a field experiment run over three different growing seasons the sugar beets were subject to differing weather condition these are outlined in Figure 3.10. Overall the season beginning in 2010 was subject to lower temperatures and increases rainfall compared to the 2009 and 2011 seasons.

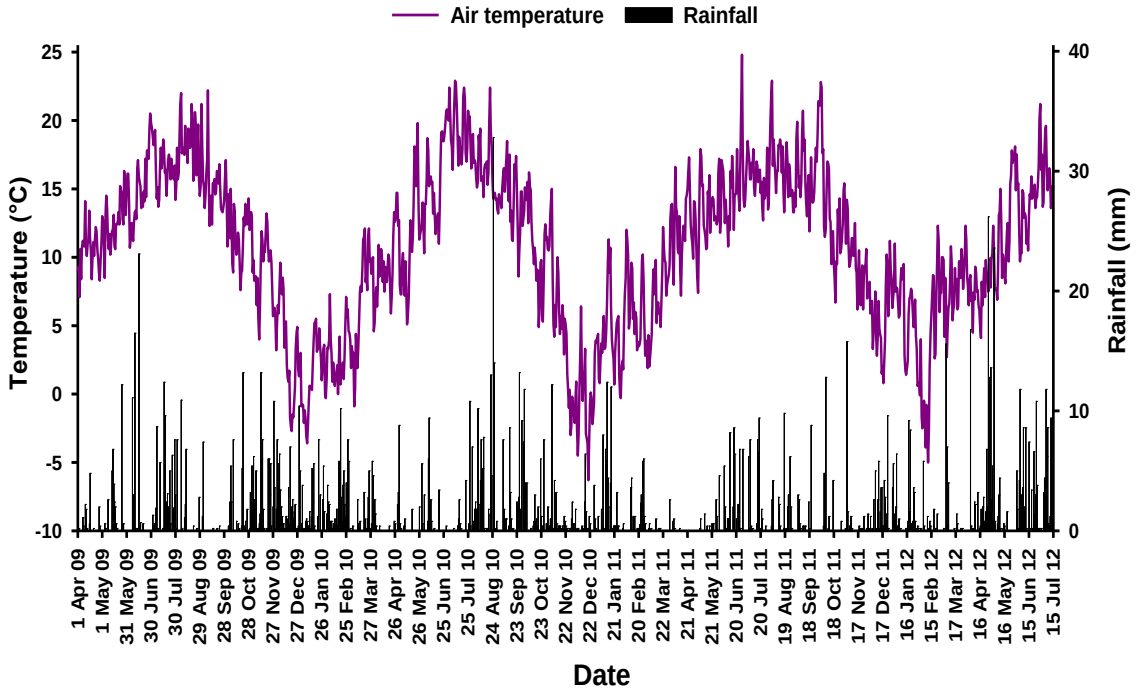

Figure 3.10 Summary of weather conditions during developmental growth seasons. Outline of weather conditions, air temperature and rainfall in the three growth seasons for the developmental study used for glycan analysis. Data and figure collated by Aiming Qi (Rothamsted Research)

3.3.5.1 Enzyme linked immunosorbent assay (ELISA) for the detection of sugar beet root cell wall glycans through development

In order to be able to efficiently assess the field grown plant material using the ELISA technique it was essential to reduce the antigen dilution usually used in an ELISA protocol. Under normal circumstances it is common to use a serial dilution of the sample to ensure that the plate wells are not overloaded and showing unreliable results. In this case to do this with each sample would only allow one harvest point to be assessed on each plate. Not only would analysing the material in this way take a long time it would also allow plate to plate variation between samples. Therefore a series of optimisation steps were undertaken to determine an appropriate dilution for the samples so that all samples of a single growing season, extraction and mAb could be plated on a single microtitre plate.

The initial experiment (Fig. 3.11) analysed both dry powdered (freeze dried and tissue lysed) plant material (Un-treated) and alcohol insoluble residues (AIR) prepared from the same dry powdered samples. This experiment was conducted using a few monoclonal antibodies which identified key polysaccharide groups; LM19 (homogalacturonan), LM25 (xyloglucan), LM13 and LM6 (arabinan). Both the commercial sugar beet variety (Sophia) and the red garden beet variety (W357B) were extracted with both CDTA and KOH and screened with the mAbs. From this initial experiment is was decided that the AIR preparation was required to maintain high epitope detection signals in both the CDTA and KOH fractions. In addition it was concluded that 0.1mg/ml was a sufficient concentration of the extract to use in subsequent ELISAs to screening of all of the field development samples. This concentration gave good absorbance readings and did not show evidence of over loading of the wells. This work allowed for the plates to be set up in such a way that there would be no technical variance between samples assessed by a single monoclonal antibody. The microtitre plant plan shown in Figure 3.12 shows how this method included three biological replicates of each sample, three technical replicates and negative control wells.

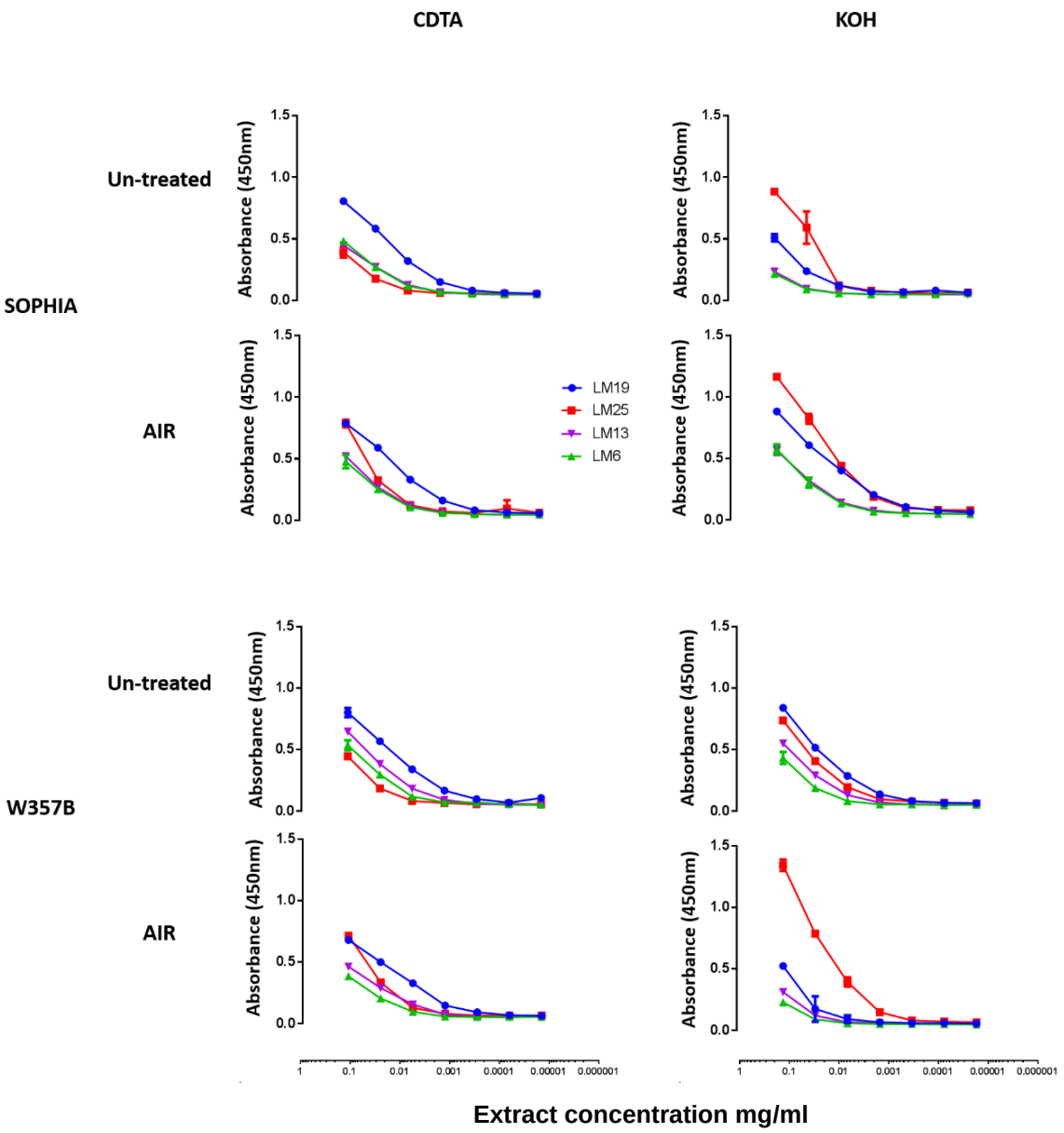

Figure 3.11 Initial detection of cell wall polysaccharides. Initial ELISA showing absorbance at 450nm for four monoclonal antibodies; Blue: LM19, Red: LM25, Purple: LM13 and Green: LM6. The results shown include absorbance detected when the sample has been prepared by alcohol insoluble residue (AIR), and when the dry powdered sample has been used without any preparation (Un-treated). Two lines of *Beta* have been used, the commercial sugar beet line (SOPHIA) and the garden beet line (W357B) to identify concentration of sample to use for further analysis.

Plate Number: Antibody: Fraction:

	1	2	3	4	5	6	7	8	9	10	11	12
A	H2.1	H2.1	H2.1	H2.2	H2.2	H2.2	H2.3	H2.3	H2.3	Control		
B	H3.1	H3.1	H3.1	H3.2	H3.2	H3.2	H3.3	H3.3	H3.3			
C	H5.1	H5.1	H5.1	H5.2	H5.2	H5.2	H5.3	H5.3	H5.3	Control		
D	H7.1	H7.1	H7.1	H7.2	H7.2	H7.2	H7.3	H7.3	H7.3			
E	H12.1	H12.1	H12.1	H12.2	H12.2	H12.2	H12.3	H12.3	H12.3	Control		
F	H13.1	H13.1	H13.1	H13.2	H13.2	H13.2	H13.3	H13.3	H13.3			
G	H15.1	H15.1	H15.1	H15.2	H15.2	H15.2	H15.3	H15.3	H15.3	Control		
H	H16.1	H16.1	H16.1	H16.2	H16.2	H16.2	H16.3	H16.3	H16.3			

Figure 3.12 Plate layout to maximise analysis efficiency. Example microtitre plate allowing all samples of a growing season to be assessed using a single monoclonal antibody at the same time. In this example H2-16 is the harvest number and the decimal .1, .2, .3 refers to the biological replicate. This arrangement allows for the reduction in technical variation and running three technical replicates per biological replicate.

After the initial experiments had been concluded the ELISA could be conducted on all samples for each of the three growing seasons. These samples were assayed using nine monoclonal antibodies which detect a variety of epitopes within cell wall polysaccharides. The results of these in Figure 3.13 show the mean of the technical and biological replicates as a heat map which indicated the relative abundance of the epitopes detected by the mAbs at the different stages of development.

Over all the results from the ELISA show good correlation between the three growing seasons with small variations year to year. The 2009 season and 2011 season show the most similar results with the 2010 season having the anomalies in most cases.

In the CDTA fraction there were two mAbs which showed consistently high relative abundance levels in all three growing seasons JIM7 (partially methylated homogalacturonan) and LM12 (feruloylated pectin). In addition to these LM19 (non-esterified homogalacturonan) remained constant at a slightly lower level to

the JIM7 and LM12 epitope detection, with the exception of the 2010 growing seasons when there was a slight decrease in relative abundance of epitope detection at harvest 5 followed by an increase to levels seen at harvest 15. Other notable mAbs in the CDTA fraction included LM13 and LM6, which both detect arabinan, showed an initial higher level of relative abundance in harvest 2 and 3 in all seasons however, the relative abundance of this epitope differed between seasons with 2009 having the highest relative abundance followed by 2011 then the 2010 season at a much lower level. LM13 and LM6 epitope detection declined during the growth period however arabinan detection by LM6 began to increase back to initial levels at harvest 15 and harvest 16 for 2009 and 2001 respectively.

The detection of the xyloglucan epitope by LM25 showed a slight increase in relative abundance in the final harvest stage (harvest 16) in all seasons. In season 2009 and 2010 the LM16 MAb detected a slight increase in arabinan at the 12 harvest stages with where the 2009 growth season showed an increase in relative abundance at harvest 12 and 13 followed by a slight decrease at harvest 15 and then another increase at harvest 16. In season 2011 there was a slight increase of the relative abundance of the LM16 epitope detected at harvest 7 followed by a decrease for the following harvests until harvest 16 where there was a peak in the relative abundance. LM26 (unpublished MAb, phloem specific) showed no signal through at three seasons with the exception of harvest 2 in the 2011 season where there was a small peak of 0.35. LM11 showed no detection for the xylan epitope in the CDTA fraction in all three seasons.

The KOH fractions showed less consistent relative abundance of epitopes throughout the growing seasons with the relative abundances fluctuating throughout. The most notable of these fluctuations is the relative abundance of the LM11 epitope, xylan. This shows peaks of relative abundance at both ends of the growing season with 2009 having the highest relative abundance at 1.12. The abundance of the xylan epitope decreases with subsequent harvests 3 and 5. Both 2009 and 2011 show a slight increase in relative abundance at harvest 7 then a drop at harvest 12 followed by a continued increase of the LM11 epitope to a peak at harvest 16 which in all three seasons has the highest relative

abundance of the LM11 epitope of the whole growing season. The most consistent relative abundance throughout development in the KOH fraction is the LM19 epitope which is detected at all harvest throughout development in all three seasons.

Figure 3.14 gives an indication of the statistical variance between biological replicates utilised in this study for the analysis of cell wall epitope abundance throughout the growing season. The initial observation from the standard deviations (SD) displayed in Figure 3.14 is that SD was low for a biological field study. This indicates that despite the replicates growing in different areas in the field the cell wall architecture varies very little. The SD's which are highlighted in more intense green show a larger SD and could indicate that these points may not be statistically significant. For example, the LM25 epitope abundance at harvests 15 and 16 in the KOH fraction for 2011 showed a higher SD and upon inspection shows that the difference in abundance seen in Figure 3.13 is in fact not statistically significant. Similarly there is a highlighted SD at harvest 16 for the LM13 epitope in 2011 however in this case this was not indicated in Figure 3.13 as a difference in epitope abundance at this point. In addition an SD of 0.343 is shown at harvest 2 for the LM26 epitope in 2011. In figure 3.13 a higher abundance of this epitope was displayed by a more intense green, in this case the SD is not great enough to remove statistical significance of this result and this variance of LM26 epitope can be considered significant.

Analysis of the SD across the cell wall analysis found that, other than those discussed above, the heat map in Figure 3.13 accurately shows the significant variance of cell wall epitopes detected utilising the ELISA technique.

Season	MAb	CDTA								KOH							
		Harvest number								Harvest number							
		2	3	5	7	12	13	15	16	2	3	5	7	12	13	15	16
2009	JIM7	1.19	1.21	1.22	1.19	1.14	1.15	1.27	1.27	0.06	0.05	0.05	0.05	0.05	0.05	0.05	0.06
	LM19	0.47	0.46	0.46	0.41	0.41	0.44	0.51	0.66	0.55	0.57	0.61	0.51	0.43	0.52	0.46	0.43
	LM6	0.82	0.78	0.65	0.65	0.66	0.65	0.78	0.91	0.22	0.18	0.13	0.10	0.08	0.10	0.13	0.16
	LM12	1.17	1.19	1.22	1.18	1.16	1.18	1.20	1.16	0.06	0.05	0.05	0.05	0.05	0.05	0.05	0.06
	LM26	0.07	0.06	0.06	0.06	0.09	0.09	0.07	0.09	0.09	0.07	0.06	0.06	0.07	0.08	0.07	0.10
	LM13	0.88	0.79	0.42	0.32	0.23	0.29	0.30	0.30	0.82	0.74	0.49	0.36	0.18	0.25	0.36	0.29
	LM16	0.17	0.14	0.11	0.11	0.39	0.42	0.25	0.43	0.15	0.11	0.11	0.11	0.20	0.26	0.22	0.26
	LM11	0.05	0.05	0.05	0.05	0.05	0.05	0.07	0.07	1.12	0.77	0.45	0.57	0.42	0.48	1.36	1.37
	LM25	0.19	0.20	0.17	0.18	0.18	0.20	0.28	0.47	0.58	0.51	0.57	0.53	0.54	0.67	0.83	1.03
2010	JIM7	0.92	0.75	0.88	0.76	0.80	0.76	0.93	1.04	0.05	0.04	0.05	0.04	0.05	0.05	0.04	0.05
	LM19	0.55	0.63	0.42	0.32	0.43	0.43	0.49	0.66	0.85	0.40	0.60	0.62	0.69	0.69	0.57	0.46
	LM6	0.29	0.21	0.21	0.19	0.20	0.20	0.23	0.25	0.14	0.06	0.07	0.06	0.07	0.07	0.06	0.07
	LM12	0.61	0.44	0.58	0.59	0.57	0.57	0.62	0.68	0.05	0.04	0.04	0.04	0.04	0.04	0.05	0.05
	LM26	0.06	0.05	0.05	0.05	0.09	0.08	0.07	0.10	0.10	0.05	0.05	0.05	0.11	0.09	0.06	0.06
	LM13	0.29	0.12	0.12	0.10	0.11	0.12	0.12	0.15	0.30	0.13	0.14	0.12	0.13	0.13	0.10	0.08
	LM16	0.08	0.06	0.05	0.07	0.14	0.11	0.10	0.18	0.09	0.05	0.06	0.06	0.17	0.13	0.08	0.10
	LM11	0.05	0.04	0.04	0.04	0.04	0.05	0.05	0.06	0.55	0.41	0.19	0.13	0.29	0.42	0.78	0.96
	LM25	0.13	0.11	0.08	0.09	0.10	0.10	0.13	0.25	0.24	0.14	0.18	0.16	0.24	0.25	0.25	0.34
2011	JIM7	0.95	0.84	0.84	0.85	0.85	0.94	0.90	0.90	0.05	0.05	0.06	0.05	0.05	0.05	0.05	0.11
	LM19	0.58	0.51	0.42	0.40	0.46	0.50	0.45	0.48	0.85	0.78	0.85	0.90	0.93	0.78	0.83	1.01
	LM6	0.47	0.36	0.34	0.30	0.29	0.35	0.35	0.39	0.16	0.12	0.08	0.09	0.10	0.09	0.09	0.15
	LM12	0.93	0.83	0.91	0.91	0.91	0.91	0.92	0.93	0.06	0.05	0.05	0.05	0.05	0.05	0.05	0.05
	LM26	0.35	0.06	0.08	0.06	0.07	0.06	0.07	0.08	0.10	0.10	0.06	0.07	0.10	0.08	0.11	0.13
	LM13	0.62	0.37	0.30	0.31	0.24	0.27	0.21	0.22	0.82	0.53	0.50	0.43	0.52	0.43	0.35	0.48
	LM16	0.17	0.11	0.09	0.27	0.16	0.12	0.19	0.49	0.12	0.16	0.08	0.11	0.30	0.16	0.18	0.36
	LM25	0.19	0.12	0.15	0.15	0.13	0.14	0.14	0.21	0.40	0.41	0.45	0.46	0.53	0.41	0.86	1.07
	LM11	0.07	0.05	0.05	0.06	0.05	0.05	0.05	0.08	0.36	0.17	0.30	0.48	0.34	0.38	0.85	1.21

Figure 3.13 Heat map of ELISA analysis of cell wall polysaccharides throughout a field development study. The relative abundance of nine cell wall polymer epitopes detected by monoclonal antibodies throughout development over three growing seasons as identified by ELISA. Two extraction fractions have been assessed CDTA (Cyclohexanediaminetetraacetic Acid) and KOH (Potassium hydroxide). Intensity of green indicates relative abundance. Each point on the heat map is shown as the absorbance at 450 nm and represents the mean of three biological replicates each of which is the mean of three technical replicates.

Season	MAb	CDTA								KOH							
		Harvest number								Harvest number							
		2	3	5	7	12	13	15	16	2	3	5	7	12	13	15	16
2009	JIM7	0.072	0.019	0.030	0.013	0.018	0.046	0.030	0.084	0.006	0.003	0.002	0.002	0.003	0.003	0.003	0.003
	LM19	0.014	0.081	0.010	0.033	0.029	0.045	0.052	0.082	0.164	0.124	0.062	0.021	0.020	0.052	0.047	0.085
	LM6	0.069	0.053	0.048	0.043	0.057	0.066	0.064	0.060	0.118	0.064	0.039	0.018	0.005	0.015	0.009	0.047
	LM12	0.061	0.038	0.040	0.019	0.044	0.037	0.030	0.018	0.002	0.002	0.001	0.002	0.003	0.003	0.004	0.008
	LM26	0.003	0.005	0.001	0.008	0.012	0.015	0.002	0.010	0.019	0.009	0.003	0.003	0.003	0.010	0.007	0.011
	LM13	0.072	0.045	0.038	0.069	0.027	0.058	0.019	0.068	0.219	0.109	0.141	0.117	0.017	0.058	0.082	0.167
	LM16	0.014	0.012	0.025	0.016	0.095	0.059	0.031	0.097	0.071	0.027	0.020	0.027	0.025	0.053	0.078	0.056
	LM11	0.002	0.005	0.003	0.003	0.002	0.003	0.039	0.009	0.067	0.183	0.178	0.012	0.029	0.141	0.212	0.150
	LM25	0.008	0.046	0.037	0.019	0.020	0.034	0.038	0.053	0.072	0.055	0.119	0.116	0.068	0.079	0.042	0.114
2010	JIM7	0.046	0.051	0.014	0.050	0.022	0.058	0.035	0.044	0.001	0.002	0.002	0.002	0.003	0.002	0.000	0.015
	LM19	0.011	0.098	0.027	0.016	0.039	0.052	0.021	0.043	0.062	0.041	0.079	0.055	0.081	0.032	0.044	0.073
	LM6	0.017	0.009	0.019	0.007	0.022	0.002	0.004	0.013	0.022	0.004	0.008	0.003	0.012	0.003	0.007	0.002
	LM12	0.007	0.032	0.022	0.027	0.017	0.013	0.023	0.030	0.001	0.001	0.001	0.001	0.001	0.001	0.001	0.003
	LM26	0.008	0.001	0.001	0.001	0.003	0.015	0.008	0.047	0.026	0.002	0.003	0.002	0.019	0.027	0.010	0.004
	LM13	0.038	0.003	0.016	0.007	0.015	0.020	0.010	0.010	0.016	0.010	0.009	0.011	0.025	0.019	0.024	0.011
	LM16	0.005	0.001	0.002	0.005	0.005	0.025	0.013	0.101	0.020	0.004	0.004	0.007	0.024	0.030	0.011	0.018
	LM11	0.002	0.001	0.001	0.002	0.001	0.001	0.008	0.016	0.108	0.040	0.030	0.048	0.078	0.091	0.098	0.088
	LM25	0.015	0.009	0.010	0.009	0.014	0.003	0.021	0.078	0.022	0.010	0.023	0.017	0.037	0.009	0.007	0.033
2011	JIM7	0.023	0.012	0.107	0.035	0.047	0.038	0.078	0.004	0.001	0.002	0.023	0.000	0.002	0.001	0.000	0.095
	LM19	0.070	0.051	0.097	0.031	0.086	0.028	0.049	0.019	0.210	0.300	0.042	0.040	0.149	0.155	0.194	0.080
	LM6	0.080	0.012	0.041	0.017	0.047	0.078	0.022	0.020	0.043	0.022	0.020	0.010	0.020	0.005	0.022	0.031
	LM12	0.019	0.058	0.041	0.053	0.040	0.055	0.035	0.017	0.003	0.003	0.002	0.001	0.002	0.002	0.002	0.003
	LM26	0.343	0.013	0.049	0.005	0.005	0.001	0.010	0.013	0.034	0.045	0.007	0.001	0.012	0.013	0.048	0.028
	LM13	0.082	0.135	0.055	0.157	0.021	0.114	0.050	0.014	0.177	0.020	0.121	0.059	0.053	0.024	0.127	0.062
	LM16	0.063	0.050	0.015	0.165	0.024	0.045	0.081	0.486	0.039	0.140	0.019	0.011	0.013	0.078	0.094	0.105
	LM11	0.011	0.002	0.004	0.005	0.003	0.003	0.003	0.037	0.193	0.031	0.115	0.182	0.027	0.105	0.024	0.061
	LM25	0.057	0.005	0.003	0.046	0.018	0.030	0.020	0.064	0.066	0.203	0.055	0.084	0.058	0.101	0.442	0.428

Figure 3.14 Heat map of the standard deviations associated with the analysis of cell wall polysaccharides throughout a field development study in Figure 3.13. The standard deviations between the biological replicates analysed for the detection of nine cell wall polymer epitopes detected by monoclonal antibodies throughout development over three growing seasons as identified by ELISA. Two extraction fractions have been assessed CDTA (Cyclohexanediaminetetraacetic Acid) and KOH (Potassium hydroxide). The intensity of the green indicates larger standard deviations between biological replicates.

3.3.5.2 Comprehensive microarray polymer profiling (CoMPP) for the detection of sugar beet root cell wall glycans through development

The comprehensive microarray polymer profiling (CoMPP) techniques is a high throughput method of identifying the relative abundance of cell wall glycans developed at the University of Copenhagen (Kračun et al., 2017). Using this semi-automated method has allowed for the same developmental samples to be screened using a larger number of mAbs than have been used for the ELISA protocol.

The CoMPP method has been used to screen the developmental samples with the same nine mAbs as the ELISA protocol (Fig 3.15) as well as an additional 16

mAbs (Fig 3.17). This has given the opportunity to compare the two protocols as well as gather more information about change in cell wall composition throughout development.

Looking at the nine mAbs also screened by the ELISA protocol shown in Figure 3.15 it is clear that the overall epitope detection over the three seasons was similar using both the CoMPP and ELISA methods. The CDTA fraction showed the same high relative abundance of JIM7 and LM12 detection throughout all eight harvests over the three seasons as well as the consistent slightly lower detection of LM19 epitope throughout all harvests. In addition, there was a similar pattern of epitope detection for the arabinan mAbs, LM13 and LM6, these showed a relatively high abundance at the beginning of the growing season (harvest 2 and 3) for all three seasons. However, the difference with this CoMPP analysis was that the relative abundance of LM13 and LM6 epitopes decrease throughout the growing season without the increase in the later stages of growth reported by the ELISA protocol in the 2009 and 2011 growing seasons. The stark difference between the ELISA and CoMPP protocols in the CDTA fraction is that there was less difference between the growing seasons, as seen by the very similar relative abundance of the 2010 season for LM13 and LM6 where the relative abundance was much lower for this year.

The KOH fraction for the CoMPP analysis again showed similarities to the ELISA results, with a few notable differences. The detected LM19 epitope signal in the KOH fraction was relatively high in the ELISA results where for the CoMPP protocol there was very little signal for the LM19 epitope. In addition to this difference there was a good signal for the LM6 epitope throughout all three growing seasons in the CoMPP KOH fraction where there was very little signal for this mAb using the ELISA protocol.

The LM6 epitope detection was strong in the first harvest and gradually decreased through the growing seasons to a relatively low level at harvest 16, the LM13 epitope showed a very similar pattern with all three seasons showing a strong detection in the initial harvest and a decrease through development. The

LM13 epitope detection differs from detection using the other arabinan mAb LM6 in that it was also detected in small amounts using the ELISA protocol.

There was a stronger signal for the LM25 epitope using the CoMPP protocol which was at a mid-range level from harvest 2-13 for all three seasons with an increase in the relative abundance for the final two harvests (harvest 15 and 16), this increase was delayed in the 2011 season where there was only an increase in the final harvest and the increase was not as large as the 2009 and 2010 growing seasons.

The LM25 epitope detection was similar to the ELISA protocol with the highest relative abundance occurring in the final two harvests (harvest 15 and 16) after a mid-range signal throughout the rest of the earlier harvests. There was very little difference between the relative abundance of the LM25 epitope between the three growth seasons with the abundance at a slightly lower level in the 2011 season. The detection of the LM11 epitope using the CoMPP protocol showed a decrease throughout the first half of the growing seasons followed by an increase at harvest 12 through to a peak in the final harvest, this is the case in all growing season except 2009 where the harvest 16 did not show a higher relative abundance of the LM11 epitope in this harvest than harvest 2.

Figure 3.16 denotes the standard deviations (SD) associated with the analysis displayed in Figure 3.15. Using these SD the significance of the data in Figure 3.15 can be assessed. SDs with high intensity green highlight potential discrepancies between the apparent increase or decrease of epitope detection shown in Figure 3.15. The majority of the highlighted SDs are in the NaOH fraction of the 2009 season and some of these reject the apparent fluctuation of detected epitopes as significant. LM11 in this fraction suggests that there is no fluctuation in the LM11 epitope across the growing season. Similarly, the levels of LM25 are not significantly different until the final two harvest points where the increase in epitope detection is significant. On the other hand, the SD for LM13 and LM6 do not disagree with the fluctuation in epitope detection shown by color intensity across the growing season. Across the rest of the seasons and both

fractions the epitope detection shown in Figure 3.15 remain significant according to the calculated SD in Figure 3.16.

		CDTA								KOH							
Season	MAb	Harvest number								Harvest number							
		2	3	5	7	12	13	15	16	2	3	5	7	12	13	15	16
2009	JIM7	85.10	88.80	86.00	84.50	82.50	83.80	74.90	74.70	0.00	0.00	0.00	0.00	0.00	0.00	0.00	0.00
	LM19	20.70	22.80	21.80	22.00	20.60	24.20	20.90	28.60	12.00	4.20	3.60	2.80	4.00	6.90	6.60	8.20
	LM6	46.70	50.10	40.40	37.40	36.90	39.00	30.60	26.90	41.90	31.40	18.30	24.40	18.70	18.80	15.70	14.10
	LM12	76.20	90.60	87.40	79.80	75.30	82.40	54.80	38.90	0.00	0.00	0.00	0.00	0.00	0.00	0.00	0.00
	LM26	0.00	0.00	0.00	0.00	0.00	1.70	0.00	0.00	7.40	0.00	0.00	0.00	9.30	5.90	0.00	4.60
	LM13	49.40	47.60	22.70	18.90	12.60	16.60	8.20	4.40	48.80	29.20	12.50	19.60	10.20	11.00	9.60	5.90
	LM16	0.00	0.00	0.00	0.00	0.00	0.00	0.00	0.00	0.00	0.00	0.00	0.00	0.00	0.00	0.00	0.00
	LM11	0.00	0.00	0.00	0.00	0.00	0.00	0.00	0.00	39.10	33.20	29.10	23.00	31.20	33.00	29.10	23.00
	LM25	0.00	0.00	0.00	0.00	0.00	0.00	0.00	0.00	37.60	31.30	27.60	34.20	34.90	32.90	56.50	51.20
2010	JIM7	81.60	68.30	82.10	78.90	79.00	76.00	73.70	70.10	0.00	0.00	0.00	0.00	0.00	0.00	0.00	0.00
	LM19	21.20	43.40	27.10	22.00	18.80	17.70	16.00	16.50	3.90	0.00	4.00	0.00	8.60	8.40	4.20	4.90
	LM6	52.70	37.90	45.20	40.30	43.20	41.70	36.00	29.00	37.50	17.50	30.60	20.10	28.10	25.50	15.70	14.10
	LM12	85.60	45.90	87.10	90.00	80.80	82.70	71.60	71.70	0.00	0.00	0.00	0.00	0.00	0.00	0.00	0.00
	LM26	0.00	0.00	0.00	0.00	1.90	3.10	0.00	0.00	0.00	3.70	0.00	0.00	21.90	17.90	6.80	6.20
	LM13	60.80	18.70	23.80	21.40	22.60	20.80	17.30	14.60	46.40	14.90	23.00	15.30	18.60	17.60	10.40	8.60
	LM16	0.00	0.00	0.00	0.00	0.00	0.00	0.00	0.00	0.00	0.00	0.00	0.00	0.00	0.00	0.00	0.00
	LM11	0.00	0.00	0.00	0.00	0.00	0.00	0.00	0.00	38.60	33.30	25.80	25.30	26.70	36.60	53.50	60.20
	LM25	0.00	0.00	0.00	0.00	0.00	0.00	0.00	0.00	38.20	32.10	26.10	25.10	26.70	35.50	54.40	60.10
2011	JIM7	79.10	79.50	74.30	74.90	79.20	77.00	74.30	71.10	0.00	0.00	0.00	0.00	0.00	0.00	0.00	0.00
	LM19	28.00	20.80	22.50	19.70	22.50	17.80	19.00	22.10	0.00	3.10	0.00	3.60	6.00	5.70	7.80	8.50
	LM6	49.70	44.10	39.30	38.60	40.50	40.80	37.80	33.30	27.40	21.50	16.10	17.50	17.70	17.60	16.20	13.30
	LM12	79.00	81.80	83.90	87.50	81.30	80.50	76.60	64.10	0.00	0.00	0.00	0.00	0.00	0.00	0.00	0.00
	LM26	0.00	0.00	0.00	0.00	0.00	0.00	0.00	0.00	3.90	2.90	0.00	1.80	6.10	5.20	4.40	4.00
	LM13	54.90	36.30	23.60	19.00	22.10	25.30	15.40	13.20	35.10	21.40	14.90	14.60	13.10	14.40	12.20	8.80
	LM16	0.00	0.00	0.00	0.00	0.00	0.00	0.00	0.00	0.00	0.00	0.00	0.00	0.00	0.00	0.00	0.00
	LM11	0.00	0.00	0.00	0.00	0.00	0.00	0.00	0.00	34.00	32.30	32.80	29.30	29.20	34.40	36.60	44.90
	LM25	0.00	0.00	0.00	0.00	0.00	0.00	0.00	0.00	33.70	31.70	30.60	28.00	28.00	34.10	36.10	44.90

Figure 3.15 heat map of CoMPP analysis of cell wall polysaccharides throughout a field development study. The relative abundance of nine cell wall polymer epitopes detected by monoclonal antibodies throughout development over three growing seasons as identified by CoMPP. Two extraction fractions have been assessed CDTA (Cyclohexanediaminetetraacetic Acid) and NaOH (Sodium hydroxide). Intensity of green indicates relative abundance. This study replicates the previous study shown in Fig 3.13. Each point on the heat map is shown as the normalised value of spot density (the highest density is assigned 100 and other values assigned relative to this). Each value on the heat map is the result of the mean of three biological replicates.

		CDTA								NaOH							
Season	MAb	Harvest number								Harvest number							
		2	3	5	7	12	13	15	16	2	3	5	7	12	13	15	16
2009	JIM7	0.000	0.000	0.000	0.000	0.000	0.000	0.000	0.000	0.000	0.000	0.000	0.000	0.000	0.000	0.000	0.000
	LM19	0.419	2.162	1.856	1.963	2.163	0.851	0.973	0.697	0.698	3.604	3.094	3.271	3.605	1.418	1.622	1.161
	LM6	2.887	6.660	3.541	8.672	1.058	2.913	1.371	1.094	4.811	11.101	5.901	14.454	1.763	4.855	2.286	1.823
	LM12	0.000	0.000	0.000	0.000	0.000	0.000	0.000	0.000	0.000	0.000	0.000	0.000	0.000	0.000	0.000	0.000
	LM26	0.449	0.000	0.000	0.000	1.119	3.069	0.000	2.582	0.749	0.000	0.000	0.000	1.865	5.115	0.000	4.303
	LM13	3.265	7.343	2.636	7.213	0.546	1.828	1.298	0.429	5.441	12.238	4.394	12.022	0.910	3.046	2.163	0.716
	LM16	0.000	0.000	0.000	0.000	0.000	0.000	0.000	0.000	0.000	0.000	0.000	0.000	0.000	0.000	0.000	0.000
	LM11	2.051	2.447	2.491	12.008	5.365	0.883	8.796	5.613	3.419	4.079	4.152	20.014	8.941	1.472	14.660	9.354
	LM25	1.788	2.867	2.834	11.875	5.353	0.280	8.940	5.697	2.980	4.779	4.724	19.791	8.922	0.466	14.899	9.495
2010	JIM7	0.000	0.000	0.000	0.000	0.000	0.000	0.000	0.000	0.000	0.000	0.000	0.000	0.000	0.000	0.000	0.000
	LM19	0.102	0.000	0.104	0.000	0.011	0.041	0.108	0.132	3.415	0.000	3.471	0.000	0.370	1.361	3.614	4.399
	LM6	0.262	0.034	0.122	0.055	0.035	0.145	0.081	0.065	8.721	1.122	4.061	1.834	1.171	4.832	2.684	2.175
	LM12	0.000	0.000	0.000	0.000	0.000	0.000	0.000	0.000	0.000	0.000	0.000	0.000	0.000	0.000	0.000	0.000
	LM26	0.000	0.096	0.000	0.000	0.005	0.355	0.065	0.024	0.000	3.198	0.000	0.000	0.177	11.845	2.159	0.793
	LM13	0.326	0.043	0.082	0.055	0.072	0.072	0.028	0.080	10.869	1.438	2.748	1.845	2.404	2.392	0.939	2.655
	LM16	0.000	0.000	0.000	0.000	0.000	0.000	0.000	0.000	0.000	0.000	0.000	0.000	0.000	0.000	0.000	0.000
	LM11	0.117	0.067	0.119	0.072	0.113	0.058	0.170	0.055	3.914	2.223	3.954	2.416	3.782	1.929	5.662	1.843
	LM25	0.122	0.074	0.115	0.074	0.136	0.047	0.176	0.035	4.062	2.456	3.821	2.480	4.546	1.577	5.859	1.158
2011	JIM7	0.000	0.000	0.000	0.000	0.000	0.000	0.000	0.000	0.000	0.000	0.000	0.000	0.000	0.000	0.000	0.000
	LM19	0.000	6.401	0.000	3.722	0.497	6.084	1.492	1.290	0.000	5.334	0.000	3.102	0.414	5.070	1.244	1.075
	LM6	4.472	1.243	3.814	1.325	0.780	0.620	1.735	0.186	3.727	1.036	3.178	1.104	0.650	0.517	1.446	0.155
	LM12	0.000	0.000	0.000	0.000	0.000	0.000	0.000	0.000	0.000	0.000	0.000	0.000	0.000	0.000	0.000	0.000
	LM26	4.146	6.122	0.000	3.726	0.865	5.629	4.688	4.162	3.455	5.102	0.000	3.105	0.720	4.691	3.907	3.469
	LM13	9.593	8.067	4.352	0.116	2.330	3.070	2.183	2.052	7.994	6.722	3.627	0.097	1.942	2.558	1.820	1.710
	LM16	0.000	0.000	0.000	0.000	0.000	0.000	0.000	0.000	0.000	0.000	0.000	0.000	0.000	0.000	0.000	0.000
	LM11	1.920	6.824	5.630	1.787	2.314	8.795	6.624	3.000	1.600	5.687	4.692	1.489	1.929	7.329	5.520	2.500
	LM25	2.162	7.881	4.088	1.099	1.267	7.854	6.707	3.076	1.802	6.567	3.406	0.916	1.056	6.545	5.589	2.564

Figure 3.16 Heat map of the standard deviations associated with the analysis of cell wall polysaccharides throughout a field development study in Figure 3.15. The standard deviations between the biological replicates analysed for the detection of nine cell wall polymer epitopes detected by monoclonal antibodies throughout development over three growing seasons as identified by CoMPP. Two extraction fractions have been assessed CDTA (Cyclohexanediaminetetraacetic Acid) and NaOH (Sodium hydroxide). The intensity of the green indicates larger standard deviations between biological replicates.

An additional 16 mAbs were selected which covered a wide range of cell wall polymers (Fig 3.17) and were used for a screen using the CoMPP protocol gave an opportunity to learn more about the sugar beet storage root cell wall composition throughout development. JIM4 (AGP) and LM9 (feruloylated galactan) mAbs gave no detection signal across the two fractions in all three seasons. The LM9 antibody was recently showing discrepancies in functionality over several different studies in different systems therefore this could have accounted for the lack of signal in this instance.

In the CDTA fraction; JIM5 detects the same epitope as LM19 (Homogalacturonan with no esterification) and therefore showed a similar

detection pattern with a slightly higher mid-range detection across the whole season for all three years with the exception of harvest 3 in 2010 where there was a spike in the relative abundance of the JIM5 epitope. LM18 again detects a similar homogalacturonan epitope and therefore showed the same consistent detection in the CDTA fraction across the whole season in all three years with the 2010 season showing a slight reduction in relative abundance towards the end of the growing season.

LM5 detecting galactan showed the same pattern in all three growing seasons in the CDTA fraction with a high relative abundance of the epitope in harvest 2, gradually reducing over the growing season with the lowest level of relative abundance detected in harvest 16. A similar pattern of relative abundance of the LM5 epitope was detected in all three seasons for the KOH fraction with a slightly reduced relative abundance level than that detected in the CDTA fraction.

The LM21 epitope (heteromannan) was detected in both the CDTA and KOH fraction with a fairly consistent relative abundance level across all harvests in all seasons for the CDTA fraction. However, the KOH fraction showed a slightly reduced relative abundance of the LM21 epitope in the 2009 season and a much reduced detection of the epitope in the 2010 and 2011 seasons.

The LM15 (xyloglucan) epitope was only detected in the KOH fraction just as the LM25 epitope was in the previous set of mAbs. However, in the case of LM15 the relative abundance levels remained consistent across all the harvest for all three growing seasons.

LM10 (xylan) was also only detected in the KOH fraction in all three seasons where there was a similar pattern in relative abundance detection to LM11 but at a lower level of detection. There was higher detection of the LM10 epitope at the beginning and the end of the growing seasons with a reduction at harvest 5 and 7 followed by an increase with the highest level of detection at harvest 15 and 16 for all seasons.

LM1 and JIM20 both detect extensin and therefore showed similar detection patterning throughout the growing seasons. There was seasonal variation in the

detection of extensin in the CDTA fraction with the 2009 season showing a rise in relative abundance between harvest 2 and 3 followed by a slight reduction at harvest 5 and then an increase at harvest 7 then a decrease over the rest of the season with very low levels detected at harvest 15 and 16. Initially 2010 showed a similar rise and fall pattern in the epitope detection however the relative abundance levels dropped off after harvest 7 with low levels detected from harvest 13 onwards. The 2011 seasons showed variation in LM1 and JIM20 epitope detection with a steady reduction in relative abundance from harvest 2 through to harvest 5 followed by an increase back to harvest 2 levels at harvest 7 with another fall in relative abundance and a rise at harvest 12 and 13 respectively. However season 2011 showed the same very low levels of epitope abundance in the final two harvest points.

LM2 and LM16 (AGP) detected their epitope at low levels throughout all harvests of all three seasons in the CDTA fraction with the highest relative abundance detected in harvest 2 and decreasing over the growing season. There was a slight peak in the detection of the LM2 epitope at harvest 12 and 13 in the KOH fraction for each of the three growing seasons. JIM13 (AGP) indicated a consistent detection of epitope in both the CDTA and KOH fractions across all harvest points, with CDTA having a higher relative abundance level than KOH throughout. LM28 (glucuronoxylan) was only detected in the final two harvests of the CDTA fraction in all growing seasons with 2009 and 2010 showing a peak at harvest 15 followed by a large decrease at harvest 16, the detected levels were relatively very low in the 2011 season.

The LM28 epitope of glucuronoxylan was detected throughout all harvests for all growing seasons with detection being at a consistent level until an increase in the final two harvests, this increase was the largest in 2009 and 2010 with the increase being less in the 2011 growing season.

LM6-M (arabinan) detected similarly to LM6 but showed a higher level of relative abundance than LM6. The detection of the LM6-M epitope is fairly level throughout the harvest points in the CDTA fraction in all three growing seasons with a slight decrease in relative abundance in harvest 15 and 16. A similar

pattern of LM6-M epitope detection is identified in the KOH fraction for all seasons with the detection being at a slightly reduced level of relative abundance. LM30 epitope detection was at very low levels throughout both the CDTA and KOH fraction at all harvests in all growing seasons.

The standard deviations (SD) associated with the data displayed in Figure 3.17 are shown in Figure 3.18. Using these SD the significance of the data in Fig 3.17 can be assessed. As in the SDs of the previous antibodies used in Fig 3.15 the largest SD are seen in the 2009 season. However, there is only one instance of where the SD alters the results significance in Figure 3.17. LM5 in the CDTA fraction in the 2009 season does not fluctuate as indicated by the reduction of green intensity towards the end of the season The SD for the detecton of LM5 across the growing season show that there is not significant difference in the detect levels across the growing season. Other than this example, the fluctuations of detected epitope levels shown in Fig 3.17 are significant.

		CDTA								KOH							
Season	MAb	Harvest number								Harvest number							
		2	3	5	7	12	13	15	16	2	3	5	7	12	13	15	16
2009	JIM5	31.30	29.40	29.00	25.60	24.70	29.80	27.20	34.40	0.00	0.00	0.00	0.00	0.00	0.00	0.00	0.00
	LM18	19.10	18.20	17.60	16.50	17.30	19.90	16.90	22.90	4.00	0.00	0.00	0.00	0.00	0.00	0.00	0.00
	LM5	42.50	39.60	30.40	28.10	20.90	23.60	15.50	10.70	41.70	25.20	15.00	22.80	17.30	15.10	12.40	11.90
	LM21	36.30	32.80	35.30	36.50	43.00	46.20	37.50	34.80	23.40	19.50	17.60	23.30	24.80	22.00	21.90	18.70
	LM15	0.00	0.00	0.00	0.00	0.00	0.00	0.00	0.00	35.00	33.00	28.70	30.40	32.70	33.90	32.30	30.50
	LM10	0.00	0.00	0.00	0.00	0.00	0.00	0.00	0.00	34.90	29.40	26.30	30.60	30.70	29.40	46.20	39.80
	LM1	15.10	24.20	19.30	26.10	19.00	14.60	5.90	4.30	8.70	9.80	9.60	13.30	12.30	9.30	5.10	5.30
	JIM20	18.20	32.00	24.10	32.10	22.20	17.60	5.60	4.20	11.10	12.50	12.00	13.50	13.70	11.20	8.50	8.90
	LM2	31.60	21.30	12.20	10.10	9.20	12.50	8.70	9.40	7.40	0.00	0.00	0.00	9.30	5.90	0.00	4.60
	JIM4	0.00	0.00	0.00	0.00	0.00	0.00	0.00	0.00	0.00	0.00	0.00	0.00	0.00	0.00	0.00	0.00
	JIM13	35.80	32.90	35.30	36.60	41.90	46.10	37.50	35.00	23.30	19.60	17.60	23.20	24.60	22.30	21.80	18.70
	JIM16	18.30	10.70	5.80	9.10	10.90	9.20	2.30	1.90	0.00	3.90	0.00	0.00	0.00	0.00	0.00	0.00
	LM9	0.00	0.00	0.00	0.00	0.00	0.00	0.00	0.00	0.00	0.00	0.00	0.00	0.00	0.00	0.00	0.00
	LM28	0.00	0.00	0.00	0.00	0.00	0.00	31.00	12.10	44.80	41.50	37.80	45.90	42.40	41.10	74.70	73.10
	LM6-M	61.00	70.00	62.30	55.10	54.80	57.80	41.00	34.80	49.70	40.00	29.10	39.70	35.30	33.40	26.80	24.90
	LM30	0.00	0.00	0.00	0.00	0.00	0.00	2.20	1.70	4.30	1.80	4.10	0.00	6.70	5.60	4.60	4.10
2010	JIM5	28.80	71.50	31.70	26.90	23.70	23.20	20.70	22.10	0.00	0.00	0.00	0.00	0.00	0.00	0.00	0.00
	LM18	19.20	39.20	20.30	16.20	14.60	13.10	11.60	12.20	0.00	0.00	0.00	0.00	0.00	0.00	0.00	0.00
	LM5	43.70	23.40	29.80	29.40	18.30	19.30	18.90	16.00	32.50	15.10	29.50	20.50	16.80	16.00	11.90	12.80
	LM21	35.90	38.60	37.90	44.30	46.80	44.80	38.60	28.10	10.80	13.40	18.40	21.60	28.50	23.60	17.30	17.50
	LM15	0.00	0.00	0.00	0.00	0.00	0.00	0.00	0.00	31.60	36.90	33.90	28.10	30.40	34.90	30.70	33.50
	LM10	0.00	0.00	0.00	0.00	0.00	0.00	0.00	0.00	32.50	27.00	22.20	19.20	24.20	31.50	44.50	43.30
	LM1	26.60	10.80	27.10	23.80	11.20	10.40	9.80	5.40	7.10	8.20	10.00	11.60	11.00	10.90	9.70	1.90
	JIM20	38.80	13.40	38.80	31.20	14.90	13.60	13.10	6.50	8.30	8.00	9.70	11.10	11.30	11.30	10.20	4.10
	LM2	29.80	24.70	17.50	15.70	14.50	13.80	13.30	9.00	0.00	3.70	0.00	0.00	21.90	17.90	6.80	6.20
	JIM4	0.00	0.00	0.00	0.00	0.00	0.00	0.00	0.00	0.00	0.00	0.00	0.00	0.00	0.00	0.00	0.00
	JIM13	35.80	38.40	37.90	44.40	46.70	44.70	38.60	28.20	10.90	13.50	18.80	21.40	29.20	26.30	20.30	20.50
	JIM16	24.20	8.00	8.20	8.90	7.50	6.10	6.30	4.00	0.00	0.00	0.00	0.00	0.00	0.00	0.00	0.00
	LM9	0.00	0.00	0.00	0.00	0.00	0.00	0.00	0.00	0.00	0.00	0.00	0.00	0.00	0.00	0.00	0.00
	LM28	0.00	0.00	0.00	0.00	0.00	0.00	36.00	4.80	41.50	44.80	37.50	32.60	35.30	42.10	75.90	86.20
	LM6-M	66.80	45.90	62.70	63.00	59.40	58.10	49.60	46.80	45.80	26.30	46.00	36.80	42.40	40.00	25.90	25.50
	LM30	0.00	0.00	0.00	0.00	8.90	5.90	0.00	0.00	0.00	0.00	3.60	0.00	16.00	11.60	4.60	2.50
2011	JIM5	32.50	29.00	29.30	24.10	30.00	24.50	26.10	27.60	0.00	0.00	0.00	0.00	0.00	0.00	0.00	0.00
	LM18	20.30	15.50	16.90	15.20	16.80	12.80	14.30	16.60	0.00	0.00	0.00	0.00	0.00	0.00	0.00	0.00
	LM5	41.20	29.00	27.00	25.30	21.20	24.20	20.70	16.40	27.40	20.70	16.40	17.70	15.50	16.00	14.80	13.00
	LM21	33.70	35.60	34.30	36.70	42.40	39.90	42.10	38.60	9.80	15.50	14.70	17.30	24.30	20.00	20.20	17.90
	LM15	0.00	0.00	0.00	0.00	0.00	0.00	0.00	0.00	32.00	31.80	30.60	31.50	31.60	30.30	31.30	28.80
	LM10	0.00	0.00	0.00	0.00	0.00	0.00	0.00	0.00	29.20	26.00	25.70	26.70	21.50	27.00	30.40	32.40
	LM1	28.40	22.00	19.80	31.90	19.00	22.10	7.90	6.50	9.20	11.40	7.80	12.20	11.20	14.70	9.90	10.20
	JIM20	43.80	32.80	29.30	46.50	26.80	33.30	11.40	8.90	8.50	10.10	7.60	10.10	10.40	12.90	9.50	9.60
	LM2	32.10	21.20	13.90	13.20	10.00	16.10	12.10	13.60	3.90	2.90	0.00	1.80	6.10	5.20	4.40	4.00
	JIM4	0.00	0.00	0.00	0.00	0.00	0.00	0.00	0.00	0.00	0.00	0.00	0.00	0.00	0.00	0.00	0.00
	JIM13	33.70	35.50	34.30	36.50	42.30	39.70	42.00	38.30	11.90	16.60	15.10	17.30	24.30	19.90	20.20	17.90
	JIM16	26.20	13.60	9.30	9.50	10.40	10.80	9.20	8.70	0.00	0.00	0.00	0.00	0.00	0.00	0.00	0.00
	LM9	0.00	0.00	0.00	0.00	0.00	0.00	0.00	0.00	0.00	0.00	0.00	0.00	0.00	0.00	0.00	0.00
	LM28	0.00	0.00	0.00	0.00	0.00	0.00	2.50	4.50	36.60	36.70	35.90	39.80	34.40	41.80	44.40	64.20
	LM6-M	62.20	59.70	57.60	58.40	57.70	57.00	52.50	45.10	35.60	33.20	28.50	31.20	31.60	29.70	27.90	23.20
	LM30	0.00	0.00	0.00	0.00	0.00	0.00	0.00	1.70	0.00	3.50	0.00	0.00	0.00	3.60	0.00	2.50

Figure 3.17 Heat map of additional CoMPP analysis of cell wall polysaccharides throughout a developmental field study. The relative abundance of 16 additional cell wall polymer epitopes detected by monoclonal antibodies throughout development over three growing seasons using the CoMPP method. Two extraction fractions have been assessed CDTA (Cyclohexanediaminetetraacetic Acid) and NaOH (Sodium hydroxide). Intensity of green indicates relative abundance. Each point on the heat map is shown as the normalised value of spot density (the highest density is assigned 100 and other values assigned relative to this). Each value on the heat map is the result of the mean of three biological replicates each of which is the mean of three technical replicates.

		CDTA								NaOH							
Season	MAb	Harvest number								Harvest number							
		2	3	5	7	12	13	15	16	2	3	5	7	12	13	15	16
2009	JIM5	6.257	0.000	2.390	0.000	0.000	0.000	0.000	0.000	3.476	0.000	0.000	0.000	0.000	0.000	0.000	0.000
	LM18	8.258	19.676	6.170	24.010	3.418	7.891	2.238	2.234	4.588	10.931	3.428	13.339	1.899	4.384	1.243	1.241
	LM5	1.761	5.081	3.375	24.235	1.555	7.259	13.609	5.320	0.979	2.823	1.875	13.464	0.864	4.033	7.561	2.955
	LM21	3.244	3.387	5.104	31.924	2.564	1.561	3.030	3.591	1.802	1.881	2.836	17.736	1.424	0.867	1.684	1.995
	LM15	3.761	3.338	5.695	31.865	13.383	5.415	18.878	10.815	2.089	1.855	3.164	17.703	7.435	3.008	10.488	6.008
	LM10	0.667	3.082	0.612	13.797	3.155	0.779	8.196	8.657	0.371	1.712	0.340	7.665	1.753	0.433	4.553	4.809
	LM1	0.197	4.259	1.349	14.012	2.638	1.313	3.144	2.702	0.109	2.366	0.749	7.784	1.465	0.730	1.747	1.501
	JIM20	1.347	0.000	0.000	0.000	3.357	9.207	0.000	7.745	0.749	0.000	0.000	0.000	1.865	5.115	0.000	4.303
	LM2	0.000	0.000	0.000	0.000	0.000	0.000	0.000	0.000	0.000	0.000	0.000	0.000	0.000	0.000	0.000	0.000
	JIM4	1.618	5.177	3.234	24.083	1.770	7.305	13.698	5.329	0.899	2.876	1.797	13.379	0.983	4.058	7.610	2.961
	JIM13	0.000	6.165	0.000	0.000	0.000	0.000	0.000	0.000	0.000	3.425	0.000	0.000	0.000	0.000	0.000	0.000
	JIM16	0.000	0.000	0.000	0.000	0.000	0.000	0.000	0.000	0.000	0.000	0.000	0.000	0.000	0.000	0.000	0.000
	LM9	7.536	6.850	15.314	47.718	19.953	3.070	39.439	25.140	4.187	3.805	8.508	26.510	11.085	1.706	21.911	13.967
	LM28	7.433	23.612	11.529	41.455	4.147	13.050	6.287	5.133	4.129	13.118	6.405	23.030	2.304	7.250	3.493	2.851
	LM6-M	6.739	5.618	12.667	0.000	1.810	8.807	14.215	12.772	3.744	3.121	7.037	0.000	1.006	4.893	7.897	7.095
	LM30	0.000	11.019	0.000	0.000	0.000	11.278	0.000	7.801	0.000	6.122	0.000	0.000	0.000	6.266	0.000	4.334
2010	JIM5	0.000	0.000	0.000	0.000	1.400	0.000	0.000	0.000	0.000	0.000	0.000	0.000	0.000	0.000	0.000	0.000
	LM18	6.502	4.875	1.877	3.630	9.773	5.505	2.116	3.705	4.645	3.482	1.341	2.593	6.981	3.932	1.511	2.647
	LM5	2.134	1.144	1.549	2.175	4.746	2.738	3.482	3.626	1.524	0.817	1.106	1.553	3.390	1.956	2.487	2.590
	LM21	0.950	3.419	5.648	2.298	4.321	3.893	3.068	1.282	0.678	2.442	4.034	1.641	3.087	2.781	2.191	0.915
	LM15	1.797	6.178	4.542	5.171	5.097	2.282	10.539	4.261	1.284	4.413	3.244	3.694	3.640	1.630	7.528	3.044
	LM10	0.843	0.449	1.441	1.477	0.595	3.003	2.193	4.554	0.602	0.321	1.030	1.055	0.425	2.145	1.567	3.253
	LM1	1.592	1.107	2.063	1.470	0.619	2.748	1.570	5.036	1.137	0.790	1.474	1.050	0.442	1.963	1.122	3.597
	JIM20	0.000	4.477	0.000	0.000	0.248	16.582	3.022	1.110	0.000	3.198	0.000	0.000	0.177	11.845	2.159	0.793
	LM2	0.000	0.000	0.000	0.000	0.000	0.000	0.000	0.000	0.000	0.000	0.000	0.000	0.000	0.000	0.000	0.000
	JIM4	1.946	0.994	1.652	1.764	5.114	3.967	3.813	4.101	1.390	0.710	1.180	1.260	3.653	2.833	2.724	2.929
	JIM13	0.000	0.000	0.000	0.000	0.000	0.000	0.000	0.000	0.000	0.000	0.000	0.000	0.000	0.000	0.000	0.000
	JIM16	0.000	0.000	0.000	0.000	0.000	0.000	2.300	0.000	0.000	0.000	0.000	0.000	0.000	0.000	0.000	0.000
	LM9	8.956	3.227	3.565	4.489	8.005	3.672	6.038	14.325	6.397	2.305	2.546	3.207	5.718	2.623	4.313	10.232
	LM28	10.677	3.471	5.483	5.052	6.104	7.771	3.077	4.176	7.626	2.480	3.916	3.609	4.360	5.551	2.198	2.983
	LM6-M	0.000	0.000	8.789	0.000	10.312	21.610	11.236	5.996	0.000	0.000	6.278	0.000	7.366	15.436	8.026	4.283
	LM30	0.000	8.571	0.000	0.000	0.000	8.772	0.000	6.068	0.000	6.122	0.000	0.000	0.000	6.266	0.000	4.334
2011	JIM5	0.000	0.000	0.000	0.000	0.000	0.000	0.000	0.000	0.000	0.000	0.000	0.000	0.000	0.000	0.000	0.000
	LM18	0.000	0.000	0.000	0.000	0.000	0.000	0.000	0.000	0.000	0.000	0.000	0.000	0.000	0.000	0.000	0.000
	LM5	1.035	0.959	1.168	0.515	0.681	0.624	0.279	0.067	3.451	3.197	3.895	1.717	2.269	2.080	0.929	0.224
	LM21	0.170	1.715	0.281	0.133	0.290	1.427	0.324	0.233	0.567	5.718	0.938	0.444	0.965	4.756	1.079	0.778
	LM15	0.045	0.551	0.552	0.393	0.784	0.337	0.436	0.409	0.151	1.836	1.841	1.310	2.614	1.122	1.453	1.363
	LM10	0.444	1.780	0.995	0.824	0.551	1.691	0.917	0.472	1.482	5.932	3.317	2.746	1.836	5.638	3.056	1.575
	LM1	0.282	0.827	0.611	0.253	0.909	0.131	0.712	0.406	0.941	2.757	2.038	0.842	3.030	0.435	2.374	1.352
	JIM20	0.045	0.518	0.175	0.220	0.530	0.132	0.579	0.324	0.151	1.728	0.582	0.734	1.767	0.439	1.930	1.080
	LM2	1.036	1.531	0.000	0.932	0.216	1.407	1.172	1.041	3.455	5.102	0.000	3.105	0.720	4.691	3.907	3.469
	JIM4	0.000	0.000	0.000	0.000	0.000	0.000	0.000	0.000	0.000	0.000	0.000	0.000	0.000	0.000	0.000	0.000
	JIM13	0.157	2.291	0.400	0.124	0.359	1.403	0.346	0.221	0.524	7.637	1.333	0.415	1.195	4.677	1.152	0.738
	JIM16	0.000	0.000	0.000	0.000	0.000	0.000	0.000	0.000	0.000	0.000	0.000	0.000	0.000	0.000	0.000	0.000
	LM9	0.000	0.000	0.000	0.000	0.000	0.000	0.000	0.000	0.000	0.000	0.000	0.000	0.000	0.000	0.000	0.000
	LM28	0.686	2.868	1.148	0.436	1.069	3.245	3.475	2.471	2.286	9.560	3.828	1.452	3.562	10.818	11.584	8.235
	LM6-M	1.418	0.887	1.562	0.709	0.371	0.879	0.344	0.190	4.727	2.957	5.207	2.362	1.238	2.930	1.148	0.635
	LM30	0.000	1.837	0.000	0.000	0.000	1.880	0.000	1.300	0.000	6.122	0.000	0.000	0.000	6.266	0.000	4.334

Figure 3.18 Heat map of the standard deviations associated with the analysis of cell wall polysaccharides throughout a field development study in Figure 3.17. The standard deviations between the biological replicates analysed for the detection of 16 additional cell wall polymer epitopes detected by monoclonal antibodies throughout development over three growing seasons as identified by CoMPP. Two extraction fractions have been assessed CDTA (Cyclohexanediaminetetraacetic Acid) and NaOH (Sodium hydroxide). The intensity of the green indicates larger standard deviations between biological replicates.

3.4 Discussion

3.4.1 Sugar beet storage root anatomy is connected to relative sucrose content

The results of the successive cambium study expanded on the findings of Artschwager (1926). Root diameter increases due to cell division and cell expansion taking place between cambial rings increasing the distance between the rings until they are more or less equidistant, with the exception of the rings closest to the periphery of the root. This study also showed that the vascular rings in a mature root are lain down during the early seedling development discussed in this chapter. The number of cambial rings is also a contributing factor in sucrose concentration as lines of *Beta* with higher sucrose content have an increased number of cambial rings, the SOPHIA line has up to eight additional cambial rings whereas the garden beet (W375B) has a maximum of 6 showing that an increased cambial ring number is a feature of storage root which the potential for increased sugar beet sucrose yield. Using C869 as a representative of sugar beet that isn't a commercial variety shows that the selective breeding programmes that have produced the Sophia line for increased sucrose concentrations in the storage root have led to the addition of cambial rings.

3.4.2 Detection of cell wall polysaccharides throughout development

The cell wall is not a static structure and can therefore change composition in response to developmental stimuli, this has been shown clearly in the field development study where the relative abundance of certain epitopes either fluctuates over the growth period or maintains at a specific level of relative abundance, in addition seasonal variation demonstrates that the cell wall can also respond to environmental signals. The epitopes which had little fluctuation in the relative abundance throughout the harvest points are those involved in the general wall structure and are required for cell division and expansion, for example the homogalacturonan (HG) epitopes detected the back bone of the pectin macromolecule and are required for general plant growth and allows primary cell wall expansion, therefore this would be a polysaccharide key to the maturation of the root as cells expand to increase root yield. In addition the epitope which detects feruloyation of pectin (LM12) are also involved in the

structural integrity of the cells and cell adhesion (Oosterveld et al., 2000, Oosterveld et al., 1997) and therefore are necessary to ensure the overall strength and shape of the root throughout all developmental stages. These structural epitopes will remain with the same relative abundance throughout harvest points as more of the polysaccharide is produced to accommodate root growth.

Some epitopes are associated with pectin but have a role in cell wall flexibility and adhesion (Moore et al., 2008, Ralet et al., 2008). These epitopes are usually associated with rhamnogalacturonan I (RGI) and form branches of galactan (LM5) or arabinan (LM6, LM13, LM16, LM6-M). Flexibility is important while the root is expanding and accumulating sucrose as the cells need to withstand the turgor pressure associated with high sucrose concentrations. After bolting (harvest 15 and 16) the turgor pressure within the storage root is reduced and the cells become more rigid. This is echoed by the fall in galactan and arabinan epitope relative abundance in the final two harvests.

The xylan antibodies (LM10, LM11 and LM28) have shown high epitope detection throughout the growing season, especially at either end of the growing season. This epitope detection patterning supports the cambial work in the previous section where vasculature is lain down in the early stages of development. Higher abundance of the xylan epitope in the early stages is due there being a higher abundance of vasculature in comparison to other tissue types as demonstrated in early seedling development in this Chapter. As the root develops cell division and expansion occurs between the cambial rings to increase root size and accommodate sucrose reducing the abundance of the xylan epitope in the storage root. After vegetative maturity, the root switches into the reproductive phase where some of the biomass in the storage root is converted to produce the elongated stem to allow flower production and therefore once again the relative abundance of the xylan epitope in relation to other cell types is increased.

The relative abundance of extensin epitopes (LM1 and JIM20) show higher signals throughout the vegetative half of the growing season. It would be expected that extensin would be abundant during these stages due to the storage

root expanding during this time to accommodate the accumulating sucrose (Carpita and Gibeaut, 1993, Taiz, 1984). After this expansion the relative levels of extensin drop at harvest point 15 where the root is no longer increasing in size. These epitopes showed the most seasonal variation which the 2010 season showing variation in abundance throughout the harvest points, the 2010 season was colder and had increased rainfall compared to the other two experimental seasons (Fig 3.9), resulting in reduced fresh weight of the sugar beets which grew during this season. The beets for the 2010 season had reduced root yield and therefore did not expand as much as the beets grown in the other two seasons, explaining the variation in relative abundance of the extensin epitopes.

3.4.2.1 A comparison of using ELISA and CoMPP for the analysis of cell wall polysaccharides

Comprehensive microarray polymer profiling, or CoMPP and enzyme linked immunosorbent assay, or ELISA are both widely used in conjunction with cell wall component specific monoclonal antibodies (mAbs) for the analysis of the occurrence and relative abundance of plant cell wall glycans. Until now no comparison between the two methods has been made using the same samples for both methods of analysis. In this study sugar beet cell wall material collected throughout a growing season has been analysed using both of the methods. The comparative merits of both procedures have been evaluated as methods of cell wall component detection and ability to profile cell wall structures and changes throughout the growing season.

An advantage of using CoMPP as a tool for profiling cell wall glycans is that is it possible to screen large sample groups many mAbs at the same time, due to the semi-automated method of the procedure. When conducting ELISAs for the samples discussed in this study the number of mAbs used was limited to about twelve due to time and space restraints, however up to thirty mAbs can be probed in one run of CoMPP (Fig 3.13). The larger screen has allowed for the assessment of interesting epitope abundance changes throughout the growing season.

Doing a large initial screen of antibodies is a useful way to utilise the high throughput nature of CoMPP. When conducting an ELISA protocol it is the norm to select the mAbs considered to be of most interest, however this could lead to missing interesting results which can be obtained through a larger screen.

While being able to using a larger screen has its advantages it is clear that the two protocols produce comparable results which have higher and lower affinity to the epitopes. The CoMPP method uses a cut-off point of 5% where any signal below this point is regarded as no signal and reported as 0.00. The ELISA protocol does not usually use a cut off and any signal above the background level is considered a true result, this could allow for subtle results to be picked up where they may have not been using the CoMPP method where background is removed before the 5% cut off is applied.

The CoMPP method is a very useful tool if a large number of samples need to be analysed as it is very easy to screen many samples with many mAbs in a relatively short timeframe. This method allows the user to identify interesting results very quickly so that they could then be assessed further. The ELISA method is much slower and less high throughput than the CoMPP method, however it is much easier to pick up subtle differences within an analysis making this useful to use if you need a more sensitive analysis of samples.

Chapter 4

Characterisation of a phloem sieve element specific antibody (LM26)

4.1 Introduction

To assess the potential sucrose yield of sugar beet storage roots this project has identified key structures within the storage root anatomy utilising the previously characterised mAb LM11. However in this analysis it is difficult to identify the tissues responsible for the translocation of sucrose to the root, the phloem. The ability to identifying these cell types is important in the understanding of phloem tissue location and cellular structure *in situ*, and how this dictates sucrose yield. There are currently no known markers for phloem sieve elements and therefore the identification of phloem cells and the positioning of these has previously been a challenge. This was an important challenge to overcome in this project as the abundance and positioning of phloem in sugar beet storage roots is an indicator of potential sucrose yield and an identifier for breeding targets to increase sucrose yield.

The study of plant developmental anatomy requires analyses which leave plant material in-tact allowing visualisation and tracking of anatomical changes over time. While chemical analysis of plant material can give insight into the composition and relative abundance of cell wall polysaccharides of plant cell walls over time these analyses relies on the complete destruction of any anatomical structures and therefore cannot give insight into the spatial positioning of these polysaccharides *in muro*. Monoclonal antibodies (mAbs) in combination with immunofluorescence microscopy allow the detection of cell wall polysaccharides *in situ* and in context of the associated tissue. Although this is an effective and widely used technique for the analysis of plant cell walls it relies on the availability of appropriate mAbs directed to specific epitopes of interest. Once mAbs are characterised and their binding specificities known they can be used in the assessment of the function and location of their respective specific cell wall structures. Currently there is a wide range of mAbs available for the detection of a diverse range of cell wall polysaccharides including those described in Fig 1.1. Despite the vast number of mAbs available, use to identify specific cell types is uncommon, this is due to cell wall polysaccharides being rarely limited to one cell type and binding patterning varying between species and taxonomic groups. An

exception are mAbs directed to heteroxylan which bind specifically to xylem vessels due to the heteroxylan rich secondary cell walls (McCartney et al., 2005).

The identification, characterisation and use of the monoclonal antibody designated LM26 are described in this chapter. The use of several analytic techniques described here show LM26 as a novel tool for the study of plant vascular anatomy with specificity to phloem sieve elements.

4.2 Materials and methods

Fluorescence microscopy of sugar beet and garlic blubs was conducted by the author as described in chapter 2. TEM microscopy and images of LM26 binding in sugar beet were supplied by Rebecca Lauder at Rothamsted research.

Glycan microarrays were provided by Mads Clausen at the technical university of Copenhagen.

Epitope detection chromatography was conducted as described in chapter 2 by the author using shop bought garlic bulb material extracted at the University of Leeds.

4.3 Results

4.3.1 Monoclonal antibody LM26 binds specifically to phloem sieve elements in a range of plant organs including sugar beet roots

The antibody designated LM26 which was secreted by a cell line arising from the immunization which led to the pectic homogalacturonan directed Mab LM7 (Willats et al., 2001), was found to bind to plant cell walls. Specifically LM26 bound to phloem sieve elements (Fig 4.1). Shown in Fig 4.1 specificity to phloem sieve elements can be identified by the presence of 'filled' companion cells with high cytoplasmic content which are associated with the cells which are bound by LM26. A range of plant species other than sugar beet show phloem specific binding of LM26 including *Arabidopsis thaliana* stems, tomato petiole and Miscanthus stems (Fig 4.2). The LM26 antibody was used to probe mature sugar beet storage root cross sections to identify binding specificity. Calcofluor White was applied to all antibody labelled sections, labelling all β-glycan linkages in plant cell walls to produce blue fluorescence when UV is applied. The Calcofluor white stain provides a structural over view of all cell walls in the sections allowing the positioning of the bound cells to be identified. The combination of monoclonal antibody binding specificity and Calcofluor white staining allows a clear view of the sugar beet storage root supernumerary cambial arrangement (Fig 4.3). In this arrangement the phloem sieve elements highlighted in the green are situated outside of its associated xylem tissue, as identified by the thickened cell walls stained with Calcofluor white coloured blue, under UV radiation. Using immunogold labelling in combination with transmission electron microscopy (TEM) (Fig 4.4) indicates that the LM26 epitope is located adjacent to the plasma membrane, as shown by the black particles restricted to the inner surface of the cell wall.

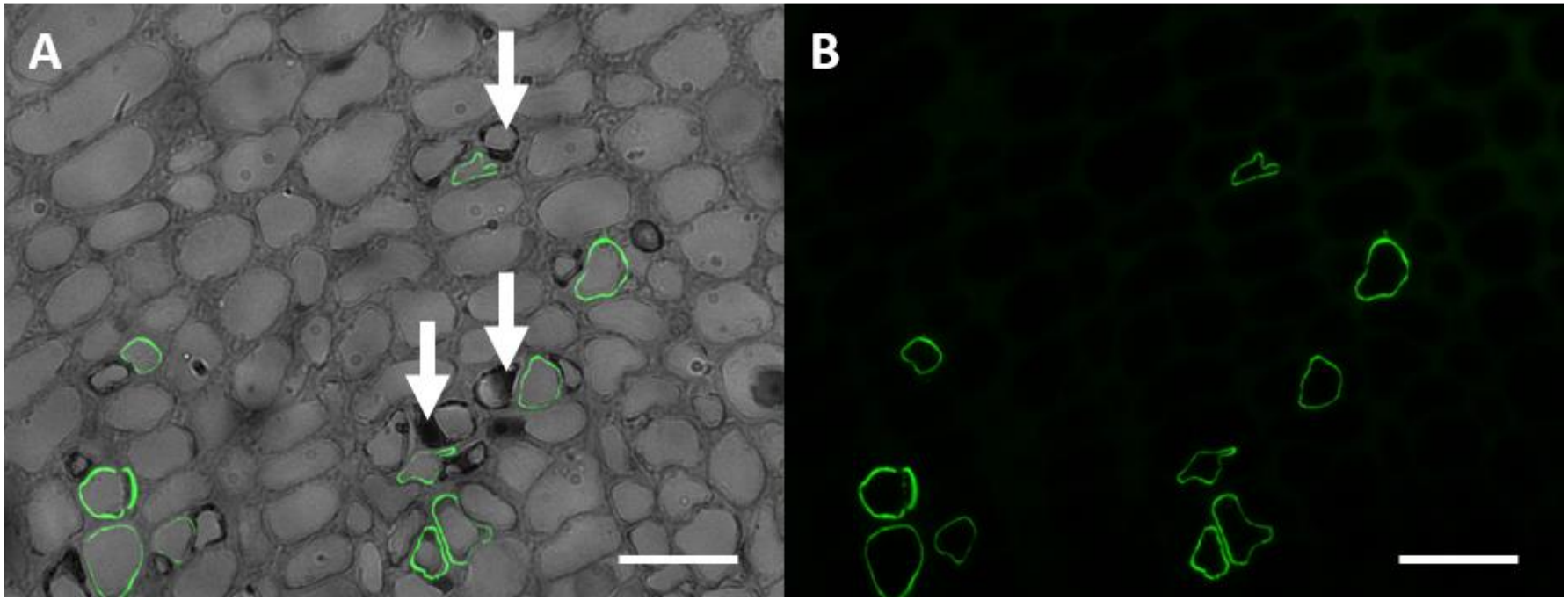

Figure 4.1 *in situ* analysis of LM26 binding to *Beta vulgaris* L. (sugar beet). *In situ* indirect immunofluorescence analysis of LM26 binding to transverse sections of resin embedded sugar beet storage root. A) Combined bright field and indirect immunofluorescence (green FITC) detection of LM26 binding to phloem sieve elements. B) Immunofluorescence (green FITC) of LM26 binding. Arrows indicate associated companion cells. Scale bars = 20 µm

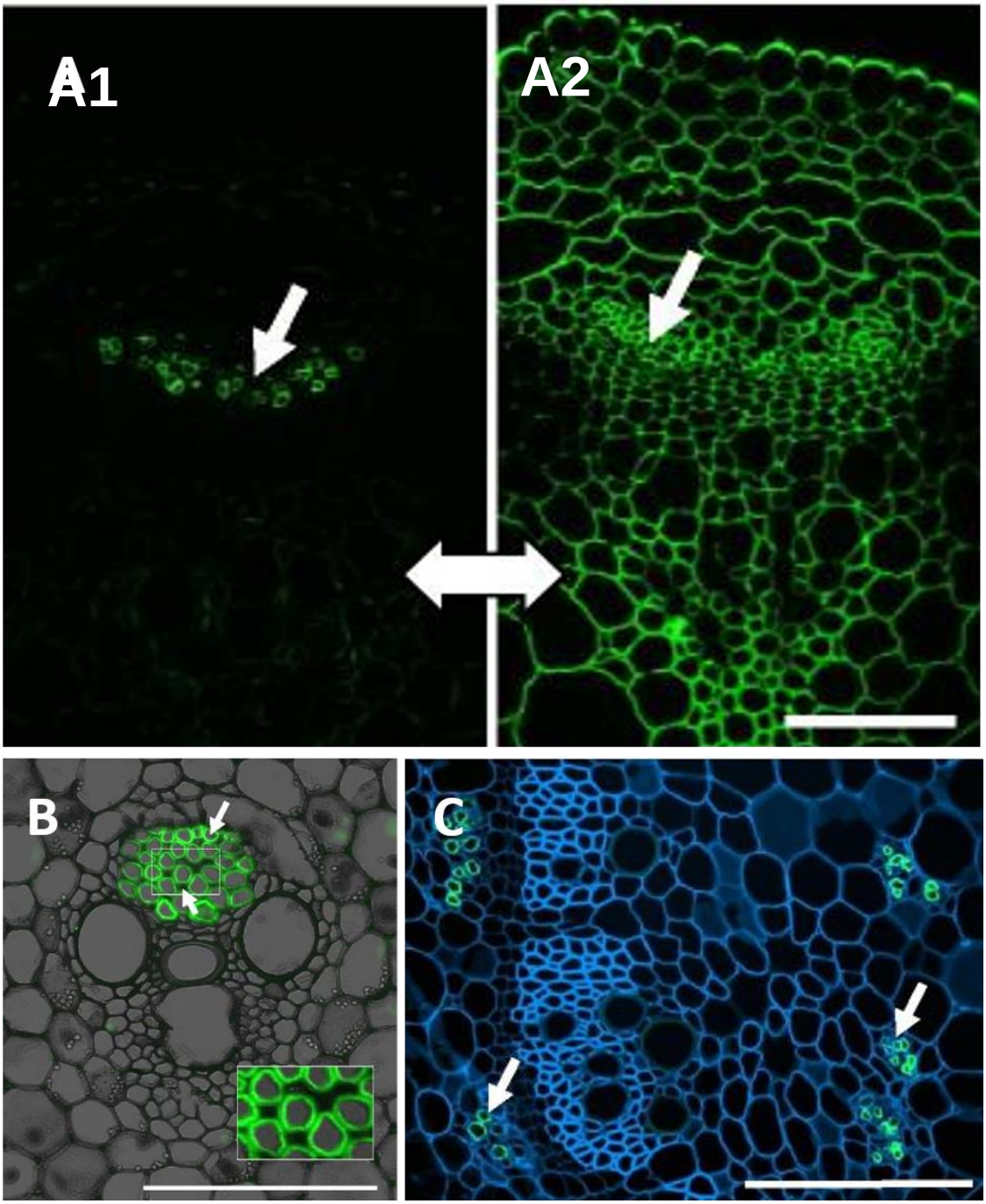

Figure 4.2 *in situ* analysis of LM26 binding patterns. *In situ* indirect immunofluorescence analysis of LM26 binding to transverse sections of resin embedded; A1) *Arabidopsis thaliana* inflorescence stem, B) *Miscanthus x giganteus* stem, C) Tomato leaf petiole. In all cases LM26 binds specifically to phloem sieve elements, indicated by single headed arrows. A2) immunolabelling of LM5 in *A. thaliana* shown for comparison, binding to all cell types (including phloem sieve elements). For *M. x giganteus* LM26 binding has been combined with bright field to show all cell types with a double magnification insert showing the absence of LM26 binding in companion cells. In the case of tomato Calcofluor White (blue fluorescence) is used to stain all cell types. Scale bars = 100 µm. (Images provided by Paul Knox and Sue Marcus, University of Leeds).

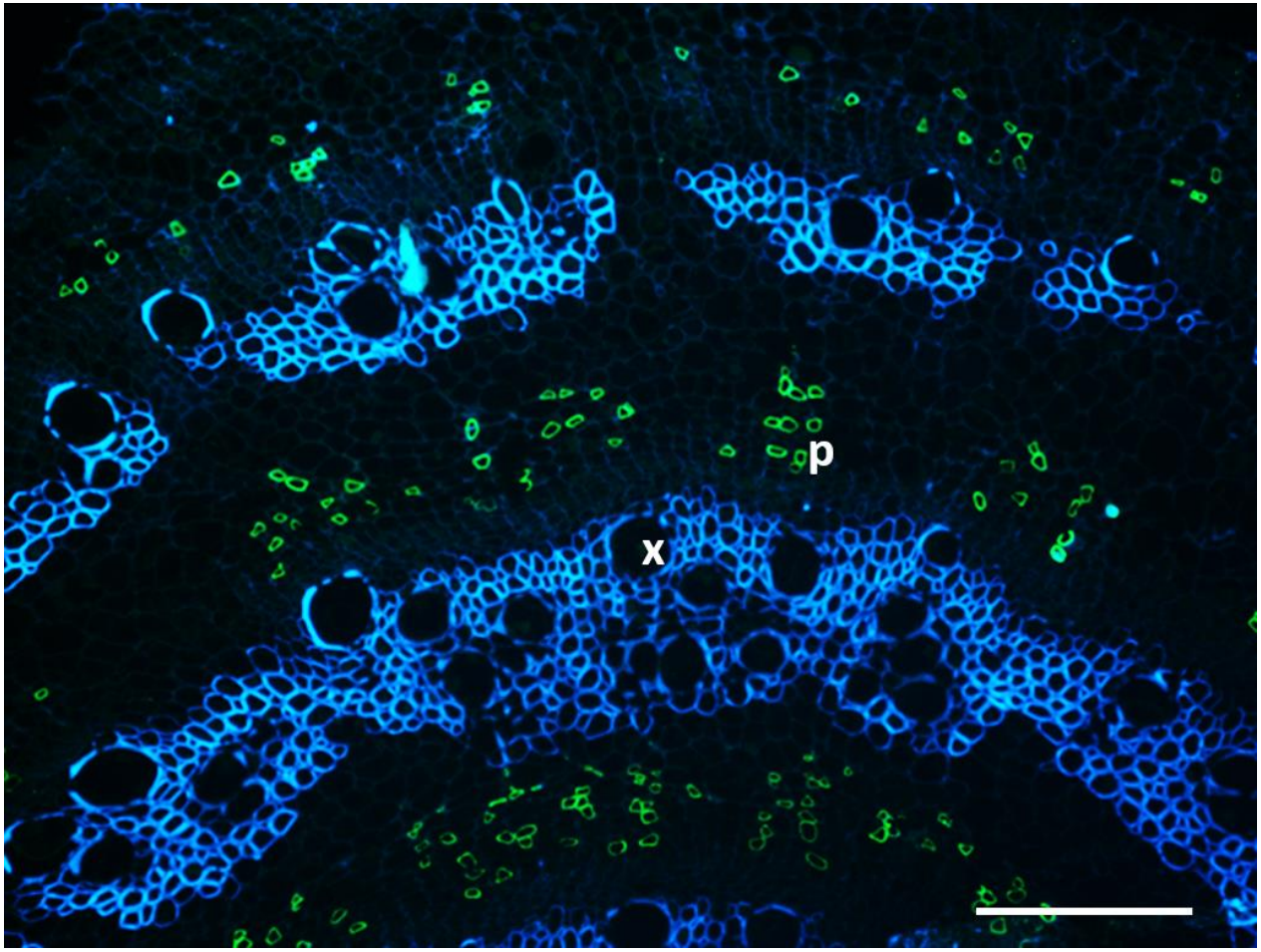

Figure 4.3 Overall vascular anatomy in sugar beet storage root. Combined indirect immunofluorescence (green FITC) detection of LM26 binding to, p; phloem sieve elements in a transverse section of a resin embedded sugar beet storage root with Calcofluor White staining (blue) highlights all cell types with x; xylem vessels highlighted most strongly. Scale bar = 400 µm.

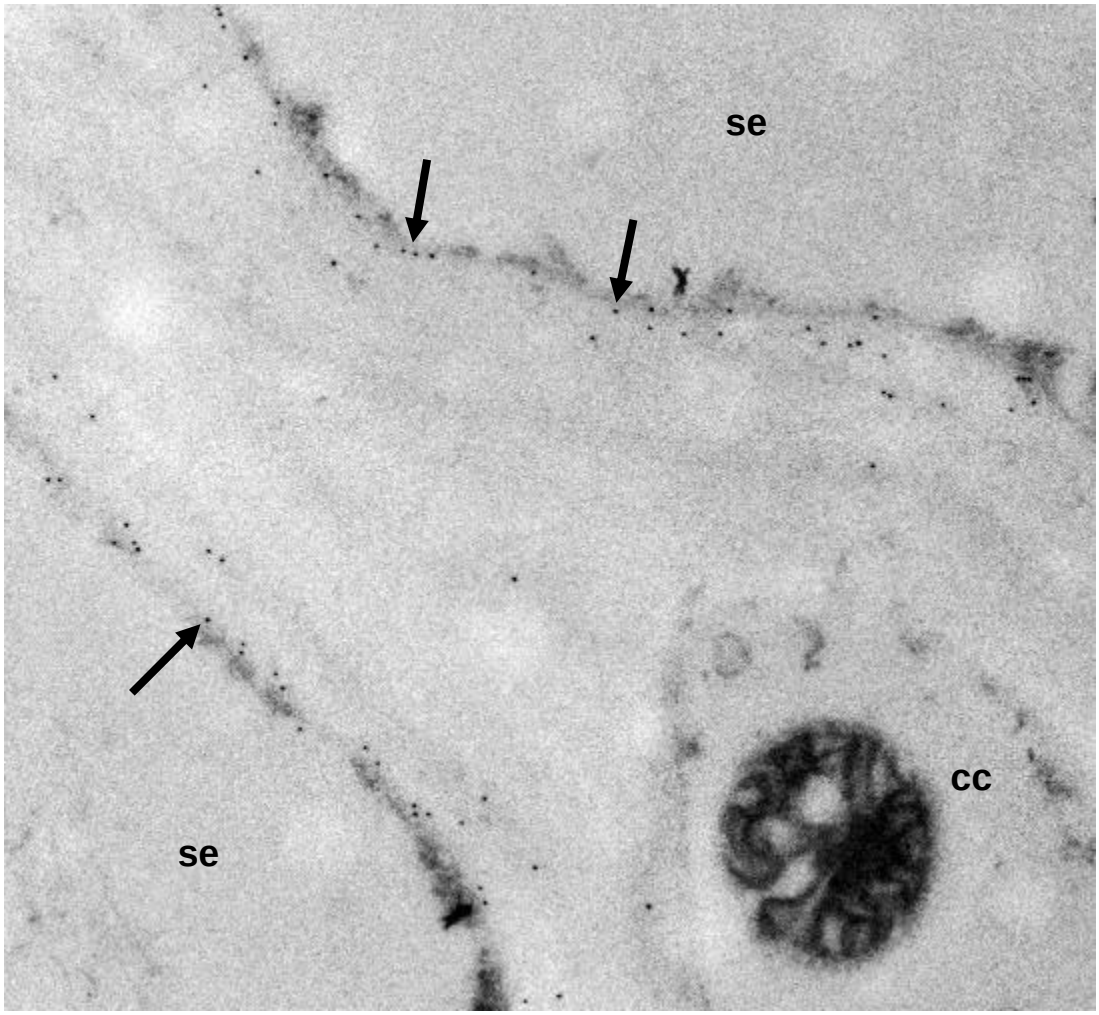

Figure 4.4 Transmission electron microscopy of sugar beet phloem sieve elements. Transmission electron microscopy and immunogold labelling of LM26 binding to phloem sieve elements in sugar beet storage roots. Gold particles (indicated with arrows) are restricted to the inner cell wall adjacent to the plasma membrane of the phloem sieve elements (se). Gold particles are not present in cell walls of neighbouring companion cells (cc). Scale bar = 1.0 µm. Image supplied by Rebecca Lauder (Rothamsted research, Harpenden, UK)

4.3.2 LM26 binds to a β-1,6-galactosyl substitution of pectic β-1,4-galactan

LM26 was used against sets of microarrays of synthetic cell wall associated oligosaccharides, produced at the Technical University of Copenhagen, to determine the epitope recognised by the antibody. The LM26 antibody was found to bind to three related β-1,4-galactosides (Fig 4.5), with the most effective recognition of 6-O-(β-Gal)-β-1,4-galactohexose (oligo 12, Fig 4.5). Weaker recognition was identified in oligosaccharides with a longer substitution or a shorter β-1,4-galactan backbone (oligos 10 and 5 respectively, Fig 4.5).

Binding of LM5 was conducted as a comparison to the recognition of LM26, and shows to have recognition specificity restricted to linear β-1,4-galactosides without the substitutions recognised by LM26 and has been previously reported (Andersen et al., 2016a).

Compound	1	2	3	4	5	6	7	8	9	10	11	12
Type	linear oligos				branched oligos							
LM26	0	0	0	0	21	0	0	0	0	18	0	100
LM5	100	81	51	0	0	0	0	0	0	0	0	0

1 β-1,4 galactotriose
2 β-1,4 galactopentaose
3 β-1,4 galactoheptaose
4 α-1,4 Ara*f*-β-1,4 galactohexaose
5 6'-*O*-(β-1,6 Gal)-β-1,4 galactotriose
6 6'-*O*-(α-1,6 Gal)-β-1,4 galactotriose
7 4'-*O*-(α-1,4 Gal)-6'-*O*-(α-1,6 Gal)-β-1,4 galactobiose
8 6'''-*O*-(α-1,6 Ara*f*)-β-1,4 galactohexaose
9 6'''-*O*-(α-1,5 Ara*f*-α-1,6 Ara*f*)-β-1,4 galactohexaose
10 6'''-*O*-(β-1,6 Gal-β-1,6 Gal)-β-1,4 galactohexaose
11 6'''-*O*-(β-1,4 Gal-β-1,6 Gal)-β-1,4 galactohexaose
12 6'''-*O*-(β-1,6 Gal)-β-1,4 galactohexaose

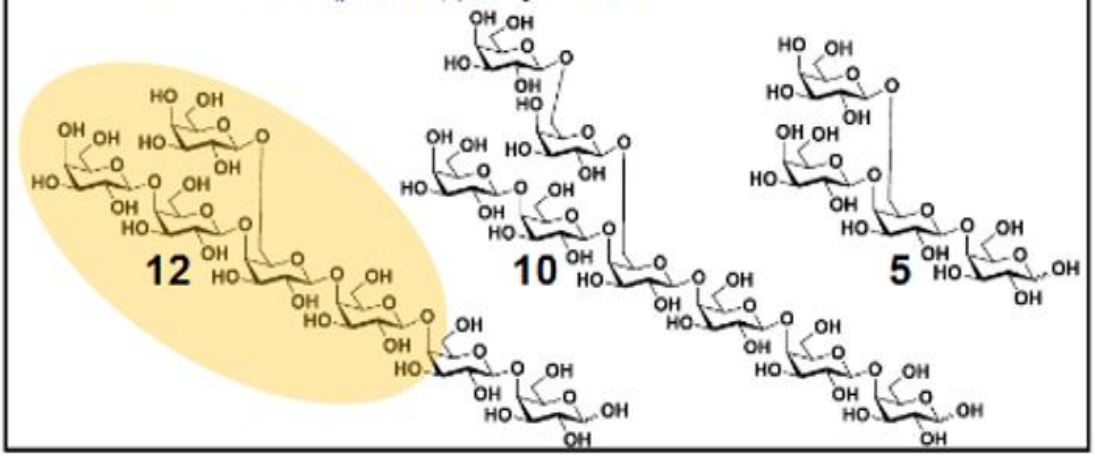

Figure 4.5 Summary of glycan microarray analysis of LM26 the binding specificities of mAbs LM5 and LM26 to synthetic 1,3-galacto-oligosaccharies are shown. The three structures bound by LM26 are shown (Oligos-12, 10 and 5) with the proposed LM26 epitope highlighted in the yellow shaded area. Values are the % of the maximal detectible signal. (Figure provided by Mads Clausen, Technical University Denmark).

4.3.3 LM26 binding occurs in most cell walls of garlic bulbs: an abundant source of the epitope for the characterisation of LM26

The structure identified as the LM26 epitope, β-1,6-galactosyl substitution of β-1,4-galactan, is rare in pectin (Ridley et al., 2001), however it has been identified in garlic bulbs (Das and Das, 1977). Using LM26 to probe garlic bulbs sections indicated that the LM26 epitope is present in most cell walls and not exclusively phloem sieve elements (Fig 4.6). This has provided an abundant source of the LM26 epitope for additional analyses where sufficient material could not be extracted from sugar beet root due to sparsity of the epitope. This source of the LM26 epitope from garlic bulbs has been used to further confirm that the epitope is linked to pectic glycans.

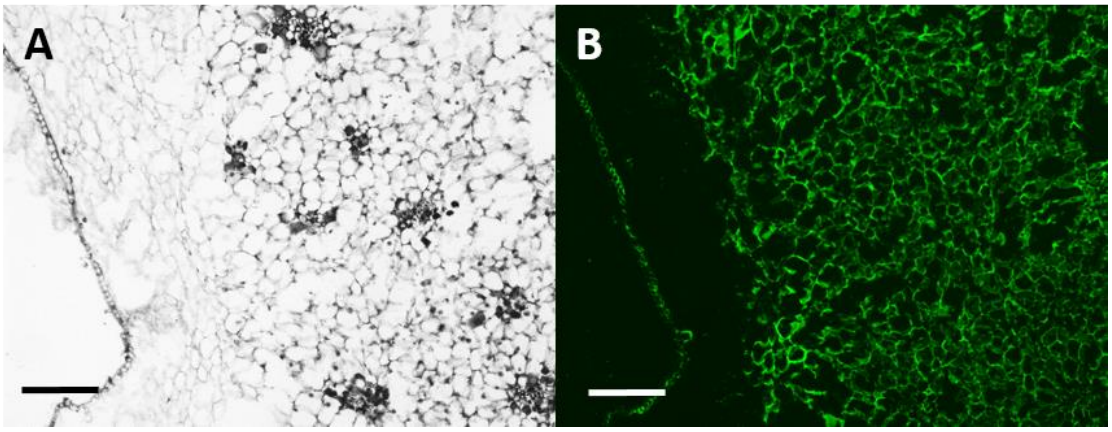

Figure 4.6 LM26 binding in garlic bulbs. A, Bright field micrograph of a transverse section of a wax embedded garlic bulb showing all cells B, Indirect immunofluorescence (green FITC) detection of LM26 binding to most cell walls s in the same section. Scale bar = 300 µm

Further analysis was conducted using LM26 and other cell wall directed mAbs in combination with anion-exchange chromatography to detect the biological associations of cell wall epitopes within the cell wall, a technique developed previously and called epitope detection chromatography (EDC) (Cornuault et al., 2014). After extraction of the garlic bulb AIR, extractions were analysed for relative abundance of the LM26 epitope by ELISA, the first extraction, water was found to have the highest relative abundance of the LM26 epitope and was used for EDC analysis. Fractions were eluted from the anion exchange column using an increasing step salt gradient producing several co-eluting peaks detected using LM26, LM5 and JIM7 (Fig 4.7). The LM26 and LM5 detection show highly similar outputs supporting that the LM26 epitope is associated with a linear galactan backbone as shown in the microarray analysis (Fig 4.5). JIM7 binds to methyl-esterified HG (Clausen et al., 2003), co-elution of LM5 and LM26 with the JIM7 peak suggests that the epitopes are associated with pectic RG-I. LM19 binds to un-esterified HG (Verhertbruggen et al., 2009) an epitope that only elutes at highest salt concentrations, producing one single peak, showing a distinct group of un-esterified HG (Fig 4.6). Running the same EDC protocol after a pre-treatment of an alkali (sodium carbonate, Na_2CO_3) shows the loss of the JIM7 epitope and an increase in the LM19 peak (Fig 4.7), the alkali pre-treatment removes methyl esterification and therefore increases the relative abundance of un-esterified HG. After the de-esterification both the LM26 and LM5 traces showed a shift with a higher elution with the LM19 epitope. However, not all the LM5 and LM26 epitopes co-eluted after the alkali treatment suggesting that not all are associated with HG domains. From this analysis it is clear that the LM26 MAb binds to a substitution of 1,4-galactan with associations to pectic RG-I.

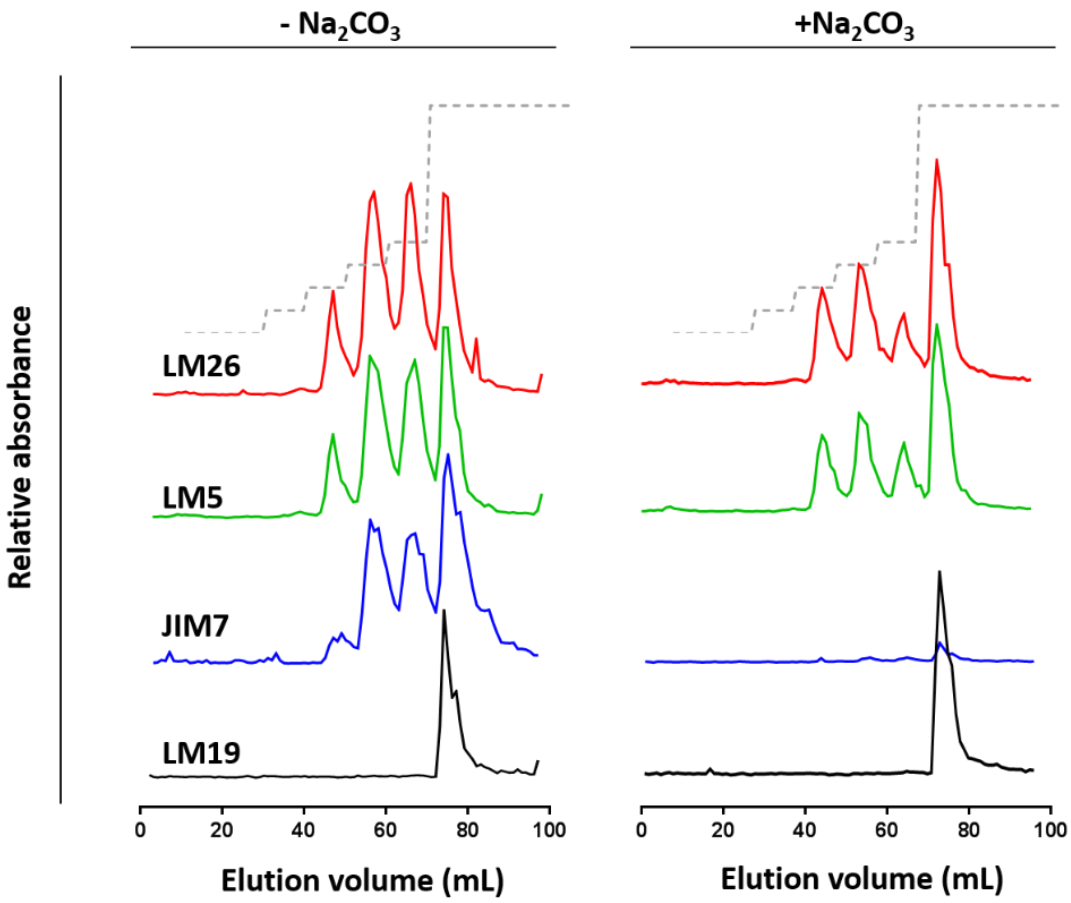

Figure 4.7 Epitope detection chromatography (EDC) of garlic bulb cell wall material. Epitope detection in water-soluble extract of garlic bulb cell walls using LM26, LM5. Including detection of pectic HG epitopes using JIM7 (methyl esterified HG) and LM19 (un-esterified HG). Samples were treated with a sodium carbonate pre-treatment (+Na_3CO_2) or without (-Na_3CO_2) in each case the traces shown are the mean of three chromographic runs. The stepped gradient used is shown for the anion exchange chromatography is shown as a dashed line.

4.4 Use of LM26 to identify phloem development in sugar beet storage root.

LM26 is an addition to a variety of cell wall marker which aid the study of vascular development and have been used to track the early development of sugar beet (*Beta vulgaris*) storage roots (Fig 4.7) In this case LM26 has the capability to indicate phloem cells within the supernumerary successive cambial anatomy at differing time points to identify the potential link between phloem abundance and position to overall sucrose yields in the commercial crop.

4.4.1 Study of phloem developmental anatomy in sugar beet storage roots

Using the LM26 MAb the development of the phloem vessels has been tracked through the early development of the storage root in three different *Beta vulgaris* lines; commercial sugar beet variety Sophia, a sugar beet variety used for breeding programmes C869 and a red garden beet variety W357B. After 3 weeks of growth after emergence (3 WAE) there is clear successive rings of phloem vessels visible in all three lines, these are interspersed with parenchyma tissue and xylem tissue, with the phloem vessels developing anterior to the xylem vessels. While the roots are still small the phloem vessels appear to be laid down in an unbroken circle, whereas with increased root size the space between rings increases and vascular tissue is detected with parenchyma separating areas of vasculature within the same vascular ring giving the vasculature a more clustered appearance with rays of xylem and phloem dispersed around the arc of each vascular ring.

In Chapter 3 the anatomy of the same three lines were assessed using LM11 to identify the xylem vessels. The binding patterning shown by LM26 in Figures 4.8, 4.9 and 4.10 show that each of the rings of xylem is associated with phloem sieve elements. The outer rings appeared to contain phloem sieve elements at a lower abundance than the more central rings. However, the Sophia line had a higher abundance of phloem sieve elements, detected by LM26, in the more outer rings than the other two lines. The W357B line showed the lowest abundance of phloem sieve elements as highlighted by the binding of LM26.

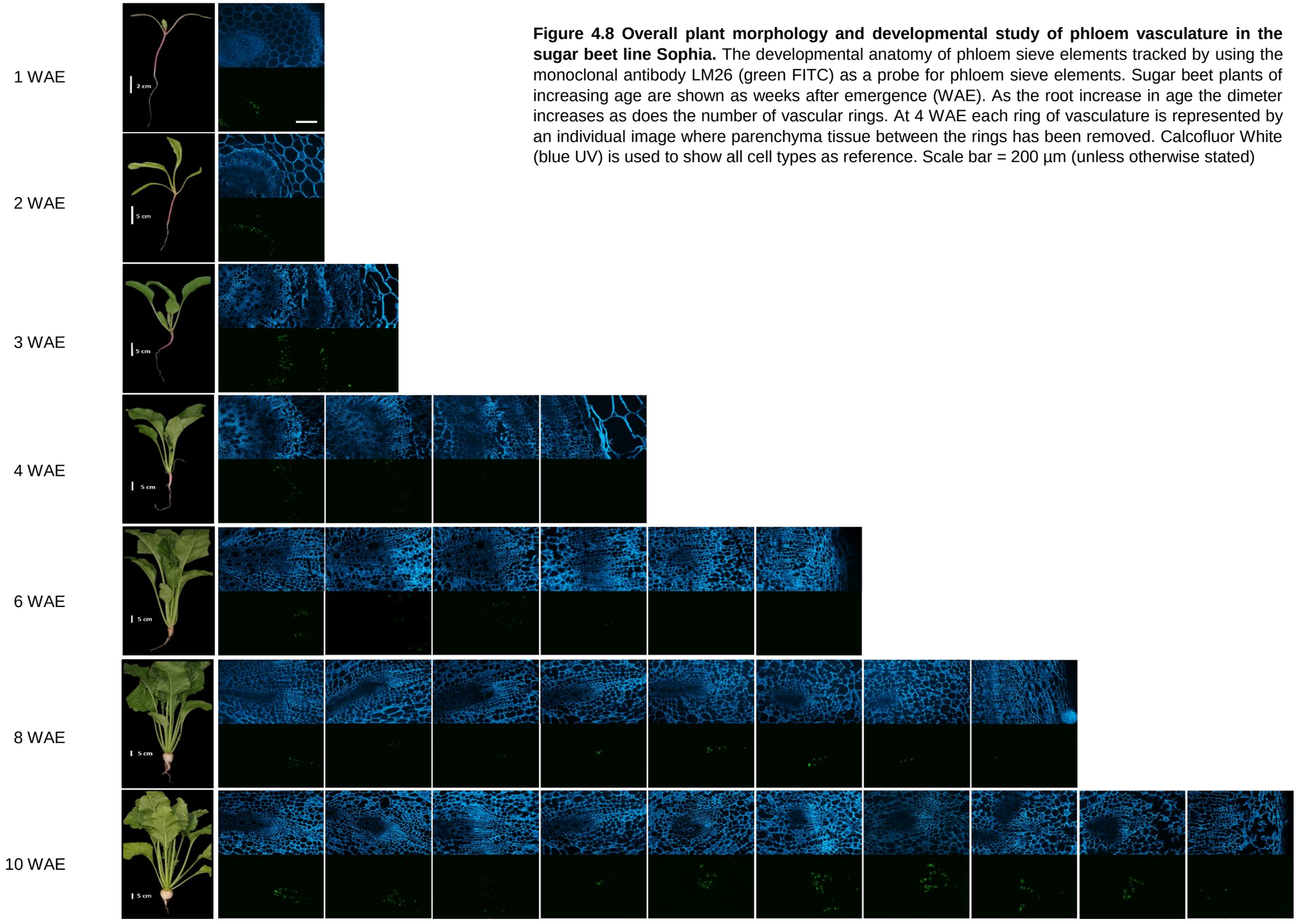

Figure 4.8 Overall plant morphology and developmental study of phloem vasculature in the sugar beet line Sophia. The developmental anatomy of phloem sieve elements tracked by using the monoclonal antibody LM26 (green FITC) as a probe for phloem sieve elements. Sugar beet plants of increasing age are shown as weeks after emergence (WAE). As the root increase in age the dimeter increases as does the number of vascular rings. At 4 WAE each ring of vasculature is represented by an individual image where parenchyma tissue between the rings has been removed. Calcofluor White (blue UV) is used to show all cell types as reference. Scale bar = 200 µm (unless otherwise stated)

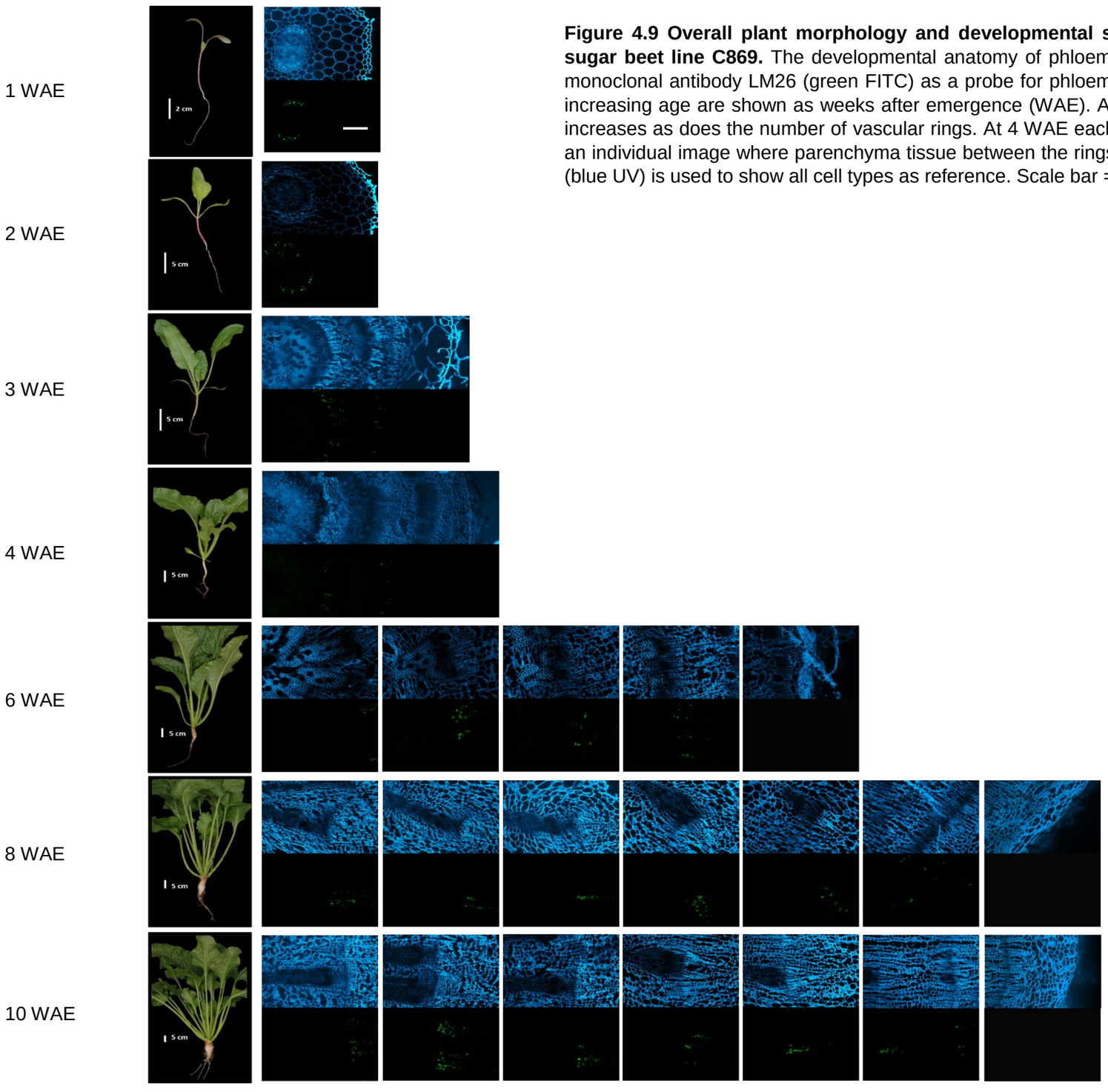

Figure 4.9 Overall plant morphology and developmental study of phloem vasculature in the sugar beet line C869. The developmental anatomy of phloem sieve elements tracked by using the monoclonal antibody LM26 (green FITC) as a probe for phloem sieve elements. Sugar beet plants of increasing age are shown as weeks after emergence (WAE). As the root increase in age the dimeter increases as does the number of vascular rings. At 4 WAE each ring of vasculature is represented by an individual image where parenchyma tissue between the rings has been removed. Calcofluor White (blue UV) is used to show all cell types as reference. Scale bar = 200 µm (unless otherwise stated)

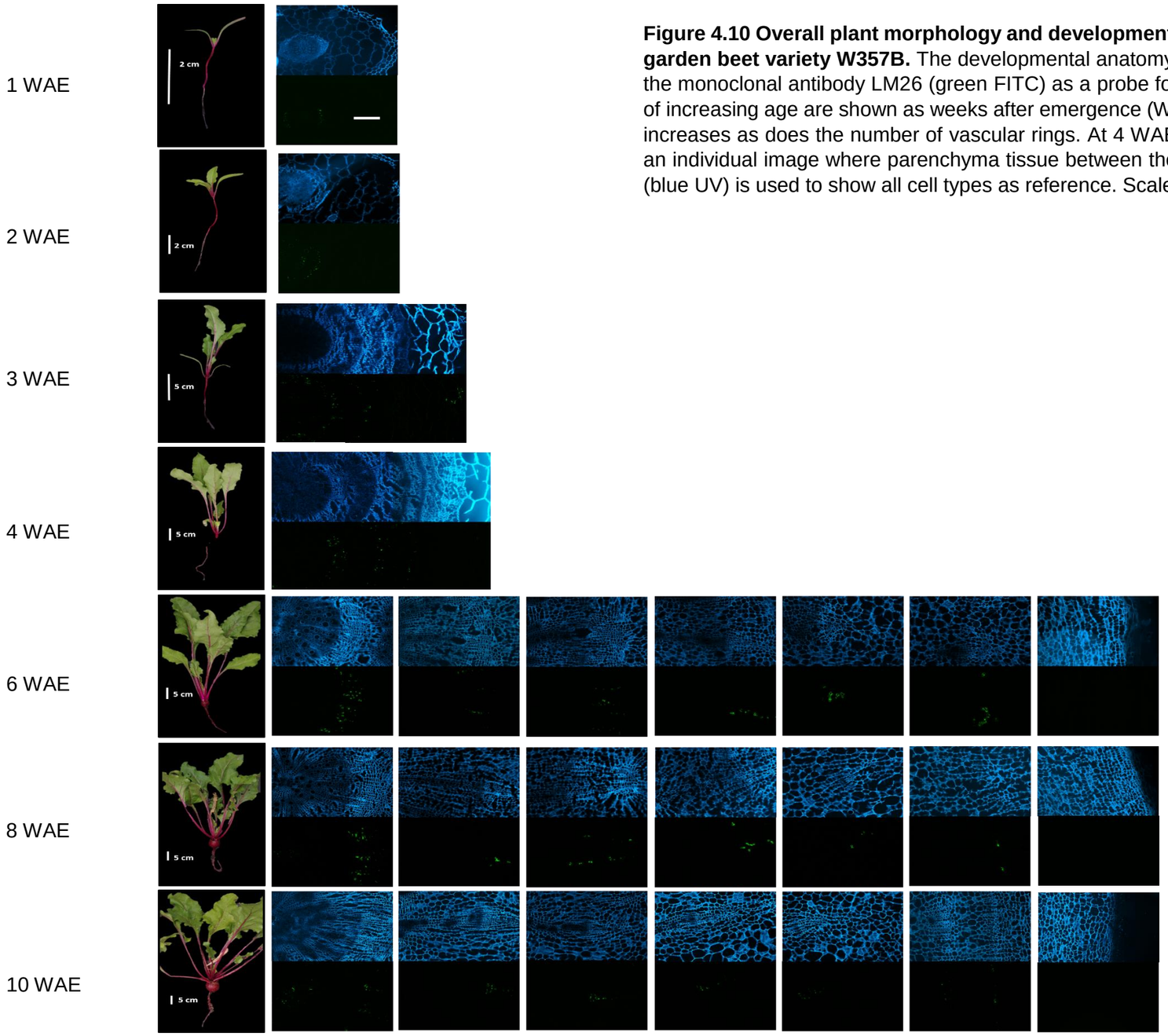

Figure 4.10 Overall plant morphology and developmental study of phloem vasculature in the red garden beet variety W357B. The developmental anatomy of phloem sieve elements tracked by using the monoclonal antibody LM26 (green FITC) as a probe for phloem sieve elements. Sugar beet plants of increasing age are shown as weeks after emergence (WAE). As the root increase in age the dimeter increases as does the number of vascular rings. At 4 WAE each ring of vasculature is represented by an individual image where parenchyma tissue between the rings has been removed. Calcofluor White (blue UV) is used to show all cell types as reference. Scale bar = 200 µm (unless otherwise stated)

4.5 Discussion

The monoclonal antibody designated LM26 binds to a β-1,6-galactosyl substitution of pectic β-1,4-galactan, which is specific in phloem sieve elements in many species. A cell wall epitope specific to phloem sieve elements is an interesting discovery. Since the theory was first proposed by Münch (1930) it has become widely accepted that mass flow through phloem sieve elements is driven by the pressure gradient generated by the accumulation of photosynthate at the source (e.g. leaves) and the unloading of these at the sinks (e.g. roots and fruits). The higher solute content of the phloem sieve elements produces a higher turgor pressure due to water entering from surrounding cells via osmosis (De Schepper et al., 2013, Gould et al., 2005). While phloem cell walls are usually thicker to accommodate the relatively increased turgor pressure associated with mass flow, the cell walls of phloem are not thickened to the extent of xylem vessels with their secondary cell walls (Heo et al., 2014). Therefore indicating that the detected branching of the 1,4-galactan plays some role in the mechanical properties of the cell wall. While the role of RG-I glycans is not completely resolved there is evidence that 1,4-galactan rich domains of pectic polysaccharides are associated with increased cell wall firmness, and conversely cell walls have increased elasticity where 1,4-galactan is less abundant (McCartney et al., 2000). The substitution recognised by the LM26 antibody may contribute to a modification of the 1,4-galactan to increase the elasticity in these regions of phloem vasculature enabling the cell walls to withstand higher turgor pressure (Torode et al., 2017). Structural modifications of galactosyl side chains are synonymous with their capacity to cross link with other cell wall components as areas with higher frequency of unsubstituted blocks are more able to interact with other cell wall components (Dea et al., 1986). Therefore the addition of the substitution detected by LM26 contributes to altering the overall mechanical properties of the cell walls which make the phloem tissue fit for function

Understanding the internal anatomy of sugar beet storage roots in respect to phloem development is key to increasing sugar yield. It has been long known that sucrose is deposited in sugar beet roots through diffusion from phloem cells to parenchyma cells down a concentration gradient (Draycott, 2006). Therefore it

is hypothesised that an increase in phloem number would increase the sucrose content of the storage root and increase overall sugar yield for the sugar beet industry. This work for the first time shows an *in situ* representation of the anatomy of the sugar beet vasculature to provide reference for the improvement of the sugar beet crop.

Chapter 5

Assessment of recombinant inbred lines of *Beta vulgaris* to identify candidate lines for future breeding targets

5.1 Introduction

When sucrose was discovered in the roots of red and white beets those with higher sugar levels were selectively bred to give rise to a majority of today's modern sugar beet varieties (Francis, 2006), which mostly trace back to these early selections. *Beta vulgaris* not only includes sugar beet (*Beta vulgaris* subsp. *vulgaris*) but also Swiss chard (*Beta vulgaris* subsp. *vulgaris*), red beet (*Beta vulgaris* subsp. *vulgaris*), fodder beet (*Beta vulgaris* subsp. *vulgaris*) and many wild varieties including sea beet (*Beta vulgaris* subsp. *maritima*). Cross fertilisation between these types has enabled breeders and scientists to tap into genetic diversity within the species, contributing to many favourable traits of commercial sugar beet such as disease resistant hybrid varieties, for example *Rhizomania* resistance (McGrath, 2010). Now modern conventional breeding methods such as marker assisted breeding are routinely used to produce novel sugar beet lines (Francia et al., 2005, Grimmer et al., 2007, Schondelmaier et al., 1996), supported by the adoption of genetic modification to introduce specific desirable traits that do not exist in the available breeding germplasm However, currently only three varieties of genetically modified sugar beet are approved, all of which convey herbicide resistance and are cultivated in USA, Canada and Japan (ISAAA, 2016). The adoption of genetically modified sugar beet in Europe is unlikely to occur in the near future (European Commission, 2009, European Commission, 2015).

Due to traditional breeding efforts involving backcrosses to remove deleterious traits the genome of commercial sugar beets are relatively similar. In this study a population of recombinant inbred lines (RILs) produced by McGrath et al. (2005) have been used in an effort to identify traits or genetic combinations which wouldn't otherwise rise from commercial sugar beet breeding programmes. The RILs used are the result of a cross between a sugar beet parent line (C869) and a red garden beet parent (W357B) produced by Mitchell McGrath at Michigan State University as part of a gene discovery study (McGrath et al., 2005). The principal behind this cross was that these two lines, while the same species, have contrasting physiological traits. The goal of this cross was to develop RILs from genetically divergent germplasm to examine

trait genetics. This resulting RIL has been utilised to assess the cell wall components and interactions of sugar beet storage roots and how these could have an effect on crop successes. The results can be used to identify potential candidate lines to be investigated and beneficial genes identified.

5.2 Materials and methods

The RIL population used in this chapter was provided by Michell McGrath, Michigan State University and grown at Broom's Barn on behalf of the author in preparation for the start of this project in October 2013. The RIL population were harvest by the author and staff at Broom's barn when measurements were taken at time of harvest and root material was coarsely cut before freezing with liquid nitrogen and storing at 80°C. After storage the samples were freeze dried and ground by the author at Rothamsted research, Harpenden.

Ground samples were prepared as alcohol insoluble residue by the author at University of Leeds and then prepared in sample tubes to be transported to University of Copenhagen. The author attended the University of Copenhagen for a research visit to conduct the CoMPP analysis and data handling for the RIL population in this chapter.

Raw data from the CoMPP analysis was provided to Stephen Powers (Rothamsted research) for statistical analysis, where groups were analysed for the effect of genotype and growing area. Some data was disregarded at this stage as being statistically unreliable and is not included in final analysis. Statistical data provided in the form of the multivariant analysis is shown in Figure 5.1 in this chapter. Statistically relevant data was utilised to perform univariate analysis by the author (Figure 5.1 – Figure 5.15)

5.3 Results

The resulting RILs from the cross between the C869 sugar beet parent and the W357B red garden beet parent produced distinct genetic lines which were used for this analysis in combination with the parent lines and a commercial variety Sophia. These lines were harvested with four individual plants representing each RIL. With potentially 800 samples including controls and replicates for the RIL population it was important to use a high throughput method to analyse the cell wall polysaccharides across the population. Therefore, comprehensive microarray polymer profiling (CoMPP) was used to identify the relative abundance of call wall polysaccharides in the roots collected from the RIL population. After processing losses from field related diseases such as violet root rot or low yield 175 lines each of which had its cell wall material extracted twice sequentially (CDTA and NaOH extractions) were analysed using CoMPP at the University of Copenhagen. This analysis utilised 30 monoclonal antibodies (mAbs), to complete a large screen of the polysaccharide epitopes across the population.

The raw data of the spot densities from the arrays were used for correlation analysis because using the adjusted values as described in chapter 3 (setting 100% as a standardised maximum) would interfere with the statistical analysis of the results. A multivariate correlation was conducted to deduce any general trends of polysaccharide epitope abundance, the correlation results included both the mAb detection and physiological traits (root fresh weight, root diameter, root dry weight, percentage dry matter, percentage sucrose of dry matter, percentage sucrose of fresh weight and sugar yield) that had been previously collected (Fig 5.1). Correlation between physiological traits were as anticipated with sugar yield having a strong positive correlation with fresh root weight, diameter, dry weight and % sucrose of dry matter. Therefore, large roots with high sucrose concentration of the dry matter confers higher overall sugar yield.

5.3.1 Verification of the method by correlations between monoclonal antibodies of the same class

Where antibodies detect similar epitopes this can serve as an internal control. Examples of these internal controls have the highest positive correlations; LM15 and LM25 which both bind to xyloglucan had a positive correlation of 0.954, LM11 and LM10 which both bind to xylan had a positive correlation of 0.945, LM18 and LM19 which both bind to homogalacturonan had a positive correlation of 0.949, LM1 and JIM20 which both bind to extensin showed a positive correlation of 0.985. These strong positive correlations show that the methods used for this analysis are reliable.

5.3.2 Correlations of different monoclonal antibodies indicate *in muro* interactions between polysaccharide groups.

The correlation between different cell wall polysaccharides gives insight in to the interactions of the polysaccharides within the wall. LM6-M detection of arabinan positively correlated with LM12 epitope abundance which was similar to the positive correlation shown by LM6 which also detects arabinan. To a lesser extent there was a positive correlation between detection of LM6-M and the detection of the JIM7 epitope (homogalacturonan). In general across the correlation matrix there was a positive correlation between mAbs which detect HG epitopes and those which detect arabinan epitopes. For example there was a strong positive correlation between detection of the LM13 epitope and JIM7 detection of at 0.583 and 0.560 for the CDTA and NaOH extractions respectively. This positive correlation occurred with the exception of LM13 detection where there was negative correlation between this epitope and those detected by LM18 and LM19 in the NaOH extraction, however there was a positive correlation between these detected epitopes in the CDTA extraction. The JIM16 and JIM13 epitope detection of AGPs had positive correlation with arabinan detection by LM6 and LM6-M as well as a positive correlation with detection of HG by LM19 and LM18.

Detection of galactan epitopes by the mAb LM5 showed a positive correlation with HG epitopes identified by JIM5 and LM19. AGP epitopes detected by JIM13 and LM2 also showed a positive correlation with the detection of

galactan. However there was a negative correlation between detection of galactan and the detection of arabinan by LM13. The anti-xylan antibodies LM11 and LM10 indicated a positive correlation with detection by several other antibodies including those detecting HG (JIM5), AGP (JIM13 and LM2) and galactan (LM5).

Detection by LM1 and JIM20 for epitopes of extensin had a positive correlation with the JIM7 epitope (homogalacturonan). With JIM20 also showed positive correlation with the anti-AGP epitopes identified by the mAb JIM16 as well as arabinan detection by LM6. The detection of xyloglucan by LM25 only showed a positive correlation with two of the anti-HG antibodies, LM19 and LM18.

5.3.3 Correlation between physiological traits and cell wall epitope detection in RIL population

The correlation between economically important physiological traits and cell wall polysaccharides can give an insight in to how the composition of sugar beet storage root cell walls can impact the overall sucrose yield from the crop. Highlighted on the correlation matrix in Figure 5.1 there are some specific mAbs epitope detections which showed correlation, both positive and negative, with physiological traits. For example, the JIM13 epitope detected in the NaOH fraction showed a negative correlation with both fresh and dry root weight. Detection of LM10 and LM11 epitopes, which both detect xylan, showed a negative correlation with fresh and dry weight. Importantly LM11 epitope detection had a negative correlation with sugar yield and to a lesser extent the LM10 epitope showed the same negative correlation. LM5 detection of a galactan epitope in the CDTA fraction had a positive correlation with both percentage of root composed of dry matter and percentage sucrose of the fresh weight. Detection of arabinan by LM13 showed positive correlation with several physiological traits; fresh weight, diameter, root dry weight and to a lesser extent sugar yield. The glucoronoxylan antibody LM28 detection showed a positive correlation with percent of root dry matter.

	Fresh Root Weight g	Diameter Average cm	% dry matter	Root Dry Weight g	% Sucrose Of Dry Matter	% Sucrose Of Fresh Weight	Sugar Yield kg/ha	LM6-M CDTA	LM6-M NaOH	JIM5 CDTA	JIM5 NaOH	JIM7 CDTA	JIM13 CDTA	JIM13 NaOH	JIM16 CDTA	JIM20 CDTA	JIM20 NaOH	LM1 CDTA	LM2 CDTA	LM2 NaOH	LM5 CDTA	LM5 NaOH	LM6 CDTA	LM6 NaOH	LM10 NaOH	LM11 NaOH	LM12 CDTA	LM13 CDTA	LM13 NaOH	LM15 CDTA	LM15 NaOH	LM18 CDTA	LM18 NaOH	LM19 CDTA	LM19 NaOH	LM21 CDTA	LM21 NaOH	LM25 CDTA	LM25 NaOH
Diameter Average cm	0.871																																					
% dry matter	0.003	0.047																																				
Root Dry Weight g	0.986	0.865	0.145																																			
% Sucrose Of Dry Matter	0.428	0.354	0.303	0.469																																		
% Sucrose Of Fresh Weight	0.230	0.227	0.864	0.352	0.731																																	
Sugar Yield kg/ha	0.984	0.859	0.161	0.992	0.533	0.397																																
LM6-M CDTA	0.092	0.120	-0.085	0.087	0.064	-0.028	0.085																															
LM6-M NaOH	-0.118	-0.029	0.188	-0.101	0.089	0.173	-0.077	0.653																														
JIM5 CDTA	0.158	0.228	0.114	0.179	-0.161	0.001	0.149	0.175	0.008																													
JIM5 NaOH	-0.317	-0.255	0.145	-0.299	-0.015	0.084	-0.284	0.077	0.465	0.007																												
JIM7 CDTA	0.151	0.212	0.076	0.173	-0.120	-0.011	0.141	0.458	0.225	0.653	0.001																											
JIM13 CDTA	-0.130	-0.085	-0.108	-0.149	0.012	-0.064	-0.132	0.355	0.326	-0.165	0.299	-0.148																										
JIM13 NaOH	-0.406	-0.306	-0.025	-0.427	-0.118	-0.076	-0.396	0.236	0.638	-0.244	0.535	-0.192	0.669																									
JIM16 CDTA	-0.008	-0.077	0.030	0.000	-0.032	0.003	-0.004	0.483	0.372	0.107	0.116	0.334	0.223	0.220																								
JIM20 CDTA	0.330	0.321	0.106	0.347	0.020	0.088	0.329	0.322	0.142	0.385	-0.101	0.701	-0.085	-0.227	0.427																							
JIM20 NaOH	0.149	0.152	-0.197	0.120	0.005	-0.134	0.109	0.119	0.199	0.001	0.224	0.169	0.208	0.257	0.216	0.232																						
LM1 CDTA	0.357	0.341	0.098	0.373	0.013	0.079	0.352	0.277	0.115	0.400	-0.094	0.705	-0.127	-0.249	0.390	0.985	0.265																					
LM2 CDTA	-0.054	-0.021	-0.126	-0.079	0.027	-0.073	-0.064	0.191	0.163	0.121	0.117	0.010	0.451	0.316	0.262	0.007	0.057	-0.006																				
LM2 NaOH	-0.384	-0.291	-0.011	-0.391	-0.106	-0.059	-0.373	0.139	0.370	-0.032	0.397	-0.041	0.385	0.641	0.251	-0.196	0.091	-0.205	0.674																			
LM5 CDTA	-0.012	-0.022	0.417	0.047	0.281	0.439	0.073	0.079	0.219	0.025	0.345	-0.164	0.429	0.248	0.143	-0.230	-0.114	-0.249	0.235	0.173																		
LM5 NaOH	-0.246	-0.254	0.236	-0.220	0.121	0.227	-0.187	0.018	0.401	-0.174	0.486	-0.314	0.467	0.590	0.293	-0.297	0.033	-0.322	0.294	0.439	0.790																	
LM6 CDTA	0.006	-0.019	-0.227	-0.019	-0.086	-0.207	-0.027	0.823	0.452	0.293	0.078	0.485	0.327	0.182	0.639	0.406	0.194	0.363	0.211	0.107	0.026	0.042																
LM6 NaOH	-0.136	-0.050	0.106	-0.125	-0.052	0.043	-0.117	0.624	0.878	0.159	0.449	0.335	0.201	0.564	0.356	0.210	0.248	0.200	0.115	0.378	0.027	0.226	0.482															
LM10 NaOH	-0.425	-0.309	0.283	-0.390	-0.134	0.135	-0.378	-0.061	0.312	0.086	0.469	-0.073	0.160	0.442	0.216	-0.142	0.093	-0.146	0.237	0.447	0.297	0.477	-0.024	0.287														
LM11 NaOH	-0.458	-0.357	0.303	-0.418	-0.162	0.133	-0.409	-0.037	0.322	0.061	0.469	-0.078	0.231	0.480	0.270	-0.110	0.057	-0.126	0.294	0.500	0.326	0.508	-0.011	0.295	0.945													
LM12 CDTA	-0.120	-0.070	0.020	-0.105	0.001	0.014	-0.108	0.892	0.654	0.057	0.238	0.349	0.436	0.357	0.480	0.190	0.112	0.139	0.176	0.270	0.189	0.180	0.682	0.602	0.074	0.124												
LM13 CDTA	0.407	0.454	-0.055	0.404	0.004	-0.037	0.377	0.461	0.112	0.572	-0.206	0.583	-0.151	-0.307	-0.100	0.295	0.005	0.313	0.039	-0.210	-0.117	-0.443	0.318	0.213	-0.286	-0.343	0.259										
LM13 NaOH	0.148	0.289	0.194	0.167	-0.037	0.111	0.160	0.303	0.410	0.461	0.087	0.560	-0.226	-0.007	-0.043	0.306	0.026	0.322	-0.022	0.025	-0.163	-0.245	0.155	0.538	0.009	-0.041	0.178	0.697									
LM15 CDTA	-0.227	-0.270	-0.177	-0.247	-0.182	-0.216	-0.251	0.104	-0.019	-0.082	0.099	-0.059	0.074	0.059	-0.006	-0.096	-0.164	-0.118	0.064	0.113	-0.142	-0.051	0.143	0.001	-0.001	0.010	0.206	-0.024	-0.076								
LM15 NaOH	-0.263	-0.393	-0.083	-0.276	-0.115	-0.126	-0.274	-0.180	-0.085	-0.072	0.125	-0.111	-0.070	0.065	-0.054	-0.105	-0.078	-0.113	-0.010	0.172	-0.119	0.007	-0.154	-0.046	0.152	0.217	-0.070	-0.264	-0.179	0.269							
LM18 CDTA	0.067	0.135	0.055	0.080	-0.215	-0.068	0.048	-0.017	-0.191	0.841	0.040	0.441	-0.102	-0.293	-0.121	0.239	-0.054	0.252	0.093	-0.040	0.042	-0.201	0.088	-0.068	0.069	0.057	-0.073	0.407	0.242	-0.040	0.043						
LM18 NaOH	-0.379	-0.300	-0.133	-0.398	-0.136	-0.162	-0.391	-0.250	0.103	-0.186	0.432	-0.278	0.217	0.464	-0.056	-0.264	0.268	-0.274	-0.030	0.235	0.084	0.394	-0.086	0.034	0.342	0.325	-0.169	-0.432	-0.264	0.089	0.109	-0.114					
LM19 CDTA	0.123	0.185	-0.028	0.115	-0.233	-0.134	0.090	-0.019	-0.211	0.820	-0.019	0.455	-0.129	-0.291	-0.162	0.262	-0.014	0.276	0.050	-0.069	-0.061	-0.289	0.105	-0.086	0.036	0.002	-0.118	0.452	0.287	0.016	0.050	0.949	-0.084				
LM19 NaOH	-0.368	-0.308	-0.097	-0.389	-0.041	-0.089	-0.366	-0.079	0.238	-0.195	0.461	-0.339	0.333	0.530	0.028	-0.315	0.129	-0.333	0.084	0.323	0.232	0.537	0.001	0.145	0.382	0.381	0.017	-0.403	-0.258	0.081	0.101	-0.110	0.831	-0.139			
LM21 CDTA	0.081	0.054	-0.291	0.042	-0.095	-0.251	0.035	-0.108	-0.390	0.185	-0.142	0.073	0.088	-0.270	-0.189	0.078	0.096	0.068	-0.026	-0.293	-0.027	-0.215	0.195	-0.396	-0.261	-0.307	-0.262	0.151	-0.145	0.030	-0.088	0.327	0.063	0.370	-0.028		
LM21 NaOH	0.006	0.071	0.023	0.001	0.080	0.059	0.013	0.163	0.317	-0.033	0.182	0.043	-0.049	0.183	-0.279	0.023	0.173	0.019	-0.186	-0.009	-0.146	-0.096	-0.023	0.299	-0.020	-0.074	0.058	0.114	0.228	0.003	0.058	0.029	0.166	0.077	0.150	0.132	
LM25 CDTA	-0.347	-0.357	-0.205	-0.382	-0.213	-0.262	-0.375	-0.043	0.034	0.026	0.156	-0.003	0.051	0.217	0.221	-0.145	0.119	-0.159	0.026	0.165	0.023	0.244	0.149	0.054	0.172	0.179	0.008	-0.218	-0.096	0.087	0.151	-0.085	0.407	-0.077	0.423	0.012	-0.110	
LM25 NaOH	-0.252	-0.374	-0.002	-0.253	-0.089	-0.055	-0.251	-0.160	-0.063	-0.036	0.108	-0.053	-0.127	0.013	-0.057	-0.076	-0.132	-0.084	-0.098	0.089	-0.095	-0.012	-0.162	-0.032	0.173	0.222	-0.052	-0.207	-0.117	0.250	0.954	0.045	0.081	0.038	0.089	-0.113	0.046	0.158
LM28 NaOH	-0.383	-0.326	0.432	-0.332	-0.136	0.230	-0.320	-0.301	0.090	0.117	0.336	-0.115	0.075	0.275	0.041	-0.121	-0.098	-0.126	0.208	0.363	0.324	0.370	-0.270	0.078	0.731	0.813	-0.143	-0.305	-0.019	-0.060	0.330	0.172	0.173	0.115	0.195	-0.232	-0.080	0.030

> 0.5

> 0.4

< -0.4

Figure 5.1 Correlation matrix of RIL population. Correlation of the relative abundance of monoclonal antibody detection of cell wall polysaccharides including economically important physiological traits of the RIL population. Correlations between cell wall polysaccharide abundance and physiological traits are highlighted in blue. Green = positive correlation greater than 0.5, Yellow = positive correlation between 0.4 and 0.5, Red = Negative correlation >-0.4

To be able to successfully identify lines from the recombinant population that may be suitable for further analysis to push forward sugar beet breeding efforts candidates need to be chosen using the information from the correlation matrix (Fig 5.1). The most obvious way to improve the crop for the sugar industry is to identify lines with the highest sugar yield, as shown in Figure 5.2. The lines all show a lower sugar yield than the commercial variety and the sugar beet parent. The red beet parent shown in red is low sugar yielding. The most relevant physiological traits to use were root diameter, % dry matter and % sucrose of dry matter. Root diameter was used because this accounted for the size of the root regardless of water content as is the case with fresh root weight. Shown in Figure 5.3 the RILs are ranked in order of root diameter with the Sophia line being the highest ranked with the largest diameter. The sugar beet parent also shows a large diameter with only one line with a larger diameter. Again the W357B line was recorded at the opposite end of the spectrum. Percentage dry matter is a useful analysis to assess dry matter partitioning, how much energy is assigned to the root. The dry matter is majority composed of sucrose, cell wall polysaccharides (Milford et al., 1988). Figure 5.4 shows the relative percentages of dry matter in all of the lines with the commercial Sophia line having the highest percentage of dry matter followed by C869. W357B has the second lowest % dry matter value from all of the lines. Assessing percentage sucrose of dry matter indicated partitioning to sucrose rather than cell wall production. Figure 5.5 showed the commercial variety had a much higher percentage sucrose of dry matter than any of the RILs, however 15 RILs had higher percentage sucrose of dry matter than the C869 line. The red garden beet showed the lowest percentage sucrose of dry matter.

In addition to physiological traits the correlation matrix identified potentially beneficial cell wall characteristics which could lead to an increased sugar yield (LM5, LM13 and LM28). The relative detection levels of these epitopes has been analysed further.

Figure 5.6 showed the relative detection levels of the LM5 epitope of galactan, the commercial variety had a high relative abundance of LM5 detection as did

the sugar beet parent C869. LM13 detection of arabinan in Figure 5.7 showed that unlike previous traits analysed the high yielding Sophia and C869 did not have the highest levels of detection with LM13. Detection of glucuronoxylan with LM28 (Fig 5.8) showed that the sugar beet parent C869 had a high relative abundance of LM28 detection with the Sophia line having a mid-range detection.

Relevant cell wall detection levels of epitopes which indicated a negative correlation with physiological traits in Figure 5.1 (LM10, LM11, JIM13, LM25, LM18 and LM19) were also analysed to identify lines with high relative abundance of these traits.

Analysis of the relative abundance of xylan detection with LM10 (Fig 5.9) and LM11 (Fig 5.10) indicated that the high yielding sugar beet parent C869 actually had a relatively high level of xylan detection as did line 325 which was one of the higher sugar yielding lines. According to work conducted in Chapter 3 and 4 of this thesis, which indicated that an increase in vasculature could contribute to an increase in sucrose concentration this epitope detection will be assessed further for indication of lines showing traits which align with this hypothesis.

Figure 5.11 indicated that the two parent lines had similar detection of the AGP epitope of JIM13 with the high yielding commercial line Sophia having a slightly higher detection level of JIM13.

LM25 also indicated a negative correlation with sugar yield in the correlation matrix and further analysis indicated that the red garden beet parent line had a much higher level of epitope detection of xyloglucan with LM25 than the sugar beet parent C869 and the commercial line Sophia (Fig 5.12).

HG detection with LM18 (Fig 5.13) and LM19 (Fig 5.14) showed that detection of Lm18 epitope was higher in the red garden beet than the sugar beet parent C869 and Sophia showed a much lower detection of the LM18 epitope. However, for LM19 the detection of the HG epitope was higher in the sugar

beet parent than the red garden beet parent but the high sugar yielding Sophia still had the lowest level of detection from the three.

In addition the detection of these cell wall polysaccharides identified by the correlation matrix as being either positively or negatively correlated with sugar yield LM12 epitope has also been considered as an interesting factor for its potential effect on downstream pulp processing (Bonnin et al., 2002b). Detection of the LM12 epitope (Fig 5.15) shows that the C869 parent line has a relatively low detection of feruloylated pectin compared to the W357B parent line.

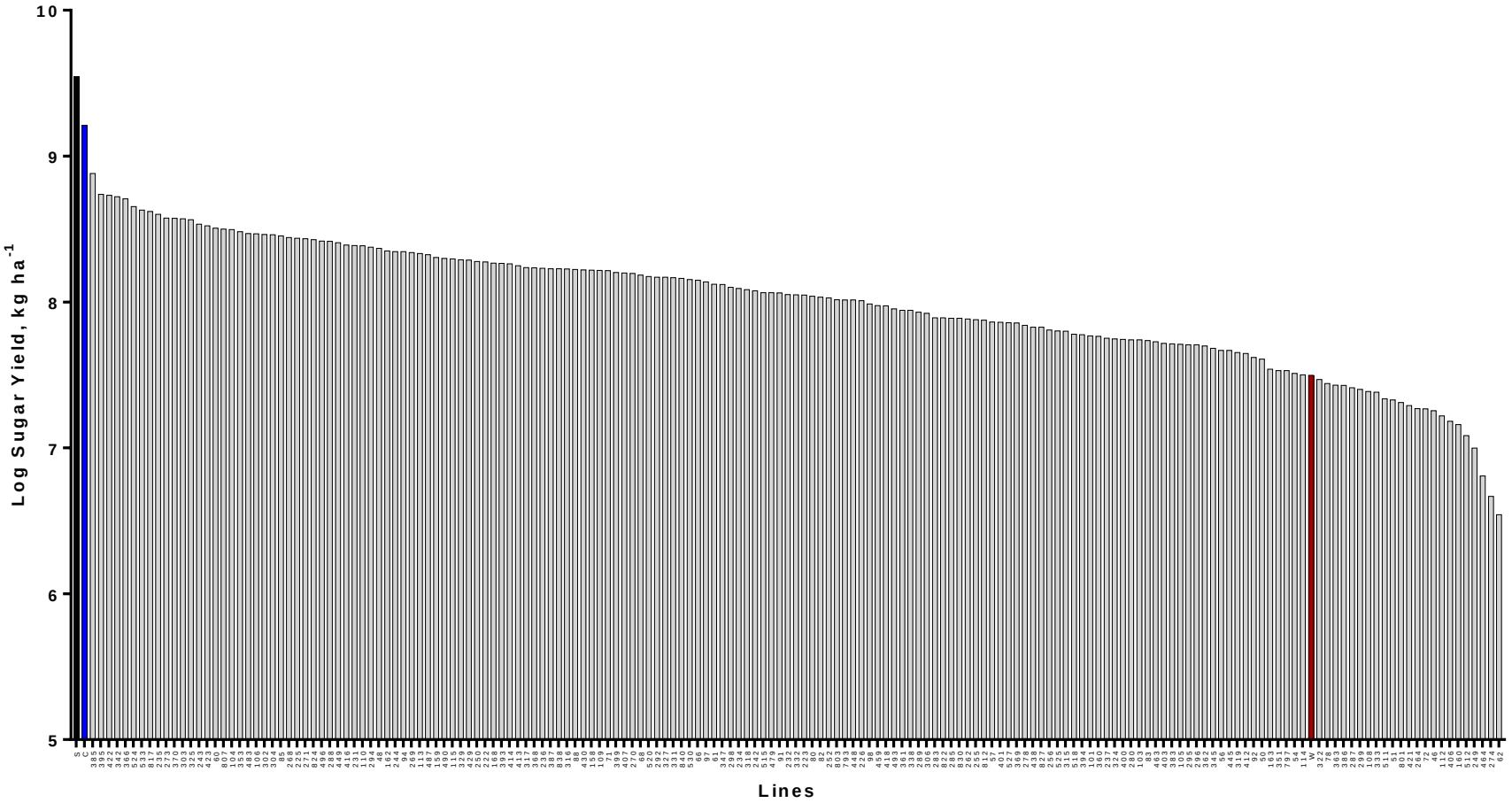

Figure 5.2. Recombinant inbred lines ranked by sugar yield. Recombinant inbred lines (RILs) shown in order of sugar yield (kg ha^{-1}). Parent lines are indicated by coloured bars; C869 (sugar beet parent) - blue, W357B (red garden beet parent) - red. The commercial variety Sophia is indicated by the black bar. Values are displayed as Log.

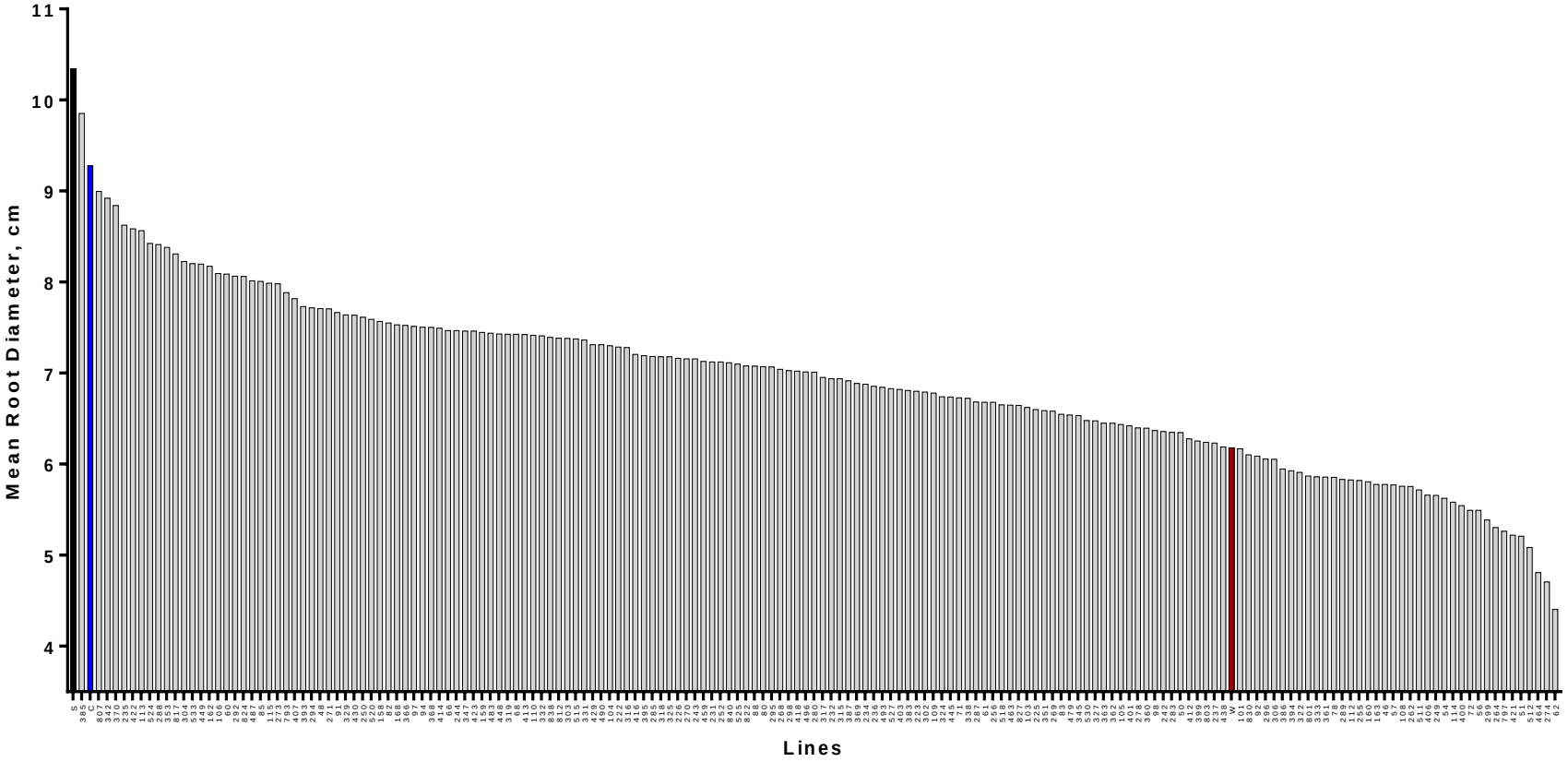

Figure 5.3. Recombinant inbred lines ranked by mean root diameter. Recombinant inbred lines (RILs) shown in order of mean root diameter (cm). Parent lines are indicated by coloured bars; C869 (sugar beet parent) - blue, W357B (red garden beet parent) - red. The commercial variety Sophia is indicated by the black bar.

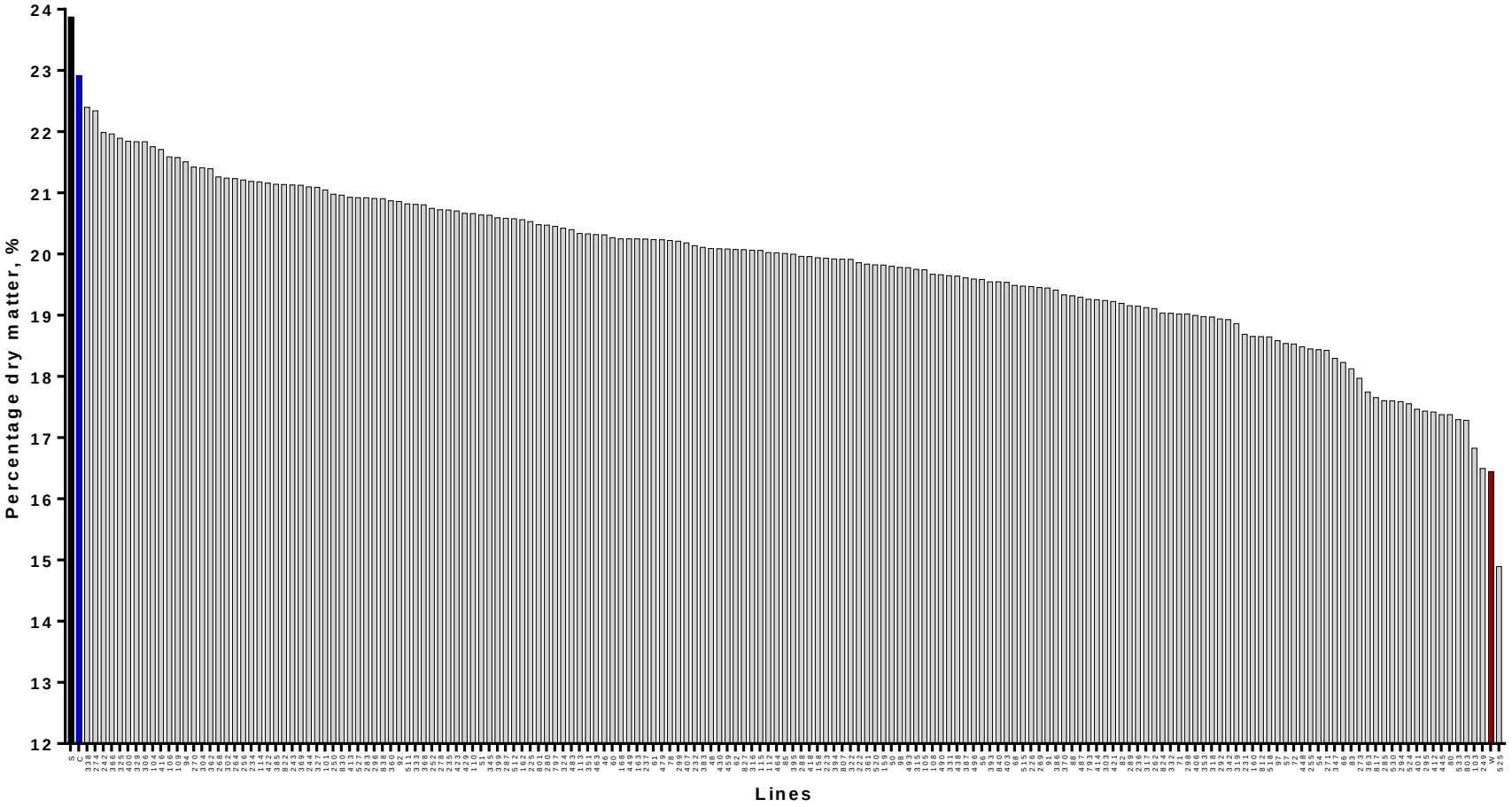

Figure 5.4. Recombinant inbred lines ranked by percentage dry matter. Recombinant inbred lines (RILs) shown in order of percentage dry matter (%) Parent lines are indicated by coloured bars; C869 (sugar beet parent) - blue, W357B (red garden beet parent) - red. The commercial variety Sophia is indicated by the black bar.

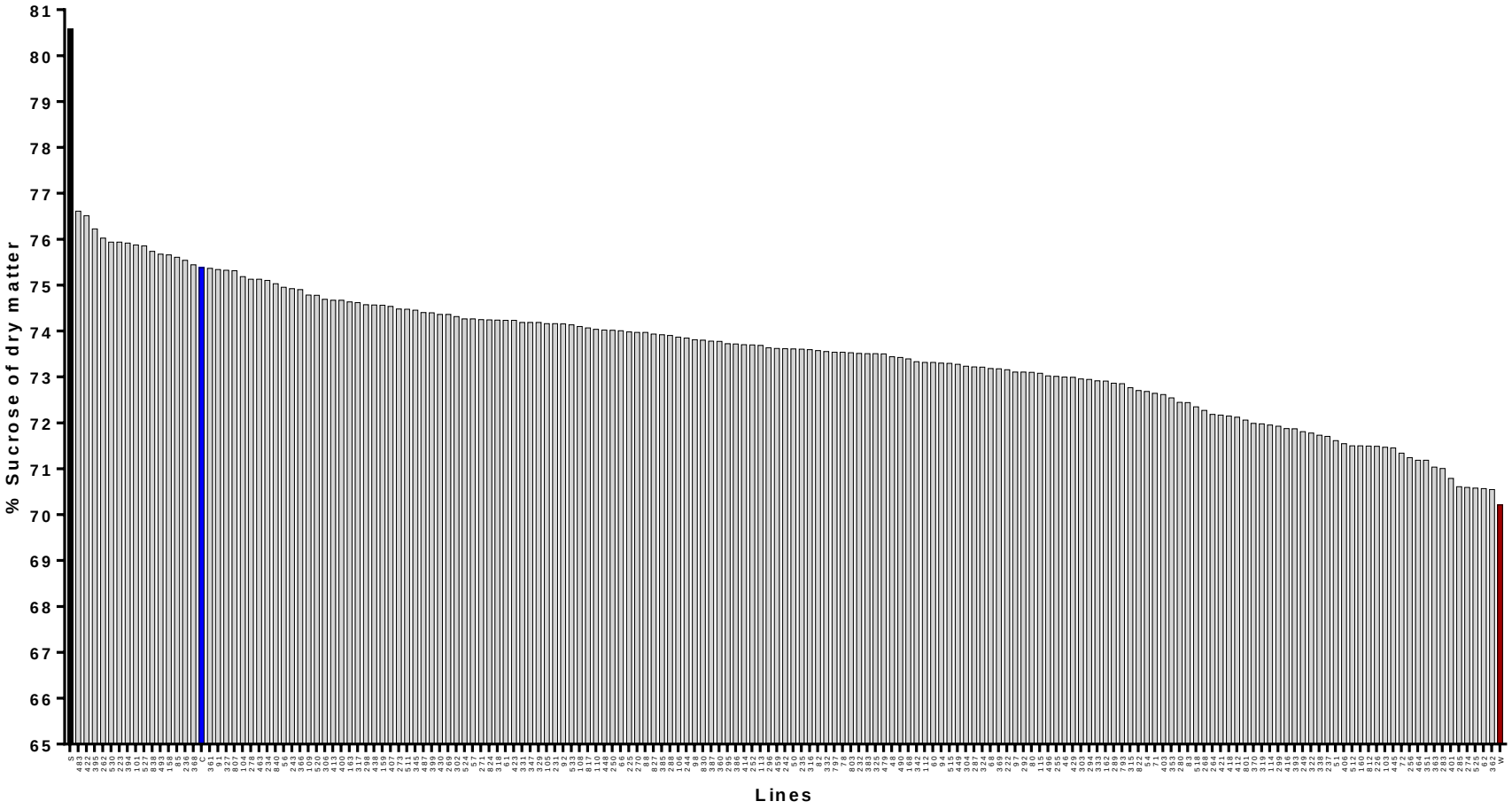

Figure 5.5. Recombinant inbred lines ranked by percentage sucrose of dry matter. Recombinant inbred lines (RILs) shown in order of percentage sucrose of dry matter (%) Parent lines are indicated by coloured bars; C869 (sugar beet parent) - blue, W357B (red garden beet parent) - red. The commercial variety Sophia is indicated by the black bar.

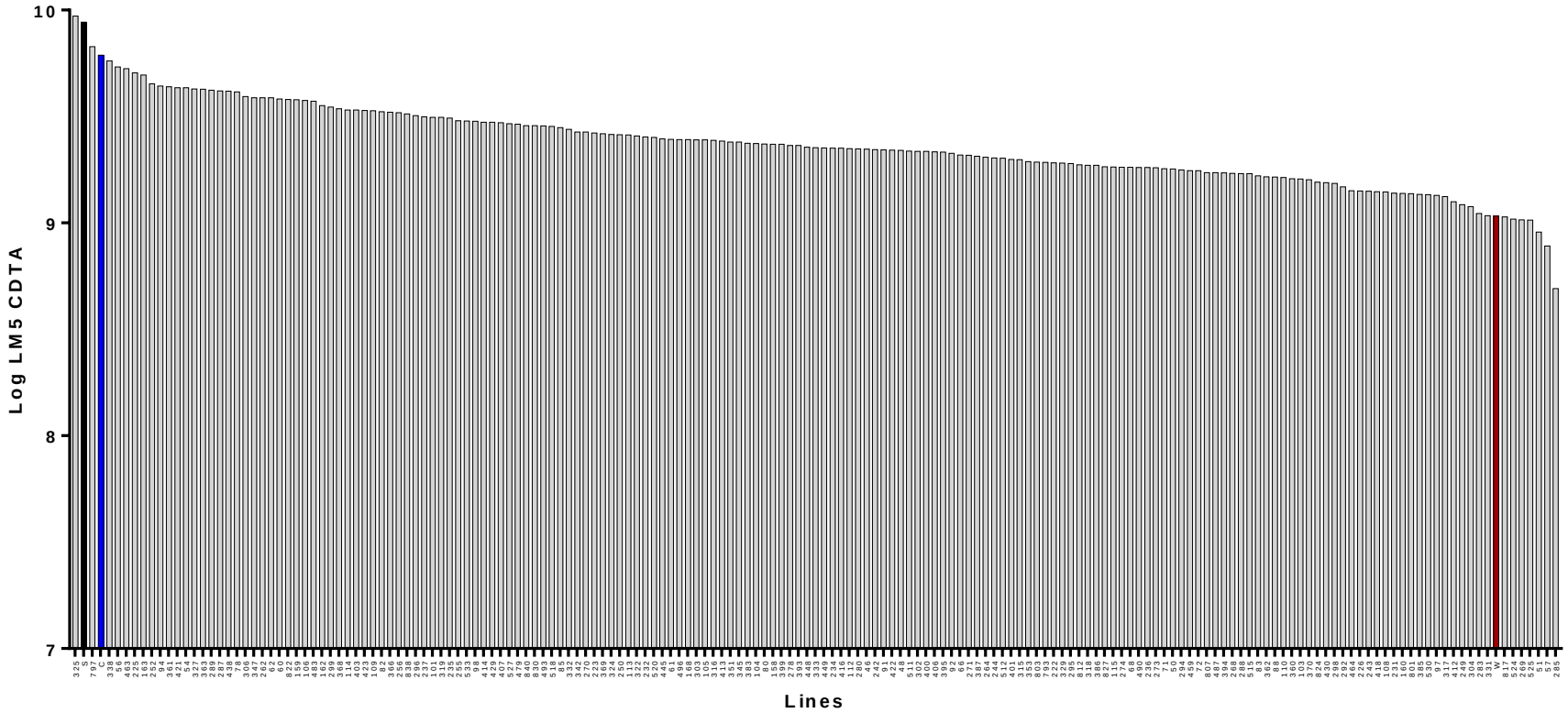

Figure 5.6. Recombinant inbred lines ranked by LM5 epitope detection. Recombinant inbred lines (RILs) shown in order of relative LM5 epitope detection (Log). Parent lines are indicated by coloured bars; C869 (sugar beet parent) - blue, W357B (red garden beet parent) - red. The commercial variety Sophia is indicated by the black bar.

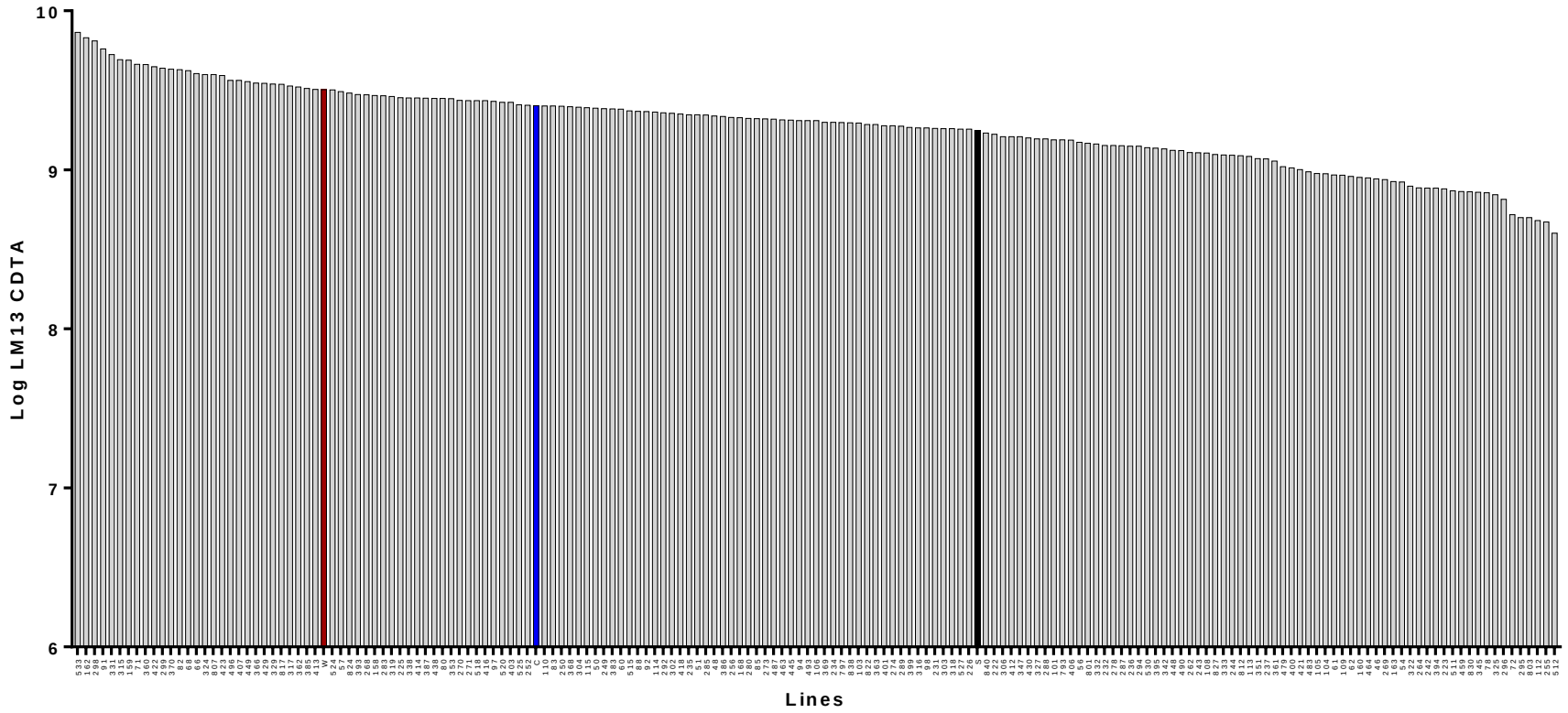

Figure 5.7. Recombinant inbred lines ranked by LM13 epitope detection. Recombinant inbred lines (RILs) shown in order of relative LM13 epitope detection (Log). Parent lines are indicated by coloured bars; C869 (sugar beet parent) - blue, W357B (red garden beet parent) - red. The commercial variety Sophia is indicated by the black bar.

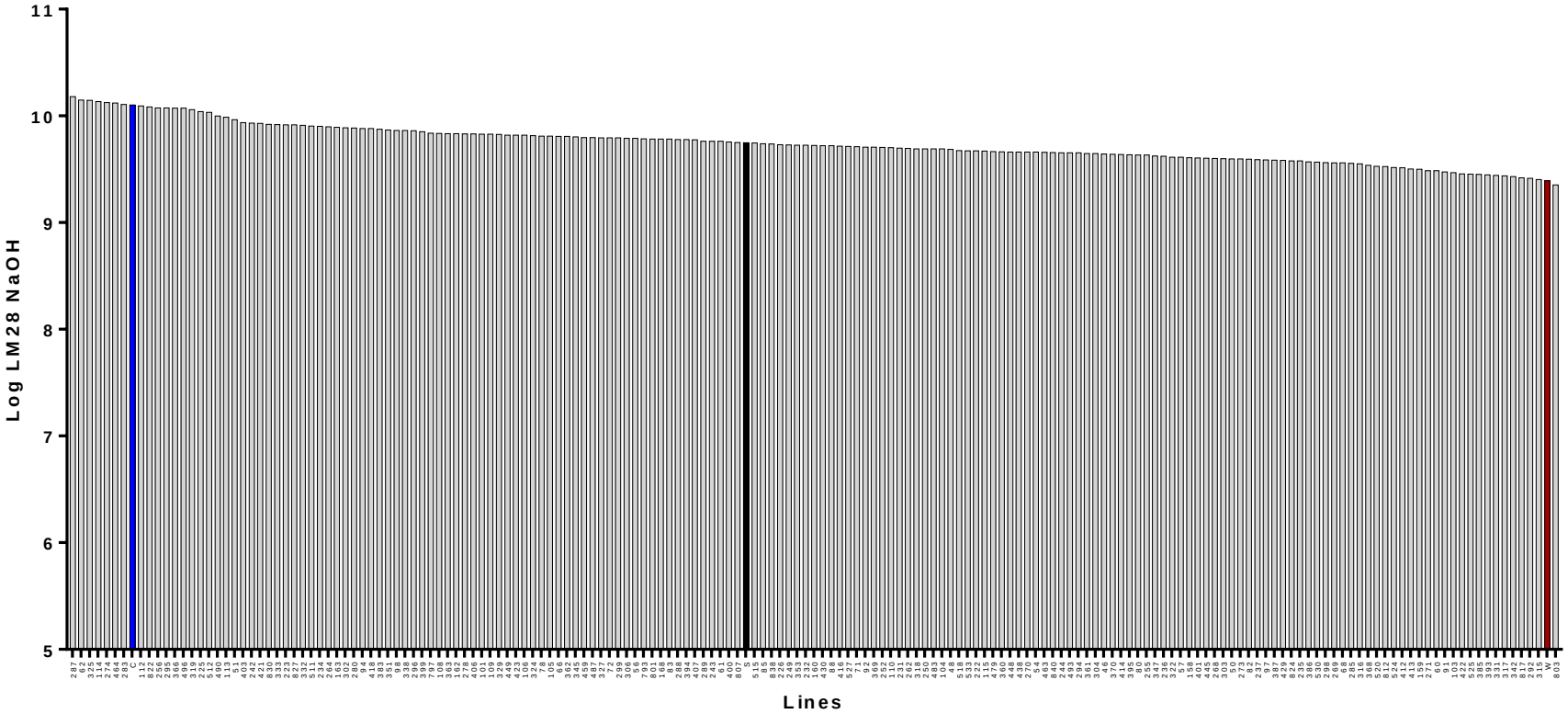

Figure 5.8. Recombinant inbred lines ranked by LM28 epitope detection. Recombinant inbred lines (RILs) shown in order of relative LM28 epitope detection (Log). Parent lines are indicated by coloured bars; C869 (sugar beet parent) - blue, W357B (red garden beet parent) - red. The commercial variety Sophia is indicated by the black bar.

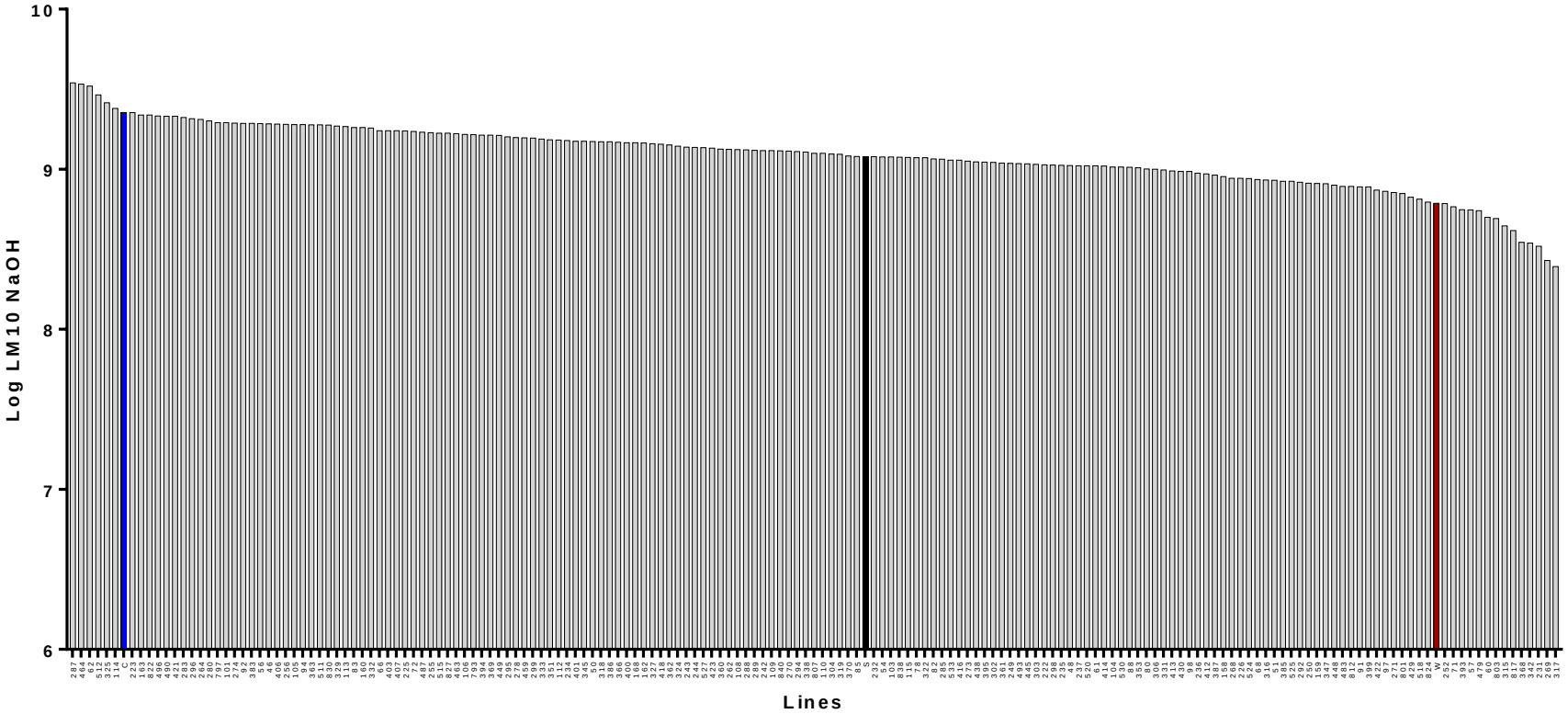

Figure 5.9. Recombinant inbred lines ranked by LM10 epitope detection. Recombinant inbred lines (RILs) shown in order of relative LM10 epitope detection (Log). Parent lines are indicated by coloured bars; C869 (sugar beet parent) - blue, W357B (red garden beet parent) - red. The commercial variety Sophia is indicated by the black bar.

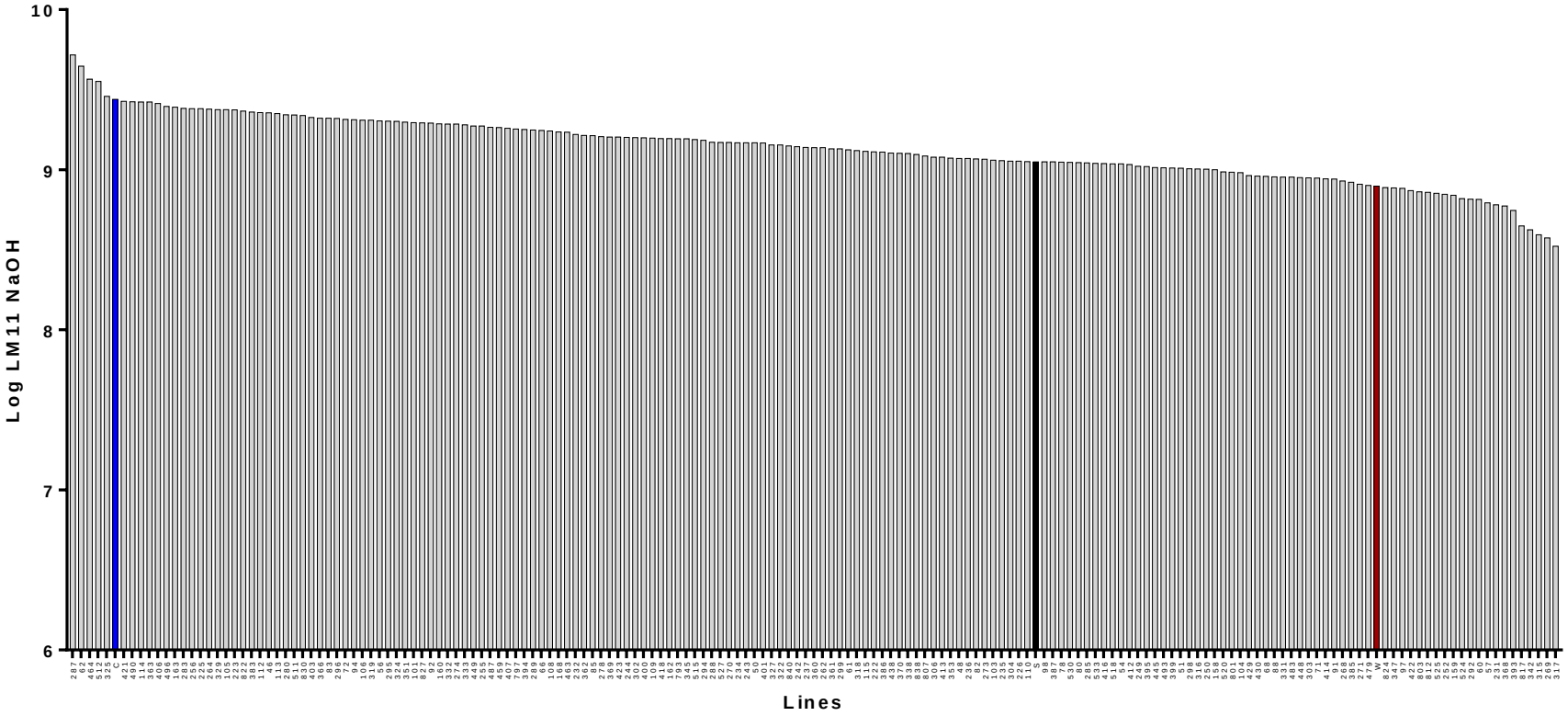

Figure 5.10. Recombinant inbred lines ranked by LM11 epitope detection. Recombinant inbred lines (RILs) shown in order of relative LM11 epitope detection (Log). Parent lines are indicated by coloured bars; C869 (sugar beet parent) - blue, W357B (red garden beet parent) - red. The commercial variety Sophia is indicated by the black bar.

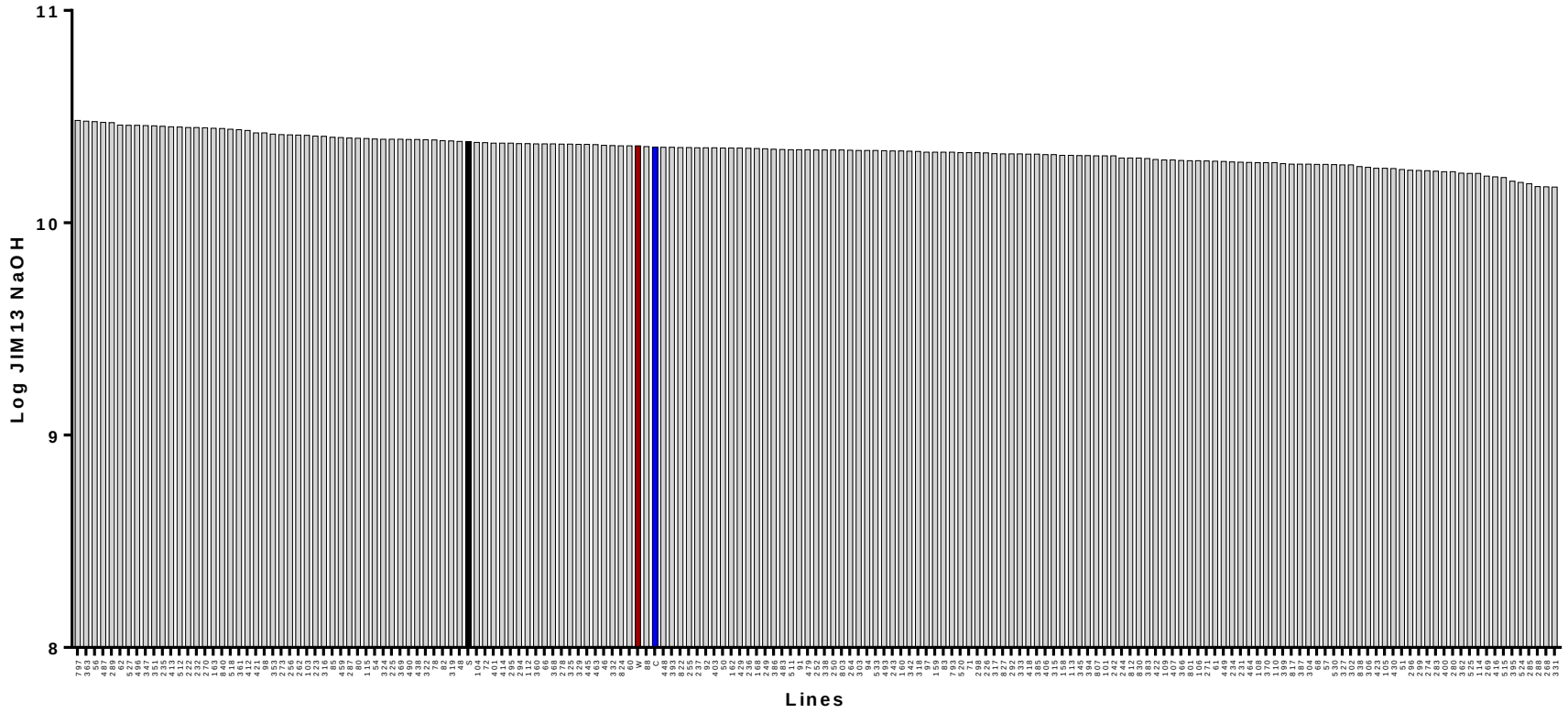

Figure 5.11. Recombinant inbred lines ranked by JIM13 epitope detection. Recombinant inbred lines (RILs) shown in order of relative JIM13 epitope detection (Log). Parent lines are indicated by coloured bars; C869 (sugar beet parent) - blue, W357B (red garden beet parent) - red. The commercial variety Sophia is indicated by the black bar.

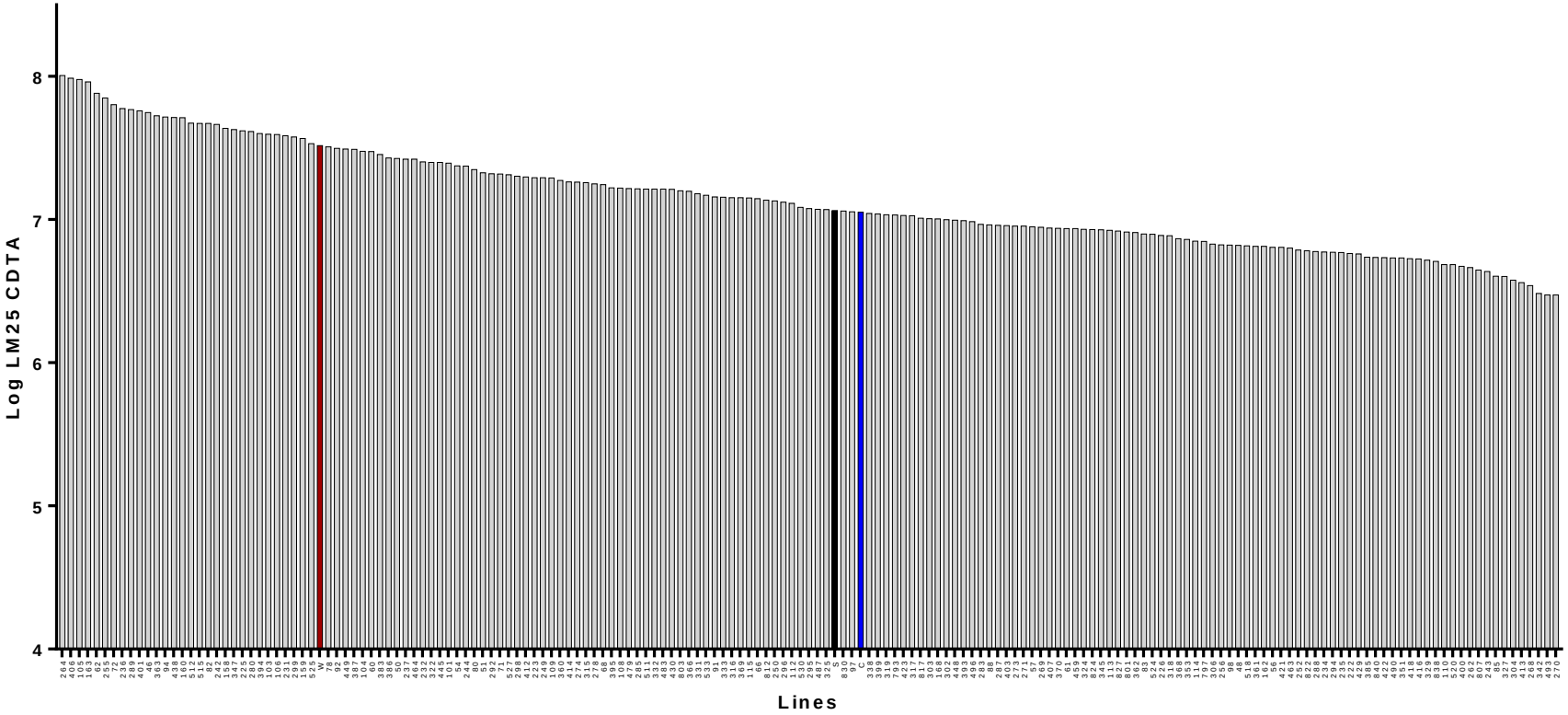

Figure 5.12. Recombinant inbred lines ranked by LM25 epitope detection. Recombinant inbred lines (RILs) shown in order of relative LM25 epitope detection (Log). Parent lines are indicated by coloured bars; C869 (sugar beet parent) - blue, W357B (red garden beet parent) - red. The commercial variety Sophia is indicated by the black bar.

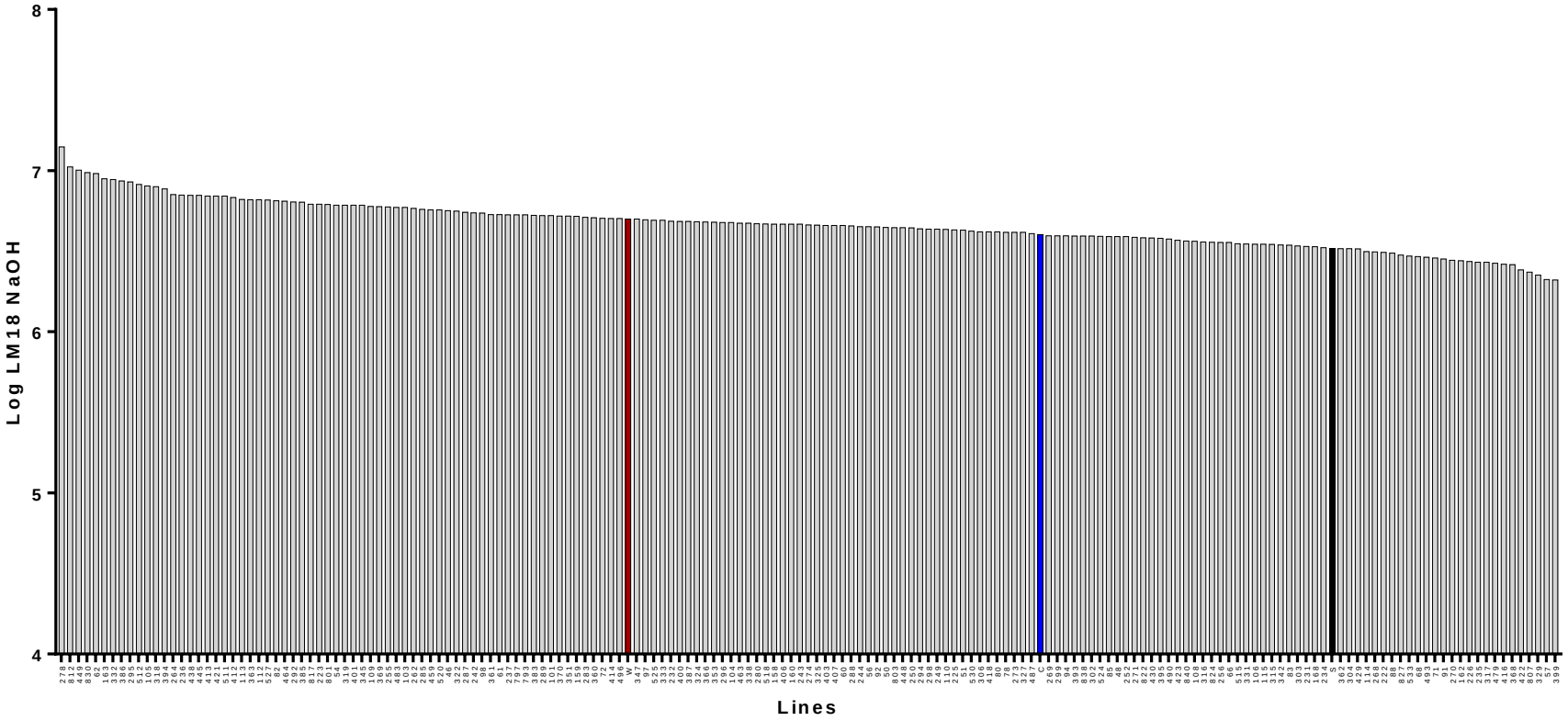

Figure 5.13. Recombinant inbred lines ranked by LM18 epitope detection. Recombinant inbred lines (RILs) shown in order of relative LM18 epitope detection (Log). Parent lines are indicated by coloured bars; C869 (sugar beet parent) - blue, W357B (red garden beet parent) - red. The commercial variety Sophia is indicated by the black bar.

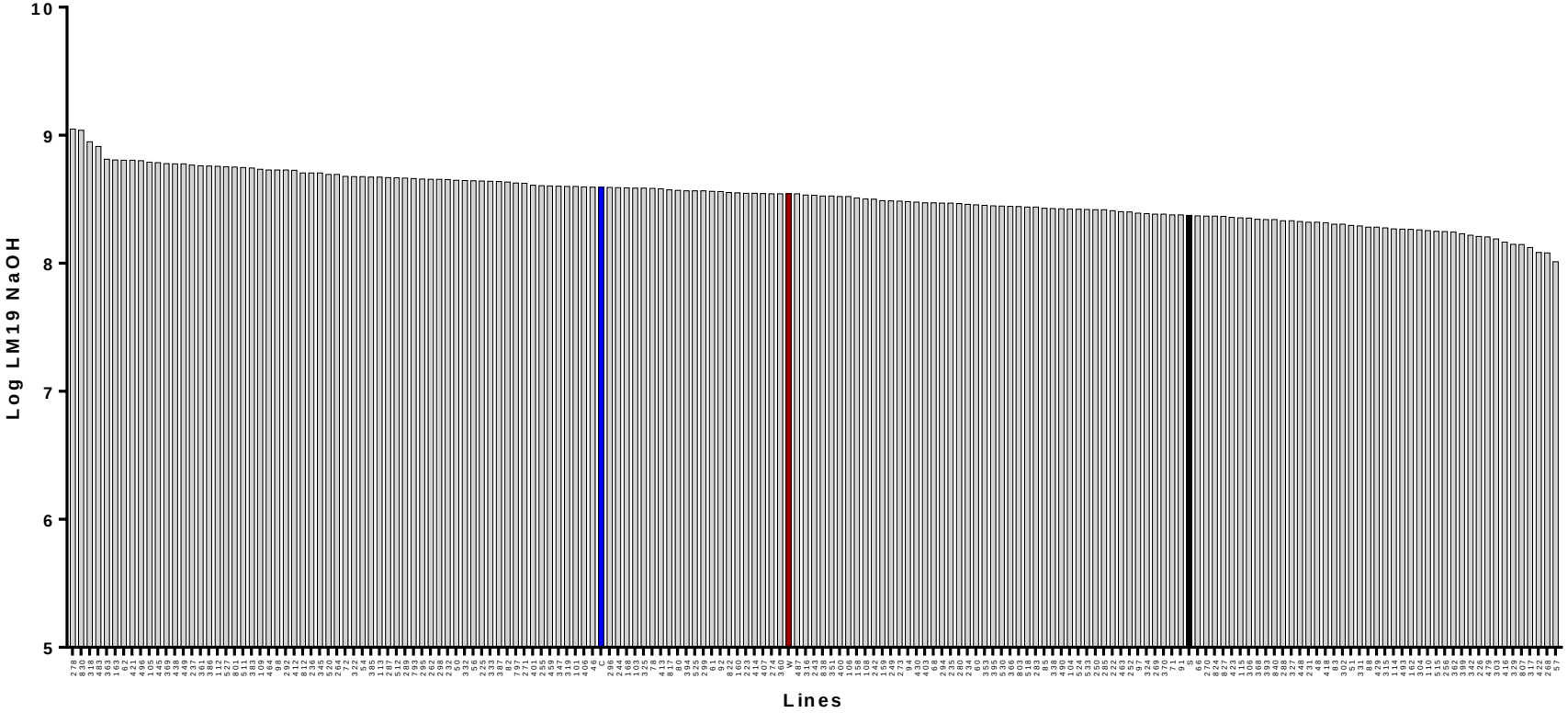

Figure 5.14. Recombinant inbred lines ranked by LM19 epitope detection. Recombinant inbred lines (RILs) shown in order of relative LM19 epitope detection (Log). Parent lines are indicated by coloured bars; C869 (sugar beet parent) - blue, W357B (red garden beet parent) - red. The commercial variety Sophia is indicated by the black bar.

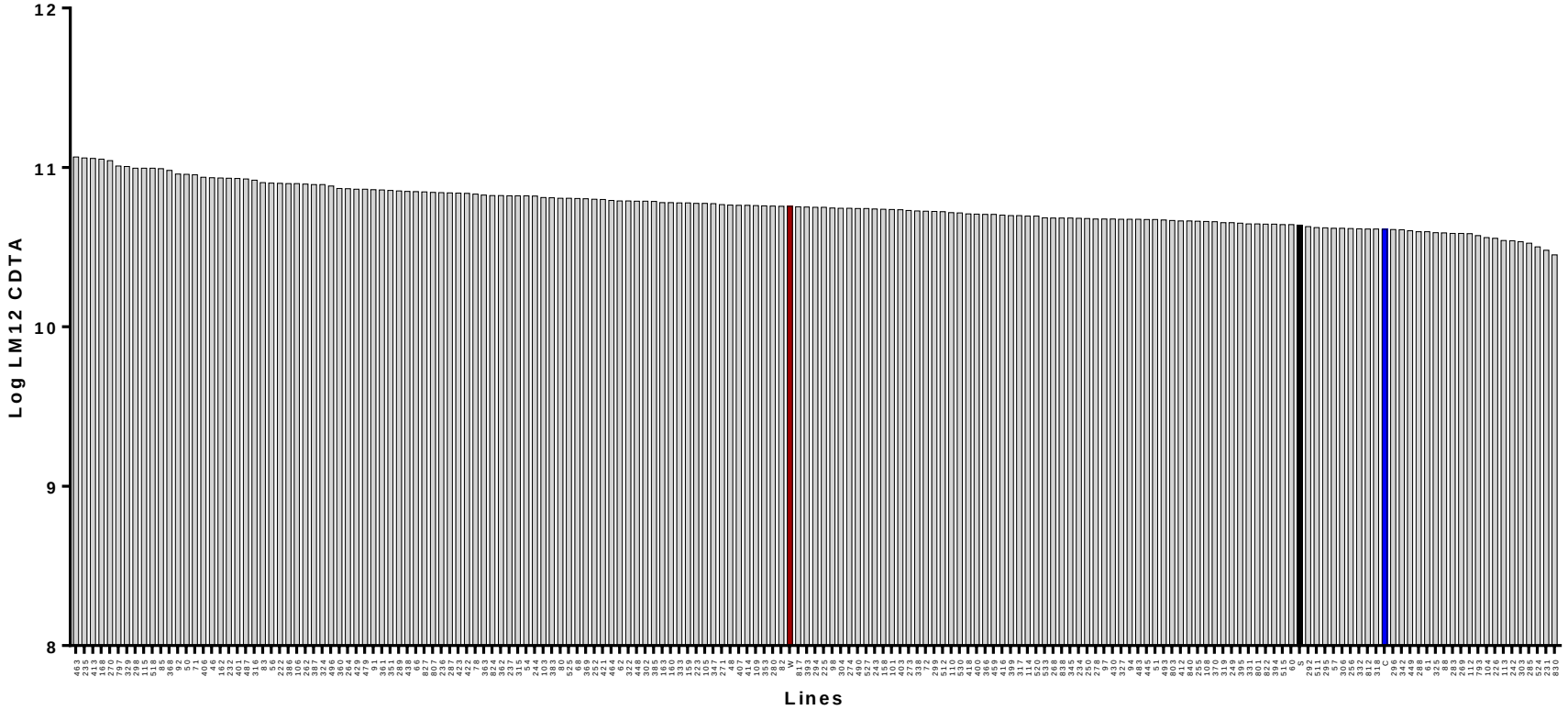

Figure 5.15. Recombinant inbred lines ranked by LM12 epitope detection. Recombinant inbred lines (RILs) shown in order of relative LM12 epitope detection (Log). Parent lines are indicated by coloured bars; C869 (sugar beet parent) - blue, W357B (red garden beet parent) - red. The commercial variety Sophia is indicated by the black bar.

5.3.4 Identifying candidate lines

In order to identify lines which should be investigated further the physiological traits and relative cell wall polysaccharide detection levels should be compared to find line which have desirable characteristics for both the sugar industry and downstream processing of pulp. In Figure 5.16 the 20 lines with the highest sugar yield per hectare have been used to identify candidates which may contain genetic when used for breeding purposes may produce beneficial traits. Comparing the line whose roots have the largest diameter many of the highest yielding lines have this trait however, none of the high yielding roots have both large diameters and high percentage dry matter. There is one line, 106, which has both high percentage dry matter and a large root diameter, this line was ranked 21 for highest sugar yielding lines.

It was important to deduce the allocation of sucrose to other dry matter such as cell walls and therefore a comparison was made for percentage sucrose of dry matter. Several of the lines with the highest sugar yields also displayed a high percentage of sucrose of dry matter. Lines; 483, 422 and 395, showed higher percentage of their dry matter being sucrose than the parent line, C869.

Discussed earlier was the negative correlation between xylan detection and sucrose yield however it has been decided to include this analyses with high yielding lines to identify any lines which have both high yield and high xylan detection. In Figure 5.16 it was shown that one of the RILs 325 had both a high relative abundance of xylan as well as a high sugar yield. In addition the C869 parent also had one of the highest detected levels of xylan by LM10 and LM11.

In addition to high xylan detection line 325 also had the highest galactan detection out of all the lines including the commercial variety and sugar beet parent line. One other line, 797, has shown high galactan detection by LM5 as well as relatively high xylan detection by LM10. No other high sugar yielding lines showed high galactan or xylan detection. In contrast LM28 detection of glucoronoxylan indicated a positive correlation with percentage dry matter. The lines, 325 and 366 both showed a high detected level of glucoronoxylan

and a high percentage dry matter. In addition the sugar beet parent line C869 also showed this correlation.

Arabinan detection by LM13 showed a positive correlation with larger roots and increased sugar yield. Therefore a comparison was made with LM13 detection and high sugar yield. Several of the highest yielding lines showed to have the highest arabinan detection. With the commercial variety and the sugar beet parent line not appearing in the top ranked 22 lines. Line 533 showed the highest arabinan detection, this line was also included in the lines with the highest root diameters. Other lines which also had high arabinan detection by LM13 and larger root diameters were 422 and 370.

Pectic feruloyation was also analysed within the comparison in Figure 5.3. However this comparison was made with lines with the lowest feruloyation rather than the highest. Three high yielding lines were found to have some of the lowest levels of detection by LM12 for feruloylated pectin; 524, 104 and 325.

It is important to also identify traits which could be detrimental to sugar yield so that these traits can be selected against during breeding programmes. Several detected epitopes indicated a negative correlation with sugar yield and therefore were assessed to identify low sugar yielding lines which also exhibited these cell wall traits.

Figure 5.17 shows the correlation between the lowest yielding RILs and the negative cell wall polysaccharide detection. Here it was shown that several of the lowest sugar yielding lines had high abundance of detection of these cell wall polysaccharides. Notably line 62 had a high detection of all the negatively correlated cell wall polysaccharides, this line was also the lowest sugar yielding line of all the RILs.

Sucrose yield kg/ha		Root Diameter		% dry matter		% sucrose of dry matter		Xylan detection				Glucuronoxylan		Galactan detection		Arabinan detection		Feruloyation detection	
								LM10 NaOH		LM11 NaOH		LM28 NaOH		LM5 CDTA		LM13 CDTA		LM12 CDTA	
Line	Value (log)	Line	Value (cm)	Line	Value (%)	Line	Value (%)	Line	Value (log)	Line	Value (log)	Line	Value (log)	Line	Value (log)	Line	Value (log)	Line	Value (log)
Sophia	9.5	Sophia	10.3	Sophia	23.9	Sophia	80.6	287	9.5	287	9.7	287	10.2	325	10.0	533	9.9	830	10.5
C869	9.2	385	9.9	C869	22.9	483	76.6	464	9.5	62	9.6	62	10.2	Sophia	9.9	162	9.8	231	10.5
385	8.9	C869	9.3	338	22.4	422	76.5	62	9.5	464	9.6	325	10.1	797^	9.8	298	9.8	524	10.5
395	8.7	807	9.0	274	22.3	395	76.2	512	9.5	512	9.6	114	10.1	C869	9.8	91	9.8	285	10.5
422	8.7	342	8.9	242	22.0	262	76.0	325	9.4	325	9.5	274	10.1	338	9.8	331	9.7	303	10.5
342	8.7	370	8.8	366	22.0	530	75.9	114	9.4	C869	9.4	464	10.1	56	9.7	315	9.7	242	10.5
366	8.7	235	8.6	325	21.9	223	75.9	C869	9.4	421	9.4	283	10.1	463	9.7	159	9.7	113	10.5
524	8.7	422	8.6	400	21.8	394	75.9	223	9.4	490	9.4	C869	10.1	225	9.7	71	9.7	226	10.6
533	8.6	113	8.6	329	21.8	101	75.9	163	9.3	114	9.4	112	10.1	163	9.7	360	9.7	104	10.6
817	8.6	524	8.4	306	21.8	527	75.9	822	9.3	363	9.4	822	10.1	252	9.7	422	9.6	793	10.6
235	8.6	288	8.4	104	21.8	838	75.7	496	9.3	406	9.4	256	10.1	94	9.6	299	9.6	112	10.6
273	8.6	353	8.4	416	21.7	493	75.7	490	9.3	496	9.4	295	10.1	361	9.6	370	9.6	269	10.6
370	8.6	817	8.3	106*	21.6	158	75.7	421	9.3	163	9.4	366	10.1	421	9.6	82	9.6	283	10.6
303	8.6	304	8.2	109	21.6	85	75.6	283	9.3	283	9.4	496	10.1	54	9.6	68	9.6	88	10.6
325	8.6	533	8.2	94	21.5	236	75.5	296	9.3	256	9.4	319	10.1	327	9.6	66	9.6	325	10.6
243	8.5	449	8.2	270	21.4	368	75.4	264	9.3	225	9.4	225	10.0	363	9.6	324	9.6	61	10.6
423	8.5	162	8.2	304	21.4	C869	75.4	280	9.3	264	9.4	512	10.0	289	9.6	807	9.6	288	10.6
60	8.5	106*	8.1	362	21.4	361	75.4	797^	9.3	329	9.4	490	10.0	287	9.6	423	9.6	449	10.6
807	8.5	60	8.1	268	21.3	91	75.3	101	9.3	105	9.4	113	10.0	438	9.6	496	9.6	342	10.6
104	8.5	292	8.1	302	21.2	327	75.3	274	9.3	223	9.4	51	10.0	78	9.6	407	9.6	296	10.6
353	8.5	824	8.1	264	21.2	807	75.3	92	9.3	822	9.4	403	9.9	306	9.6	449	9.6	C869	10.6
483	8.5	487	8.0	256	21.2	104	75.2	383	9.3	383	9.4	242	9.9	347	9.6	366	9.5	318	10.6
106*	8.5							Sophia	9.1	Sophia	9.1								

Lowest to highest

Figure 5.16 Comparison of the highest sugar yielding recombinant inbred lines. The 20 highest sugar yielding lines (kg ha^{-1}) compared to other significant physiological and detected cell wall characteristics identified by the correlation matrix in Figure 5.1. High yielding lines have been assigned a colour code to allow cross referencing across different traits. The commercial variety Sophia and the sugar beet parent have been included where appropriate as the highest yielding lines. All traits are ordered from highest to lowest except of feruloyation detection where this is lowest to highest.

Sucrose yield kg/ha		HG detection				Xyloglucan detection		AGP detection	
		LM18 NaOH		LM19 NaOH		LM25 CDTA		JIM13 NaOH	
Line	Value (log)	Line	Value (log)	Line	Value (log)	Line	Value (log)	Line	Value (log)
62	6.5	278	7.1	278	9.1	264	8.0	62	10.0
274	6.7	812	7.0	830	9.0	406	8.0	163	9.9
464	6.8	449	7.0	318	9.0	105	8.0	50	9.9
249	7.0	830	7.0	483	8.9	163	8.0	401	9.9
512	7.1	62	7.0	363	8.8	62	7.9	464	9.9
160	7.2	163	7.0	163	8.8	255	7.9	487	9.8
406	7.2	332	6.9	62	8.8	72	7.8	351	9.8
112	7.2	386	6.9	421	8.8	236	7.8	264	9.8
46	7.3	295	6.9	496	8.8	289	7.8	46	9.8
72	7.3	512	6.9	105	8.8	401	7.8	72	9.8
264	7.3	105	6.9	445	8.8	46	7.7	115	9.8
421	7.3	318	6.9	369	8.8	363	7.7	223	9.8
801	7.3	394	6.9	438	8.8	94	7.7	325	9.8
51	7.3	264	6.9	449	8.8	438	7.7	394	9.8
511	7.3	236	6.9	237	8.8	160	7.7	56	9.8
333	7.4	438	6.8	361	8.8	512	7.7	512	9.8
108	7.4	445	6.8	386	8.8	515	7.7	830	9.8
299	7.4	413	6.8	112	8.8	82	7.7	249	9.8
287	7.4	421	6.8	527	8.8	242	7.7	413	9.8
386	7.4	511	6.8	801	8.8	158	7.6	232	9.8
363	7.4	412	6.8	511	8.8	347	7.6	236	9.8
78	7.4	113	6.8	383	8.7	225	7.6	353	9.8
322	7.5	363	6.8	109	8.7	280	7.6	85	9.8
W357B	7.5	112	6.8	464	8.7	394	7.6	412	9.8

Figure 5.17 Comparison of the lowest sugar yielding recombinant inbred lines. The lowest sugar yielding lines (kg ha^{-1}) compared to significant detected cell wall characteristics identified by the correlation matrix in Figure 5.1. Low yielding lines have been assigned a colour code to allow cross referencing across different traits. The red garden beet parent (W357B) has been included as one of the lowest yielding lines.

5.4 Discussion

5.4.1 Physiological trait analysis

Candidate lines with beneficial traits could be used to identify markers for genetic regions of interest. An ideal variety for sugar production is a sugar beet with a high sugar yield, which has a high percentage of dry matter and therefore does not contain relatively high amount of water. In addition this individual would have a high percentage of sucrose of dry matter, demonstrating its potential to allocate a higher proportion of carbon resources to sucrose rather than other sugars such as cell wall components. This line would also produce relatively large roots with these characteristics to allow a high per hectare sugar yield. These are traits that were illustrated to have positive correlation in Figure 5.1. Therefore finding line which indicate one or more of these traits could provide targets for breeding programmes.

Work described in Chapter 4 concluded that in order for a sugar beet root to accumulate high levels of sucrose it would be important for there to be abundance phloem to deposit sucrose into the root, and therefore an increase in cambial rings. From the correlation analysis it was clear that higher relative abundance of the xylan epitopes had a negative correlation with sugar yield. However as correlation is based on the relative abundance of xylan detected, very small roots which confer low sugar yield on a field scale, would indicate a high relative abundance of xylan. In Chapter 3 with was demonstrated that vasculature develops early in growth before expansion, therefore if a root grew very little during the expansion stage xylan would account for a higher proportion of the root composition and therefore skew the correlation. Using the analysis in Figure 5.11 it is clear that a high xylan detection does not always confer to low sugar yield as demonstrated by RIL 325. Line 325 has one of the highest detected relative abundances of the LM10 and LM11 epitope (Fig 5.2) with an average sugar yield of 5705 kg/ha which is the 13th highest sugar yield of the RILs. However this high yield was achieved in smaller root as this was not one of the lines with the largest root diameter. Therefore, this supports the hypothesis that combining increased vasculature with smaller cells contributes to higher concentrations of sucrose.

Xylan detection is an indicator of relative abundance of vasculature, both xylem and phloem, within the root. Further to this, increased galactan detection indicated a positive correlation with percentage of dry matter and percentage sucrose of fresh weight and to a lesser extent an increase of percentage of sucrose of dry matter. Work in Chapter 4 indicated that the epitope of the LM26 antibody which identifies phloem sieve elements was associated with the galactan backbone, therefore this positive correlation could indicate an increase in phloem vessels in lines which have an increased percentage. An increased abundance of galactan can also have mechanical implications in the root, increasing cell wall firmness (McCartney et al., 2000), giving the whole root more strength and resistance to mechanical stress. However in this case the special deposition of galactan is unknown. The comparison analysis in Figure 5.3 identified two lines which had both high xylan detection as well as high galactan detection; 325 and 797. While 797 was not one of the highest yielding lines, 325 was ranked as the 13th highest yielding line. This result makes line 325 an interesting candidate for further work as it has been identified to have an increased amount of detection of epitopes associated with vasculature. Traits which could have allowed this line with smaller roots to accumulate relative high concentrations of sugar.

Arabinan detection has also shown a positive correlation with physiological traits involved with root size (fresh root weight, diameter and root dry weight). Like galactan arabinan has a structural role in plant cell walls, increased relative arabinan content has been identified as conferring flexibility in cell walls as well as cell to cell adhesion. Arabinan In sugar beet specifically has been indicated as cross linking through ferulic acids (Ralet et al., 2006, Levigne et al., 2004c, Levigne et al., 2004b) and therefore a higher relative abundance of these could provide the tensile strength for a root to grow larger. However this type of interaction could have implications in downstream processing of sugar beet pulp by industries other than sugar production. The comparison analysis in Figure 5.3 has confirmed that many of the highest sugar yielding lines has also got some of the highest levels of detection of arabinan suggesting that higher levels of arabinan give the roots beneficial mechanical properties for accumulating increased concentrations of sugar. In addition the analysis of the feruloyation

detection by LM12 indicated that some of the lines had reduced levels of feruloyation of their pectin. These lines are interesting candidates as they could show reduced cross-linking while still accumulating relatively large concentrations of sucrose. These traits are of interest to downstream processors of sugar beet pulp as a reduction in these strong interactions could make digestion more efficient.

As discussed earlier it is clear that the storage root needs to expand to accumulate sugar while maintaining high levels of dry matter rather than water. Ideally rather than cells expanding to increase diameter cells would undertake cell division and increase cell wall content, this would combat the issue of large cells contain lower concentrations of sucrose due to water uptake (Draycott, 2006b). The lines identified as have higher percentage of dry matter are not included in the 20 lines with the largest diameter. However these lines do not have the largest root have the highest sugar yields per hectare. This indicates that these roots may have smaller cells containing a high concentration of sucrose and therefore these are ideal candidates breeding targets towards increasing sucrose concentration. Line 104 is especially interesting in this regards as this line is also included in the 20 lines with the highest percentage sucrose from dry matter.

It is also important during breeding to be able to identify negative traits which could lead to a decrease in sugar yield. The correlation matrix (Fig 5.1) indicated four epitopes which could have a negative effect on sugar yield; JIM13, LM25, LM18 and LM19.

The correlation of high JIM13 detection with sucrose yield could indicate that the increased abundance of AGP could be effecting growth. AGPs have been identified as having a role in suppressing development and cell proliferation (Basile and Basile, 1993, Basile et al., 1986). Therefore a line with high levels of AGP detection would indicate repressed growth and reduced cell number and therefore affecting sucrose assimilation. There were several lines identified as having high detection of JIM13 with line 62 having the highest detection (Fig 5.17).

LM25 detects an epitope of xyloglucan (Pedersen et al., 2012) which is a factor in the mechanical strength of cell walls (Peña et al., 2004, Hayashi, 1989) due to interactions with cellulose microfibrils. There are many studies on the role of xyloglucan in reducing cell expansion and elongation (Takeda et al., 2002, Labavitch and Ray, 1974), and increase in xyloglucan could reduce cell expansion and cell wall flexibility and therefore could reduce sucrose assimilation. Again line 62 had a high detection of LM25 as did line 264 and 406.

Increased HG detection by LM18 and LM19 also indicated a negative correlation with sugar yield. These mAbs identify HG which is partially methylated or have no methyl esterification (Verhertbruggen et al., 2009a). Homogalacturonan is a key polysaccharide in the pectin supramolecule. The de-methyl-esterified (de-Me) portions of HG are responsible for the ionic interactions with Ca^{2+} to form the pectic gel (Caffall and Mohnen, 2009) contributing to wall strength. An increase of these interactions has been attributed to decreased cell wall expansion and increased wall stiffening (Stolle-Smits et al., 1999). In this study Stolle-Smits et al. (1999), found that at maturation pea pod cell wall degraded RGI components but increased de-Me-HG which prevented further expansion or growth. This increased detection of de-Me-HG in the low sugar yielding lines could be due to reduced expansion reducing accommodation of increased turgor pressure due to sucrose assimilation. Again, line 62 was found to have high detection of both the LM18 and LM19 epitope. Other lines which also showed high detection of LM19 were 363 which also detected relatively high levels of xyloglucan and 421 which showed high detected levels of both LM18 and LM19.

Interestingly it has also been found that reducing the amount of de-methyl-esterified HG has been found to increase the efficiency of enzymatic saccharification of plant cell wall material (Lionetti et al., 2010). This is an interesting note for utilising sugar beet pulp for biomass saccharification.

5.4.*2 In muro* interactions

Positive correlation between the detection of arabinan epitopes by mAbs (LM6-M, LM6, LM13, and LM16) and the detection of homogalacturonan (JIM5, JIM7,

LM18, LM19) indicates that these are associated with each other within the wall. From current understanding of the structure of *in muro* pectin these associations should be expected, with RGI and HG making up the pectin supramolecule where arabinan side chains are located on the RGI portion of the molecule.

Arabinan epitopes showing positive correlation with LM12 detection of feruloylated pectic confirms that feruloyation occurs on the arabinose residues of arabinan chains in sugar beet pectin (Ralet et al., 2006). Therefore, the higher the abundance of arabinan in the cell walls the higher the abundance of feruloyation. This is potentially an important consideration for the downstream processing of sugar beet pulp as these diferulic cross-bridges are known to decrease digestibility in grasses (Kroon et al., 1999b), although the implications in sugar beet are still unknown.

5.5 Conclusion

From the work in this Chapter a group of candidate lines for further study can be collated in Table 5.1 and Table 5.2. These have been chosen based on their individual traits, both physiological and cell wall related.

Table 5.1 Selected candidate recombinant inbred lines for further study for crop improvement.

Line	Traits
325	High percentage dry matter, high xylan detection, high glucuronoxylan detection, high galactan detection, low feruloylation detection
104	High % dry matter, high % sucrose of dry matter, low feruloylation detection
524	Large root diameter, low feruloyation detection
807	Large root diameter, high % sucrose of dry matter, high arabinan detection
422	Large root diamter, high % sucrose of dry matter
395	High % sucrose of dry matter
483	High % sucrose of dry matter
533	Large root diameter, high arabinan detection
366	High % dry matter, high glucoronoxylan detection, high arabinan detection
106	Large root diameter, high % dry matter
370	Large root diameter, high arabinan detection

Table 5.2 Selected candidate recombinant inbred lines for further study into decreased sugar yield.

Line	Traits
62	High homogalacturonan detection, high xyloglucan detection, high AGP detection
264	High homogalacturonan detection, high xyloglucan detection, high AGP detection
363	High homogalacturonan detection, high xyloglucan detection
512	High homogalacturonan detection, high xyloglucan detection, high AGP detection
46	High xyloglucan detection, high AGP detection
464	High homogalacturonan detection, high AGP detection
511	High homogalacturonan detection
249	High AGP detection
160	High xyloglucan detection

Chapter 6

General discussion

This project involved an extensive analysis of *Beta vulgaris* root anatomy regarding relative positioning of the vascular tissues, xylem and phloem, in context of supernumerary successive cambium. In addition, cell wall analysis has provided key information regarding the relative abundance of a range of cell wall epitopes throughout crop development. Key candidate lines from the RIL populations have also been identified to steer future sugar beet breeding for crop improvement, for both agronomically important and accompanying cell wall components.

The study of the internal anatomies of three *Beta vulgaris* lines has indicated that the successive cambial arrangement, which is hypothesised to contribute to sucrose concentrations, is established in early stages of development. The development of successive cambial rings is highly conserved across all three lines studied (Sophia, W357B and C869) and is a contributing factor to overall root size. The commercial sugar beet line Sophia showed the highest number of cambial rings as well as the largest root diameter, both factors appear to contribute to a higher sucrose concentration and overall sugar yield.

Utilising the newly characterised mAb LM26 it was possible to identify the relative positioning of the phloem sieve elements to the xylem vessels within the cambial arrangement. This indicates why increasing the number of cambial rings increased sucrose concentration by reducing the length diffusion pathway from phloem sieve elements to storage parenchyma.

The increased number of cambial rings in the commercial variety, Sophia, is the result of traditional breeding techniques where selection has been based on potential sucrose concentrations rather than root anatomy. This work provides an understanding of the basis of sugar yield and suggests that breeding for sugar beets with an increased number of cambial rings could lead to a higher potential for sucrose accumulation in commercial sugar beets.

This understanding of root anatomy allowed the analysis of the relative abundance of xylan epitope detection in relation to sugar yield within the RIL population. This detection gave the indication that an increase in vasculature can lead to high sugar yield ha^{-1} without excessive root expansion.

Knowing that root vasculature develops early in the growth period informed the decision to discount xylan detection as detrimental to increased sugar yield when found to be negatively correlated with sugar yield in the correlation matric (Fig 5.1). This negative correlation was caused by a number of low sugar yielding lines showing a high relative abundance of xylan detection, however, these lines also showed high relative abundance of epitopes which can suppress development (AGPs and xyloglucan) preventing effective sucrose accumulation. These roots were small and had undergone very little expansion and therefore the relative abundance of vascular tissue (shown by xylan detection) in comparison to parenchyma was high. However lines were identified which had high sugar yield and high xylan detection suggesting that these lines potentially contain the genetic information for increased number of cambial rings.

The characterisation of the LM26 monoclonal antibody (mAb) was important for this project during the developmental study of cambial arrangement. This mAb is directed to phloem sieve elements and its epitope has been identified as a β-1,6-galactosyl substitution of pectic β-1,4-galactan, which we now know occurs discretely in the phloem sieve elements of sugar beet and other key species including *Miscanthus* and *Arabidopsis.* The identification of the epitope gives an insight into the cell wall modifications associated with this specific type of tissue and its related function.

For studying sugar beet this novel monoclonal antibody has been a valuable tool for the further assessment of the internal anatomies of the *Beta vulgaris* lines. This sugar storage crop relies on phloem vessels to accumulate sucrose in its root parenchyma cells and the microscopic visualisation of these tissues enables an increased understanding of the mechanisms involved in the success of this process. Using the LM26 antibody *in situ* has given in insight into the successive cambial arrangement within the storage root and the spatial relationships between the xylem, the phloem and the parenchyma cells. Sugar beet phloem sieve elements have never been assessed in this way before and the developmental work has provided a valuable opportunity to visualise the spatial variation of phloem abundance in the cambial rings throughout growth in different *Beta vulgaris* lines. It is now possible to pinpoint at what stage of seedling

development phloem develop and when new rings are added. This information shows that this early development is the most important part of the sugar beet growth period in terms of sugar yield potential.

Utilising the LM26 antibody for quantitative studies such as ELISA, CoMPP or EDC has been difficult due to the low relative abundance of the LM26 epitope in the sugar beet root. Due to the epitope being so localised to the phloem sieve elements in sugar beet roots there is such a low level of the epitope in a homogenised sample it has not been possible to use the antibody for quantitative developmental analysis of cell wall composition as shown in chapter 4 where convincing levels of the epitope were not detected. During the CoMPP analysis of the RIL population in chapter 5 the LM26 signal was so low that it was found to be statistically unreliable. The rarity of this epitope in a homogenised sample is a limitation to the use of this mAb for quantitative studies, this issue could potentially be limited by selective sampling rather than holistic. Selective sampling in sugar beet was tempted through the duration of this study however, the microscopic nature of the phloem sieve elements made efforts unsuccessful, therefore requiring the use of the garlic samples to provide a sufficient source of the epitope for analysis during characterisation of LM26. Despite these limitations the characterisation of the LM26 mAb it can now be used as a tool for identifying phloem sieve elements, useful for various studies across many species to study how vasculature develops and changes in response to developmental and environmental stimuli.

Studying sugar beet cell walls beyond early seedling stage has allowed an assessment of changes in cell wall composition throughout development. It is uncertain if plant development drives cell wall modification or cell wall composition drives development. However, a combination of biotic and abiotic factors will effect crop performance (Atkinson and Urwin, 2012), including cell wall properties (Cosgrove, 1997). Looking into cell wall composition in sugar beet throughout three different growing seasons has allowed the investigation of the effect environmental factors have upon cell wall composition and how this effects the overall success of the crop. This work contributes to efforts to tease apart the function of the cell wall in growth and development. It is clear from several studies

that cell wall mechanics is greatly affects by cell wall composition. Many of these studies have stated that cell turgor has a role in altering cell wall composition, an important consideration for sugar beet study due to high turgor of cells with high levels of sucrose held within. Ali and Traas (2016) described how load bearing cell walls undergo polymerisation to increase cellular matrix (pectin components) when exposed to increases in turgor pressure. This expansion of cell walls has been again described in other species where mechanic stress has induced elastic extensibility (Peters et al., 2001, Braybrook and Jönsson., 2016) Work on characterisation of LM26 in this project also showed that cell wall structures are key in the physical properties of the cell, as shown by Torode et al. (2017) where the LM26 epitope (6-O-(β-Gal)-β-1,4-galactohexose) showed to increase elasticity of the walls identified to contain this rare modulation. The analysis described in this thesis can be used to support these hypotheses, that the cell wall composition can be altered in response to a variety of stresses both abiotic and biotic (e.g. environment, soil type and growing season). In addition, field studies conducted in this project provide important insight into and how modifications in cell walls could impact crop performance.

The list of candidate lines can now be used for gene discovery or further analysis. Combining the results from this work into ongoing work in collaboration with the University of Michigan the search for a gene for crop improvement can be directed. The sugar beet genome (Dohm et al., 2014) and the ongoing sequencing of the RIL parental lines (C869 and W357B) by McGrath and Townsend (unpublished) will make the identification of SNPs via genotyping by sequencing possible. This work will lead to the identification of QTLs (Quantitative Trait Locus) to provide causal genes or mutations an early step in identifying and sequencing actual genes which can cause trait variation. This information can be fed into current breeding efforts and marker assisted breeding for crop improvement.

Utilising monoclonal antibodies to assess the cell wall composition of the RIL population has allowed the identification of potential gene pools for crop improvement. This is a valuable asset to any breeding programme and has clear economic importance. The genetic diversity between sugar beet and garden beet

has been exploited to develop RILs where novel mutations become fixed via sequential self-fertilisation (McGrath et al., 2005). This makes it is possible to capture novel genetic variation outside of the current germplasm widely used for sugar beet breeding. Through the assessment of the *Beta vulgaris* RIL population a set of candidate lines have been identified for further investigation. These lines have been selected based on factors identified to increase overall sugar yield with a correlated cell wall epitope level. In addition, those lines which expressed traits detrimental to sugar yield have also been selected for further study into genetic markers to select against to prevent low sugar yield.

For the sugar industry it is important to focus on increased sugar yield as this is the priority income from the crop. This work has indicated that in addition to traditional physiological traits, it has identified that some cell wall characteristics may contribute to increase sugar yield. Cell wall characteristics are not usually considered during variety development, however, the cell wall analysis of the RIL population has shown that cell wall properties could potentially be scored using tools such as mAbs in combination with high throughput methods such as CoMPP.

In addition to the sugar industry there is an interest in the properties of sugar beet storage root cell walls for downstream processes such as those involved in biofuels. Some RILs from this study have been identified to have lower amounts of feruloyation, something that is hypothesised to increase saccharification of second generation biofuel feed stocks (Reem et al., 2016, Grabber et al., 1998). The lines selected for this trait also had some of the highest sugar yields therefore making these and exciting avenue to follow up.

6.1 Conclusion

In conclusion, this project has confirmed *Beta vulgaris* storage root internal anatomies in regard to vascular tissues with the assistance of cell wall directed monoclonal antibodies including the newly characterised monoclonal antibody LM26. This work utilised CoMPP as a high throughout method for the first time in this type of system to collate cell wall characteristics throughout a population. By

correlating the detected levels of cell wall polysaccharides with physiological traits, lines with potentially beneficial traits have been identified for future work to identify genes of interest for the improvement of the sugar beet crop. Potential improvements include, increased sugar yield, in field performance and downstream processing of sugar beet pulp as a lignocellulosic biomass source.

6.2 Future perspectives

This thesis has outlined several promising areas for future work and impactful publication:

- A technical report and analysis of two quantitative techniques for the analysis of plant cell walls. Both CoMPP and ELISA are widely used in the plant cell wall research community to detect specific cell wall epitopes which translate to cell wall traits. However, these two techniques have never been directly compared using the same samples as in this project. There is now an opportunity to report the differences and similarities of detection sensitivity as well as practicality of utilising these techniques for a variety of sample sizes and extraction methods.

- The novel antibody LM26 developed as part of this project provides a new addition to the tools available for the analysis of multiple species physiology. The use of this antibody has been invaluable as part of this project and this example can be used to direct research into vasculature in future work. Work outlined in this project can be expanded utilising LM26 during the next stages in the analysis of the RIL population described in chapter 5. Candidate lines can be analysed *in situ* to deduce if their vasculature hold the key to potentially more successful plants whether increased sugar yield or additional uses downstream. This will provide even more detail into sugar beet vasculature and further inform efforts towards crop improvement.

Chapter 7

References

Ali, O. and Traas, J., 2016. Force-driven polymerization and turgor-induced wall expansion. *Trends in plant science*, *21*(5), pp.398-409.

Alkaya, E. & Demirer, G. N. 2011. Anaerobic mesophilic co-digestion of sugar-beet processing wastewater and beet-pulp in batch reactors. *Renewable Energy,* 36**,** 971-975.

Amor, Y., Haigler, C. H., Johnson, S., Wainscott, M. & Delmer, D. P. 1995. A membrane-associated form of sucrose synthase and its potential role in synthesis of cellulose and callose in plants. *Proceedings of the National Academy of Sciences,* 92**,** 9353-9357.

Anders, N., Wilkinson, M. D., Lovegrove, A., Freeman, J., Tryfona, T., Pellny, T. K., Weimar, T., Mortimer, J. C., Stott, K., Baker, J. M., Defoin-Platel, M., Shewry, P. R., Dupree, P. & Mitchell, R. A. C. 2012. Glycosyl transferases in family 61 mediate arabinofuranosyl transfer onto xylan in grasses. *Proceedings of the National Academy of Sciences of the United States of America,* 109**,** 989-993.

Andersen, M. C., Boos, I., Marcus, S. E., Kracun, S. K., Rydahl, M. G., Willats, W. G., Knox, J. P. & Clausen, M. H. 2016. Characterization of the LM5 pectic galactan epitope with synthetic analogues of beta-1,4-d-galactotetraose. *Carbohydr Res,* 436**,** 36-40.

Anderson, C. T., Carroll, A., Akhmetova, L. & Somerville, C. 2010. Real-time imaging of cellulose reorientation during cell wall expansion in *Arabidopsis* roots. *Plant Physiol,* 152**,** 787-796.

Andrews, D. 2008. *Bio-methane fulled vehicles- John balwin CNG Services* [Online]. Claverton Energy Research Group. Available: http://www.claverton-energy.com/bio-methane-fuelled-vehicles-john-baldwin-cng-services.html [Accessed January 2014].

Antoni, D., Zverlov, V. & Schwarz, W. 2007. Biofuels from microbes. *Applied Microbiology and Biotechnology,* 77**,** 23-35.

Artschwager, E. 1926. Anatomy of the vegetative organs of the sugar beet. *Journal of Agricultural Research,* 33**,** 0143-0176.

Atkinson, N. J. & Urwin, P. E. 2012. The interaction of plant biotic and abiotic stresses: from genes to the field. *J Exp Bot,* 63**,** 3523-3543.

Basile, D., Basile, M. & Varner, J. The occurance of arabinogalactan-protein in Plagiochila-arctica Bryhn and Kaal (Hepaticae). American Journal of Botany, 1986. Botanical Soc Amer Inc Ohio State Univ-Dept Botany, 603-604.

Basile, D. V. & Basile, M. R. 1993. The role and control of the place-dependent suppression of cell division in plant morphogenesis and phylogeny. *Memoirs of the Torrey Botanical Club***,** 63-84.

Baver, L. & Farnsworth, R. 1941. Soil structure effects in the growth of sugar beets. *Soil Science Society of America Journal,* 5**,** 45-48.

BBRO 2017. Recommended list 2017. *In:* BRITISH BEET RESEARCH ORGANISATION (ed.).

Beeckman, T., Przemeck, G. K., Stamatiou, G., Lau, R., Terryn, N., De Rycke, R., Inzé, D. & Berleth, T. 2002. Genetic complexity of cellulose synthase A gene function in Arabidopsis embryogenesis. *Plant Physiol,* 130**,** 1883-1893.

Bennett, R., Phipps, R., Strange, A. & Grey, P. 2004. Environmental and human health impacts of growing genetically modified herbicide-tolerant sugar beet: a life-cycle assessment. *Plant Biotechnology Journal,* 2**,** 273-278.

Berndes, G., Hoogwijk, M. & van den Broek, R. 2003. The contribution of biomass in the future global energy supply: a review of 17 studies. *Biomass & Bioenergy,* 25**,** 1-28.

Bhambie, S. & Sharma, A. Ontogeny of cambium in Amaranthus caudatus L. and Achyranthes aspera L. Proceedings of the Indian Academy of Sciences, 1985. 295-301.

Biancardi, E., Lewellen, R. T., De Biaggi, M., Erichsen, A. W. & Stevanato, P. 2002. The origin of rhizomania resistance in sugar beet. *Euphytica,* 127**,** 383-397.

Bonnin, E., Dolo, E., Le Goff, A. & Thibault, J. F. 2002a. Characterisation of pectin subunits released by an optimised combination of enzymes. *Carbohydrate Research,* 337**,** 1687-1696.

Bonnin, E., Saulnier, L., Brunel, M., Marot, C., Lesage-Meessen, L., Asther, M. & Thibault, J. F. 2002b. Release of ferulic acid from agroindustrial by-products by the cell wall-degrading enzymes produced by *Aspergillus niger* I-1472. *Enzyme and Microbial Technology,* 31**,** 1000-1005.

Brentrup, F., Küsters, J., Kuhlmann, H. & Lammel, J. 2001. Application of the Life Cycle Assessment methodology to agricultural production: an example of sugar beet production with different forms of nitrogen fertilisers. *European Journal of Agronomy,* 14**,** 221-233.

Brett, C. T. 2000. Cellulose microfibrils in plants: biosynthesis, deposition, and integration into the cell wall. *International review of cytology,* 199**,** 161-199.

British Sugar. 2010. *Sites:Our UK operations* [Online]. British Sugar plc. Available: http://www.britishsugar.co.uk/Sites.aspx [Accessed 20th May 2014].

Bromley, J. R., Busse-Wicher, M., Tryfona, T., Mortimer, J. C., Zhang, Z., Brown, D. M. & Dupree, P. 2013. GUX1 and GUX2 glucuronyltransferases decorate distinct domains of glucuronoxylan with different substitution patterns. *Plant J,* 74**,** 423-34.

Brouns, F., Edwards, S. & English, P. 1997. The effect of dietary inclusion of sugar-beet pulp on the feeding behaviour of dry sows. *Animal Science,* 65**,** 129-133.

Brown, D. M., Zeef, L. A., Ellis, J., Goodacre, R. & Turner, S. R. 2005. Identification of novel genes in *Arabidopsis* involved in secondary cell wall formation using expression profiling and reverse genetics. *Plant Cell,* 17**,** 2281-2295.

Brummell, D. A. 2006. Cell wall disassembly in ripening fruit. *Functional Plant Biology,* 33**,** 103-119.

Buhre, C., Kluth, C., Bürcky, K., Märländer, B. & Varrelmann, M. 2009. Integrated Control of Root and Crown Rot in Sugar Beet: Combined Effects of Cultivar, Crop Rotation, and Soil Tillage. *Plant Disease,* 93**,** 155-161.

Burton, R. A., Gidley, M. J. & Fincher, G. B. 2010. Heterogeneity in the chemistry, structure and function of plant cell walls. *Nature chemical biology,* 6**,** 724-732.

Busse-Wicher, M., Gomes, T. C. F., Tryfona, T., Nikolovski, N., Stott, K., Grantham, N. J., Bolam, D. N., Skaf, M. S. & Dupree, P. 2014. The pattern of xylan acetylation suggests xylan may interact with cellulose microfibrils as a twofold helical screw in the secondary plant cell wall of *Arabidopsis thaliana*. *Plant Journal,* 79**,** 492-506.

Caffall, K. H. & Mohnen, D. 2009. The structure, function, and biosynthesis of plant cell wall pectic polysaccharides. *Carbohydr Res,* 344**,** 1879-1900.

Camposeo, S. & Rubino, P. 2003. Effect of irrigation frequency on root water uptake in sugar beet. *Plant and Soil,* 253**,** 301-309.

Canilha, L., Chandel, A. K., Milessi, T. S. D., Antunes, F. A. F., Freitas, W. L. D., Felipe, M. D. A. & da Silva, S. S. 2012. Bioconversion of Sugarcane Biomass into Ethanol: An Overview about Composition, Pretreatment Methods, Detoxification of Hydrolysates, Enzymatic Saccharification, and Ethanol Fermentation. *Journal of Biomedicine and Biotechnology*.

Carlquist, F. S. & Gowans, D. A. 1995. Secondary growth and wood histology of Welwitschia. *Botanical Journal of the Linnean Society,* 118**,** 107-121.

Carlquist, S. 2003. Wood and stem anatomy of woody Amaranthaceae ss: ecology, systematics and the problems of defining rays in dicotyledons. *Botanical Journal of the Linnean Society,* 143**,** 1-19.

Carlquist, S. 2007. Successive cambia revisited: ontogeny, histology, diversity, and functional significance. *Journal of the Torrey Botanical Society,* 134**,** 301-332.

Carpita, N. C. & Gibeaut, D. M. 1993. Structural models of primary cell walls in flowering plants: consistency of molecular structure with the physical properties of the walls during growth. *The Plant Journal,* 3**,** 1-30.

Chen, X.-Y. & Kim, J.-Y. 2009. Callose synthesis in higher plants. *Plant signaling & behavior,* 4**,** 489-492.

Clausen, M. H., Ralet, M. C., Willats, W. G. T., McCartney, L., Marcus, S. E., Thibault, J. F. & Knox, J. P. 2004. A monoclonal antibody to feruloylated-(1 -> 4)-beta-D-galactan. *Planta,* 219**,** 1036-1041.

Colquhoun, I. J., Ralet, M. C., Thibault, J. F., Faulds, C. B. & Williamson, G. 1994. Structure Identification of Feruloylated Oligosaccharides from Sugar-Beet Pulp by Nmr-Spectroscopy. *Carbohydrate Research,* 263**,** 243-256.

Cooke, D. A. & Scott, J. 2012. *The sugar beet crop*, Springer Science & Business Media.

Cornuault, V., Buffetto, F., Marcus, S. E., Crépeau, M.-J., Guillon, F., Ralet, M.-C. & Knox, P. 2017. LM6-M: a high avidity rat monoclonal antibody to pectic α-1,5-L-arabinan. *bioRxiv*.

Cornuault, V., Buffetto, F., Rydahl, M. G., Marcus, S. E., Torode, T. A., Xue, J., Crepeau, M. J., Faria-Blanc, N., Willats, W. G. T., Dupree, P., Ralet, M. C. & Knox, J. P. 2015. Monoclonal antibodies indicate low-abundance links between heteroxylan and other glycans of plant cell walls. *Planta,* 242**,** 1321-1334.

Cornuault, V., Manfield, I. W., Ralet, M. C. & Knox, J. P. 2014. Epitope detection chromatography: a method to dissect the structural heterogeneity and inter-connections of plant cell-wall matrix glycans. *Plant J,* 78**,** 715-22.

Cosgrove, D. J. 1993. Wall Extensibility - Its Nature, Measurement and Relationship to Plant-Cell Growth. *New Phytologist,* 124**,** 1-23.

Cosgrove, D. J. 1997. Relaxation in a high-stress environment: the molecular bases of extensible cell walls and cell enlargement. *Plant Cell,* 9**,** 1031-1041.

Cosgrove, D. J. 2000. Loosening of plant cell walls by expansins. *Nature,* 407**,** 321.

Cosgrove, D. J. 2005. Growth of the plant cell wall. *Nature Reviews Molecular Cell Biology,* 6**,** 850-861.

Daas, P. J. H., Boxma, B., Hopman, A. M. C. P., Voragen, A. G. J. & Schols, H. A. 2001. Nonesterified galacturonic acid sequence homology of pectins. *Biopolymers,* 58**,** 1-8.

De Boer, A. & Volkov, V. 2003. Logistics of water and salt transport through the plant: structure and functioning of the xylem. *Plant, Cell & Environment,* 26**,** 87-101.

Dodić, S., Popov, S., Dodić, J., Ranković, J., Zavargo, Z. & Mučibabić, R. J. 2009. Bioethanol production from thick juice as intermediate of sugar beet processing. *Biomass and Bioenergy,* 33**,** 822-827.

Dohm, J. C., Minoche, A. E., Holtgräwe, D., Capella-Gutiérrez, S., Zakrzewski, F., Tafer, H., Rupp, O., Rossleff Soerensen, T., Stracke, R. & Reinhardt, R. 2014. The genome of the recently domesticated crop plant sugar beet (*Beta vulgaris*). *Nature,* 505**,** 546-+.

Draycott, A. P. 2006a. Development of Sugar Beet. *In:* DRAYCOTT, A. P. (ed.) *Sugar Beet.* Blackwell Publishing UK.

Draycott, A. P. 2006b. *Sugar Beet*, Blackwell Publishing.

Draycott, A. P. & Farley, R. F. 1971. Effect of sodium and magnesium fertilisers and irrigation on growth, composition and yield of sugar beet. *J Sci Food Agric,* 22**,** 559-63.

Duan, X. & Burris, J. S. 1997. Film coating impairs leaching of germination inhibitors in sugar beet seed. *Crop Science,* 37**,** 515-520.

Edwards, M., Bowman, Y., Dea, I. & Reid, J. 1988. A beta-D-galactosidase from nasturtium (*Tropaeolum majus* L.) cotyledons. Purification, properties, and

demonstration that xyloglucan is the natural substrate. *Journal of Biological chemistry,* 263**,** 4333-4337.

El-Mezawy, A., Dreyer, F., Jacobs, G. & Jung, C. 2002. High-resolution mapping of the bolting gene B of sugar beet. *Theoretical and applied genetics,* 105**,** 100-105.

Elbehri, A., Segerstedt, A. & Lui, P. 2013. Biofuels and the sustainability challenge: A global assessment of sustainability issues, trends and policies for biofuels and related feedstocks.: Food and Agriculture Organisation (FAO).

Elliott, M. C. & Weston, G. D. 1993. Biology and physiology of the sugar-beet plant. *In:* COOKE, D. A. & SCOTT, R. K. (eds.) *The Sugar Beet Crop.* Dordrecht: Springer Netherlands.

Ergun, M. & Mutlu, S. F. 2000. Application of a statistical technique to the production of ethanol from sugar beet molasses by *Saccharomyces cerevisiae*. *Bioresource Technology,* 73**,** 251-255.

Esau, K. & Hoefert, L. L. 1972. Development of infection with beet western yellows virus in the sugarbeet. *Virology,* 48**,** 724-738.

European Commission 2009. Directive 2009/41/EC of the European Parliament and of the Council on the contained use of genetically modified micro-organisms (Recast). *Official Journal of the European Union,* 125**,** 75-97.

European Commission 2015. Directive 2015/412 of the European Parliament and of the Council amending Directive 2001/18/EC as regards the possibility for the Member States to restrict or prohibit the cultivation of genetically modified organisms (GMOs) in their territory. *Official Journal of the European Union,* 68**,** 1-8.

Fahn, A. & Zimmermann, M. 1982. Development of the successive cambia in *Atriplex halimus* (Chenopodiaceae). *Botanical Gazette,* 143**,** 353-357.

Fares, K., Renard, C. M. G. C., R'Zina, Q. & Thibault, J.-F. 2001. Extraction and composition of pectins and hemicelluloses of cell walls of sugar beet roots grown in Morocco. *International Journal of Food Science & Technology,* 36**,** 35-46.

Fincher, G. B., Stone, B. A. & Clarke, A. E. 1983. Arabinogalactan-proteins: structure, biosynthesis, and function. *Annual Review of Plant Physiology,* 34**,** 47-70.

Francia, E., Tacconi, G., Crosatti, C., Barabaschi, D., Bulgarelli, D., Dall'Aglio, E. & Vale, G. 2005. Marker assisted selection in crop plants. *Plant Cell, Tissue and Organ Culture,* 82**,** 317-342.

Francis, S. A. 2006. Development of sugar beet. *Sugar Beet***,** 9-29.

Fry, S. C. 1988. *The growing plant cell wall: chemical and metabolic analysis*, Longman Group Limited.

Fry, S. C. 1989. The Structure and Functions of Xyloglucan. *J Exp Bot,* 40**,** 1-11.

Geiger, D. R., Giaquinta, R. T., Sovonick, S. A. & Fellows, R. J. 1973. Solute distribution in sugar beet leaves in relation to phloem loading and translocation. *Plant Physiol,* 52**,** 585-589.

Giaquinta, R. T. 1979. Sucrose translocation and storage in the sugar beet. *Plant Physiol,* 63**,** 828-832.

Goubet, F., Jackson, P., Deery, M. J. & Dupree, P. 2002. Polysaccharide analysis using carbohydrate gel electrophoresis: a method to study plant cell wall polysaccharides and polysaccharide hydrolases. *Anal Biochem,* 300**,** 53-68.

Grabber, J., Hatfield, R. & Ralph, J. 1998. Diferulate cross-links impede the enzymatic degradation of non-lignified maize walls. *J Sci Food Agric,* 77**,** 193-200.

Grimmer, M., Trybush, S., Hanley, S., Francis, S., Karp, A. & Asher, M. 2007. An anchored linkage map for sugar beet based on AFLP, SNP and RAPD markers and QTL mapping of a new source of resistance to Beet necrotic yellow vein virus. *Theoretical and applied genetics,* 114**,** 1151-1160.

Hanson, A. D. & Wyse, R. 1982. Biosynthesis, translocation, and accumulation of betaine in sugar beet and its progenitors in relation to salinity. *Plant Physiol,* 70**,** 1191-1198.

Harholt, J., Suttangkakul, A. & Scheller, H. V. 2010. Biosynthesis of Pectin. *Plant Physiology,* 153**,** 384-395.

Harris, P. J. 2006. Primary and secondary plant cell walls: a comparative overview. *New Zealand Journal of Forestry Science,* 36**,** 36.

Harveson, R. 2016. *History of sugarbeets* [Online]. Cropwatch: Intitute of agriculture and natural resources - University of Nebraska-Linoln. 2017].

Hayashi, T. 1989. Xyloglucans in the primary cell wall. *Annual Review of Plant Biology,* 40**,** 139-168.

Hergert, G. W. 2010. Sugar beet fertilization. *Sugar Tech,* 12**,** 256-266.

Hernandez-Gomez, M. C., Runavot, J.-L., Guo, X., Bourot, S., Benians, T. A., Willats, W. G., Meulewaeter, F. & Knox, J. P. 2015. Heteromannan and Heteroxylan Cell Wall polysaccharides display different dynamics during the elongation and secondary Cell Wall deposition phases of cotton fiber cell development. *Plant and Cell Physiology,* 56**,** 1786-1797.

Him, J. L., Pelosi, L., Chanzy, H., Putaux, J. L. & Bulone, V. 2001. Biosynthesis of (1→ 3)-β-d-glucan (callose) by detergent extracts of a microsomal fraction from Arabidopsis thaliana. *The FEBS Journal,* 268**,** 4628-4638.

Hosoya, T., Kawamoto, H. & Saka, S. 2007. Cellulose–hemicellulose and cellulose–lignin interactions in wood pyrolysis at gasification temperature. *Journal of analytical and applied pyrolysis,* 80**,** 118-125.

Huang, X., Li, D. & Wang, L.-j. 2017. Characterization of pectin extracted from sugar beet pulp under different drying conditions. *Journal of Food Engineering,* 211**,** 1-6.

Huhtanen, P. 1988. The effects of barley, unmolassed sugar-beet pulp and molasses supplements on organic matter, nitrogen and fibre digestion in the rumen of cattle given a silage diet. *Animal Feed Science and Technology,* 20**,** 259-278.

ISAAA 2016. ISAAA's GM approval database.

Ishii, T., Matsunaga, T., Pellerin, P., O'Neill, M. A., Darvill, A. & Albersheim, P. 1999. The plant cell wall polysaccharide rhamnogalacturonan II self-assembles into a covalently cross-linked dimer. *Journal of Biological chemistry,* 274**,** 13098-13104.

Jarvis, M. 2003. Chemistry - Cellulose stacks up. *Nature,* 426**,** 611-612.

Jensen, P. & Spliid, N. 2003. Deposition of pesticides on the soil surface. *Pesticides research,* 65.

Jones, L., Milne, J. L., Ashford, D. & McQueen-Mason, S. J. 2003. Cell wall arabinan is essential for guard cell function. *Proceedings of the National Academy of Sciences,* 100**,** 11783-11788.

Joseleau, J. P. & Perez, S. 2017. *Secondary Wall Hemicellulose* [Online]. GlycoPedia.

Kabel, M. A., van den Borne, H., Vincken, J.-P., Voragen, A. G. & Schols, H. A. 2007. Structural differences of xylans affect their interaction with cellulose. *Carbohydrate Polymers,* 69**,** 94-105.

Kenter, C., Hoffmann, C. M. & Märländer, B. 2006. Effects of weather variables on sugar beet yield development (*Beta vulgaris* L.). *European Journal of Agronomy,* 24**,** 62-69.

Kerstens, S. & Verbelen, J. P. 2002. Cellulose orientation in the outer epidermal wall of angiosperm roots: Implications for biosystematics. *Annals of Botany,* 90**,** 669-676.

Khan, M. F. 2010. Introduction of glyphosate-tolerant sugar beet in the United States. *Outlooks on Pest Management,* 21**,** 38-41.

Kim, S. & Dale, B. E. 2004. Global potential bioethanol production from wasted crops and crop residues. *Biomass and Bioenergy,* 26**,** 361-375.

Kimura, S., Laosinchai, W., Itoh, T., Cui, X., Linder, C. R. & Brown, R. M., Jr. 1999. Immunogold labeling of rosette terminal cellulose-synthesizing complexes in the vascular plant *Vigna angularis*. *Plant Cell,* 11**,** 2075-86.

Kissner. 2015. *Sugar processing* [Online].

Knox, J. P., Day, S. & Roberts, K. 1989. A set of cell surface glycoproteins forms an early position, but not cell type, in the root apical carota L. *Development,* 106**,** 47-56.

Knox, J. P., Linstead, P. J., King, J., Cooper, C. & Roberts, K. 1990a. Pectin Esterification Is Spatially Regulated Both within Cell-Walls and between Developing-Tissues of Root Apices. *Planta,* 181**,** 512-521.

Knox, J. P., Linstead, P. J., King, J., Cooper, C. & Roberts, K. 1990b. Pectin esterification is spatially regulated both within cell walls and between developing tissues of root apices. *Planta,* 181**,** 512-21.

Knox, J. P., Linstead, P. J., Peart, J., Cooper, C. & Roberts, K. 1991. Developmentally Regulated Epitopes of Cell-Surface Arabinogalactan Proteins and Their Relation to Root-Tissue Pattern-Formation. *Plant Journal,* 1**,** 317-326.

Koelsch, L. M. 1969. Sugar beet processing. Google Patents.

Kračun, S. K., Fangel, J. U., Rydahl, M. G., Pedersen, H. L., Vidal-Melgosa, S. & Willats, W. G. 2017. Carbohydrate Microarray Technology Applied to High-Throughput Mapping of Plant Cell Wall Glycans Using Comprehensive Microarray Polymer Profiling (CoMPP). *Metastasis Research Protocols, 2nd Edition,* 1503**,** 147-165.

Kroon, P. A., Garcia-Conesa, M. T., Fillingham, I. J., Hazlewood, G. P. & Williamson, G. 1999a. Release of ferulic acid dehydrodimers from plant cell walls by feruloyl esterases. *Journal of the Science of Food and Agriculture,* 79**,** 428-434.

Kroon, P. A., Garcia-Conesa, M. T., Fillingham, I. J., Hazlewood, G. P. & Williamson, G. 1999b. Release of ferulic acid dehydrodimers from plant cell walls by feruloyl esterases. *J Sci Food Agric,* 79**,** 428-434.

Kumar, P., Barrett, D. M., Delwiche, M. J. & Stroeve, P. 2009. Methods for Pretreatment of Lignocellulosic Biomass for Efficient Hydrolysis and Biofuel Production. *Industrial & Engineering Chemistry Research,* 48**,** 3713-3729.

KWS. 2005. *Roundup Ready sugar beet:application for approval as food and feed* [Online].

Labavitch, J. M. & Ray, P. M. 1974. Relationship between promotion of xyloglucan metabolism and induction of elongation by indoleacetic acid. *Plant Physiol,* 54**,** 499-502.

Lamport, D. T. 1966. The protein component of primary cell walls. *Advances in botanical research,* 2**,** 151-218.

Lamport, D. T., Varnai, P. & Seal, C. E. 2014. Back to the future with the AGP–Ca2+ flux capacitor. *Annals of Botany,* 114**,** 1069-1085.

Lange, W., Brandenburg, W. A. & De Bock, T. S. 1999. Taxonomy and cultonomy of beet (*Beta vulgaris* L.). *Botanical Journal of the Linnean Society,* 130**,** 81-96.

Lee, K. J., Marcus, S. E. & Knox, J. P. 2011. Cell wall biology: perspectives from cell wall imaging. *Molecular Plant,* 4**,** 212-219.

Levigne, S., Ralet, M. C., Quemener, B. & Thibault, J. F. 2004a. Isolation of diferulic bridges ester-linked to arabinan in sugar beet cell walls. *Carbohydrate Research,* 339**,** 2315-2319.

Levigne, S., Ralet, M. C., Quemener, B. & Thibault, J. F. 2004b. Isolation of diferulic bridges ester-linked to arabinan in sugar beet cell walls. *Carbohydr Res,* 339**,** 2315-2319.

Levigne, S., Ralet, M. C. & Thibault, J. F. 2002. Characterisation of pectins extracted from fresh sugar beet under different conditions using an experimental design. *Carbohydrate Polymers,* 49**,** 145-153.

Levigne, S. V., Ralet, M. C. J., Quemener, B. C., Pollet, B. N. L., Lapierre, C. & Thibault, J. F. J. 2004c. Isolation from sugar beet cell walls of Arabinan oligosaccharides esterified by two ferulic acid monomers. *Plant Physiol,* 134**,** 1173-1180.

Lewellen, R., Skoyen, I. & Erichsen, A. Breeding sugar beet for resistance to rhizomania: Evaluation of host-plant reactions and selection for and inheritance of resistance. 50. Winter Congress of the International Institute for Sugar Beet Research, Bruxelles (Belgium), 11-12 Feb 1987, 1987. IIRB. Secretariat General.

Lima, D. U., Loh, W. & Buckeridge, M. S. 2004. Xyloglucan-cellulose interaction depends on the sidechains and molecular weight of xyloglucan. *Plant Physiology and Biochemistry,* 42**,** 389-394.

Lin, T. Y., Elbein, A. D. & Su, J. C. 1966. Substrate specificity in pectin synthesis. *Biochem Biophys Res Commun,* 22**,** 650-7.

Lionetti, V., Francocci, F., Ferrari, S., Volpi, C., Bellincampi, D., Galletti, R., D'Ovidio, R., De Lorenzo, G. & Cervone, F. 2010. Engineering the cell wall by reducing de-methyl-esterified homogalacturonan improves saccharification of plant tissues for bioconversion. *Proceedings of the National Academy of Sciences,* 107**,** 616-621.

Liwanag, A. J. M., Ebert, B., Verhertbruggen, Y., Rennie, E. A., Rautengarten, C., Oikawa, A., Andersen, M. C. F., Clausen, M. H. & Scheller, H. V. 2012. Pectin Biosynthesis: GALS1 in *Arabidopsis thaliana* Is a beta-1,4-Galactan beta-1,4-Galactosyltransferase. *Plant Cell,* 24**,** 5024-5036.

Longland, A. & Low, A. 1989. Digestion of diets containing molassed or plain sugar-beet pulp by growing pigs. *Animal Feed Science and Technology,* 23**,** 67-78.

Ma, S., Yu, S.-j., Zheng, X.-l., Wang, X.-x., Bao, Q.-d. & Guo, X.-m. 2013. Extraction, characterization and spontaneous emulsifying properties of pectin from sugar beet pulp. *Carbohydrate Polymers,* 98**,** 750-753.

Mannerlof, M., Tuvesson, S., Steen, P. & Tenning, P. 1997. Transgenic sugar beet tolerant to glyphosate. *Euphytica,* 94**,** 83-91.

Marcus, S. E., Blake, A. W., Benians, T. A., Lee, K. J., Poyser, C., Donaldson, L., Leroux, O., Rogowski, A., Petersen, H. L., Boraston, A., Gilbert, H. J., Willats, W. G. & Knox, J. P. 2010. Restricted access of proteins to mannan polysaccharides in intact plant cell walls. *Plant J,* 64**,** 191-203.

Marcus, S. E., Verhertbruggen, Y., Herve, C., Ordaz-Ortiz, J. J., Farkas, V., Pedersen, H. L., Willats, W. G. & Knox, J. P. 2008. Pectic homogalacturonan masks abundant sets of xyloglucan epitopes in plant cell walls. *BMC Plant Biol,* 8**,** 60.

Mathew, S. & Emilia Abraham, T. 2004. *Ferulic Acid: An Antioxidant Found Naturally in Plant Cell Walls and Feruloyl Esterases Involved in its Release and Their Applications*.

May, M. 2003. Economic consequences for UK farmers of growing GM herbicide tolerant sugar beet. *Annals of Applied Biology,* 142**,** 41-48.

Mazumder, K., Pena, M. J., O'Neill, M. A. & York, W. S. 2012. Structural characterization of the heteroxylans from poplar and switchgrass. *Metastasis Research Protocols, 2nd Edition,* 908**,** 215-28.

McCann, M. C., Wells, B. & Roberts, K. 1992. Complexity in the spatial localization and length distribution of plant cell-wall matrix polysaccharides. *Journal of Microscopy,* 166**,** 123-136.

McCartney, L., Marcus, S. E. & Knox, J. P. 2005a. Monoclonal antibodies to plant cell wall xylans and arabinoxylans. *Journal of Histochemistry & Cytochemistry,* 53**,** 543-546.

McCartney, L., Marcus, S. E. & Knox, J. P. 2005b. Monoclonal antibodies to plant cell wall xylans and arabinoxylans. *J Histochem Cytochem,* 53**,** 543-6.

McCartney, L., Ormerod, A. P., Gidley, M. J. & Knox, J. P. 2000. Temporal and spatial regulation of pectic (1-->4)-beta-D-galactan in cell walls of developing pea cotyledons: implications for mechanical properties. *Plant J,* 22**,** 105-13.

McGrath, J. M., Koppin, T. K. & Duckert, T. M. Breeding for genetics: development of recombinant inbred lines (RILs) for gene discovery and deployment. Proceedings from the 33rd biennial meeting, 2005 Palm Springs, CA. USA. American society of sugar beet technologists.

McGrath, M. 2010. A primer: Sugar beet breeding and genetics. *Sugarbeet grower.*

McMahon, H. T. & Gallop, J. L. 2005. Membrane curvature and mechanisms of dynamic cell membrane remodelling. *Nature,* 438**,** 590.

McNeil, M., Darvill, A. G. & Albersheim, P. 1980. Structure of Plant-Cell Walls .10. Rhamnogalacturonan-I, a Structurally Complex Pectic Polysaccharide in the Walls of Suspension-Cultured Sycamore Cells. *Plant Physiology,* 66**,** 1128-1134.

McQuilken, M., Whipps, J. & Cooke, R. 1990. Control of damping off in cress and sugar beet by commercial seed coating with *Pythium oligandrum*. *Plant Pathology,* 39**,** 452-462.

Meier, H. & Reid, J. 1982. Reserve polysaccharides other than starch in higher plants. *Plant carbohydrates I.* Springer.

Meier, U., Bleiholder, H., Buhr, L., Feller, C., Hack, H., Heß, M., Lancashire, P. D., Schnock, U. & Stauß, R. 1993. The BBCH system to coding the phenological growth stages of plants–history and publications.

Melton, L. D., Mcneil, M., Darvill, A. G., Albersheim, P. & Dell, A. 1986. Structure of Plant-Cell Walls .17. Structural Characterization of Oligosaccharides Isolated from the Pectic Polysaccharide Rhamnogalacturonan-Ii. *Carbohydrate Research,* 146**,** 279-305.

Milford, G. F. J. 1973. Growth and Development of Storage Root of Sugar-Beet. *Annals of Applied Biology,* 75**,** 427-&.

Milford, G. F. J., Travis, K. Z., Pocock, T. O., Jaggard, K. W. & Day, W. 1988. Growth and dry-matter partitioning in sugar beet. *The Journal of Agricultural Science,* 110**,** 301-308.

Modelska, M., Berlowska, J., Kregiel, D., Cieciura, W., Antolak, H., Tomaszewska, J., Binczarski, M., Szubiakiewicz, E. & Witonska, I. 2017. Concept for Recycling Waste Biomass from the Sugar Industry for Chemical and Biotechnological Purposes. *Molecules,* 22**,** 1544.

Mohdaly, A. A. A., Sarhan, M. A., Smetanska, I. & Mahmoud, A. 2010. Antioxidant properties of various solvent extracts of potato peel, sugar beet pulp and sesame cake. *J Sci Food Agric,* 90**,** 218-226.

Mohnen, D. 2008. Pectin structure and biosynthesis. *Curr Opin Plant Biol,* 11**,** 266-277.

Molinari, H. B., Pellny, T. K., Freeman, J., Shewry, P. R. & Mitchell, R. A. 2013. Grass cell wall feruloylation: distribution of bound ferulate and candidate gene expression in *Brachypodium distachyon*. *Frontiers in plant science,* 4.

Moller, I., Marcus, S. E., Haeger, A., Verhertbruggen, Y., Verhoef, R., Schols, H., Ulvskov, P., Mikkelsen, J. D., Knox, J. P. & Willats, W. 2008. High-throughput screening of monoclonal antibodies against plant cell wall glycans by hierarchical clustering of their carbohydrate microarray binding profiles. *Glycoconj J,* 25**,** 37-48.

Moller, I., Sørensen, I., Bernal, A. J., Blaukopf, C., Lee, K., Øbro, J., Pettolino, F., Roberts, A., Mikkelsen, J. D., Knox, J. P., Bacic, A. & Willats, W. G. T. 2007. High-throughput mapping of cell-wall polymers within and between plants using novel microarrays. *The Plant Journal* [Online], 50.

Moore, J. P., Farrant, J. M. & Driouich, A. 2008. A role for pectin-associated arabinans in maintaining the flexibility of the plant cell wall during water deficit stress. *Plant signaling & behavior,* 3**,** 102-104.

Moore, P. J. & Staehelin, L. A. 1988. Immunogold localization of the cell-wall-matrix polysaccharides rhamnogalacturonan I and xyloglucan during cell expansion and cytokinesis inTrifolium pratense L.; implication for secretory pathways. *Planta,* 174**,** 433-445.

Mutasa-Göttgens, E. S., Qi, A., Zhang, W., Schulze-Buxloh, G., Jennings, A., Hohmann, U., Müller, A. E. & Hedden, P. 2010. Bolting and flowering control in sugar beet: relationships and effects of gibberellin, the bolting gene B and vernalization. *AoB Plants,* 2010**,** plq012.

Nordic Sugar 2012. Sugar Beet Fibre: Physiological effects & Clinical studies.

O'Neill, M., Albersheim, P. & Darvill, A. 1990. 12 The Pectic Polysaccharides of Primary Cell Walls. *Carbohydrates,* 2**,** 415.

O'Neill, M. A., Eberhard, S., Albersheim, P. & Darvill, A. G. 2001. Requirement of Borate Cross-Linking of Cell Wall Rhamnogalacturonan II for *Arabidopsis* Growth. *Science,* 294**,** 846-849.

O'Neill, M. A., Ishii, T., Albersheim, P. & Darvill, A. G. 2004. Rhamnogalacturonan II: Structure and function of a borate cross-linked cell wall pectic polysaccharide. *Annual Review of Plant Biology,* 55**,** 109-139.

Oosterveld, A., Beldman, G., Schols, H. A. & Voragen, A. G. J. 2000. Characterization of arabinose and ferulic acid rich pectic polysaccharides

and hemicelluloses from sugar beet pulp. *Carbohydrate Research,* 328**,** 185-197.

Oosterveld, A., Grabber, J. H., Beldman, G., Ralph, J. & Voragen, A. G. 1997. Formation of ferulic acid dehydrodimers through oxidative cross-linking of sugar beet pectin. *Carbohydr Res,* 300**,** 179-181.

Panella, L. 2010. Sugar Beet as an Energy Crop. *Sugar Tech,* 12**,** 288-293.

Park, Y. B. & Cosgrove, D. J. 2015. Xyloglucan and its Interactions with Other Components of the Growing Cell Wall. *Plant and Cell Physiology,* 56**,** 180-194.

Pattathil, S., Avci, U., Baldwin, D., Swennes, A. G., McGill, J. A., Popper, Z., Bootten, T., Albert, A., Davis, R. H. & Chennareddy, C. 2010. A comprehensive toolkit of plant cell wall glycan-directed monoclonal antibodies. *Plant Physiol,* 153**,** 514-525.

Pauly, M. & Keegstra, K. 2008. Physiology and metabolism 'Tear down this wall'. *Curr Opin Plant Biol,* 11**,** 233-235.

Pauly, M., Qin, Q., Greene, H., Albersheim, P., Darvill, A. & York, W. S. 2001. Changes in the structure of xyloglucan during cell elongation. *Planta,* 212**,** 842-850.

Peaucelle, A., Braybrook, S. A., Le Guillou, L., Bron, E., Kuhlemeier, C. & Höfte, H. 2011. Pectin-induced changes in cell wall mechanics underlie organ initiation in *Arabidopsis*. *Current biology,* 21**,** 1720-1726.

Pedersen, H. L., Fangel, J. U., McCleary, B., Ruzanski, C., Rydahl, M. G., Ralet, M. C., Farkas, V., von Schantz, L., Marcus, S. E., Andersen, M. C., Field, R., Ohlin, M., Knox, J. P., Clausen, M. H. & Willats, W. G. 2012. Versatile high resolution oligosaccharide microarrays for plant glycobiology and cell wall research. *J Biol Chem,* 287**,** 39429-38.

Peña, M. J., Ryden, P., Madson, M., Smith, A. C. & Carpita, N. C. 2004. The galactose residues of xyloglucan are essential to maintain mechanical strength of the primary cell walls in *Arabidopsis* during growth. *Plant Physiol,* 134**,** 443-451.

Peña, M. J., Zhong, R. Q., Zhou, G. K., Richardson, E. A., O'Neill, M. A., Darvill, A. G., York, W. S. & Ye, Z. H. 2007. *Arabidopsis* irregular xylem8 and irregular xylem9: Implications for the complexity of glucuronoxylan biosynthesis. *Plant Cell,* 19**,** 549-563.

Perez, S., Mazeau, K. & du Penhoat, C. H. 2000. The three-dimensional structures of the pectic polysaccharides. *Plant Physiology and Biochemistry,* 38**,** 37-55.

Pettolino, F. A., Walsh, C., Fincher, G. B. & Bacic, A. 2012. Determining the polysaccharide composition of plant cell walls. *Nature protocols,* 7**,** 1590.

Ralet, M.-C., Crépeau, M.-J., Lefèbvre, J., Mouille, G., Höfte, H. & Thibault, J.-F. 2008. Reduced number of homogalacturonan domains in pectins of an *Arabidopsis* mutant enhances the flexibility of the polymer. *Biomacromolecules,* 9**,** 1454-1460.

Ralet, M. C., Andre-Leroux, G., Quemener, B. & Thibault, J. F. 2006. Sugar beet (*Beta vulgaris*) pectins are covalently cross-linked through diferulic bridges in the cell wall (vol 66, pg 2800, 2005). *Phytochemistry,* 67**,** 844-844.

Ralet, M. C., Cabrera, J. C., Bonnin, E., Quemener, B., Hellin, P. & Thibault, J. F. 2005. Mapping sugar beet pectin acetylation pattern. *Phytochemistry,* 66**,** 1832-1843.

Ralet, M. C., Crepeau, M. J., Buchholt, H. C. & Thibault, J. F. 2003. Polyelectrolyte behaviour and calcium binding properties of sugar beet pectins differing in their degrees of methylation and acetylation. *Biochemical Engineering Journal,* 16**,** 191-201.

Ralet, M. C., Thibault, J. F., Faulds, C. B. & Williamson, G. 1994. Isolation and Purification of Feruloylated Oligosaccharides from Cell-Walls of Sugar-Beet Pulp. *Carbohydrate Research,* 263**,** 227-241.

Reem, N. T., Pogorelko, G., Lionetti, V., Chambers, L., Held, M. A., Bellincampi, D. & Zabotina, O. A. 2016. Decreased polysaccharide feruloylation compromises plant cell wall integrity and increases susceptibility to necrotrophic fungal pathogens. *Frontiers in plant science,* 7.

Reif, J. C., Liu, W., Gowda, M., Maurer, H. P., Möhring, J., Fischer, S., Schechert, A. & Würschum, T. 2010. Genetic basis of agronomically important traits in sugar beet (*Beta vulgaris* L.) investigated with joint linkage association mapping. *Theoretical and applied genetics,* 121**,** 1489-1499.

Renard, C. M. G. C. & Jarvis, M. C. 1999. A cross-polarization, magic-angle-spinning, C-13-nuclear-magnetic-resonance study of polysaccharides in sugar beet cell walls. *Plant Physiology,* 119**,** 1315-1322.

Rennie, E. A. & Scheller, H. V. 2014. Xylan biosynthesis. *Current Opinion in Biotechnology,* 26**,** 100-107.

Rezic, T., Oros, D., Markovic, I., Kracher, D., Ludwig, R. & Santek, B. 2013. Integrated hydrolyzation and fermentation of sugar beet pulp to bioethanol. *J. Microbiol. Biotechnol,* 23**,** 1244-1252.

Richardson, K. 2010. Traditional Breeding in Sugar Beet. *Sugar Tech,* 12**,** 181-186.

Richmond, T. 2000. Higher plant cellulose synthases. *Genome Biol,* 1**,** REVIEWS3001.

Richmond, T. A. & Somerville, C. R. 2000. The cellulose synthase superfamily. *Plant Physiol,* 124**,** 495-8.

Ridley, B. L., O'Neill, M. A. & Mohnen, D. A. 2001. Pectins: structure, biosynthesis, and oligogalacturonide-related signaling. *Phytochemistry,* 57**,** 929-967.

Robert, E. M. R., Schmitz, N., Boeren, I., Driessens, T., Herremans, K., De Mey, J., Van de Casteele, E., Beeckman, H. & Koedam, N. 2011. Successive Cambia: A Developmental Oddity or an Adaptive Structure? *Plos One,* 6**,** e16558.

Rodríguez-Gacio, M. d. C., Iglesias-Fernández, R., Carbonero, P. & Matilla, Á. J. 2012. Softening-up mannan-rich cell walls. *J Exp Bot,* 63**,** 3976-3988.

Rombouts, F. M. & Thibault, J. F. 1986. Feruloylated Pectic Substances from Sugar-Beet Pulp. *Carbohydrate Research,* 154**,** 177-187.

Saftner, R. A., Daie, J. & Wyse, R. E. 1983. Sucrose uptake and compartmentation in sugar beet taproot tissue. *Plant Physiol,* 72**,** 1-6.

Saulnier, L. & Thibault, J. F. 1999. Ferulic acid and diferulic acids as components of sugar-beet pectins and maize bran heteroxylans. *Journal of the Science of Food and Agriculture,* 79**,** 396-402.

Scheller, H. V. & Ulvskov, P. 2010. Hemicelluloses. *Annual Review of Plant Biology,* 61**,** 263-89.

Schols, H. A., Bakx, E. J., Schipper, D. & Voragen, A. G. J. 1995. A xylogalacturonan subunit present in the modified hairy regions of apple pectin. *Carbohydrate Research,* 279**,** 265-279.

Schondelmaier, J., Steinrücken, G. & Jung, C. 1996. Integration of AFLP markers into a linkage map of sugar beet (*Beta vulgaris* L.). *Plant breeding,* 115**,** 231-237.

Schreiber, L., Hartmann, K., Skrabs, M. & Zeier, J. 1999. Apoplastic barriers in roots: chemical composition of endodermal and hypodermal cell walls. *J Exp Bot,* 50**,** 1267-1280.

Scott, R., English, S., Wood, D. & Unsworth, M. 1973. The yield of sugar beet in relation to weather and length of growing season. *The Journal of Agricultural Science,* 81**,** 339-347.

Showalter, A. 2001. Arabinogalactan-proteins: structure, expression and function. *Cellular and Molecular Life Sciences,* 58**,** 1399-1417.

Showalter, A. M. 1993. Structure and function of plant cell wall proteins. *The Plant Cell Online,* 5**,** 9-23.

Smallwood, M., Beven, A., Donovan, N., Neill, S. J., Peart, J., Roberts, K. & Knox, J. P. 1994. Localization of Cell-Wall Proteins in Relation to the Developmental Anatomy of the Carrot Root Apex. *Plant Journal,* 5**,** 237-246.

Smallwood, M., Martin, H. & Knox, J. P. 1995. An epitope of rice threonine- and hydroxyproline-rich glycoprotein is common to cell wall and hydrophobic plasma-membrane glycoproteins. *Planta,* 196**,** 510-22.

Sørensen, I. & Willats, W. G. 2011. Screening and characterization of plant cell walls using carbohydrate microarrays. *The Plant Cell Wall: Methods and Protocols***,** 115-121.

Spackman, V. M. T. & Cobb, A. H. 2002. An enzyme-based method for the rapid determination of sucrose, glucose and fructose in sugar beet roots and the effects of impact damage and postharvest storage in clamps. *J Sci Food Agric,* 82**,** 80-86.

Steudle, E. & Peterson, C. A. 1998. How does water get through roots? *J Exp Bot,* 49**,** 775-788.

Stevenson, D. W. & Popham, R. A. 1973. Ontogeny of the Primary Thickening Meristem in Seedlings of *Bougainvillea spectabilis*. *American Journal of Botany,* 60**,** 1-9.

Stolle-Smits, T., Beekhuizen, J. G., Kok, M. T., Pijnenburg, M., Recourt, K., Derksen, J. & Voragen, A. G. 1999. Changes in cell wall polysaccharides of green bean pods during development. *Plant Physiol,* 121**,** 363-372.

Strube. 2017. *Suagr Beet Seed Research* [Online].

Sutton, M. & Doran Peterson, J. 2001. Fermentation of sugarbeet pulp for ethanol production using bioengineered *Klebsiella oxytoca* strain P2. *Journal of Sugar Beet Research,* 38**,** 19-34.

Taiz, L. 1984. Plant cell expansion: regulation of cell wall mechanical properties. *Annual Review of Plant Physiology,* 35**,** 585-657.

Takeda, T., Furuta, Y., Awano, T., Mizuno, K., Mitsuishi, Y. & Hayashi, T. 2002. Suppression and acceleration of cell elongation by integration of xyloglucans in pea stem segments. *Proceedings of the National Academy of Sciences,* 99**,** 9055-9060.

Tamaio, N., Vieira, R. C. & Angyalossy, V. 2009. Origin of successive cambia on stem in three species of Menispermaceae. *Brazilian Journal of Botany,* 32**,** 839-848.

Taylor, N. G. 2008. Cellulose biosynthesis and deposition in higher plants. *New Phytologist,* 178**,** 239-252.

Thomas, L. H., Forsyth, V. T., Šturcová, A., Kennedy, C. J., May, R. P., Altaner, C. M., Apperley, D. C., Wess, T. J. & Jarvis, M. C. 2013. Structure of cellulose microfibrils in primary cell walls from collenchyma. *Plant Physiol,* 161**,** 465-476.

Torode, T. A., O'Neill, R., Marcus, S. E., Cornuault, V., Pose, S., Lauder, R. P., Kracun, S. K., Rydahl, M. G., Andersen, M. C. F., Willats, W. G. T., Braybrook, S. A., Townsend, B. J., Clausen, M. H. & Knox, J. P. 2018. Branched Pectic Galactan in Phloem-Sieve-Element Cell Walls: Implications for Cell Mechanics. *Plant Physiol,* 176**,** 1547-1558.

Turkenburg, W. C. & et al. 2000. Renewable energy technologies. *Energy and the Challenge of Sustainability. World Energy Assessment.*: UNDP/UNDESA/WEC.

Turner, S. R. & Somerville, C. R. 1997. Collapsed xylem phenotype of *Arabidopsis* identifies mutants deficient in cellulose deposition in the secondary cell wall. *Plant Cell,* 9**,** 689-701.

Tzilivakis, J., Warner, D., May, M., Lewis, K. & Jaggard, K. 2005. An assessment of the energy inputs and greenhouse gas emissions in sugar beet (*Beta vulgaris*) production in the UK. *Agricultural Systems,* 85**,** 101-119.

Ueland, P. M. 2011. Choline and betaine in health and disease. *Journal of Inherited Metabolic Disease,* 34**,** 3-15.

Ulrich, A. 1952. The influence of temperature and light factors on the growth and development of sugar beets in controlled climatic environments. *Agronomy Journal,* 44**,** 66-73.

Van der Poel, P. 1998. Sugar Technology Beet and Cane Sugar Manufacture PW van der Poel, H. Schiweck, T. Schwartz. *Berlin: Verlag Dr. Albert Vartens KG*.

Verhertbruggen, Y. & Knox, J. P. 2006. Pectic polysaccharides and expanding cell walls. *The expanding cell.* Springer.

Verhertbruggen, Y., Marcus, S. E., Haeger, A., Ordaz-Ortiz, J. J. & Knox, J. P. 2009a. An extended set of monoclonal antibodies to pectic homogalacturonan. *Carbohydr Res,* 344**,** 1858-62.

Verhertbruggen, Y., Marcus, S. E., Haeger, A., Verhoef, R., Schols, H. A., McCleary, B. V., McKee, L., Gilbert, H. J. & Knox, J. P. 2009b. Developmental complexity of arabinan polysaccharides and their processing in plant cell walls. *Plant J,* 59**,** 413-25.

Voragen, A. G., Coenen, G.-J., Verhoef, R. P. & Schols, H. A. 2009. Pectin, a versatile polysaccharide present in plant cell walls. *Structural Chemistry,* 20**,** 263.

Vorwerk, S., Somerville, S. & Somerville, C. 2004. The role of plant cell wall polysaccharide composition in disease resistance. *Trends in Plant Science,* 9**,** 203-209.

Watson, D. J. & Baptiste, E. C. D. 1938. A comparative physiological study of sugar-beet and mangold with respect to growth and sugar accumulation I. Growth analysis of the crop in the field. *Annals of Botany,* 2**,** 437-480.

Watson, D. J. & Selman, I. W. 1938. A comparative physiological study of sugar-beet and mangold with respect to growth and sugar accumulation II. Changes in sugar content. *Annals of Botany,* 2**,** 827-846.

Weiland, P. 2003. Production and energetic use of biogas from energy crops and wastes in Germany. *Applied Biochemistry and Biotechnology,* 109**,** 263-274.

Wightman, R. & Turner, S. R. 2008. The roles of the cytoskeleton during cellulose deposition at the secondary cell wall. *The Plant Journal,* 54**,** 794-805.

Willats, W. G., McCartney, L., Mackie, W. & Knox, J. P. 2001. Pectin: cell biology and prospects for functional analysis. *Plant Mol Biol,* 47**,** 9-27.

Williams, G. & Asher, M. 1996. Selection of rhizobacteria for the control of Pythium ultimum and Aphanomyces cochlioides on sugar-beet seedlings. *Crop Protection,* 15**,** 479-486.

Wyse, R. 1979. Sucrose Uptake by Sugar-Beet Tap Root-Tissue. *Plant Physiol,* 64**,** 837-841.

Yapo, B. M. 2011. Pectic substances: From simple pectic polysaccharides to complex pectins—A new hypothetical model. *Carbohydrate Polymers,* 86**,** 373-385.

Yates, E. A., Valdor, J. F., Haslam, S. M., Morris, H. R., Dell, A., Mackie, W. & Knox, J. P. 1996. Characterization of carbohydrate structural features recognized by anti-arabinogalactan-protein monoclonal antibodies. *Glycobiology,* 6**,** 131-9.

York, W. S., Darvill, A. G., McNeil, M., Stevenson, T. T. & Albersheim, P. 1986. Isolation and characterization of plant cell walls and cell wall components. *Methods in enzymology,* 118**,** 3-40.

Zamski, E. & Azenkot, A. 1981. Sugarbeet vasculature. I. Cambial development and the three-dimensional structure of the vascular system. *Botanical Gazette,* 142**,** 334-343.

Zandleven, J., Sørensen, S. O., Harholt, J., Beldman, G., Schols, H. A., Scheller, H. V. & Voragen, A. J. 2007. Xylogalacturonan exists in cell walls from various tissues of *Arabidopsis thaliana*. *Phytochemistry,* 68**,** 1219-1226.

Zykwinska, A. W., Ralet, M. C. J., Garnier, C. D. & Thibault, J. F. J. 2005. Evidence for in vitro binding of pectin side chains to cellulose. *Plant Physiol,* 139**,** 397-407.